THE UNIVERSITY OF OKLAHOMA

GRADUATE COLLEGE

EVALUATION OF RESILIENT MODULI AND LAYER COEFFICIENTS OF AGGREGATE MATERIALS FOR AASHTO FLEXIBLE PAVEMENT DESIGN

A Dissertation

SUBMITTED TO THE GRADUATE FACULTY

in partial fulfillment of the requirements for the

degree of

Doctor of Philosophy

By

PING TIAN

Norman, Oklahoma

1998

UMI Number: 9822823

EVALUATION OF RESILIENT MODULI AND LAYER COEFFICIENTS OF AGGREGATE MATERIALS FOR AASHTO FLEXIBLE PAVEMENT DESIGN

A Dissertation APPROVED FOR THE
SCHOOL OF CIVIL ENGINEERING AND ENVIRONMENTAL SCIENCE

BY

Md. Musharrafuzzaman 2/18/98

K. K. M[illegible] 01/20/98

M. A. Moa[illegible] 1/29/98

Luther White 1-30-98

James B. Nevels, Jr 2/2/98

To My Wife, My Daughter and My Parents

ACKNOWLEDGMENTS

I would like to express my sincere appreciation to my adviser, Dr. Musharraf Zaman, Kerr McGee Presidential Professor, for his continued help, valuable guidance, constructive criticism, and active interest that led to the successful completion of this research work. His boundless energy, wide knowledge and effective mentorship made my doctoral work at the University of Oklahoma challenging and memorable. I would also like to thank my committee members Dr. K. K. Muraleetharan and Dr. Michael Mooney for their valuable comments and advice. Thanks are also due to my committee members Dr. Luther White of the Department of Mathematics, and Dr. James B. Nevels, Jr. of the Oklahoma Department of Transportation (ODOT), for their time, support, and encouragement. I would also like to express my deepest gratitude to Dr. Joakim G. Laguros, David Ross Boyd Professor Emeritus, for his special attention and help during this research work.

The financial support in the form of a research assistantship from the Oklahoma Department of Transportation (ODOT), in cooperation with the Federal Highway Administration (FHWA) is gratefully acknowledged. I would like to thank Mr. Curtis J. Hayes and Mr. Wilson Brewer, both from the ODOT, for their help in locating the quarries, and for sampling and transporting the aggregates used in this study. A special appreciation is extended to Mr. Mike Schmitz of the School of Civil Engineering and Environmental Science for his help in solving different testing problems.

I would also like to thank Dr. Dar-Hao Chen and Mr. Luping Yi, my friends and colleagues, for their help in the initial work of this research. Mr. Eddie Eckart and Mr. Kin-Lam Ng's help in the specimen preparation and testing is also greatly appreciated.

Finally, I would like to express my sincerest gratitude to my family, especially my wife, my parents, and my daughter, for their moral support and encouragement throughout the entire course of my student life. It is their help that made me successful in achieving my academic goals.

TABLE OF CONTENTS

LIST OF TABLES

LIST OF FIGURES

ABSTRACT

In this study, an evaluation of resilient modulus (RM) of aggregate materials and its application in AASHTO flexible pavement design were investigated. Two different aggregates, a limestone and a sandstone, that are considered good quality aggregates and are commonly used as the base/subbase course of pavements in Oklahoma were used. A series of RM tests was conducted to investigate the effects of testing procedure, material gradation, moisture content, drainage condition, and material type on the RM values. The variabilities of RM values due to these effects were investigated in detail and the layer coefficients required by the AASHTO design equation were evaluated.

The AASHTO standard testing procedure T 294-94 was used in conducting the RM tests. The major differences between the standard and the interim (T 292-91I) testing procedures were compared and their effects on RM values were evaluated with respect to the sample conditioning, applied stress sequence, number of loading cycles, loading duration and frequency, and loading waveform.

Three gradations and three moisture contents were selected to investigate the effects of gradation and moisture content on the RM values. Undrained RM tests were conducted and the excess pore pressure generated during the tests was measured to examine the effect of drainage condition on the RM values. Two types of undrained cyclic triaxial tests were used in order to simulate the different traffic situations in the field.

Unconfined compressive strength and triaxial compression tests were conducted to evaluate the static strength properties of the tested specimens. Multiple linear regression models were developed to correlate the RM with other important properties such as the bulk

stress, moisture content, and gradation factors.

Layer coefficients were calculated for use in the design of flexible pavements by using the AASHTO design methodology. Multiple linear regression models were developed for predicting the layer coefficients of the two aggregates. Finally, the effects of gradation, moisture content, and drainage condition on the design parameters were explained through design examples involving the design of three layer flexible pavements.

CHAPTER 1

INTRODUCTION

1.1 Introduction

Aggregate base and subbase layers are important components of a flexible pavement. Base and subbase layers are designed to support the stresses imposed by repeated wheel loads and to reduce distresses on pavements such as rutting and fatigue cracking. Also, a drainable aggregate base is designed to remove water efficiently from pavements and to minimize the distresses induced by moving vehicles; hence, to help prolong the service life of pavements (Huang 1993).

A proper characterization of pavement materials is important in the pavement design process. An accurate determination of the material properties that describe the material behavior under traffic loading is critical in the prediction of stresses, strains, and associated deflections of a pavement under traffic loading.

The 1993 AASHTO Guide for Design of Pavement Structure recommended the use of resilient modulus (RM) as a fundamental property for characterizing pavement materials in the mechanistic-empirical design of flexible pavements (AASHTO 1993). While the AASHTO recommendations address the importance of material property, they do not adequately address issues such as state standards, acceptability criteria, environmental variation effects, and construction practice. Moreover, the standards for RM testing are continuously being revised. In 1992, AASHTO adopted a new testing method T 294-92I (AASHTO 1992a) in accordance with the Strategic Highway Research Program (SHRP) recommendations. The RM testing procedure in this method is significantly different from that recommended previously by AASHTO such as the T 274-82 (AASHTO 1982) and T 292-91I (AASHTO 1991) methods. In 1994, AASHTO proposed the standard testing procedure T 294-94 (AASHTO 1994a), which is same as the interim test procedure T 294-92I, except for the units used. The testing procedures T 292-91I and T 294-92I are the two new versions provided by AASHTO in order to overcome the deficiencies in the T 274-82 method. However, there are significant differences between the two procedures in terms of loading duration, loading frequency, number of loading cycles, loading waveform, applied stress sequence, and location of LVDTs.

Since their introduction, the aforementioned testing procedures have been subjected to criticism and discussion. At the same time, a number of investigations have been conducted on the resilient response of aggregate materials (Rada et al. 1981; Raad et al. 1992; and Zaman et al. 1994). These studies have contributed significantly to the understanding of the resilient properties of aggregate materials. However, most of the tests in these studies were conducted by using the interim testing procedures (AASHTO T 274-82, T 292-91I, and T 294-92I). It has been reported that different testing procedures will result in different RM values, hence the differences in pavement design (Mohammad et al. 1994).

The stress-strain characteristic of base course materials is a very important factor in the pavement analysis process since it will show any variation in the RM and other properties, and in the stress-strain distribution in the pavement. Because of this it is necessary to measure the resilient response correctly and accurately in the laboratory. Since the development of the RM test, researchers have made efforts to investigate the cyclic response of aggregate materials. However, in general, each study was directed toward a specific type of material or identifying the effect of a particular parameter on the RM response for a given material. In the past, very few studies have been addressed on the RM of aggregate materials and more studies have been conducted on cohesive materials like clay or silt. A detailed investigation of RM for aggregate materials with the AASHTO testing procedure T 294-94 has not been pursued yet, although such a study would be very useful for implementing the AASHTO Guide for Design of Pavement Structure (AASHTO 1993).

The AASHTO design procedure requires only a single RM value for each flexible layer to determine the layer coefficient used in the evaluation of structural number (SN) of the entire pavement system (AASHTO 1993). However, the RM value depends on the stress at a specific point in the pavement layer induced by gravity and traffic loads. Moreover, the RM values determined from laboratory testing are usually represented as a function of bulk stress rather than a single RM (Laguros et al. 1993). Therefore, when using the AASHTO design guidelines, it becomes imperative to determine only one stress state which will lead to the determination of a single RM value to be used in the design. However, variations in stresses within base/subbase layers depend on the thickness and RM of each pavement layer (Chen et al. 1995). This type of variation in material response was not considered in the earlier AASHTO Design Guide (AASHTO 1972). Unfortunately, the recent AASHTO Guide (AASHTO 1993) does not provide any methodology as to how to consider this RM-thickness-stress relationship in pavement design. Therefore, in the present study the RM-thickness-stress relationship was evaluated using the finite element method to compute appropriate equivalent bulk stress which was used in the determination of layer coefficients.

As a general rule, void ratio has a significant influence on the stiffness characteristics of aggregate materials (Rada and Witczak 1981). In practical applications, open or coarse aggregates are frequently used in constructing a drainage layer in order to drain water out of the pavement efficiently. Aggregates with dissimilar grain size distribution may be used in base/subbase layers to meet various needs of the pavement structure. Also, the gradation may change during construction because more fines are produced due to the breakage of particles in the rolling compaction. On the other hand, if the gradation used in the field does not satisfy the gradation requirement established by specifications, a certain level of tolerance should be considered in the design to account for such effects. Previous research investigations indicated that the degree of influence of gradation appears to be related to the aggregate investigated and there is no uniform trend applicable for all aggregate types (Hicks and Monismith 1971; Rada and Witczak 1981; and Thompson and Smith 1990). In the present study, the gradation variation within a specified range was selected and the influence of the gradation variation on the RM values was investigated.

Drainage of water from pavements has always been an important consideration in pavement design (Rahman et al. 1996). However, as indicated by the AASHTO design guide (AASHTO 1993), current design methods often result in base courses that do not drain well. The generated excess pore water pressure, combined with increased traffic volumes and loads, often leads to early distress in the pavement structure. Water enters the pavement structure in many ways, such as through cracks, joints, or as groundwater from an interrupted aquifer, a high water table, or localized springs. Effects of this water on flexible pavements include: (1) reduced strength of unbounded aggregate materials, (2) reduced strength of roadbed soils, and (3) expulsion of fines in aggregate base under pavements with a resulting loss of support.

In the AASHTO pavement design procedure (AASHTO 1993), drainage is treated by considering the effect of water on the properties of the pavement layers and their consequences to the structural capacity of a pavement. However, in real design practice, it is still unclear as to how to select the material properties (RM) during the pavement wetting phase under different drainage conditions. It has been pointed out in the design guide (AASHTO 1993) that additional work is needed to document the actual effect of drainage on pavement life. Therefore, properly characterizing the material properties during the pavement wetting phase is an important element in improving pavement design and performance. To this end, the present study addresses the influence of drainage conditions on the RM values of aggregate base materials.

Another practical consideration is that, during saturation, pavement sublayers could experience excess pore water pressure as a result of repeated traffic loads. An increase in pore water pressure reduces the effective stress and, consequently, the strength and stiffness of the associated materials. Increasing pore pressure is possibly one of the worst scenarios with respect to pavement performance and is referred to as an "undrained condition."

Raad et al. (1992) examined the behavior of crushed aggregates with different gradations under saturated, undrained, and repeated triaxial loading conditions by using the AASHTO Method T 274-82. Of particular interest is the comparative behavior of open-graded and dense-graded base courses and the influence of fines on the cyclic response. Their results indicated that most dense-graded aggregates exhibit the highest RM values. However, the saturated dense-graded aggregates will develop excess pore water pressure under undrained conditions, which could lead to a decrease in RM values. In recent years, more states have built permeable base pavements, which allow rapid drainage of the infiltrated moisture. Field observations of drainable bases (open graded aggregate bases) in Oklahoma

(Rahman et al. 1996) indicated that none of the bases became completely saturated, even for very poor drainage conditions. Additional studies are needed to investigate if the real saturation state can exist in the pavement base layer. Chen (1994) found that in order to simulate the wet season in the field, the specimens can be prepared at the optimum moisture content and maximum dry density and then immersed into a water tank for a desired period of time. It was found (Chen 1994) that soaking compacted specimens can realistically simulate the actual field conditions.

Until now, no systematic study has been conducted on evaluation of RM of soaked specimens under undrained condition. This study is expected to have a significant effect on understanding the resilient behavior of aggregate materials under traffic loading.

1.2 Objectives and Scope of the Study

This study was pursued with two major objectives in view: (i) to determine the resilient moduli and layer coefficients of some commonly encountered aggregate base/subbase materials so that they can be used in the mechanistic design of flexible pavement in accordance with the AASHTO design guidelines; (ii) to investigate the major influencing factors such as the testing method, material gradation, moisture content, and drainage condition on the RM values and the pavement performance. Chen et al. (1994 and 1994a) investigated the RM variation of six types of aggregate which are commonly used in Oklahoma as pavement base/subbase layers. It was found that the differences of the RM values due to the variation of aggregate types are approximately in the range of 20 to 50%. Since the gradation, moisture content, and drainage effects on the RM values were not included in that study (Chen 1994), Chen concluded that further study regarding these effects can be focused on two representative aggregates. Richard Spur (RS) and Sawyer aggregates were selected for this purpose. These two aggregates are commonly used in Oklahoma as pavement base/subbase layers, and they are representative of other similar aggregates used in the state (Chen et al. 1993 and 1994a). To achieve the objectives of this study, an extensive laboratory testing program was undertaken for the RS and the Sawyer aggregates. The following were the specific tasks of this study:

1. Conduct RM tests for the RS aggregate by using the different AASHTO testing procedures T 292-91I and T 294-94 to investigate the influence of testing procedures on RM values. The combined effect of sample conditioning, applied stress sequence, number of loading cycles, loading duration, and loading waveform on the RM values were evaluated based on the RM test results.
2. Conduct RM tests for the two aggregates based on three different gradations (median, coarser limit, and finer limit of ODOT gradation range). Evaluate the effect of gradation on RM values.
3. Conduct RM tests for the two aggregates based on three different moisture contents (optimum, 2% below, and 2% above optimum). Evaluate the effect of moisture content on RM values.
4. Conduct RM tests for the two aggregates under undrained conditions. Investigate the drainage condition and excess pore pressure effects on RM values.
5. After the RM test, conduct static triaxial compression and unconfined compressive strength tests for all of the RM specimens to evaluate the cohesion (C), friction angle (ϕ), and unconfined compressive strength (U_C) for the two aggregates.
6. Evaluate the material property coefficients (k_1 and k_2) required by the AASHTO

design equation ($RM = k_1\theta^{k2}$). Study the effects of gradation, moisture content, and drainage conditions on these material property coefficients.

7. Develop multiple linear regression models for predicting the RM values of the two investigated aggregates based on the correlations between the RM and other important material properties (e.g., bulk stress (θ), gradation (percent passing the No. 200 sieve) and moisture content (MC)).

8. Calculate layer coefficients to facilitate the implementation of RM in the AASHTO flexible pavement design. Develop multiple linear regression models for predicting the layer coefficients of the two aggregate bases investigated. With the help of design examples, the effect of RM variation on the pavement performance due to the variations of gradation, moisture content, and drainage conditions can be further demonstrated.

1.3 Format of the Dissertation

Following the introduction and the objectives of the study discussed in Chapter 1, Chapter 2 provides a detailed literature review on the RM concept, RM testing methods, factors influencing the RM values, and a review of the mechanistic-empirical (ME) pavement design methodology. Chapter 3 provides a discussion on the material sources, the laboratory tests conducted, and the experimental methodology adopted. A detailed discussion of the RM test results and analyses conducted are presented in Chapter 4. Chapter 5 discusses the material model parameter values and the multiple linear regression models correlating RM with other important material properties. The layer coefficients of the various aggregate bases and AASHTO flexible pavement design examples illustrating the use of layer coefficients are presented in Chapter 6. In Chapter 7, the summary and conclusions of the study are presented along with recommendations for further research. The detailed results of RM tests conducted on the individual duplicate specimens are presented in Appendix A. SI units are followed throughout the dissertation. However, whenever English units are used, conversion factors are provided. In addition, a conversion table is provided in Appendix B.

CHAPTER 2

LITERATURE REVIEW

2.1 Introduction

This chapter provides an overview of the relevant studies conducted by various researchers on resilient modulus of aggregate materials. The various topics discussed in this chapter are: concept of resilient modulus, resilient modulus testing and testing procedures, material models, factors influencing resilient modulus of aggregate materials, and existing mechanistic-empirical flexible pavement design methodologies.

2.2 Resilient Modulus

A proper characterization of pavement materials is important in the pavement design process. Accurate determination of the material properties that describe the material behavior under traffic loading is critical in the prediction of stresses, strains, and associated deflections of a pavement under traffic loading.

An aggregate base course has a significant effect on the resilient deflection as well as on the residual deformation of a flexible pavement. The response of aggregate materials under cyclic loading that simulates actual traffic loading is different from the response under static loading. Most paving materials are not elastic but experience some permanent strain after each load application and withdrawal as in the case of traffic loading. However, if stresses due to traffic loads are small compared to the strength of the material, even after a large number of repeated loading and unloading sequences, only a very small amount of permanent deformation (ε_p) is accumulated. Most deformation under each load repetition is recoverable (ε_r) and proportional to the load (Huang 1993). To examine this behavior, researchers have used the concept of resilient modulus (RM), which is defined mathematically as the cyclic deviator stress σ_d divided by the resilient strain ε_r

$$RM = \sigma_d / \varepsilon_r \tag{2-1}$$

The RM defined above is a fundamental material property that describes the load-deformation behavior of the pavement material under traffic loading. Conceptually it is same as the modulus of elasticity; however, it describes the stress-strain relationship under a cyclic loading. Figure 2-1 shows the stress-strain characteristics of pavement materials under cyclic loading, and the RM can be represented by the slope of the scant line of the unloading-reloading stress-strain cycle.

2.3 Resilient Modulus Testing

The RM values of pavement materials are usually determined either by laboratory testing of the pavement materials or by in-situ non-destructive deflection testing (NDT) of the pavement. In the laboratory, the cyclic triaxial test is usually conducted on the pavement materials for measuring the RM values. The Falling Weight Deflectometer (FWD), however, is the most commonly used non-destructive field testing method for evaluation of the RM values of the individual layers of an existing flexible pavement. A NDT method is used to measure the deflections at the different points of a pavement surface, and the RM of individual pavement layers can be backcalculated with the obtained deflection values. The major drawback of the NDT method is that the thickness of the layer needs to be precisely known (Cosentino and Chen 1991). Other limitations of this method include: (1) relatively small loading magnitudes; (2) inability in capturing the nonlinear material behavior; and (3) requiring favorable weather (Pezo et al. 1992). Irwin (1993) reported that the NDT method is not sensitive to thin layers, adjacent layers of similar modulus, large modular ratios, and the degree of bonding between layers. Also, there are no adequate criteria for evaluating the reasonableness of the moduli arising from backcalculation.

A comparison between backcalculated moduli and laboratory moduli is difficult because of the variability in sampling materials, testing, and result interpretation (Lee et al. 1988; Wu 1993). It has been found that discrepancies are existed between backcalculated moduli from FWD field testing data and laboratory determined triaxial test values. For example, Elliott (1992) reported that the backcalculated subgrade RM values for cohesive soils are unconservative and need to be multiplied by a factor no greater than 0.33 to be consistent with the 21 MPa RM value assumed for the subgrade in the AASHTO Road Test. Maree et al. (1982) indicated that the laboratory constant confining pressure triaxial tests overestimate the moduli of the crushed-stone bases, and a shift factor of 0.3 to 0.5 needs to be applied.

2.4 Resilient Modulus Testing Procedures

As a result of more than 10 years of testing, the testing procedure for the laboratory determination of RM values was finally standardized in 1994. Historically, AASHTO has proposed several test methods for RM testing, namely, AASHTO T 274-82 (AASHTO 1982), T 292-91I (AASHTO 1991), T 294-92I (AASHTO 1992a), and T 294-94 (AASHTO 1994a). A review of these testing procedures reveals that the basic differences are particularly related to: (1) sample conditioning, (2) applied confining pressure, (3) applied stress sequence, (4) waveform of cyclic loading, (5) number of loading cycles, and (6) location of LVDTs. A detailed comparison in terms of the magnitudes of confining pressure (σ_c), deviator stress (σ_d), and the applied stress sequence for the AASHTO testing methods T 274-82, T 292-91I, T 294-92I, and T 294-94 is shown in Table 2-1. Table 2-2 shows a comparison between the important features of these test methods.

Since its introduction, the testing procedure T 274-82 (AASHTO 1982) has been a target of widespread criticism (Pezo et al. 1992). The main criticism for the T 274-82 method is that the required loading conditions are too severe and therefore, a specimen may fail in the conditioning stage (Chen 1994). For example, Ho (1989) stated that the heavy sample conditioning stage in the T 274-82 may cause different levels and types of stresses and was very severe for Florida subgrade soils. The T 274-82 method requires an evaluation of RM under a substantial number of stress states for both cohesive and granular soils that many researchers believe to be excessive and unnecessary (Vinson 1989). For these reasons, AASHTO modified the T 274-82 and proposed the T 292-91I method in 1991. Then in 1992, AASHTO adopted the T 294-92I method in accordance with the Strategic Highway Research Program (NCHRP) recommendations. Later, in 1994, AASHTO proposed the standard testing procedure T 294-94 which is same as the T 294-92I method except for the units used.

The RM values of aggregate materials can be influenced by various factors among which the applied confining pressure is considered a very important factor (Rada et al. 1981). Thus, in order to adequately characterize such materials, it is desirable to conduct the RM tests under a wide range of confining pressures expected within the pavement base and subbase layers. The AASHTO T 292-91I and T 294-94 (T 294-92I) methods use a variety of constant confining pressures and cyclic deviator stresses. However, the sequences of the applied pressures and stresses are completely different. The T 292-91I starts with a higher confining pressure and deviator stress and ends with a lower confining pressure and deviator stress. On the other hand, the T 294-94 uses a reverse sequence which starts with a lower confining pressure and deviator stress and ends with a higher confining pressure and deviator stress (Table 2-2). Zaman et al. (1994) investigated these two stress sequences by using the rectangular waveform, in which two sets of RM tests were conducted under identical conditions, except for the stress application sequence. Their test results indicate that the stress sequence used in the T 294-94 method yielded higher RM values (15-34% higher) than those produced by the stress sequence used in the T 292-91I method. This variation was attributed to the cyclic stress having a stiffening effect on the specimen structure because the stress application sequence goes from lower to higher in the T 294-94 testing method.

Axial deformation of the aggregate specimens is measured using Linear Variable Differential Transducers (LVDTs). Generally, there are two ways to install the LVDTs for specimen deformation measurement: (1) over the entire length; (2) over a portion of the specimen. The AASHTO T 274-82 and T 292-91I methods recommend that the LVDTs be internally mounted to measure the deformation of the specimen over the middle 1/3 to 1/4 of the length of the specimen. On the other hand, the AASHTO T 294-92I and T 294-94 methods recommend that the LVDTs be externally mounted and the deformation along the entire length of the specimen be measured. In general, an externally mounted LVDT, which measures the deformation of the entire length of a specimen, yields higher deformation and hence, gives lower RM values than a test using an internally mounted LVDT. As reported by

Mohammad et al. (1994), RM values were higher for the specimens with the internal LVDT, located at the middle one third of the specimen, than the specimens with the external LVDT located at the end of the specimen. Similar results were reported by Burczyk (1994) in that RM measurements made with LVDTs mounted on the specimen inside the testing chamber consistently gave higher values than the LVDTs located outside of the triaxial cell and mounted on the loading piston. Generally, the internally mounted LVDTs avoid the end effect of a specimen caused by the relatively rigid porous stones and steel platens. However, it is difficult to mount the internal LVDTs, particularly for aggregate specimens. Also, the internal LVDTs cause some degree of disturbance on a specimen.

It has been reported that different testing procedures will result in different RM values; the magnitude of influence seems to depend on the material tested. Mohammad et al. (1994) reported that the testing procedure influenced the RM values of blasting sands more significantly than those of silty clays. Zaman et al. (1994) also studied one sandstone aggregate and found that the influence of testing procedure for this material is significant. A number of factors were examined by Tian et al. (1997) in order to investigate the reasons for the differences in RM results.

2.5 Material Models

The existence of nonlinear stress-strain characteristics of aggregate materials has been well known for many years. To reflect the stress-dependent behavior of an aggregate, the k-θ model (Eq. (2-2)) has been used for a long time in pavement analysis and design. The AASHTO test methods (AASHTO T 292-91I, T 294-92I, and T 294-94) have recommended this model to describe the stress dependent nonlinear behavior of aggregate materials.

$$RM = k_1 \theta^{k_2} \tag{2-2}$$

where, k_1 and k_2 are the material constants and θ is the bulk stress defined as the first stress invariant ($\theta = \sigma_1 + \sigma_2 + \sigma_3$).

Eq. (2-2) has been implemented in various pavement analysis computer programs by using an iterative computation scheme. For most pavement sections, stresses induced by traffic load provide the shear effect, while the bulk stress is primarily dominated by the overburden pressure (Chen 1994). May and Witczak (1981) and Uzan (1985) have pointed out that the model given by Eq. (2-2) does not consider the effect of shear stress which is believed to have an effect on RM values. Uzan (1985) suggested an improved model which includes the effect of shear stress.

$$RM = k_3 \theta^{k_4} \sigma_d^{k_5} \tag{2-3}$$

where, k_3, k_4, and k_5 are the material constants and σ_d is the deviator stress.

Nataatmadja (1994) also reported that the coefficient of determination determined from the k-θ model is very low ($R^2 = 0.4658$) for his RM test results. However, when the RM is normalized by means of the ratio of the deviator stress to the sum of principal stresses, a significant relationship is obtained.

$$RM * \sigma_d / \theta = A + B \sigma_d \tag{2-4}$$

where A (kPa) and B (dimensionless) are material constants.

Barksdale et al. (1990) stated that the k-θ model, as given by Eq. (2-2), gives a good representation of the measured shear strain but a very poor prediction of volumetric strain. Also, the k-θ model does not describe the significant decrease in the RM values which occurs with the increasing strain observed in the laboratory. Furthermore, Witczak and Uzan (1988) modified Eq. (2-3) by replacing the deviator stress σ_d with the octahedral shear stress τ_{oct} because they believed that the RM values of granular materials increase with increasing confinement but decrease with increasing shear, which appears to be more theoretical, as shown in Eq. (2-5).

$$RM = k_6 P_a \theta^{k_7} \tau_{oct}^{-k_8} \tag{2-5}$$

where k_6, k_7, and k_8 are material constants, and Pa is the pressure of atmosphere.

Brown and Pappin (1981) stated that confusion has often arisen over the use of the k-θ model because the constant k_1 is not dimensionless. Furthermore, a distinction is rarely made between total stress and effective stress. Although it is of no consequence for dry materials, it is of fundamental importance when pore water is present.

2.6 Resilient Modulus of Untreated Granular Materials

Rada and Witczak (1981) conducted a comprehensive evaluation of 271 RM test results obtained from 10 different research agencies. Six unique sets of k_1 and k_2 values for six different granular material types were presented, as reproduced in Table 2-3. The data indicates that the crushed stone type aggregate shows the largest variation in k_1 and k_2. The mean k_1 and k_2 values for all granular materials were found to be 63,756 kPa and 0.52, respectively.

Researchers from several agencies also have reported k_1 and k_2 values for untreated aggregate materials. These values are reproduced in Table 2-4. Chen (1994) conducted laboratory RM tests using the AASHTO T 292-91I method on six aggregate types sampled from different parts of Oklahoma. The k_1 and k_2 values obtained from these aggregate materials are presented in Table 2-5.

The Asphalt Institute (AI 1991b) suggests design RM values ranging from less than 103 MPa to greater than 345 MPa. Typical values of k_1 and k_2 for unbound base and subbase materials, as recommended by the AASHTO Guide for Design of Pavement Structures (AASHTO 1993), are presented in Table 2-6.

In view of the above k_1 and k_2 values, it can be observed that there are certain differences in k_1 values reported by different research agencies. The k_1 values are dependent on the material type, moisture content, and material gradation used. However, the variation of k_2 value is not significant. For design purposes, taking the k_2 value as 0.5 to 0.7 is generally a safe assumption, as specified by the AASHTO Design Guide (AASHTO 1993). The k_1 value, however, should be carefully selected in the design practice.

2.7 Factors Influencing Resilient Modulus of Granular Materials

In recent years, some studies have been performed to investigate the influence of various factors affecting the RM values of granular materials. Generally, the following factors are believed to have significant influence on the resilient characteristics of granular materials: (1) loading condition, (2) degree of saturation, (3) compaction level (dry density), (4) material gradation, (5) drainage condition, and (6) material type.

2.7.1 Loading Condition

The effect of loading conditions in the RM test for granular materials is generally well understood from previous research investigations. The most significant loading factor that affects the modulus is the stress level (Rada and Witczak 1981). Hicks and Monismith (1971) reported that for a constant principal stress ratio (σ_1/σ_3), the RM increased as the confining pressure increased. It was also found that the RM generally increased with increasing axial stress for principal stress ratios greater than 2. In general, it is customary to relate either bulk stress θ or confining pressure σ_c to RM. Because of its ease of adaptation into nonlinear solutions of a layered pavement system, the RM and θ relation is used by most researchers.

Other load factors, such as stress sequence, stress frequency, and number of stress cycles necessary to reach a stable permanent response, have little, if any, effect on the RM response (Rada and Witczak 1981). Kaicheff and Hicks (1973) demonstrated that if the stress pulse is rapidly applied, and then sustained; the resilient response is the same as that obtained from a rapidly applied and released short duration stress pulse of same magnitude. Hence, it was concluded that there was no evidence of a change in resilient behavior with a change in load duration or frequency (for a duration of time in the range of 0.1 to 0.2 second), and also the number of stress cycles had little effect on RM values. Hicks (1970) reported that the sequence in which different stress states are applied has little effect on resilient response as long as the principal stress ratio (σ_1/σ_3) is kept below 6 to 7. Studies by Hicks and Monismith (1971) and Kalcheff and Hicks (1973) indicated that one specimen can be used to evaluate resilient response of granular materials over a reasonably wide range of stress levels. However, the specimen should be preconditioned with about 100 load repetitions.

2.7.2 Degree of Saturation

Degree of saturation, if other factors are held constant, plays a major role in the RM response of granular materials. The degree of saturation is a more fundamental parameter than water content and should always be specified with the RM test results (Pandey 1996). Barksdale et al. (1990) stated that the degree of saturation is more closely related than the water content to the soil suction and capillary tension forces which can have significant effect on the stiffness of a material. Generally, most previous research concluded that the RM of granular materials decreases as the degree of saturation increases beyond a certain range (80 to 85%) (Hicks and Monismith 1971; Rada and Witczak 1981; and Thompson 1989). However, although this is true in a general sense, the exact influence of saturation appears to be dependent on the aggregate type (Rada and Witczak 1981). Degree of saturation is found to affect the k_1 parameter, in the k-θ model, more than the k_2 parameter. Seed et al. (1967) found that, for well-graded gravels, k_1 was reduced and k_2 remained unchanged with increasing saturation (S_r) values. Repeated load triaxial tests, conducted by Haynes and Yoder (1963) on gravels and crushed stone, indicated that there was a critical degree of saturation near 80 to 85%. Above this critical degree of saturation, the RM decreased rapidly particularly if tests were performed under an undrained condition. Below the critical point, the degree of saturation had small influence on the RM. Rada and Witczak (1981) concluded that, in general, the effect of moisture can change the typical k_1 values from 207 MPa (dry) to 7 MPa (saturation), with resultant changes in RM value from 276 MPa to 69 MPa or less.

Barksdale and Itani (1989) reported that different granular materials presented different levels of sensitivity to moisture. For granitic gneiss, the RM decreased by a factor of about 40% and 20% after soaking at bulk stresses of 103 kN/m^2 and 690 kN/m^2 , respectively. However, for the river gravel specimens, the RM decreased, upon soaking, by a factor of 50% and 25% at bulk stresses of 103 kN/m^2 and 690 kN/m^2, respectively. It should be noted that these test results are for tests conducted on drained specimens. Had the undrained tests been performed, the effect of moisture content on the RM would undoubtedly have been greater.

Thom (1988) reported that the elastic behavior of granular materials as a function of moisture content can be divided into two categories. The first category is the case where the material is initially wetted, and the elastic stiffness changes slightly with the increasing moisture content. In the second category, subsequent drying and rewetting take place, and as a result, the elastic stiffness changes significantly with the increase in moisture content.

Thom and Brown (1987) studied the behavior of a crushed stone under drained, repeated loading conditions. It was found that the RM values decreased slightly with the increase in moisture content. However, increasing the degree of saturation did have a significant effect on the permanent deformation behavior. They also found that for an open-graded stone having only 2 to 3% fines, the RM values were almost not affected by saturation level. Therefore, the effect of water on the resilient behavior of granular materials increases with the increasing amount of fines.

Based on the findings discussed above, Barksdale et al. (1990) concluded that the following important points are directly related to laboratory testing of granular materials: (1) the RM can be significantly affected at high degrees of saturation depending upon whether the test is performed under a drained or undrained condition. This finding is not surprising considering the principle of effective stress. Generally, the positive pore water pressure developed during the undrained test can significantly affect the RM of granular materials at a high degree of saturation as it affects the effective stress level. (2) large permanent deformations can occur in conventional aggregate base materials at high levels of saturation.

2.7.3 Compaction Level (dry density)

Several studies have been conducted by previous researchers including the effect of density on the RM response of granular materials (Rada and Witczak 1981). These studies have indicated that, although an increase in dry density results in an increase in RM values, the effect is relatively small compared with changes caused by stress level and moisture content. Rada and Witczak (1981) also reported that the k_1 value increases gradually with increasing the compaction effort and the k_2 value remains essentially constant. The average increase in k_1 value was nearly 48% when the compaction was changed from standard to modified proctor. Therefore, it was concluded that the influence of compaction in improving the modulus (k_1) cannot be ignored in this case.

Barksdale and Itani (1989) found that as the dry density of a granitic gneiss increased from 95 to 100% of the AASHTO T 180 value (AASHTO 1993a), the RM increased by 50 to 160% at a low bulk stress of 103 kPa. However, at a high bulk stress of 690 kPa, the effect of an increase in density was considerably reduced to only about 15 to 25%.

2.7.4 Material Gradation

Rada and Witczak (1981) reported that the gradation and its influence on k_1 and k_2 values are dependent on the type of material considered and there is no general trend regarding the influence of fines (passing the standard sieve No. 200 (0.075 mm)) on the RM values. For crushed, angular materials there was little, if any, change in either k_1 and k_2 values over a range of 3 to 17% that passes the No. 200 sieve (0.075 mm). However, for a sand-gravel material, the k_1 parameter had a maximum value near gradation with optimum fines content (6%) and then a marked decrease in k_1 values with increasing the fines content. Hicks and Monismith (1971) found that the k_2 values decreased while k_1 increased with increasing fines content for the crushed aggregate tested. Thompson and Smith (1990) reported that, for gradations that only differed (4 to 8%) in the permissible amount passing the 0.075 mm (No. 200) sieve, limited differences in RM (197 to 244 MPa at 138 kPa bulk stress) were noted among the various granular materials tested. However, more open-graded granular materials with reduced fines are less moisture sensitive and generally provide an improved granular base performance.

Kamal et al. (1993) reported that the RM value increased as the gradation changed from the finer to the coarser end of the gradation envelope. By comparing the resilient behavior of an uncrushed base material (uniformly graded with a maximum size of 5 cm with 37% aggregate fracture) with a crushed base material (uniformly graded with a maximum size of 2.5 cm with 85% aggregate fracture), Johnson and Hicks (1987) reported that, contrary to previous research and experience in crushed and uncrushed gravels, the uncrushed base course performed better than the crushed base coarse; the RM was higher, and the permanent deformation was lower. The uncrushed base is superior because of larger maximum particle size and greater maximum density. Also, Johnson and Hicks (1987) performed an analysis of the future performance of the roadway with equal thicknesses of asphalt, which indicates that a pavement over an uncrushed base would have a longer life than a pavement over a crushed base by 54%.

Barksdale and Itani (1989) studied the influence of gradation on RM values for the granitic gneiss. It was found that the coarse gradation of this material consistently resulted in higher RM values than those of the medium and fine gradations. As the gradation became finer (with the amount of fines going from 0 to 10%), the RM decreased by about 60%.

2.7.5 Drainage Condition

Hicks and Monismith (1971) conducted a series of RM tests on saturated aggregate specimens under drained and undrained conditions. It was observed that the drained and undrained stress-strain paths were nearly the same. For the undrained tests, pore pressure measurements were also recorded throughout the test. Generally, static pore pressure (back pressure) remained relatively constant over the duration of a particular test. Transient pore pressure (due to the repeated load) developed almost instantaneously and was generally of the order of 5 to 10% of the repeated load.

Raad et al. (1990) studied the behavior of crushed aggregate materials with different gradations under saturated, undrained, and repeated triaxial loading conditions. Of particular interest is the comparative behavior of open-graded and dense-graded base courses and the influence of fines on the cyclic response. Their results indicated that most dense-graded aggregates exhibit the highest RM values, while the open-graded aggregate has the lowest values. However, the saturated dense-graded aggregates will develop excess pore water pressure under undrained conditions, which could lead to a decrease in RM values.

2.7.6 Material Type

Barksdale (1989) reported that the aggregate type had a significant influence on the RM values when other factors were held constant. The RM values of the rough and angular materials were higher than those of the rounded gravel by a factor of about 50% at low values of bulk stress. At high bulk stresses, the RM of the angular granite was higher than that of the gravel by a factor of 25%.

Thompson (1989) reported that for a given gradation (either crushed or uncrushed materials), the source (limestone, sandstone, granite, etc.) is usually not a significant factor in terms of RM values. Thompson and Smith (1990) also observed that the RM values of various aggregates are similar and the type of aggregates used as base courses of roadway pavement (crushed stone/gravel) has a limited effect on the RM values. However, Chen et al. (1994b) investigated six different aggregate materials that are commonly used in Oklahoma as subbases or bases and indicated that the differences in the RM values due to the variation in aggregate type are approximately in the range of 20 to 50%; this suggests that the source of aggregate has a effect on the RM values.

2.8 Mechanistic-Empirical Flexible Pavement Design Methodology

The design equations presented in the 1993 AASHTO Design Guide (AASHTO 1993) were obtained empirically from the results of the extensive AASHTO Road Test conducted in Ottawa, Illinois, in the late 1950s and early 1960s. The empirical performance equations obtained from the AASHTO Road Test are still being used as the basic models in the current guide but were modified and extended to make them applicable to other regions of the nation. The empirical design procedures are usually acceptable only for exact conditions and within the range of variables under which they were developed and may actually give unacceptable/erroneous results outside of these ranges. In recent years, the mechanistic-empirical (ME) design method has been widely used in pavement design because it has the potential to improve the reliability of pavement design. The ME procedure stems from the fact that the theoretical or structural models are used to analyze the structural response of pavements (stress, strain, and deformation), while the distress models empirically related or calibrated to the structural responses give the pavement service life for a given limited strain criterion (Chen et al. 1994c). The calibrated mechanistic procedure is a more appropriate term for describing the ME procedure (Huang 1993). The ME method contains a number of mechanistic distress models which require careful calibration and verification to ensure that a satisfactory agreement is achieved between predicted and actual distress.

2.8.1 Pavement Structural Analysis Models

In a mechanistic design procedure, a structural analysis tool is required to predict the stress-strain and displacement response of pavements. A number of computer programs based on the Finite Element (FE) or the multi-layered elasticity (MLE) method have been developed and utilized for structural analysis of flexible pavements (Shell 1978, Thompson 1987, and Huang 1993). Overall, the MLE methods are more widely used (Thompson and Barenberg 1989) due to their simplicity, but they may suffer from the inability to evaluate the stress-dependent behavior of soil and granular materials and may yield tensile stresses in granular materials, which do not occur in the field. Chen (1994) indicated that a comprehensive analysis of flexible pavements should include the stress-dependent behavior of granular base course and the cohesive subgrade, the geostatic force of the pavement itself, finite width of the asphalt concrete (AC) pavement, multiple wheel loading at any location of the given domain being analyzed, and partial bonding between the AC and the granular layer. However, none of the structural models or computer programs is capable of incorporating all these parameters simultaneously in the analysis.

The ILLI-PAVE (Thompson and Barenberg 1990), developed at the University of Illinois, and the MICH-PAVE (Harichandran et al. 1989), developed at Michigan State University, are the two FE computer programs devoted to the structural analysis of flexible pavements with the capability to account for stress-dependent characterization of granular materials and subgrade soils through an iterative scheme. The computer program DAMA (AI 1991a), developed at the University of Maryland, was based on MLE and was used to obtain the structural design charts included in the Asphalt Institute's MS-1 manual (AI 1991b). The nonlinear characterization of granular materials in DAMA is achieved by using an approximate equation which was obtained from a multiple regression analysis. The computer program KENLAYER (Huang 1993), developed at the University of Kentucky, can be applied to a multi-layered system under stationary or moving multiple wheel loads with each pavement layer being either linear elastic, nonlinear elastic, or viscoelastic.

Chen et al. (1995) performed a comprehensive assessment of existing structural analysis models. The most appropriate model for the routine structural analysis of flexible pavement was selected based on the commonly used criteria for flexible pavement design (maximum surface deflection, tensile strain at the bottom of AC layer, and compressive strain at the top of subgrade). Chen et al. (1995) recommended that MICH-PAVE is one of the most appropriate models for the routine structural analysis of flexible pavements.

To develop a mechanistic pavement analysis and design procedure suitable for future versions of the AASHTO guide, a research project entitled "Calibrated Mechanistic Structural Analysis Procedures for Pavements" funded by NCHRP was conducted by Thompson and Barenberg (1989). The use of elastic layer programs (ELP) and ILLI-PAVE for the development of future AASHTO design guides was recommended from this study. It was suggested in this study to use the modulus-depth relationship obtained from ILLI-PAVE to establish the various moduli for the ELP, thus capitalizing on the stress-sensitive feature of ILLI-PAVE and the multiple wheel capability of ELP (Huang 1993).

2.8.2. Distress Models or Transfer Functions

Distress models, often referred to as transfer functions, which relate structural responses to various types of distress, are the weak link in the ME design methods; extensive field calibrations and verifications are needed to establish reliable distress predictions (Huang 1993). Several distress models have been reported so far (e.g., Ullidtz 1977; Shell 1978; AI 1982a; Verstraeten et al. 1982; Powell et al. 1984; Thompson 1987). Some of the existing distress models are developed from laboratory data while others are based on the observed in-service performance of pavements. These models are used to estimate the maximum number of repetitions for a given level of stress, strain, or deflection that a pavement can withstand before reaching an unacceptable state of serviceability. Two types of pavement distress, namely, fatigue cracking and rutting, are considered most critical for the design of flexible pavements (AI 1982a; Huang 1993). Fatigue cracking is caused by the tensile strain at the bottom of the asphalt layer, while rutting is caused by the accumulation of compressive strains on the top of subgrade, which is often responsible for much of the permanent deformation or rutting in flexible pavements (Lotfi et al. 1988).

Table 2-1 Comparison of the Different AASHTO RM Testing Procedures

	AASHTO T 274-82			AASHTO T 292-91I			AASHTO T 294-92I and T 294-94		
	σc (kPa)	σd (kPa)	No. of Cycles	σc (kPa)	σd (kPa)	No. of Cycles	σc (kPa)	σd (kPa)	No. of Cycles
Sample conditi-oning	34	34	200						
	34	69	200						
	69	69	200						
	69	103	200						
	103	103	200						
	103	138	200	138	103	1000	103	103	1000
Test	138	7	200	138	69	50	21	21	100
	138	14	200	138	138	50	21	41	100
	138	34	200	138	207	50	21	62	100
	138	69	200	138	276	50	34	34	100
	138	103	200	103	69	50	34	69	100
	138	138	200	103	138	50	34	103	100
	103	7	200	103	207	50	69	69	100
	103	14	200	103	276	50	69	138	100
	103	34	200	69	34	50	69	207	100
	103	69	200	69	69	50	103	69	100
	103	103	200	69	138	50	103	103	100
	103	138	200	69	207	50	103	207	100
	69	7	200	34	34	50	138	103	100
	69	14	200	34	69	50	138	138	100
	69	34	200	34	103	50	138	276	100
	69	69	200	21	34	50			
	69	103	200	21	48	50			
	34	7	200	21	62	50			
	34	14	200						
	34	34	200						
	34	69	200						
	34	103	200						
	7	7	200						
	7	14	200						
	7	34	200						
	7	52	200						
	7	69	200						

Table 2-2 Important Features of the AASHTO RM Testing Procedures for Granular Materials (after Chen 1994)

	AASHTO T 292-91I	AASHTO T 294-92I and AASHTO T 294-94
Sample conditioning	Confining Pressure: 138 kPa Deviatoric Stress: 103 kPa	Confining Pressure: 103 kPa Deviatoric Stress: 103 kPa
Stress Sequence	From a higher confining pressure and deviatoric stress to a lower confining pressure and deviatoric stress	Opposite to T 292-91I
Number of loading cycles	Conditioning: 1000 RM testing: 50	Conditioning: 1000 RM testing: 100
Stress pulse	Haversine, Triangular, Rectangular	Haversine
LVDT Location	Internal, at 1/3 to 1/4 of the specimen; or external, at the top of the specimen	External, at the top of the specimen
Compaction Method	Vibration	Vibration
Bulk Stress	From 97 to 690 kPa	From 83 to 690 kPa

Table 2-3 Summary of k_1 and k_2 Values by Aggregate Class (Rada and Witczak 1981)

Aggregate Class	No. of Data Points	k_1 Parameter (psi)			k_2 Parameter		
		Mean	SD	Range	Mean	SD	Range
Silty sands	8	1620	780	710 - 3830	0.62	0.13	0.36 - 0.80
Sand gravel	37	4480	4300	860 - 12840	0.53	0.17	0.24 - 0.80
Sand-aggregate blends	78	4350	2630	1880 - 11070	0.59	0.13	0.23 - 0.82
Crushed stone	115	7210	7490	1705 - 56670	0.45	0.23	-0.16 - 0.86
Limerock	13	14030	10240	5700 - 83860	0.40	0.11	0.00 - 0.54
Slag	20	24250	19910	9300 - 92360	0.37	0.13	0.00 - 0.52
All data	271	9240	11225	710 - 92360	0.52	0.17	-0.16 - 0.86

SD = Standard Deviation; 1 psi = 6.9 kPa

Table 2-4 Ranges of k_1 and k_2 for Untreated Granular Materials (after Chen 1994)

Reference	Material Type	k_1 (psi)	k_2
Hicks, 1970	Partially crushed gravel, crushed rock	1600 - 5000	0.57 - 0.73
Allen, 1973	Gravel, crushed stone	1800 - 8000	0.32 - 0.7
Kalcheff and Hicks, 1973	Crushed stone	4000 - 9000	0.46 - 0.64
Hicks and Finn, 1970	Untreated base at San Diego Test Road	2100 - 5400	0.61
Boyce et al., 1976	Well-graded crushed limestone	8000	0.67
Elliott, 1992	Gravel, crushed stone	4120	0.476

1 psi = 6.9 kPa

Table 2-5 Summary of k_1 and k_2 Values of Six Aggregate Types Tested Using the RM Testing Procedure AASHTO T 292-91I (Chen 1994)

County	Material Type	k_1 (psi)	SD	k_2	SD
Comanche	Limestone	4151	1082	0.3918	0.1175
		3908		0.3683	
		2168		0.5825	
Cherokee	Limestone	2283	2465	0.5017	0.1133
		4685		0.3472	
		7213		0.2882	
Creek	Limestone	4449	518	0.3698	0.0246
		4317		0.3858	
		3494		0.4180	
Choctaw	Sandstone	1388	165	0.5309	0.0295
		1691		0.5847	
		1427		0.5734	
		1498		0.6073	
		2029		0.5364	
		1440		0.5533	
Johnston	Granite	2041	173	0.5242	0.0449
		2366		0.4350	
		2102		0.4889	
Murry	Rhyolite	2747	580	0.4338	0.056
		2417		0.4949	
		3099		0.4612	
		2160		0.4769	
		1673		0.5230	
		1652		0.5949	

SD = Standard Deviation; 1 psi = 6.9 kPa

Table 2-6 Typical Values of k_1 and k_2 for Unbound Base and Subbase Materials (AASHTO 1993)

Material	Moisture Condition	k_1 (psi)	k_2
Base	Dry	6000 - 10000	0.5 - 0.7
	Damp	4000 - 6000	0.5 - 0.7
	Wet	2000 - 4000	0.5 - 0.7
Subbase	Dry	6000 - 8000	0.4 - 0.6
	Damp	4000 - 6000	0.4 - 0.6
	Wet	1500 - 4000	0.4 - 0.6

1 psi = 6.9 kPa

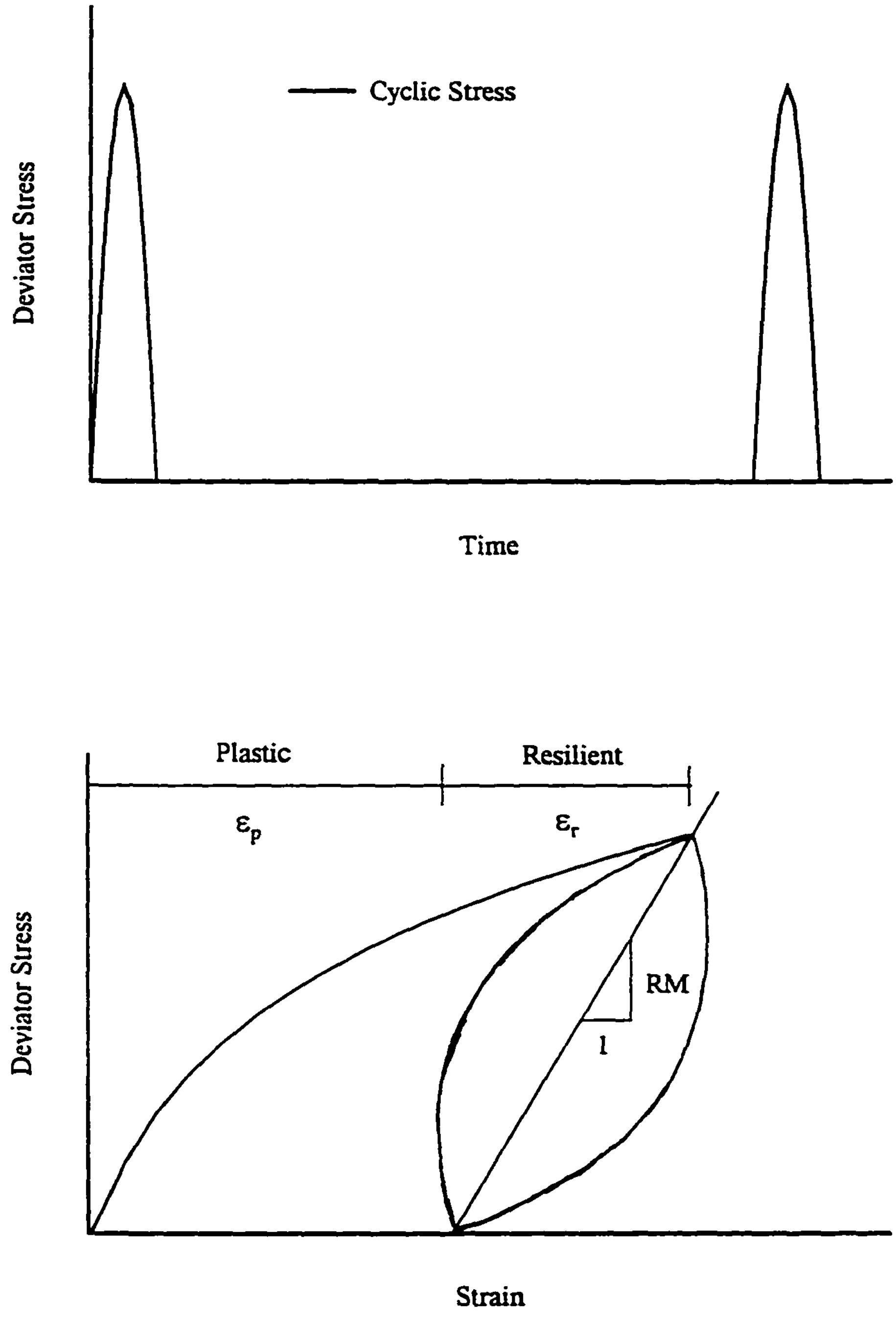

Figure 2-1 Typical Cyclic Load Response of Aggregate Material

CHAPTER 3

EXPERIMENTAL METHODOLOGY AND TESTING

3.1 Introduction

This chapter describes the experimental methodology adopted and the various laboratory tests conducted in order to achieve the goals of the study. The characteristics and origin of the materials used in this study are also presented in this chapter. Two types of aggregates, namely, Richard Spur and Sawyer aggregates were used in this study. The laboratory material property tests (e.g. grain size distribution, moisture-density relationship, Los Angeles abrasion, specific gravity, and Atterberg limit tests) and the triaxial tests (resilient modulus, unconfined compressive strength, and static triaxial compression tests) were conducted on these two aggregates. The procedure adopted to prepare aggregate specimens for RM testing and a brief description of the testing method are also presented.

3.2 Material Sources

Richard Spur (RS) and Sawyer aggregates, which are commonly encountered in Oklahoma for the construction of pavement bases, were selected in this study. The RS aggregate (limestone) was sampled from a quarry at Richard Spur in Comanche County, and the Sawyer aggregate (sandstone) was sampled at Sawyer in Choctaw County, Oklahoma. The locations of the two quarries are shown in Figure 3-1.

The RS limestones crop out in a series of small hills appropriately called the "Limestone Hills" (Rowland 1972); these rocks belong to the Arbuckle Group of Cambrian-

Ordovician age, comprising limestones and dolomites of the Kindblade and West Spring Creek formations. This group rock has an overall homogeneity of character, consisting of thin beds of brittle, comprehensively cemented limestone and dolostone. The RS limestones can be characterized generally as interbedded mud-supported and grain-supported rocks with zones containing chert, quartz sand, and silt; hence it is a hard and durable aggregate material. Most of this stone has been used as concrete aggregate and road-base material.

The Sawyer sandstones belong to the Jackfork group and have the Wildhorse Mountain formation (Huffman et al. 1975). It presents a light - brown to light - purple color and stratifies in beds up to 30 cm. It contains mostly quartzitic sands and generally is a hard and durable aggregate material.

Figures 3-2 and 3-3 show the stock-pile and the sampling process of the RS and the Sawyer aggregates, respectively. The aggregates were transported and brought to the laboratory in 20 kg bags, and a total of 80 bags were sampled for each type of aggregate.

3.3 Material Property Tests

Figure 3-4 shows the sequence of tasks performed in terms of laboratory testing in this study. The grain size distribution, moisture-density relationship, Los Angeles abrasion, specific gravity, and Atterberg limit tests were conducted on the RS and the Sawyer aggregates, respectively, for a characterization of the aggregates in terms of their basic engineering properties (e.g. liquid limit (LL), plasticity index (PI), maximum dry density (MDD), optimum moisture content (OMC), specific gravity (SG), and index of resistance to abrasion (LA)).

3.3.1 Grain Size Distribution Test

After the aggregates were brought to the laboratory, they were dried in an oven for 24 hours at a temperature of 110 degrees. Then the grain size distribution test was performed using a mechanical sieve shaker in accordance with the AASHTO T 27-93 method (AASHTO 1993b). Table 3-1 presents the results of grain size distribution tests for the RS and the Sawyer aggregates. The gradations obtained for the field samples are compared with the gradation envelope specified by the Oklahoma Standard Specifications for Highway Construction (ODOT 1996) for Type A aggregate in Figure 3-5. The gradation envelope specified by ODOT is intended to achieve the optimum strength of an aggregate blend; permeability is not addressed in defining the gradation limits.

It is observed that the field gradations of the RS and the Sawyer aggregates are similar and all meet the gradation envelope of the ODOT 1996 specifications. In order to study the gradation effect on the material property and to ensure uniformity among the various aggregate types, three different gradations, namely, coarser limit (the lower limit of the ODOT gradation envelope), median (the median points of the ODOT envelope), and finer limit (the upper limit of the ODOT envelope), were selected in this study to investigate the effect of gradation on RM values. The grain size distributions of the three selected gradations are also presented in Table 3-1. Figure 3-6 shows the three corresponding gradation curves. In the laboratory, the aggregates sampled in the field were separated into different sizes using a mechanical shaker having a set of sieves. The ODOT median, coarser limit, and finer limit gradations were achieved by mixing the particles of different sizes based on the percentage requirement of each size particle in the three gradations.

3.3.2 Moisture - Density Test

Moisture-density tests were conducted according to the AASHTO T 180-93 method (AASHTO 1993a). The purpose of this test is to determine the maximum dry density and the corresponding optimum moisture content of the aggregates. Moreover, this test provides an insight into the variations in the densities as a result of the variations in the moisture contents.

The moisture-density tests were conducted for the RS and the Sawyer aggregates based on the three gradations selected in this study. For each gradation, five to seven modified proctor tests were conducted to obtain the moisture - density relationship. Then the optimum moisture content (OMC) and maximum dry density (MDD) were determined based on the obtained moisture-density curves. The moisture - density curves for each gradation were plotted in Figures 3-7 and 3-8 for the RS and the Sawyer aggregates, respectively. The test results in terms of OMC and MDD for each gradation of the two aggregates are presented in Table 3-2. It can be observed that the median gradation produced a higher MDD than the coarser and the finer limit gradations for both aggregates. This is because the median gradation is well graded and less void ratio was produced in the compacted sample. It was also observed that the RS aggregate has a higher MDD and a lower OMC than those of the Sawyer aggregate for all of the three gradations selected. For example, the median gradation yielded the MDD of 2.380 g/cm^3 for the RS aggregate and 2.232 g/cm^3 for the Sawyer aggregate. The OMC, however, is 4.6% and 6.0% for the RS and the Sawyer aggregates, respectively. It was also found that the finer limit gradation yielded the highest OMC among the three gradations for both aggregates; one of the possible reasons for this observation is that a larger amount of fines contained in the specimen with the finer limit gradation can absorb more water than specimens with other gradations.

3.3.3 Atterberg Limit Test

Atterberg limit tests were conducted to determine the liquid limit (LL) and the plasticity index (PI) of the RS and the Sawyer aggregates. The LL and PI tests were conducted according to the AASHTO T 89-94 and T 90-94 methods (AASHTO 1994b and 1994c), respectively. The Atterberg limit test is widely used to identify soils and to give an indication of certain properties, such as plasticity, cohesiveness, and bonding characteristics (Spangler and Handy 1973). The purpose of this test in this study is to examine the property and behavior of the fine particles contained in the two aggregates. It is believed that fine particles play a critical role in contributing to the cohesion. Three gradations, the median, the finer limit, and the coarser limit, were used to prepare the test samples based on the percent of fines passing the No. 40 (0.425 mm) sieve. The test results are presented in Table 3-2. It can be observed that the plasticity index (PI) values of the RS aggregate range from 3.6 to 4.0 which are higher than those of the Sawyer aggregate (2.6 to 3.0) in the corresponding cases. However, in general, both aggregates give low PI values which means that the fine particles contained in the two aggregates have a low plasticity.

As suggested in the ODOT Standard Specifications for Highway Construction (ODOT 1996), the aggregate base material passing the No. 40 (0.425 mm) sieve shall conform to the following:

(1) Plasticity index shall not exceed 6;

(2) Liquid limit shall not exceed 25; and

(3) The blending of separate aggregates will be permitted to produce an aggregate mixture meeting the above requirements, providing no individual aggregate has a plasticity index in excess of 8.

It can be observed that the PI and LL values of the two aggregates at the different gradations meet the ODOT requirements described above.

3.3.4 Los Angeles Abrasion Test

The Los Angeles abrasion test is a measure of degradation of mineral aggregates of standard gradation resulting from a combination of actions including abrasion or attrition, impact, and grinding in a rotating steel drum. This test is widely used as an indicator of the relative quality or competence of aggregates from various sources having similar mineral compositions. Since the rolling compaction is one of the most frequently used compaction methods in the construction of pavements, the behavior of aggregate materials against the abrasion, impact, and grinding becomes more important. The LA abrasion tests were conducted according to the AASHTO T 96-94 method (AASHTO 1994d). Four tests were conducted for each aggregate and the test results are presented in Table 3-3. The LA abrasion values of the RS aggregate range from 23.54 to 24.19 with a mean value of 24, and the values of the Sawyer aggregate range from 27.69 to 29.09 with a mean value of 28.

The limiting value of the LA abrasion for a good quality aggregate is 40 according to the ODOT specification and above which the aggregate does not qualify as an aggregate suitable for base course construction (ODOT 1996). This is due to the reason that if an aggregate has a LA value greater than 40, the aggregate is assumed to be too weak against the rolling compaction in the pavement construction process. The LA values of the RS and the Sawyer aggregates are less than 40, therefore, these two aggregates are both considered good quality aggregates. Also, the LA values indicate that the RS aggregate is more resistant to deterioration as a result of abrasion and impact than the Sawyer aggregate.

3.3.5 Specific Gravity Test

Specific gravity (SG) is an important property that is generally used in the calculation of volume occupied by an aggregate in various mixtures. Bulk specific gravity is also used in the computation of voids in an aggregate and in the determination of moisture (degree of saturation) in a given aggregate mixture. The specific gravity tests were conducted according to the AASHTO T 84-94 method (AASHTO 1994e). For each of the aggregates at the median gradation, four specific gravity tests were conducted, and the test results are presented in Table 3-3. The SG values of the RS aggregate range from 2.688 to 2.717 with a mean value of 2.7, and the values of the Sawyer aggregate range from 2.537 to 2.560 with a mean value of 2.552.

3.4 Resilient Modulus Test

3.4.1 Test Specimen Preparation

The primary factors affecting the stiffness characteristics of aggregate materials are water content, compaction method, and compaction effort. The vibration compaction method has been used successfully by Chen et al. (1994a and 1994b) and is recommended by the AASHTO T 294-94 method for aggregates (AASHTO 1994a). For granular type materials, it is desirable to use a vibratory compaction method because it can prevent the breakage of particles. The AASHTO T 294-94 suggests using the OMC and MDD for a given aggregate type in accordance with the AASHTO T 180-93 (AASHTO 1993a), then using the OMC and 95% of MDD for specimen preparation. Experimental investigation conducted by Chen (1994) indicated that the vibratory compaction method gave the density values in a range of 93 to 97% of the maximum density produced by the AASHTO T 180-93 method.

Steel split molds having 152 mm diameter (inside), 305 mm height, and 6 mm thickness were used to prepare the test specimens of the desired dimensions. The mold was fitted with a hose connected to the vacuum pump so that the vacuum could be applied to the space between the membrane and the inner surface of the mold. The vacuum helps to fit the membrane tightly against the inner surface of the mold during specimen compaction. A vibrating table was used for compacting the specimen.

Figure 3-9 shows the split mold and the vibrating table used. The vibrating table consists of 760 mm x 760 mm square and 6 mm thick steel plate resting on four 38 mm x 38 mm x 6 mm steel angle legs. The split mold mounted with membrane was bolted tightly on top of the vibrating table. The membrane was fitted tightly against the mold with the help of the vacuum provided by the vacuum pump. The aggregates were mixed at optimum moisture content and compacted in ten equal layers in the molds. The vibration of the table was controlled by a controller with a maximum speed of 3600 vibrations per minute. For each of the first 8 layers, 30 seconds vibration was applied and for the last 2 layers, 4 minutes vibration was applied in order to obtain a uniform compaction along the length of the specimens. A steel tamping rod was used to tamp the aggregate during compaction along with the vibration to aid in the compaction. The densities of the compacted specimens were found to be above 98% of the maximum dry density obtained from the AASHTO T 180-93 test method which indicates that satisfactory compaction was attained.

The procedure described above was used for preparing RM test specimens of the two aggregates. In this study, generally, a total of six replicate specimens were prepared for the following study cases.

(1). **Effect of Testing Procedure**: test specimens were prepared based on the ODOT median gradation and the corresponding OMC for the RS aggregate.

(2). **Effect of Gradation**: three gradations, namely, the median, the coarser, and the finer limits of the ODOT specified gradation range, were used to prepare the RM test specimens for the two aggregates. The corresponding optimum moisture content (OMC) for each gradation (Table 3-2) was used to mix the aggregate.

(3). **Effect of Moisture Content**: the ODOT specified median gradation was adopted for test specimen preparation in this case. The moisture contents, however, were selected as OMC, 2% above, and 2% below the OMC for the RS and the Sawyer aggregates, respectively.

(4). **Effect of Drainage**: The ODOT median gradation and the corresponding OMC were selected for specimen preparation. By using other material properties measured (e.g., moisture content, dry density, and specific gravity) in this study, the initial degree of saturation was calculated. The OMC for the RS aggregate is 4.6% which is equivalent to 83% of the degree of saturation. However, for the Sawyer aggregate, the degree of saturation of 78% was attained at the OMC of 6.0%, and therefore it was decided to soak the specimens in order to increase the degree of saturation. By soaking the specimens prepared at the OMC in a water tank for one week, the degree of saturation increased to about 91%. It is expected that specimens prepared using this approach can simulate the pavement wetness duration in a reasonable manner because even after a pavement experiences an extended rainfall and the drainage of the pavement does not function properly, the pavement itself still has the same structure as represented by the specimen prepared at the OMC and only the moisture content of the pavement sub-layers is increased.

Two hours after preparation, the specimens were brought to the loading frame with minimum disturbance and were extracted from the split molds at the loading plate. Then, a new membrane was mounted on the specimen to ensure proper sealing. The new membrane was needed because the membrane used during compaction was usually found to be punctured and hence, was unable to hold the specimen tightly sealed. Figure 3-10 shows a photographic view of specimen preparation steps involving vibration of the mold and compaction of the specimen in layers.

3.4.2 Resilient Modulus Testing Equipment

The RM testing equipment setup consists of: (a) a loading device controlled by an MTS repeated load actuator, (b) a load frame, (c) a triaxial chamber, (d) a chamber pressure gauge, (e) a chamber pressure regulator, (f) an MTS 458.20 Microconsole and Microprofiler, (g) a personal computer for data acquisition, (h) a load cell , (i) two LVDTs, and (j) a numerical gauge to measure pore pressure. The overall setup of the RM testing equipment is shown in Figure 3-11.

The specimen was mounted in the triaxial chamber between the bottom and the top platens. Porous stones were placed at both the bottom and the top ends of the specimen between the platens and the specimen. The load cell, which is connected to the deviator rod, was placed on top of the specimen above the top platen. The triaxial cell was then secured tightly with the help of bolts and the two LVDTs were clamped onto the deviator rod as shown in Figure 3-12.

After the triaxial chamber was assembled with the specimen and air tightness of the chamber was ensured, the air supply hose was connected to the chamber. The chamber was then subjected to the desired confining pressure with the help of the chamber pressure regulator. Air was used as the confining medium (cell fluid) instead of water because the load cell was located inside the triaxial chamber and air pressure is easy to operate and available in most laboratories. The air pressure inside the chamber was precisely controlled by the chamber pressure regulator and an air pressure gauge which was installed on the triaxial cell to measure the confining pressure. The main advantage of this system is that the load cell is housed within the triaxial cell to allow in-vessel load measurement and to overcome the detrimental effects of friction caused by the push rod. The quality of test results is generally improved by monitoring the in-vessel load and confining pressures (Chen 1994).

After the specimen was subjected to the desired confining pressure, the RM test was started with the help of the MTS testing system (Figure 3-11). The MTS Microconsole and Microprofiler provide an excellent facility to apply various types of cyclic loading in an efficient and accurate manner. The Microprofiler (a digital function generator) was programmed to conduct a test under the desired load intensity, load frequency, and the number of loading cycles on the specimen. The Microconsole was used to operate the MTS repeated load actuator. The RM test was conducted under the stress control mode. With the start of the test, the MTS repeated load actuator came in contact with the push rod and applied the required loading intensity for the required number of loading cycles on the specimen. A 270-kg load cell mounted inside the triaxial chamber and attached to the loading piston was used to monitor the applied deviator load. Two external LVDTs were mounted on the top of the triaxial chamber to measure the deformation of the specimen.

A Gateway 2000, 486 DX2 personal computer with a 50 MHZ microprocessor was mounted with a data acquisition board DT 2801 (Data Translation, Inc.) for use in the acquisition of test data (Figure 3-11). The load cell and the LVDTs were connected to the computer for acquiring the stress-strain data. Thus, the test data were electronically collected and stored by the computer during the test. The AASHTO T 294-94 testing procedure requires the specimen to be subjected to a haversine waveform having a 0.1 second loading period followed by a 0.9 second relaxation period. This requirement calls for a data acquisition system that can acquire and store a sufficient number of data points during the one second loading cycle. The data acquisition system used in this test can collect more than 200 data points per second; this rate is suitable for executing the T 294-94 testing method. Figure 3-13 shows the flow diagram of the test equipment setup for RM testing.

After the RM test, the air pressure inside the chamber was released with the help of the chamber pressure release valve and the chamber pressure regulator (Figure 3-12). Then, the specimen was used for the unconfined compressive strength or the static triaxial compression test.

3.4.3 Testing Procedure

Except for studying the effect of testing procedure on RM, the AASHTO standard RM testing method, AASHTO T 294-94 (AASHTO 1994a), was used to conduct the RM tests in this study. The deviator stress, confining pressure, load sequence, and the number of loading cycles specified by this method are presented in Table 2-1. Figure 3-14 shows the haversine - shaped stress pulse with a loading duration of 0.1 second, a rest period of 0.9 second, and a total cycle duration of 1 second, as suggested by the AASHTO T 294-94 method. The rectangular and triangular stress pulses suggested by the AASHTO T 292-91I method are also presented for the purpose of comparison in Figure 3-14.

The drainage lines were kept open for most of the RM tests, except for studying the effect of drainage conditions on the RM values. For the undrained RM tests, two undrained testing methods were used in order to approximately simulate two possible situations in the field. In the first method (undrained I), the pore pressure is allowed to dissipate at the end of each deviator stress application; this method enables the measurement of the amount of pore pressure increase for each deviator stress cycle. In terms of field situation, it assumes that the traffic is halted over a period of time, so that the pore pressure can dissipate before another cycle of traffic transverses the pavement. In the second method (undrained II), the pore pressure is allowed to build up during the entire testing period and the accumulated pore pressure is measured. In terms of real application, this can simulate a continuous traffic situation.

3.5 Unconfined Compressive Strength Test

As mentioned earlier, following the cyclic triaxial testing, unconfined compressive strength (UC) tests or conventional triaxial compression (CTC) tests were performed. The six replicate RM specimens were separated into two groups. Specimens in one group were used for the UC tests to obtain the unconfined compressive strength (U_C), and specimens in the other group were used for the CTC tests to obtain the cohesion (C), and the friction angle (ϕ). The cyclic triaxial test served as "conditioning" of the sample for triaxial compression tests that could be imposed by moving vehicles. Thompson and Smith (1990) reported that the rapid shear strength of an unconditioned specimen does not represent the strength of an in service compacted aggregate base material subjected to traffic loading. Strength increases from 34 to 217% by the conditioning were found in their tests. Chen (1994) also examined the strength increase through conditioning induced by the cyclic stress repetitions for two aggregate types. The strength increase through "conditioning" was found to vary from 18 to 85%, depending upon the confining pressure and aggregate type.

The UC tests were conducted under the strain control mode in accordance with the AASHTO T 208-92 method (AASHTO 1992b). The MTS load frame and the MTS loading device were used for loading the specimen. The MTS Microconsole and the Microprofiler were used to control the strain intensity, the rate of the load application, and to operate the MTS loading devices. The test data was acquired and stored by the computer as in the case of RM testing. Figure 3-15 shows a typical stress-strain plot of the results obtained from the UC test. The maximum value of the stress represents the unconfined compressive strength U_C value of the specimen tested.

The UC tests were conducted for all of the RM testing cases, and the unconfined compressive strength (U_C) values for these cases are presented in Table 3-4.

3.6 Triaxial Compression Test

The CTC tests were conducted according to the AASHTO T 297-94 method (AASHTO 1994f), with the exception that the drainage was open during the test and the material was aggregate instead of cohesive soils. The CTC test was conducted under the strain control mode. The triaxial chamber was assembled similar to the RM test and the loading device was the same as the UC test. Generally, 34, 69, and 104 kPa confining pressures were applied on three replicate specimens and the specimens were sheared until failure. Mohr's circles were drawn based on the CTC test results and the shear strength parameters of cohesion (intercept) and friction angle (slope) were obtained. Figure 3-16 shows the typical Mohr circles from which the cohesion (C) and the friction angle (ϕ) were determined.

The CTC tests were conducted for all of the RM testing cases, and the values of cohesion (C) and the friction angle (ϕ) for all of the cases are presented in Table 3-4.

It has been mentioned early that all the UC and CTC tests were conducted after the RM testing. The RM testing can be thought of as "conditioning" of the sample for triaxial compression test. In order to examine the effect of the conditioning on the material strength properties (e.g., U_C, C, and ϕ), the UC and CTC tests were conducted on the "raw" Sawyer aggregate specimens which were not subjected the RM testing. The raw specimens were prepared at the median gradation and the corresponding OMC (6.0%), and the obtained material strength properties U_C, C, and ϕ for the raw specimens are presented in Table 3-4. It can be observed that the U_C increases from 262.2 to 416.7 kPa and the ϕ increases from 50.8° to 55.4° due to the conditioning stage, where the cohesion C remains constant. The corresponding increases for U_C is 59%. This is consistent with the observation made by other researchers (Thompson and Smith 1990; Chen 1994). The reason probably is that the conditioning stage has a stiffening effect on the specimen and the specimen becomes stronger after the RM testing.

Table 3-1 Particle Size Distribution of the RS and the Sawyer Aggregates as Sampled from the Quarries and the ODOT Specified Gradation Limits

U.S. Standard Sieve Size or No.	Sieve Opening (mm)	ODOT Specified Gradation Limits for Type A Aggregate (%) Passing			As Sampled Gradation (%) Passing	
		Coarser	Finer	Median	RS	Sawyer
1-1/2 in.	38.1	100	100	100	100	100
1-1/4 in.	31.75				98.1	95.0
1.0 in.	25.4				91.2	84.0
0.75 in.	19.0	40	100	70	79.5	70.0
0.5 in.	12.7				63.8	54.8
0.375 in.	9.5	30	75	52.5	59.3	47.8
4	4.75	25	60	42.5	48.6	34.5
40	0.425	8	26	17	14.8	20.3
200	0.075	4	12	8	5.6	4.8

Table 3-2 The Atterberg Limits, Optimum Moisture Content (OMC) and Maximum Dry Density (MDD) of the RS and the Sawyer Aggregates

Material	Gradation	LL (%)	PI	MDD (g/cm^3)	OMC (%)
RS	Median	13.0	3.6	2.380	4.6
	Finer Limit	13.6	4.0	2.331	5.3
	Coarser Limit	14.0	4.0	2.278	5.5
Sawyer	Median	18	2.6	2.232	6.0
	Finer Limit	19	3.0	2.190	6.3
	Coarser Limit	19	3.0	2.193	5.0

Table 3-3 Specific Gravity (SG) and Los Angeles Abrasion (LA) Values of the RS and the Sawyer Aggregates

	RS Aggregate		Sawyer Aggregate	
Test No.	SG	LA (%)	SG	LA (%)
Test 1	2.688	23.98	2.550	28.09
Test 2	2.717	23.54	2.537	28.09
Test 3	2.703	24.08	2.559	29.09
Test 4	2.688	24.19	2.560	27.69
Average	2.700	24.00	2.552	28.00

Table 3-4 Average Unconfined Compressive Strength (U_c), Cohesion (C), and Friction Angle (ϕ) Measured for the Two Aggregates

	RS			Sawyer		
	U_c (kPa)	C (kPa)	ϕ °	U_c (kPa)	C (kPa)	ϕ °
T 292-91I	347.9	68.9	58.2			
T 294-94	299.0	120.6	50.1	416.7	68.9	55.4
Coarser Limit	120.6	83.4	52.9	177.9	34.5	58.4
Finer Limit	295.6	134.4	46.9	283.6	75.8	51.2
2% below OMC	226.7	82.7	46.7	255.8	65.5	53.7
2% above OMC	150.9	44.8	55.5	214.0	51.7	56.8
Undrained I	267.6	62.0	55.0	257.1	48.2	57.5
Undrained II	316.6	68.9	54.7	302.8	55.1	56.9
Raw Sample				262.2	68.9	50.8

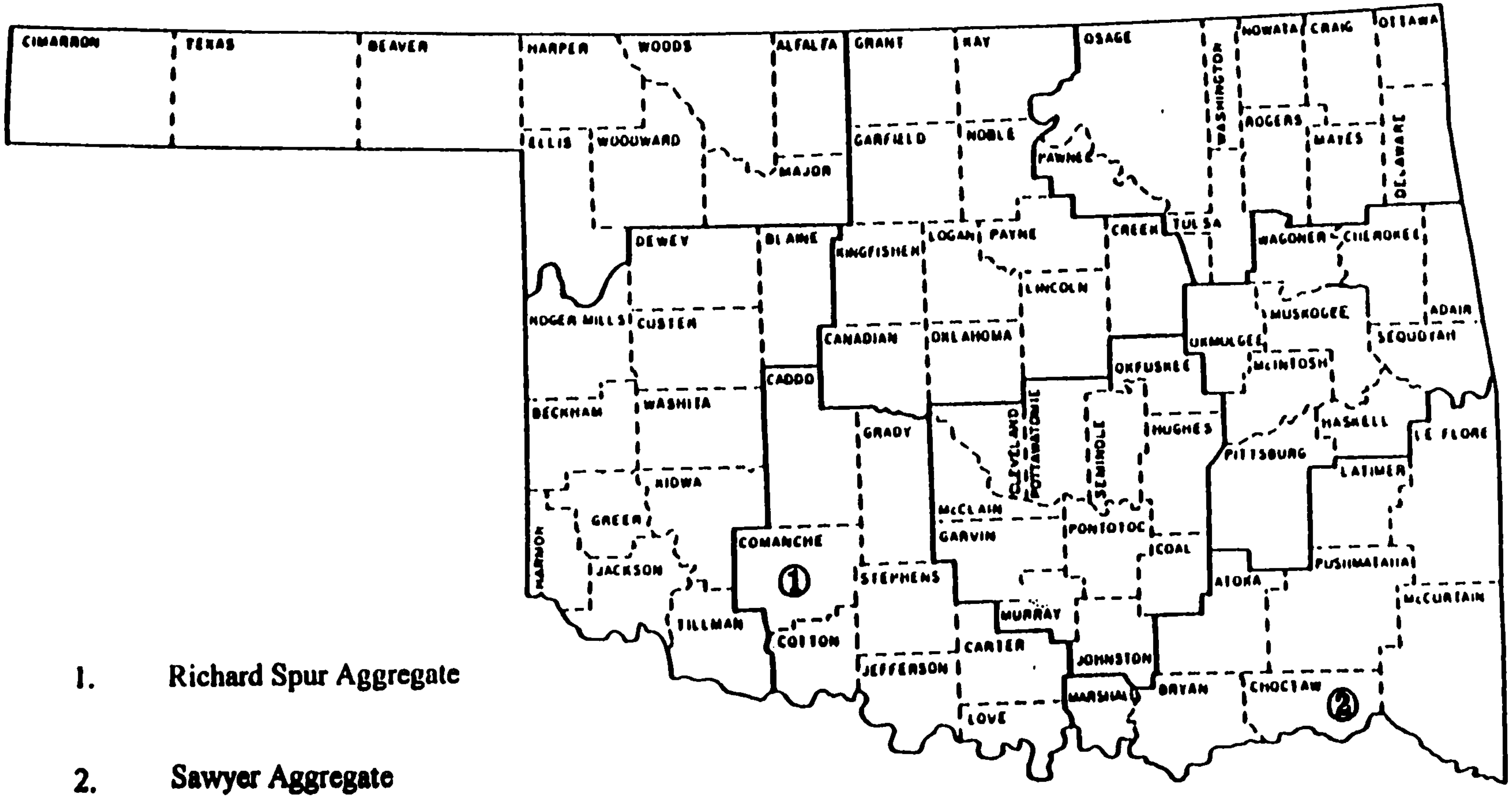

1. Richard Spur Aggregate

2. Sawyer Aggregate

THE STATE OF OKLAHOMA

Figure 3-1 Location Map Showing the Material Source Sites.

Figure 3-2 (a) Richard Spur Aggregate Quarry Site - Aggregate Stockpile

Figure 3-2 (b) Close up View of the Sampled RS Aggregate

Figure 3-3 (a) Sawyer Aggregate Quarry Site - Aggregate Stockpile

Figure 3-3 (b) Sawyer Aggregate Quarry Site - Sampling in Progress

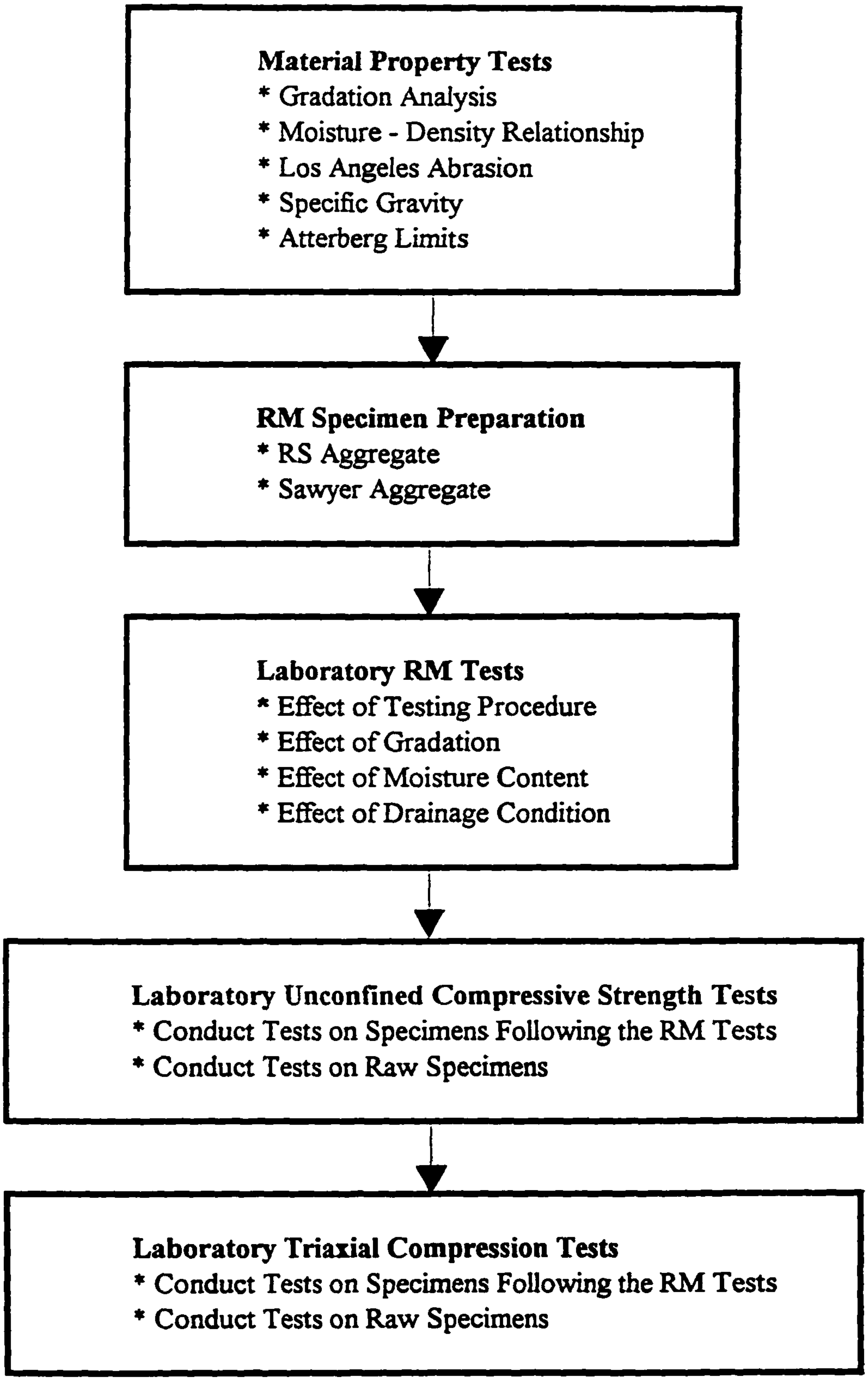

Figure 3-4 Flow Chart for the Sequence of Activities Involved in the Laboratory Testing

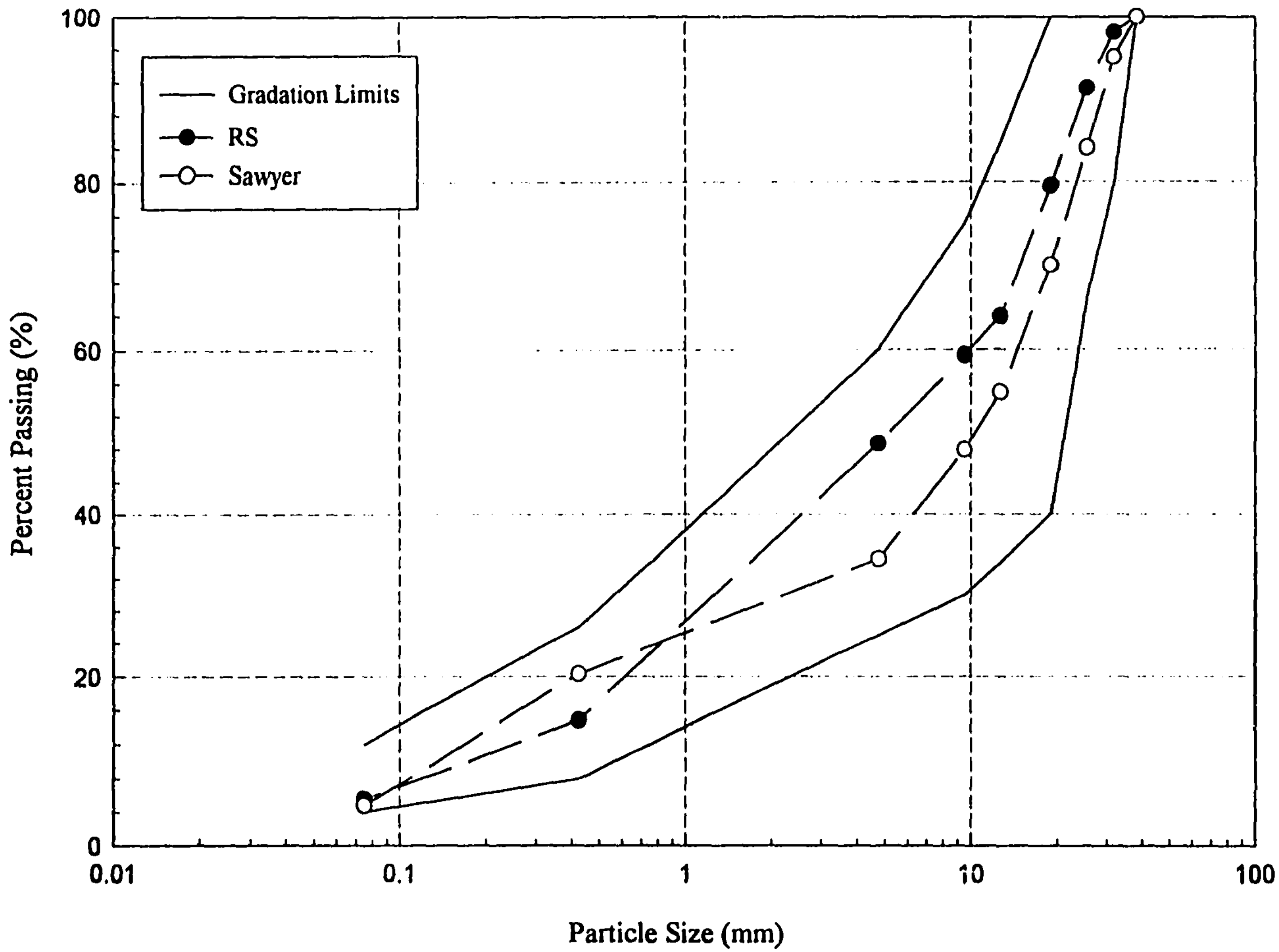

Figure 3-5 Grain Size Distribution of the RS and the Sawyer Aggregates

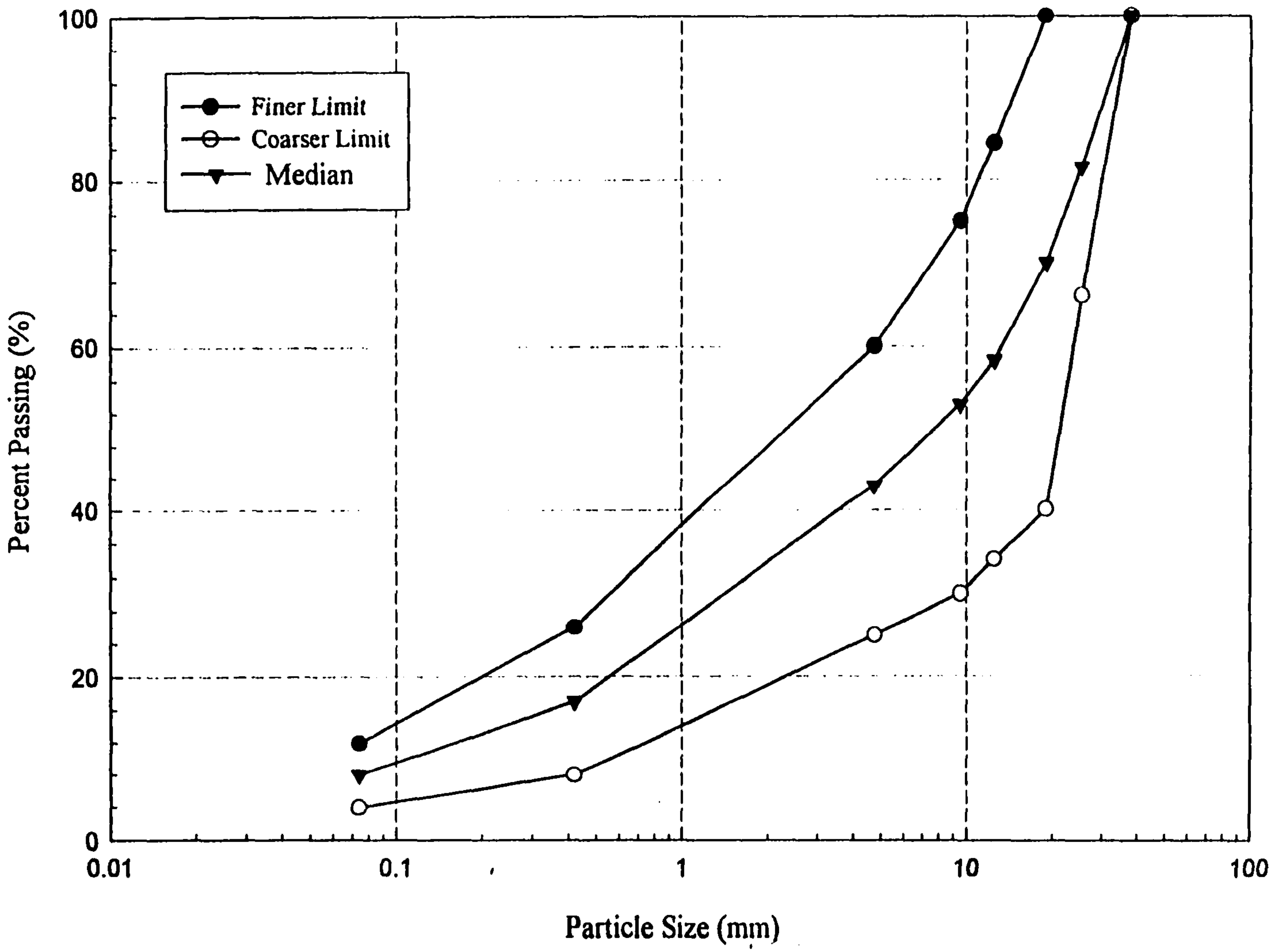

Figure 3-6 The ODOT Median, Finer Limit, and Coarser Limit Gradations Used in This Study

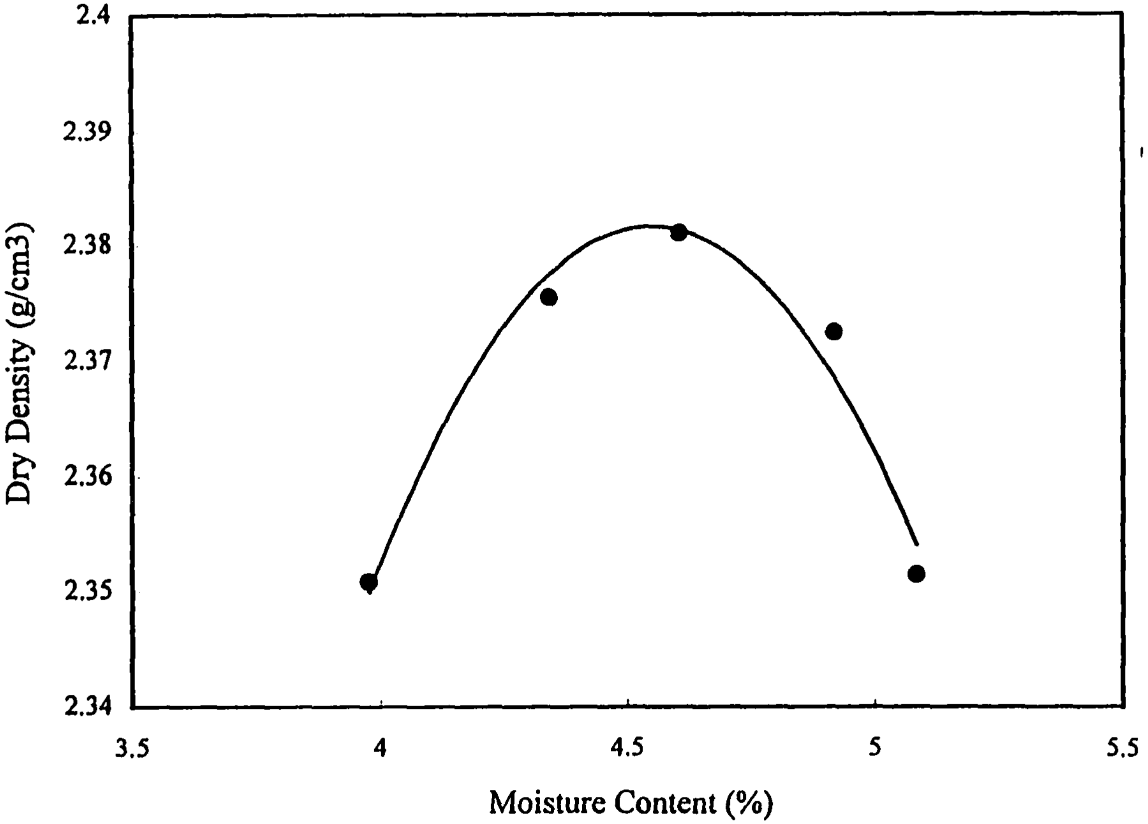

Figure 3-7 (a) Moisture - Density Curve of the RS Aggregate at the Median Gradation

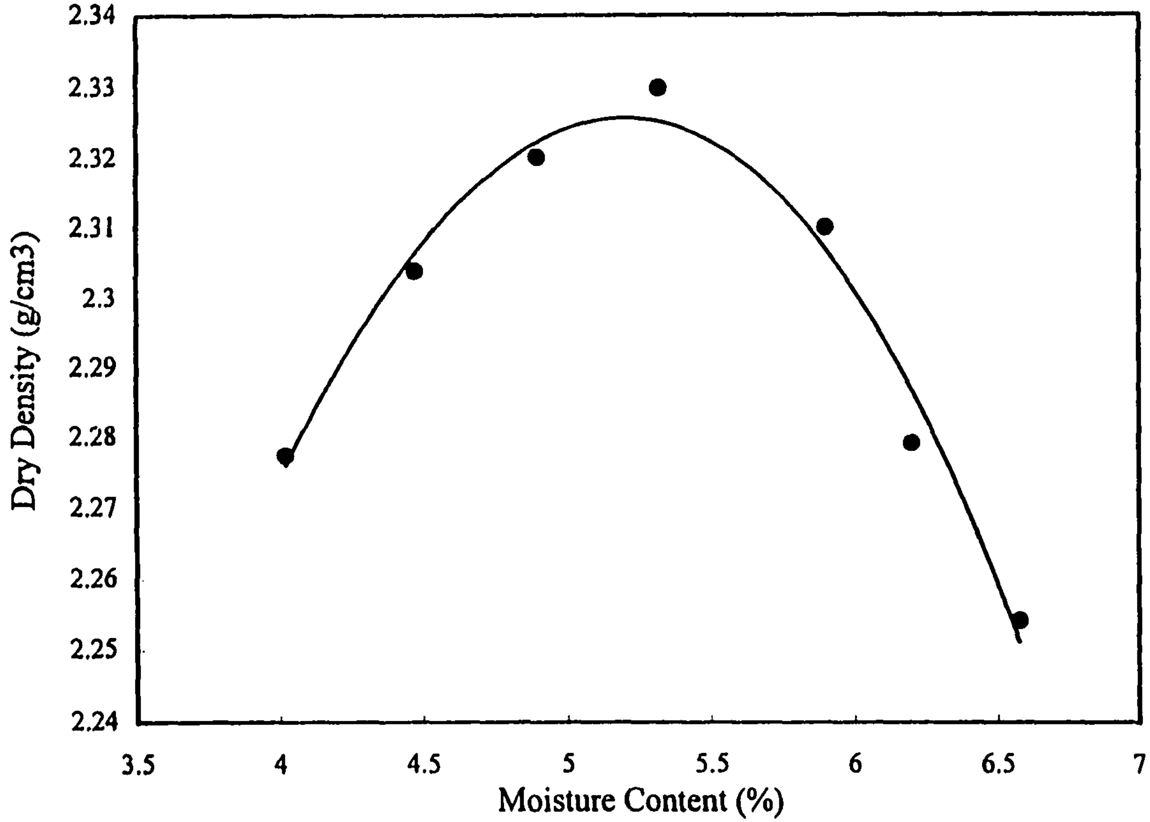

Figure 3-7 (b) Moisture - Density Curve of the RS Aggregate at the Finer Limit Gradation

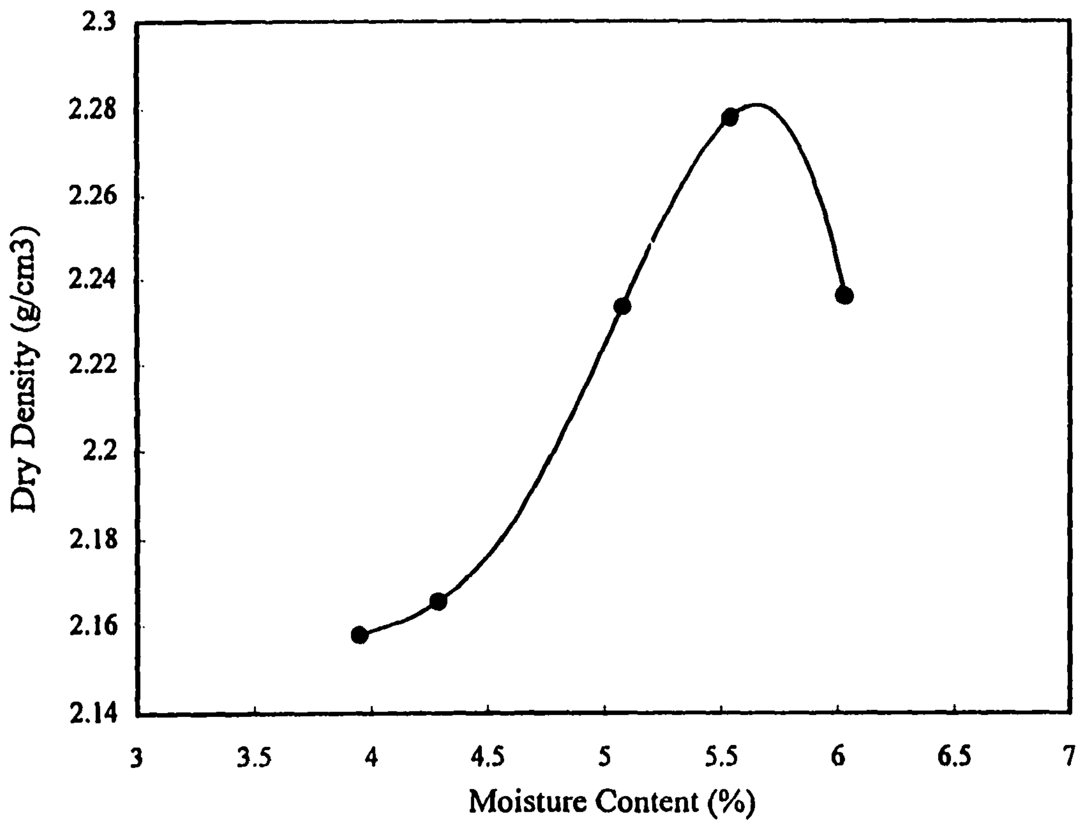

Figure 3-7 (c) Moisture - Density Curve of the RS Aggregate at the Coarser Limit Gradation

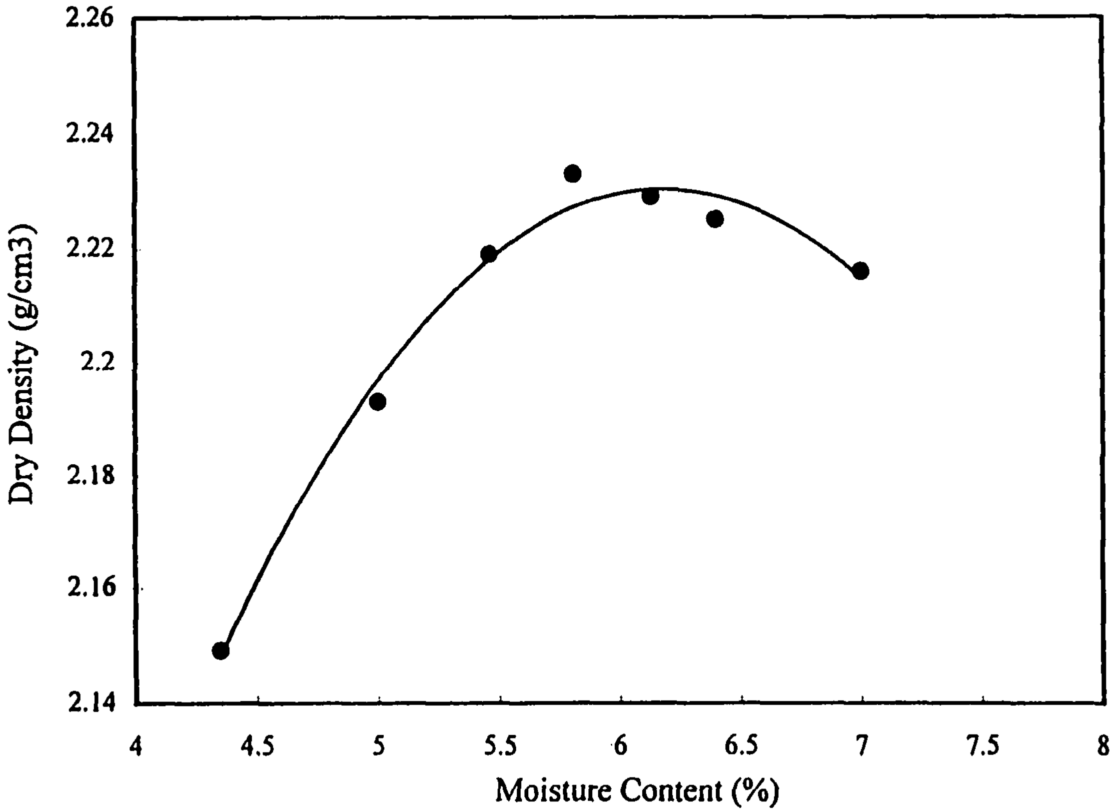

Figure 3-8 (a) Moisture - Density Curve of the Sawyer Aggregate at the Median Gradation

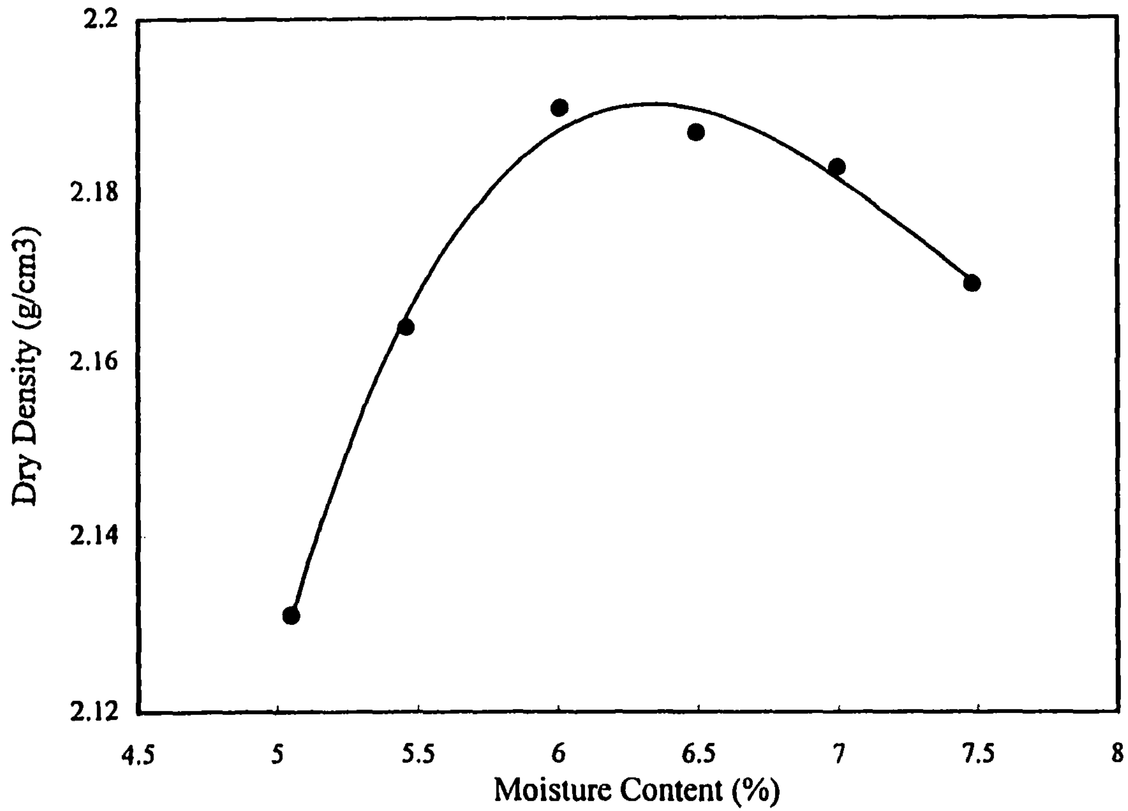

Figure 3-8 (b) Moisture - Density Curve of the Sawyer Aggregate at the Finer Limit Gradation

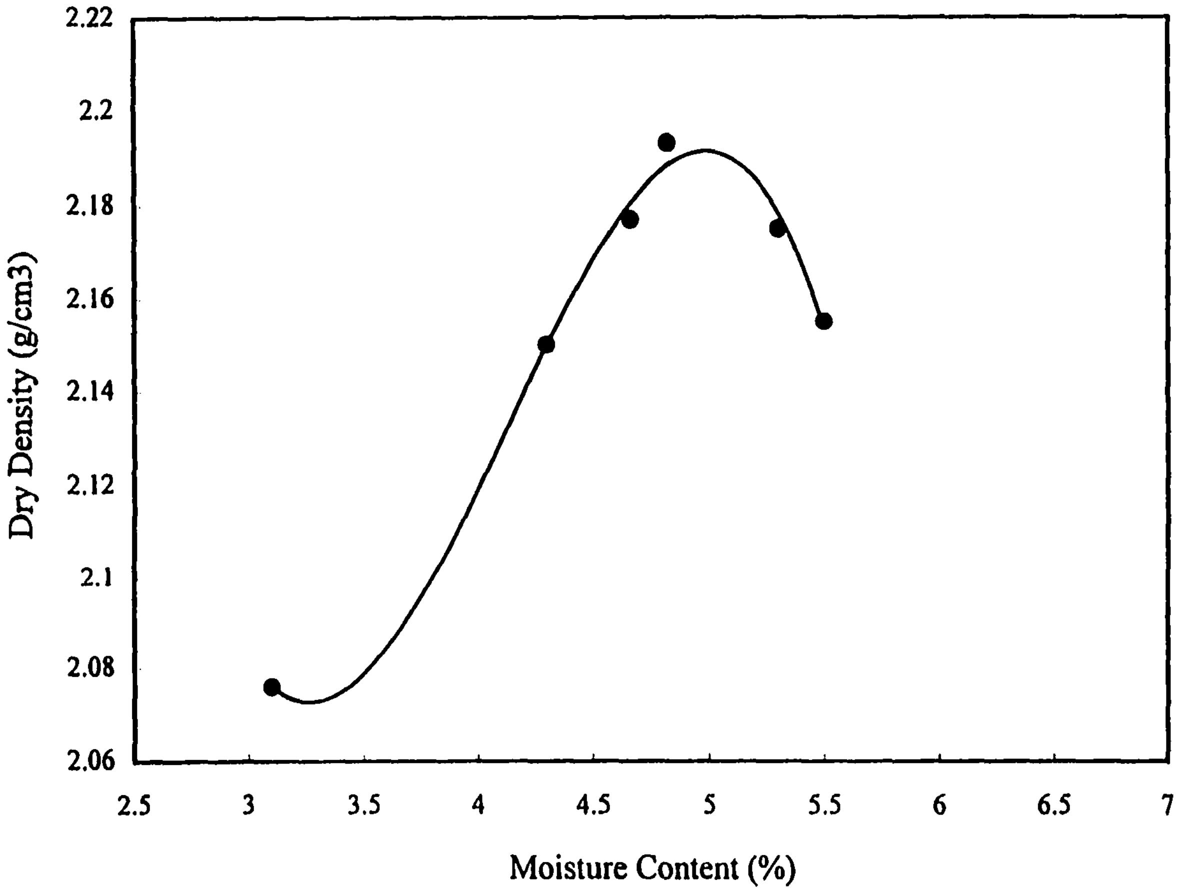

Figure 3-8 (c) Moisture - Density Curve of the Sawyer Aggregate at the Coarser Limit Gradation

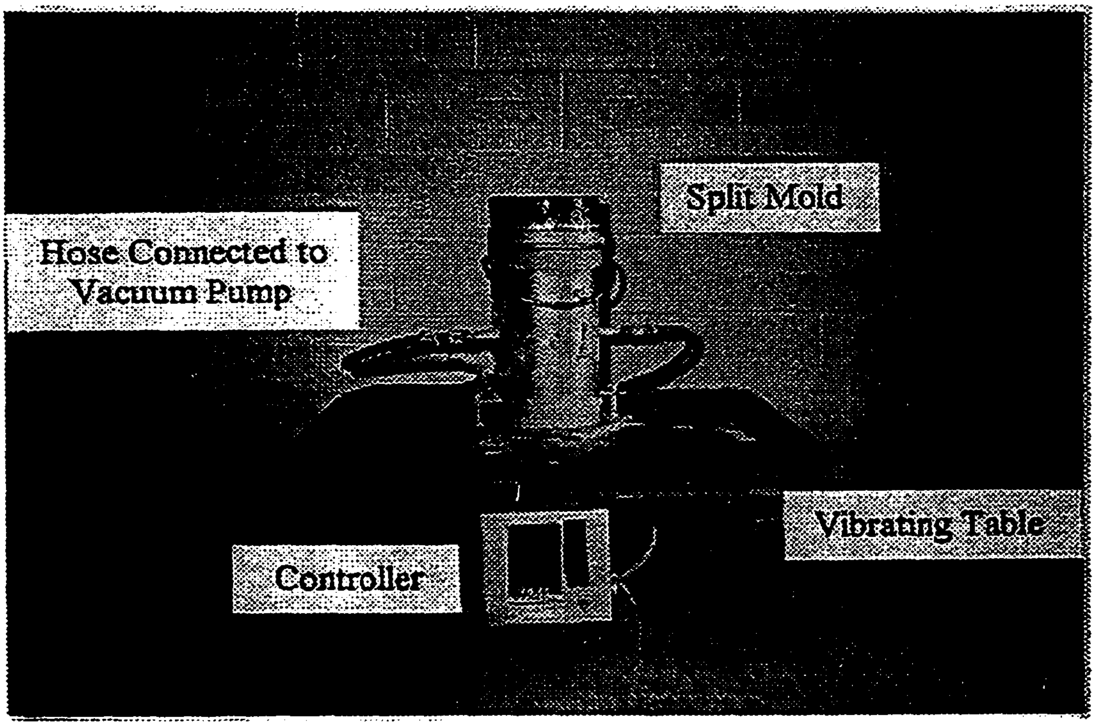

Figure 3-9 Apparatus for the RM Specimen Preparation

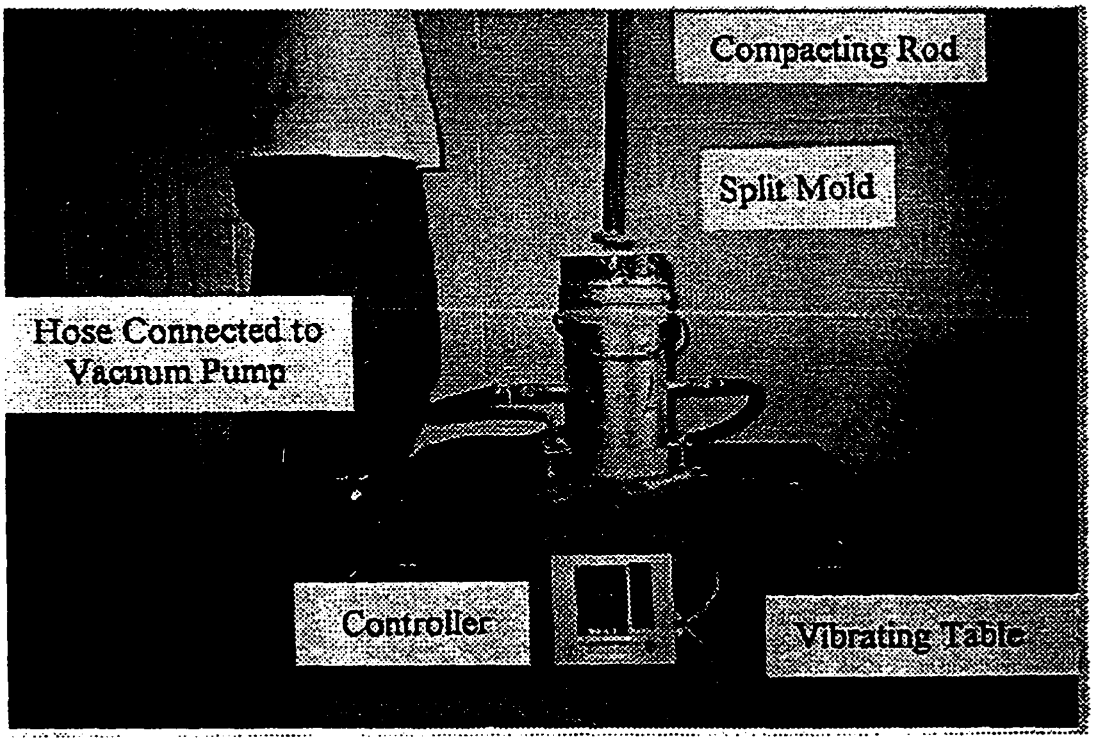

Figure 3-10 Photograph View of Specimen Preparation Process

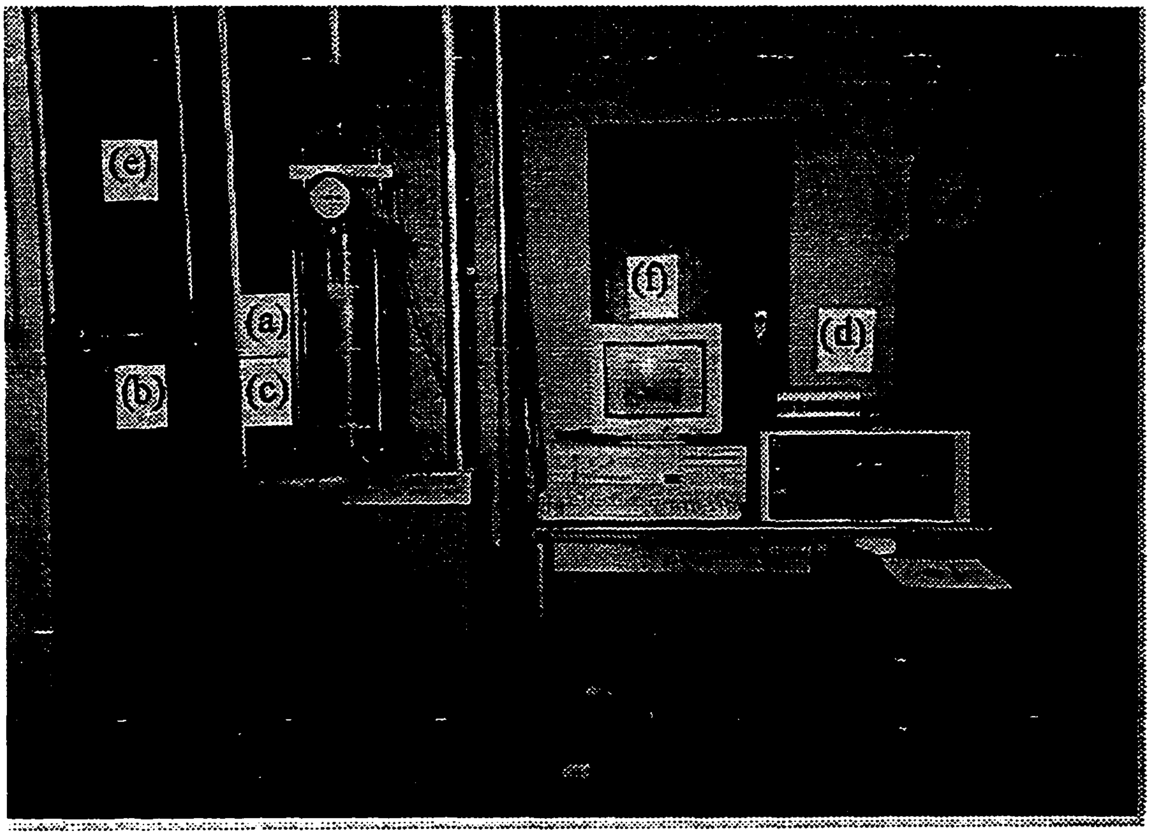

(a)	Triaxial Chamber	(b)	Chamber Pressure Regulator
(c)	Test Specimen	(d)	MTS Microconsole and Microprofile
(e)	MTS Load Frame	(f)	Personal Computer

Figure 3-11 Over Setup of the RM Testing Equipment

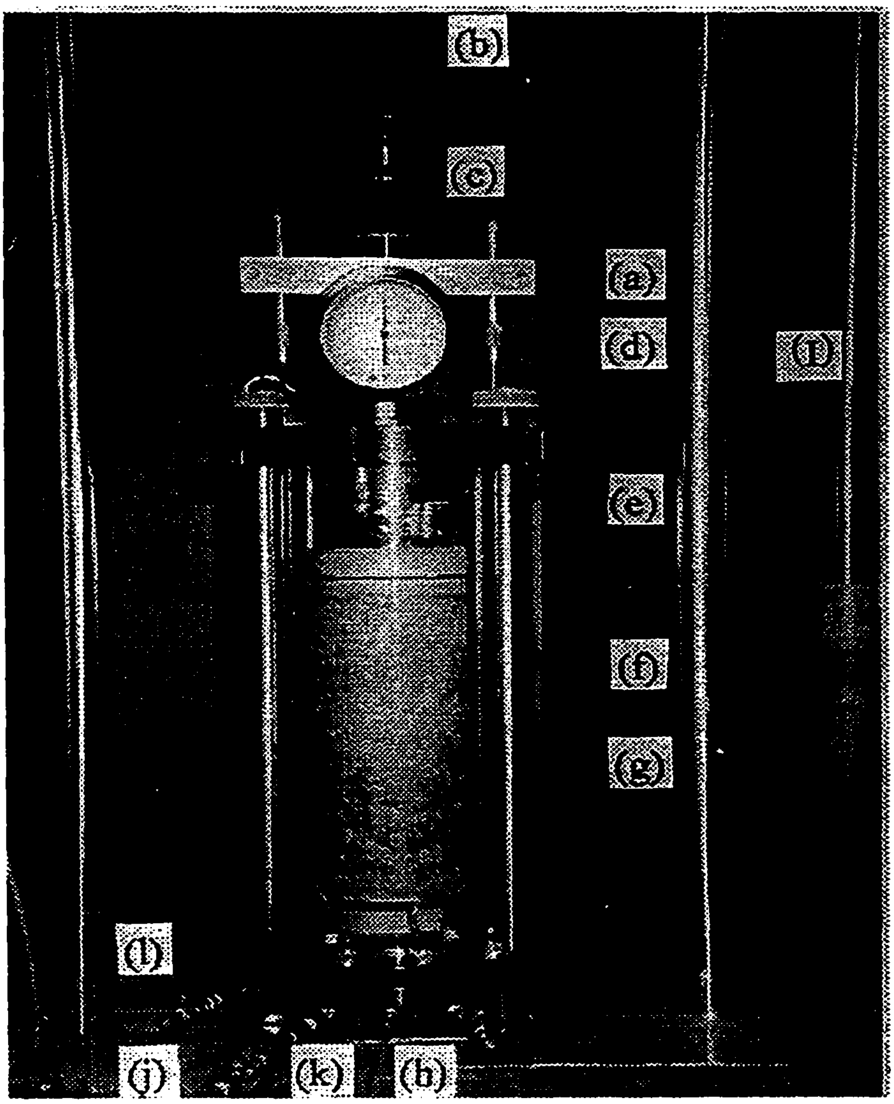

(a)	LVDTs	(b)	MTS Repeated Load Actuator
(c)	Deviator Rod	(d)	Chamber Pressure Gauge
(e)	Load Cell	(f)	Triaxial Chamber
(g)	Test Specimen	(h)	Chamber Pressure Hose
(i)	MTS Load Frame	(j)	Chamber Pressure Release Valve
(k)	Drainage Valve	(l)	Pore Pressure Gauge

Figure 3-12 Triaxial Cell for Resilient Modulus Test

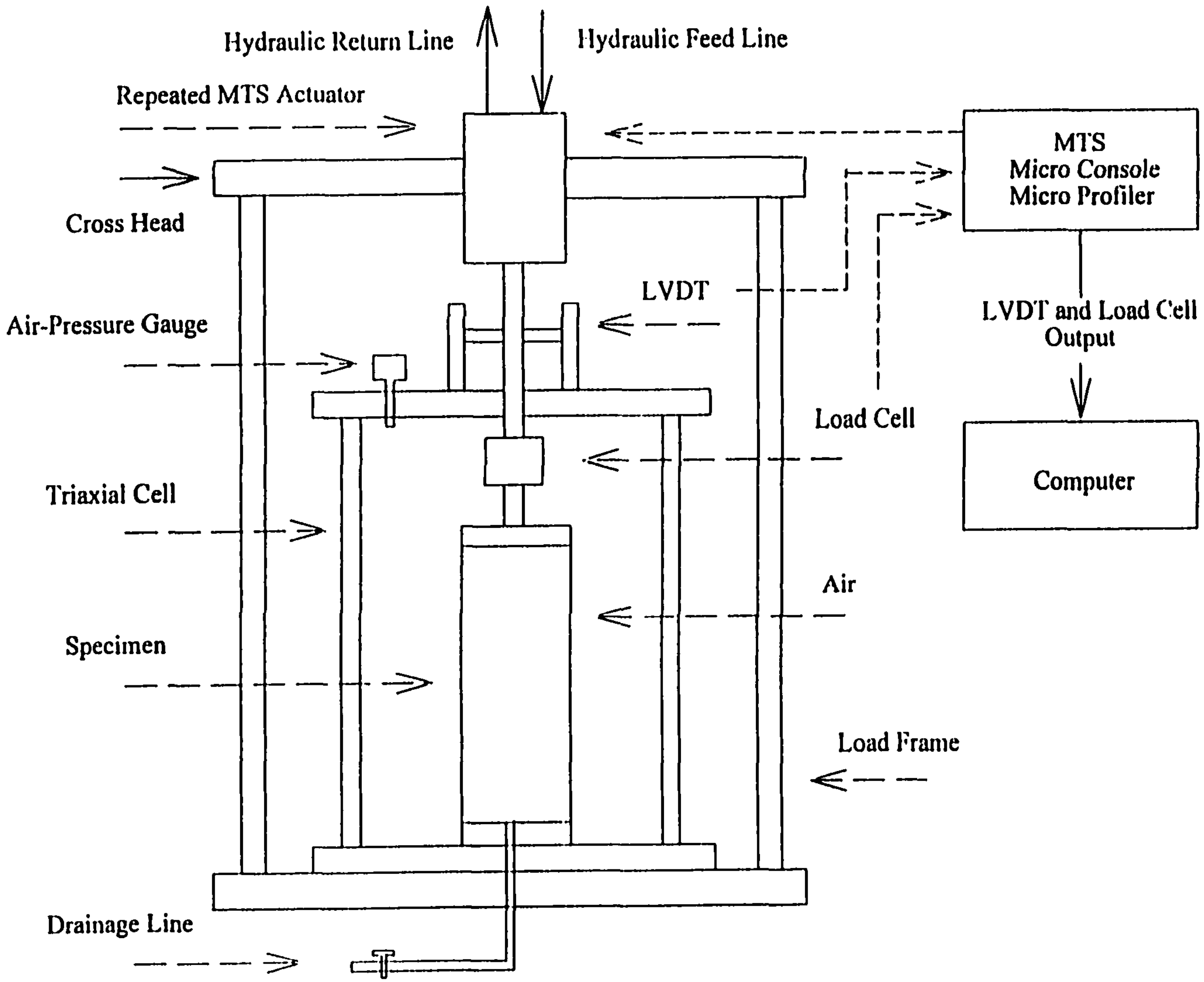

Figure 3-13 Flow Diagram of the Test Equipment Setup for RM Testing

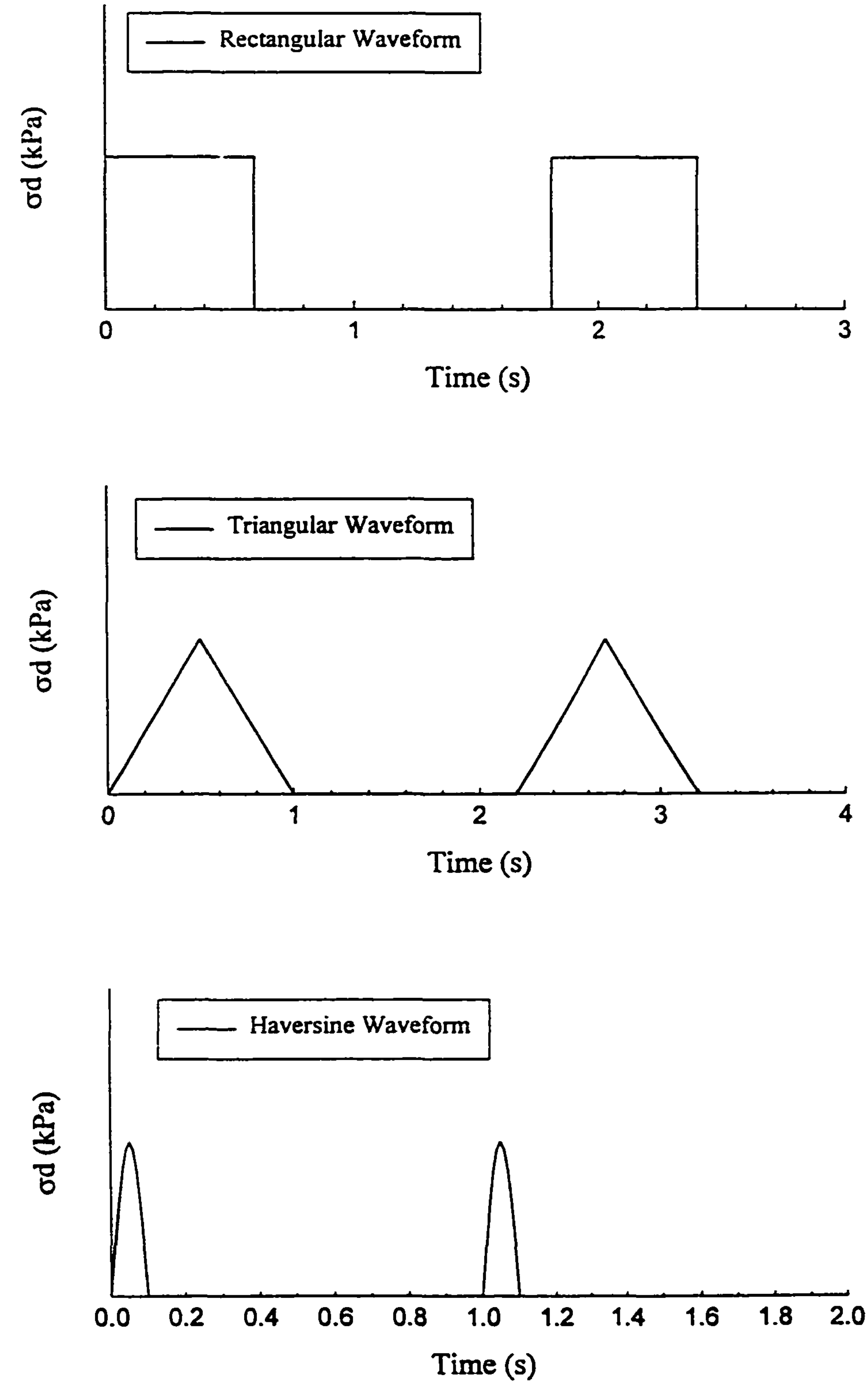

Figure 3-14 Haversine, Triangular, and Rectangular Waveforms Used in This Study

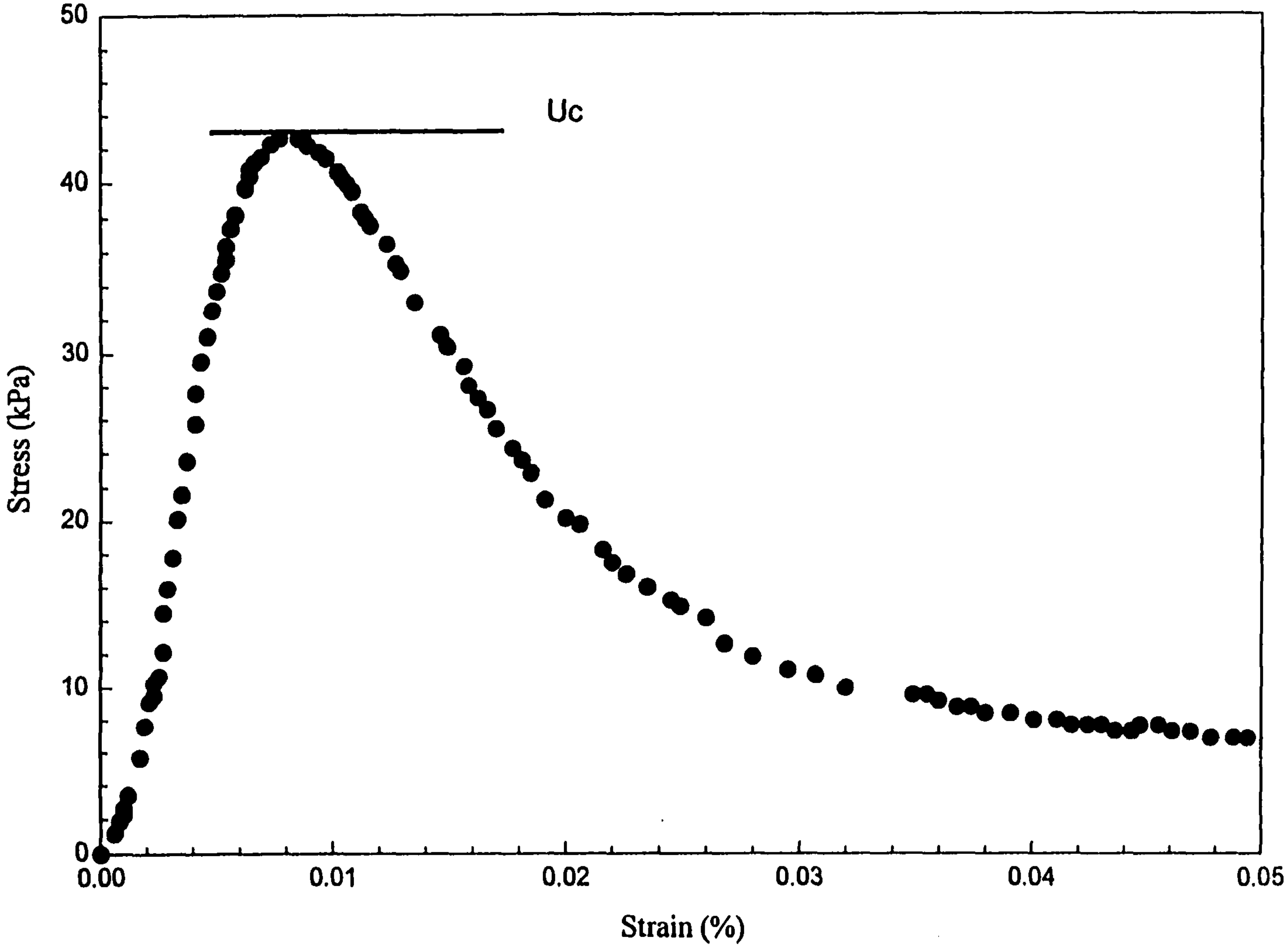

Figure 3-15 Typical Stress - Strain Diagram for the Determination of Unconfined Compressive Strength

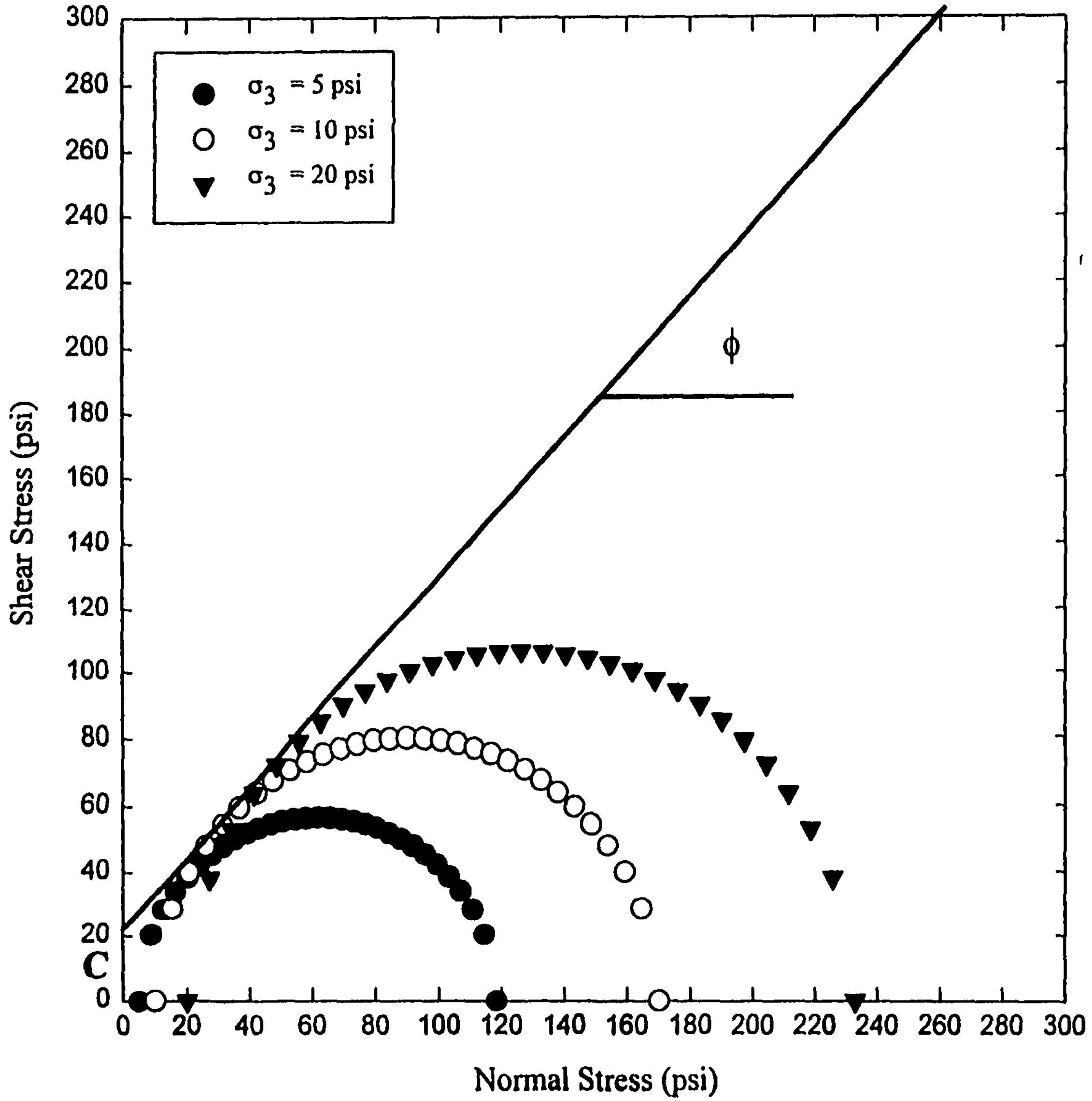

Figure 3-16 Typical Mohr Circle Diagram for the Determination of Cohesion and Friction Angle

CHAPTER 4

PRESENTATION AND DISCUSSION OF RESULTS

4.1 Introduction

The resilient moduli for the RS and the Sawyer aggregates obtained from the laboratory testing are presented in this chapter. The influence of testing procedure, gradation, moisture content, drainage condition, and aggregate type on the RM values is discussed. Discussion between the various U_C, C, and ϕ values is also conducted with respect to the effects of testing procedure, gradation, and moisture content. Finally, the error and variability of the experimental results and their significance are analyzed.

4.2 Influence of Testing Procedure

Historically, AASHTO has proposed several testing methods for the determination of RM in the laboratory, namely, AASHTO T 274-82, T 292-91I, T 294-92I, and T 294-94. The basic differences among these methods are presented in Tables 2-1 and 2-2.

The AASHTO T 292-91I, T 294-92 I, and T 294-94 procedures were intended to overcome the deficiencies in procedure T 274-82 (Pezo et al. 1992). Since the T 294-92I and the T 294-94 are essentially the same except for the unit used, the testing procedures T 292-91I and T 294-94 were used in this study to investigate the effect of testing procedures on RM values.

Two sets of RM tests were conducted for the RS aggregate at the median gradation and the corresponding OMC using the AASHTO T 292-91I and the T 294-94 procedures, respectively. The mean RM values were calculated from the six individual test results and are presented in Table 4-1. The RM values obtained from each of the six replicate tests are presented in Tables A-1 and A-2 in Appendix A, and their graphical representations are presented in Figures A-1 and A-2 in Appendix A. Following the RM tests, the material properties including cohesion (C), friction angle (ϕ), and unconfined compressive strength (U_C) were evaluated and the results are presented in Table 3-4. Based on the obtained test results in this study, the influences of the T 292-91I and the T 294-94 methods on the RM values are discussed in terms of sample conditioning, number of loading cycles, and applied loading waveform. Finally, The combined effect of the testing methods T 292-91I and T 294-94 on the RM values was evaluated based on the RM test results.

4.2.1 Sample Conditioning

In order to minimize the effects of initially imperfect contact between the end platens and the test specimen, the sample conditioning stage is applied before RM testing in both testing procedures. This stage can also be viewed as a way to simulate the real situation of the pavement base in service. The sample conditioning stages for the T 292-91I and T 294-94 differ only in the magnitude of the confining pressure σ_C applied. In the T 292-91I method, the σ_C is 138 kPa, and in the T 294-94 method, the σ_C is 103 kPa. However, the same magnitude of cyclic loading (σ_d = 103 kPa) and the same number of loading cycles (1000) are used in both testing methods. Due to the little difference in sample conditioning stage between the two testing methods, it is expected that this difference cannot have any significant effect on the RM test results.

4.2.2 Number of Loading Cycles

To determine the number of loading cycles necessary to reach a stable permanent deformation, the T 292-91I method suggests comparing the recoverable axial deformation at the twentieth and the fiftieth cycles. If the difference is greater than 5%, an additional 50 cycles are necessary at that stress state. On the other hand, the T 294-94 method suggests comparing the recoverable axial deformation at the seventieth and the hundredth cycles to check if the difference is less than 5%. However, both testing methods require to report the mean RM value from the last five cycles. It has been reported by Khedr (1985) that the response of granular materials is fairly steady and stable after approximately 100 cycles of constant cyclic loading because the rate of permanent strain accumulation decreases logarithmically with the number of load cycles. The number of loading cycles required by the T 292-91I and the T 294-94 methods in the conditioning stage is the same (1000); however, it is different in the RM testing stages (50 and 100, respectively). In the T 292-91I method, the waveform is rectangular and has a 0.6 second loading duration and a 1.2 second rest period. However, in the T294-94 method, the waveform is haversine and has a 0.1 second loading duration and a 0.9 second rest period (Figure 3-14). The recoverable axial deformations at the twentieth and the fiftieth cycles for the T 292-91I method and at the seventieth and the hundredth cycles for the T 294-94 method were calculated for the last applied deviator stresses, respectively, and the results are reported in Table 4-2. It can be observed that the recoverable axial deformations measured from the T 292-91I method are very stable and the difference of the recoverable axial deformation at the twentieth and the fiftieth cycles is less than 5%. However, in the T 294-94 method, the loading duration and rest period are shorter than those in the T 292-91I method. Therefore, when using the T 294-

94 method to conduct a RM test, it needs a larger number of load cycles to reach the stable permanent deformation. It can be observed from Table 4-2 that the difference of the recoverable axial deformation at the seventieth and the hundredth cycles ranges from 0 to 2.1% which is less than 5%. Hence, it can be concluded that 50 and 100 loading cycles are adequate for the testing methods T 292-91I and T 294-94, respectively, to reach the stable permanent deformation.

4.2.3 Loading Waveform

According to the AASHTO T 292-91I either a triangular or a rectangular waveform can be used in RM testing of subgrade soils and base/subbase materials to simulate traffic loading. However, the T 294-94 method recommends that a haversine waveform with 0.1 second loading, followed by a 0.9 second rest period be used in RM testing for both soil and granular materials. A fixed loading duration of between 0.1 and 1.0 seconds and a fixed cycle duration of between 1.0 and 3.0 seconds are specified by the T 292-91I method. Further, for a granular specimen, a minimum of 0.9 second relaxation between the end and the beginning of consecutive load repetitions is required in the T 292-91I method. The same loading magnitude was used for all three waveforms.

Seed et al. (1962) showed that the applied loading pulse in the field is approximately sinusoidal with its magnitude decreasing and the duration increasing with depth below the pavement structure. It was also shown by Barksdale (1971) that the magnitude and duration of the loading pulse are a function of the vehicle speed and depth beneath the pavement surface. The stress pulse can be approximated by a haversine or a triangular function.

In order to compare the effect of different loading waveforms, three sets of RM tests with rectangular, triangular, and haversine waveforms were conducted by using the T 294-94 procedure. The three different waveforms used in this series of tests are shown schematically in Figure 3-14. In order to render the test results comparable, the areas under the rectangular and the triangular loading forms are kept nearly same. In these tests only the waveforms were varied, while all other factors were kept the same. The RM values obtained from the replicate tests are presented in Tables A-3 and A-4 in Appendix A, and their graphical representations are presented in Figures A-3 and A-4 in Appendix A. The mean (average) RM values from the above tests are given in Table 4-1 and are also plotted in Figure 4-1, wherein it is observed that the haversine waveform produced substantially higher RM values (nearly 80% higher), overall, than the triangular and the rectangular waveforms. However, the RM values are nearly equal for the triangular and the rectangular waveforms. For example, at the bulk stress of 104 and 690 kPa, the haversine waveform produced 141 and 368 MPa RM values, while the triangular waveform yielded 73 and 208 MPa, and the rectangular waveform yielded 77 and 234 MPa, respectively. One of the reasons for this difference could be that the longer loading period in case of the triangular and rectangular waveforms is likely to produce more viscoelastic deformation, and hence more elastic strains, compared to the elastic strains produced by the haversine waveform having a short loading duration. Therefore, it can be postulated that RM values decrease with increased loading duration. Of course, other factors such as different loading frequencies and rest periods used in these waveforms may have also contributed to these differences in the RM values. Nonetheless, these results demonstrate the importance of the influence of loading waveform on the RM values.

4.2.4 General Comparison

In order to generally compare the effect of testing procedure on RM values, the mean RM values obtained from the T 292-91I and T 294-94 methods are grouped in Figure 4-2. It can be observed that the RM values from the T 294-94 method are 32 to 122% higher than the values from the T 292-91I method. For example, at the bulk stress levels of 125 and 690 kPa, the T 294-94 method yielded 149 and 368 MPa RM values, and the T 292 -91I method produced 103 and 235 MPa RM values. Some of the potential reasons, as mentioned above, are: (i) the stress sequence used in the T 294-94 method has a stiffening effect on the specimen; (ii) the haversine waveform used in the T 294-94 method has a shorter loading duration that produced less viscoelastic strain than the strain produced by the rectangular waveform used in the T 292-91I method.

From Table 3-4, it can be observed that there are some discernible changes in the static material properties which were measured after RM testing. For cohesion (C), the specimens subjected to the T 294-94 RM testing present higher values than the specimens subjected to the T 292-91I RM testing. On the other hand, the friction angle (ϕ) and the unconfined compressive strength (U_C) present lower values for the specimens which were subjected to the T 294-94 RM testing. For example, the C value of 120.6 kPa obtained after the T 294-94 RM testing is higher than the C value of 68.9 kPa obtained after the T 292-91I RM testing. On the other hand, the U_C value of 299 kPa obtained after the T 294-94 RM testing is less than the U_C value of 348 kPa obtained after the T 292-91I RM testing. The corresponding measured ϕ values are 50.1° and 58.2° after the two different RM testings. One of the possible reasons for the increase in U_C and ϕ values is as follows. It has been observed that the T 292-91I method produced lower RM values than the T 294-94 method which means higher elastic strains were produced in the specimen by the T 292-91I method. As noted by Huang (1993), generally, plastic strains are proportional to elastic strains in paving materials including an aggregate base. Accordingly, a higher permanent deformation is expected to be induced in a specimen due to the T 292-91 I method than in the T 294-94 method. As a result, the void ratio of the specimen would become smaller, making the specimen stronger and thereby resulting in higher U_C and ϕ values when such tests are conducted following the RM testing using the T 292-91I method.

4.3 Effect of Gradation

Three gradations of the RS and the Sawyer aggregates were produced, compacted, and tested at OMC and 95% of MDD in order to evaluate the effect of gradation on RM. The three gradations, which are presented in Figure 3-6, are the median, finer limit, and coarser limit gradations suggested by the ODOT specification (ODOT 1996). The mean RM values from each gradation type were calculated from the six individual test results, and are presented in Tables 4-3 and 4-4 for the RS and the Sawyer aggregates, respectively. The RM values obtained from each of the six replicate tests are presented in Tables A-5 through A-9 and their graphical representations are presented in Figures A-5 through A-9 in Appendix A. Following the RM tests, unconfined compressive strength and triaxial compression tests were conducted to determine the cohesion (C), friction angle (ϕ), and unconfined compressive strength (U_C), as presented in Table 3-4.

For untreated granular materials, Asphalt Institute (AI 1991b) suggests that RM values ranging from 103.4 to 344.5 MPa be used in the design of flexible pavements. In view of Tables 4-3 and 4-4, the RM values obtained in the present study ranged from 52 to 368 MPa (values varying with bulk stress θ). Therefore, these RM values are in the acceptable range compared with those reported by Asphalt Institute (AI 1991b).

For comparative reasons, the mean RM values for each gradation are presented graphically in Figures 4-3 and 4-4 for the two aggregates, respectively. In view of Figure 4-3, the median gradation of the RS aggregate produced substantially higher RM values (41 to 129% higher) than the finer limit gradation but only slightly higher values (nearly 0 to 26% higher) than the coarser limit gradation. However, in Figure 4-4, the coarser limit gradation of the Sawyer aggregate produced the highest RM values (nearly 10 to 36% higher than the finer limit and the median gradations), and the RM values of the median and the finer limit gradations are nearly in the same range. In comparing the data in Figures 4-3 and 4-4, it becomes evident that the finer limit gradation in both cases gives lower RM values than those of the coarser limit gradation. This difference is more obvious for the RS aggregate. The reasons for this difference between the finer and the coarser limit gradations may be: (1) the drainage rate of the finer limit aggregates is slower than that of the coarser limit aggregates; (2) the finer limit aggregates lack larger irregular particles (maximum size 1.27 cm) to provide a strong interlock between particles; (3) the large top size particles (themselves) in the coarser limit aggregates can provide a strong aggregate structure.

In documenting the effect of gradation on RM values, similar results were also reported by other studies. For example, Kamal et al. (1993) reported that the RM value increased as the gradation changed from the finer to the coarser end of the gradation envelope. By comparing the resilient behavior of an uncrushed base material with a crushed base material, Johnson and Hicks (1987) reported that the uncrushed base course performed better than the crushed base coarse. The uncrushed base is superior because of larger maximum particle size and greater maximum density. Barksdale and Itani (1989) studied the RM values of granitic gneiss, and it was found that the coarse gradation of this material consistently resulted in higher RM values than those of the medium and fine gradations.

Extending the findings in this study into pavement design, it is safe to state that the pavement designed by using the median gradation of the RS aggregate, or the coarser limit gradation of the Sawyer aggregate, which yielded the highest RM values, would require less thickness and provide good performance. However, the coarser limit gradation of the RS aggregate produced the RM values which are closer to those of the median gradation. Considering the factor that the coarser limit aggregate provides faster drainage, it can be expected that coarser limit aggregates are less likely to induce damage in pavements under saturated condition and hence, lead to more durable pavements. Johnson and Hicks (1987) once reported that the future performance of the roadway with equal thicknesses of asphalt indicates that a pavement over an uncrushed base would have a 54% longer life than a pavement over a crushed base.

The findings in this study may have significant consequences in terms of field applications because aggregate particles may break down during the compaction process producing more fines than accounted for in specifications. It is generally agreed that having a certain amount of fines is beneficial, but any excess amount would lead to a reduced strength (RM values) and, hence, reduced pavement performance. Monitoring of aggregate break down during construction and development of appropriate specifications will be necessary to help avoid any detrimental effect, particularly when aggregates with lower LA abrasion values are involved in pavement construction.

From Table 3-2, it can be observed that the median gradation produced the maximum dry densities (2.38 and 2.23 g/cm^3 for the RS and the Sawyer aggregates), and specimens with this gradation have the maximum RM values (RS aggregate) and intermediate RM values (Sawyer aggregate). However, the coarser limit gradation produced the lowest dry densities (2.278 and 2.193 g/cm^3 for the RS and the Sawyer aggregates), but the corresponding RM values are the highest (Sawyer aggregate) or the intermediate (RS aggregate). A similar relationship was also observed with respect to the unconfined compressive strength (Table 3-4) . So one cannot simply say that the RM values are proportional to the dry density and unconfined compressive strength.

It can be observed from Table 3-4 that, as the amount of fines (percent passing the No. 200 (0.075 mm) sieve) increased from 4 to 12% between the coarser limit and the finer limit gradations, the cohesion (C) increases from 83.4 to 134.4 kPa and 34.5 to 75.8 kPa, however, the friction angle (ϕ) decreases from 52.9° to 46.9 ° and 58.4 ° to 51.2 ° for the RS and the Sawyer aggregates, respectively. This is consistent with the general principles of soil mechanics, because the fine particles are the primary contributing factor to cohesion, and the coarser particles are the major contributing factor to friction angle. This finding also has a significance for practical application, since the amount of fines can increase significantly due to the rolling compaction used in the pavement construction.

4.4 Effect of Moisture Content

An attempt was made to investigate the effect of moisture content on RM by considering three different moisture contents: the OMC, 2% above, and 2% below the OMC.

Median gradation was used in this phase of the study. The mean RM values were calculated from the six individual tests and are reported in Tables 4-5 and 4-6 for the RS and the Sawyer aggregates, respectively. The RM values of the six replicate tests are presented in Tables A-10 through A-13 and their graphical representations are presented in Figures A-10 through A-13 in Appendix A. Following the RM tests, the material properties including cohesion (C), friction angle (ϕ), and unconfined compressive strength (U_C) were also evaluated and the results are presented in Table 3-4.

In order to study the variability of RM values, the mean RM values for each moisture content are grouped together and graphically presented in Figures 4-5 and 4-6, which show that an increase in moisture content leads to a decrease in RM values for both aggregates. For example, at the bulk stress level of 125 kPa, as the moisture content increases from 2.6 to 6.6%, the RM values decrease from 189 to 105 MPa for the RS aggregate. For the Sawyer aggregate, the RM values decrease from 105 to 62 MPa as the moisture content increases from 4.0 to 8.0%. This finding for aggregate materials is consistent with observations by Rada and Witczak (1981) and Thompson (1989) who demonstrated that relatively small changes in the water content can result in substantial differences in the RM values. For example, Thompson (1989) indicated that increased moisture contents (above optimum) tend to decrease RM values. Moisture sensitivity will vary depending on specific gradations and the amount and nature of the fines. Lary and Mahoney (1984) developed moisture sensitivity data for several granular base materials sampled from a number of typical roads and indicated that for an initial modulus of 138 MPa, a 1% increase in moisture content would induce RM decrease from about 4.1 to 11 MPa. One of the possible reasons for this trend could be the matric suction present in an unsaturated specimen. When the moisture content increases, the matric suction decreases, hence reduced the strength of the specimen. Spangler and Handy (1973) also stated that the capillary water in soil pores sets up compressive stress for soil skeleton which are directed inward and contribute to the strength and stability of soils. However, the capillary induced strength is temporary and may disappear entirely if the soils become saturated, since saturation eliminates the capillary menisci.

From Figures 4-5 and 4-6, it can be observed that the variation of the RM values between 2% below the OMC and the OMC is nearly -13 to 27% (RS aggregate) and 11 to 37% (Sawyer aggregate), while the variation between the OMC and 2% above the OMC is more than 25 to 80% (RS aggregate) and 18 to 71% (Sawyer aggregate). Obviously, when the moisture content is greater than the OMC, the increasing moisture content has a greater influence on the decreasing of RM values. The reason could be that the specimen compacted at 2% above the OMC produces a smaller dry density than that at the OMC; also, the specimen has less suction at the higher moisture content. Both of the factors are detrimental in terms of the strength of the specimen. However, at 2% below the OMC, the specimen has a higher suction that offsets the factor of the smaller dry density (because the maximum dry density is achieved at the OMC); hence, the smaller variation in the RM values. It should be noted that only a 2% increase in moisture content (above OMC) changes the degree of saturation (S_r) considerably. The S_r increases from 83 to 95% and 78 to 86% for the RS and the Sawyer aggregates, respectively. In fact, Haynes and Yoder (1963) conducted cyclic triaxial tests on gravels and crushed stone and indicated that there was a critical degree of saturation near 80 to 85%. Above this critical degree of saturation, the RM decreases rapidly as the degree of saturation increases. Below the critical point, the degree of saturation has small influence on the RM values. In the present study, 2% above the OMC gave the initial degree of saturation 95% and 86% for the RS and the Sawyer aggregates, respectively. Although this moisture content did not cause the specimen saturation, the decreasing of RM values is obvious. Therefore, the conclusion can be made that the RM values are likely to decrease significantly when specimens reach the state of saturation or near saturation. Of course, while other variables such as the void ratio (the amount of fines) and drainage during the tests are important factors to consider, these results clearly demonstrate the importance of the influence of moisture content on the RM values.

The results obtained from the present study are helpful in understanding the behavior of pavement base materials under different moisture conditions. When the drainage of a pavement base does not function properly or during an excessive rainfall, the moisture in the pavement base may increase and could possibly reach saturation; this is possibly the worst scenario with respect to the pavement performance. On the other hand, when the base of a pavement goes through a dry season, the pavement is expected to exhibit good performance due to the relatively higher RM values. For example, in discussing the effect of seasonal variations of RM values on the pavement performance, Elliott and Thornton (1988) gave a design example and concluded that, except for January and February, the RM values of pavement subgrade are found in a similar fashion. The relative damage of the pavement in January was 0.005, however, in February it was 0.25. The reason is that the subgrade will be frozen resulting in the lowest moisture content at January, hence, the highest RM values (30 ksi). However, February is assumed to be a period of thawing, resulting in the highest moisture content in subgrade, hence the lowest RM values (5.5 ksi).

From Table 3-4, as the moisture changed, for both aggregates, regardless of which side of the OMC, the cohesion (C) decreases compared to the case of OMC. However, the friction angle (ϕ) increases as the moisture increases. For example, the cohesion values of the RS aggregate are 82.7 and 44.8 kPa at the moisture contents of 2.6% and 6.6% are less than the cohesion value of 120.6 kPa at the OMC (4.6%). However, as the moisture increases from 2.6 to 6.6%, the friction angle increases from 46.7° to 55.5°. This could be partly attributed to the fines losing in the sample preparation process. As the specimen compacted at 2% above the OMC, the excess water was pumped out from the top and bottom sides of the model that carried out fines from the specimen. As the fines reduced in a specimen, the cohesion decreases, and at the same time the specimen has a coarser gradation, which results in a higher friction angle.

4.5 Effect of Drainage Condition

The effect of drainage condition on RM was investigated for the two selected aggregates. The ODOT median gradation and the corresponding OMC were used for preparing the specimens which were tested using the undrained I and undrained II test methods. The mean RM values were calculated from the individual tests and reported in Tables 4-7 and 4-8 for the RS and the Sawyer aggregates, respectively. The RM values obtained from the individual tests are presented in Tables A-14 through A-17, and their graphical representations are presented in Figures A-14 through A-17 in Appendix A. Similarly, the material properties including cohesion (C), friction angle (ϕ), and unconfined compressive strength (U_C) were evaluated after RM tests and presented in Table 3-4. The effects of pore pressure, degree of saturation, and drainage condition on RM values are discussed as following.

4.5.1 *Pore Pressure Generation*

An attempt was made to measure the excess pore pressure build-up in the specimens during the RM testing under the undrained condition. The average measured pore pressure values are reported in Tables 4-9 and 4-10, and also graphically presented in Figures 4-7 and 4-8 for the RS and the Sawyer aggregates, respectively. It is observed that as the stress level (bulk stress) increases, the pore pressure also increases. Since the pore pressure was allowed to accumulate in the undrained II test, but not in the undrained I test, it produced higher excess pore pressures in the former, as expected. The pore pressure increases from the undrained II to the undrained I tests are substantial, 146% (average) for the RS aggregate and 162% (average) for the Sawyer aggregate. For example, for the RS aggregate, when the bulk stress is 125 kPa, the pore pressures generated are 3.45 kPa and 1.61 kPa in the undrained II and undrained I tests, respectively. For the Sawyer aggregate, the corresponding pore pressures generated are 5.51 kPa and 2.43 kPa.

In terms of practical consequences, the generation of pore pressure in the pavement base layer could be one of the major causes for the rapid deterioration of pavement structures. An increase in pore pressure reduces the strength and the stiffness of the underlying base layer, causing an increased surface deflection and eventually a reduction of pavement service life. Also, the dissipation of pore pressure is conducive to decrease in void ratio and subsequent settlement of the base layer, causing an additional loss of pavement support and increased surface cracking.

An effort was made to investigate the effect of degree of saturation (S_r) on the magnitude of pore pressure generation. The initial S_r of the specimens, calculated from other material properties (e.g., moisture content, dry density, and specific gravity) measured in this study, was 83% for the RS aggregate and 91% for the Sawyer aggregate. It was observed that, in the undrained I test, the generated pore pressure ranges from 1.61 to 9.42 kPa for the RS aggregate (S_r = 83%) and 2.58 to 14.97 kPa for the Sawyer aggregate (S_r = 91%). However, in the undrained II test, the corresponding pore pressure ranges from 1.46 to 23.49 kPa and 3.72 to 37.29 kPa for the RS and the Sawyer aggregates, respectively. Therefore, it may be deduced that as the degree of saturation increases, the range of pore pressure generation also increases.

4.5.2 *Drainage Condition*

The mean RM values from the drained and the undrained tests are presented in Figures 4-9 and 4-10 for the RS and the Sawyer aggregates, respectively. In view of these figures, the drained RM values are significantly higher than the corresponding undrained RM values. For example, the RM values from the drained tests are 34 to 88% higher than those obtained from the undrained I tests and 53 to 124% higher than those obtained from the undrained II tests for the RS aggregate. For the Sawyer aggregates, the RM values from the drained tests are 25 to 53% higher than those obtained from the undrained I tests and 28 to 58% higher than those obtained from the undrained II tests. This is so possibly because of the following reasons: (1) the pore pressure was generated in the undrained tests; an increase in pore pressure reduces the effective stress and, hence, reduces the strength and stiffness of a material; (2) the water was allowed to drain out in the drained tests and the moisture contents of the specimens reduced during the drained testing, and consequently, the dry densities of the specimens increased. Generally, a decrease in moisture content and an increase in dry density lead to an increase in the material strength, and hence, the increased RM values.

Very few researchers have examined the influence of drainage conditions on the RM values of aggregate materials. Hicks (1970) performed an experiment under undrained conditions and pore pressures were measured throughout the tests. As the number of cyclic loads increased, pore water pressure developed and weakened the specimen. Chen (1994) made an attempt to investigate the possibility of conducting RM tests under undrained conditions but specimens failed during the conditioning stage due to the development of excess pore pressure resulting from cyclic loading. Hicks (1970) and Das (1990) stated that the undrained conditions probably do not occur in a pavement, but it indicates the propensity of a reduction in the modulus when the pavement is near saturated.

Under undrained loading conditions, the RM decreases as a result of the increase in pore pressure and the resulting decrease in effective stresses. Such a decrease is illustrated graphically by the variation of the modulus ratio with respect to the pore pressure ratio (Figures 4-11 and 4-12). The modulus ratio is defined as the ratio of the RM value under the undrained loading to the corresponding bulk stress used. The pore pressure ratio is simply the pore pressure divided by 21 kPa, which is the minimum confining stress used in the RM tests. Furthermore, the general trend of the curves reflected in Figures 4-11 and 4-12 indicates that as the magnitude of pore pressure ratio increases, the modulus ratio decreases showing that the pore pressure has a significant influence on RM values. Extending this finding to pavement design, it can be postulated that constructing permeable base, maintaining the drainage efficiently, and reducing moisture in pavement base are important factors in ascertaining pavement quality and extended service life.

4.6 Effect of Aggregate Type

The effect of aggregate type on RM can be achieved based on the RM values obtained so far. Figures 4-13 through 4-17 show the RM variations between the RS and the Sawyer aggregates due to the different gradations and moisture contents. The following observations can be made from these figures.

(1) In view of Figures 4-13 to 4-15, generally, the RS limestone aggregate has higher RM values (about 47% higher) than those of the Sawyer sandstone aggregate. This could be attributed to the following reasons: (i) the big size particles of the RS aggregate are more irregular than those of the Sawyer aggregate, hence, higher interlock was produced in the RS aggregate; (ii) the LA values of the RS and the Sawyer aggregates are 24 and 28 (Table 3-3), which indicate that the RS aggregate is more resistant and stronger to deterioration as a result of abrasion and impact than the Sawyer aggregate; (iii) the RS aggregate produced higher maximum dry densities (MDD) than those of the Sawyer aggregate at different gradations (Table 3-2). As indicated by Rada and Witczak (1981) an increase in density could result in an increase in RM values; (iv) another possible reason is the behavior of the fine particles, since the fine particles contribute the cohesion. It was found that the cohesion produced in the RS aggregate is higher than that of the Sawyer aggregate (Table 3-4). Therefore, the RS aggregate, in general, produced higher RM values than those of the Sawyer aggregate.

Pandey (1996) evaluated the RM values for one marginal aggregate (Meridian aggregate) which has a LA value of 38. The testing specimens were prepared at the ODOT median gradation and the corresponding OMC (7.3%). By comparing the RM values obtained from the marginal aggregate with those obtained from the good quality aggregates used in this study, the RM values of the RS and the Sawyer aggregates are 185% and 63% (average) higher than those of the marginal Meridian aggregate, respectively.

(2) As gradation varies within the median and the coarser limit of the ODOT specified gradation range, the effect of aggregate type on RM values become more significant. For example, in Figure 4-13, the RS aggregate at the median gradation yielded 75% (average) higher RM values than those of the Sawyer aggregate at the same gradation. In Figure 4-14, the RS aggregate at the coarser limit gradation yielded 34% (average) higher RM values than those of the Sawyer aggregate at the corresponding gradation. However, as a gradation varies within the median to the finer limit of the ODOT specified gradation range, the effect of aggregate type on RM values become less significant. For example, in Figure 4-15, the RS aggregate at the finer limit gradation yielded almost the same RM values as the Sawyer aggregate at the same gradation.

(3) In view of Figures 4-16 and 4-17, as the moisture content varies from 2% below the OMC, to 2% above the OMC, for the same median gradation, the RS aggregates yielded 60% and 70% (average) higher RM values than those of the Sawyer aggregates at the corresponding moisture contents. It indicates that the effect of moisture content on RM values is less susceptible in terms of the aggregate type compared to the effect of aggregate gradation.

Chen (1994) evaluated the RM for six different types of aggregates (Table 2-5). It was found that the differences of the RM values due to the variation of aggregate types are approximately in the range of 20 to 50%. One type of aggregate in Chen's study was from the same source as the RS aggregate used in the present study. It is interesting to compare the RM values obtained from both studies. In that study (Chen 1994), the RM tests were conducted by using the AASHTO T 292-91I method, and the specimens were prepared at a gradation which is close to the ODOT median gradation. Also, the water content at the corresponding OMC (5.6%) was used in the specimen preparation. In the present study, the RM values of the RS aggregate at the ODOT median gradation and corresponding OMC (4.6%) were also evaluated by using the AASHTO T 292-91I method. By comparing the obtained RM values, it is observed that the RM values of the RS aggregate in this study are 19% (average) higher than those obtained from Chen's study. This is reasonable because the little difference in terms of gradation and moisture content existed between the two materials could result in the difference in the obtained RM values. Also, the RS aggregate used in the two studies was sampled at different times, which could result in a certain level of difference in terms of material strength behavior.

4.7 Variability of the Experimental Results

4.7.1 Error Analysis of the Measured RM Values

Testing errors involved in laboratory measurement play a critical role in the accuracy of measured data. RM values are determined by the measured deviator stress and the elastic strain. It was found that the RM values are very sensitive in terms of the amount of the elastic strain measured. The elastic strain was measured by the LVDTs, hence, the resolution of the LVDTs has a significant influence on the measured strain values. Other factors such as the membrane strength and specimen size may also influence the measured RM values. The effects of these experimental errors on the measured RM values were analyzed as follows.

Strain Error in the Measurement System

In the present study, the data acquisition board installed in the computer for the elastic strain measurement is 12 bytes. Hence the resolution of the data collecting board is $1/2^{12}$. The LVDTs which were used in the elastic strain measurement can measure the specimen deformation within ±1 in (25.4 mm). Therefore, the minimum measurable amount of deformation by using the current LVDTs is 2/4096 in (0.0124 mm). By dividing the sample height, the equivalent minimum measurable strain is $4.069*10^{-3}$ %. This is the elastic strain error involved in the data measurement system. If the measured elastic strain is represented by ε_m, hence, the real strain produced in the specimen should be within the range of $\varepsilon_m \pm 2.035*10^{-3}$ %.

The strain error indicated above can cause errors in the measured RM values, since at the same deviator stress, RM values can be determined by any strain value within the range of $\varepsilon_m \pm 2.035*10^{-3}$ %. If the measured resilient modulus is represented by RM, the maximum possible RM (RM_{max}) can be determined by the elastic strain of $\varepsilon_m - 2*2.035*10^{-3}$ % at the same deviator stress, and the minimum possible RM (RM_{min}) can be determined by the strain of $\varepsilon_m + 2*2.035*10^{-3}$ %. The difference between the RM_{max} and RM and the difference between the RM and RM_{min} are the RM errors induced by the strain error. The relative RM errors can be represented by ±m/n% [+m% = (RM_{max} - RM) / RM; -m% = (RM_{min} - RM) / RM]. The magnitude of the RM errors depends on the magnitude of the elastic strain produced in the specimen. Generally, the smaller the strain, the larger the errors. Therefore, the RM errors are mainly depended on the confining pressure (σ_c) and the deviator stress (σ_d) used in the RM testing.

According to the AASHTO T 294-94 method, the RM values were reported by using the mean value from the last five cycles. The deviation of the RM values from the last five cycles is an important factor in terms of the accuracy of the measured RM values. It is believed that this deviation is partly attributed to the strain error involved in the measurement system. In the present study, the deviation of the RM values obtained from the last five cycles as well as the corresponding RM errors (± m/n%) induced by the strain error were calculated for the RS and the Sawyer aggregates in terms of different confining pressures and deviator stresses used in the RM testing. For the RS aggregate, the RM values at the median gradation and 2% below OMC (Test 1) were used for the above analysis, and for the Sawyer aggregate, the RM values at the finer limit gradation and OMC (Test 1) were used. The calculated results are presented in Tables 4-11 and 4-12 for both aggregates, respectively.

In view of Tables 4-11 and 4-12, the following observations can be obtained: (1) for the same confining pressure (σ_c), as the deviator stress (σ_d) increases, the relative RM error (±m/n%) decreases. For example, for the σ_c = 69 kPa, as the σ_d increases from 69 to 207 kPa (Case 7, 8, and 9), the ±m/n% decreases from ±17/13 to ±6.0/5.4% for the RS aggregate and ±14/11 to ±4.0/3.7% for the Sawyer aggregate; (2) for the stress ratio $\sigma_d/\sigma_c \leq 1$, if the bulk stress (θ) ≤ 136 kPa, relative higher ±m/n% was produced. However, if the θ > 136 kPa, relative lower ±m/n% was yielded. For example, as the $\sigma_c = \sigma_d$ = 21 kPa, and the θ = 84 kPa (Case 1), ±78/32% and ±55/24% relative errors were yielded for the RS and the Sawyer aggregates, respectively. On the other hand, as the $\sigma_c = \sigma_d$ = 69 kPa, and the θ = 276 kPa (Case 7), ±17/13% and ±14/11% relative errors were yielded for the RS and the Sawyer aggregates, respectively; (3) if the stress ratio σ_d/σ_c > 1, for any level of bulk stress, the yielded relative error ±m/n% is quite small. For example, as the σ_d/σ_c = 3 (Case 3, 6, and 9), the corresponding relative errors are in the range of ±6.0/5.4 to ±14/11% and ±4.0/3.7 to

±10/8.6% for the RS and the Sawyer aggregates, respectively. Therefore, it can be generally concluded that the RM values measured in this study are more reliable at the higher bulk stresses (θ > 136 kPa) than those at the lower bulk stresses.

The last column of Tables 4-11 and 4-12 present the standard deviation (SD) as a percentage of the mean RM values measured from the last five cycles of RM testing. The SD/Mean represents the relative error measured from the five RM values. Since the magnitudes of the relative errors (SD/Mean) are within the range of the RM errors (±m/n%) induced by the strain error in an accepted degree, therefore, it is believed that the strain error is the major reason for causing the deviation of the measured RM values. Obviously, other reasons, such as the accuracy of the load cell and the noise recorded during the testing could also have some effects on the RM values, however, these effects are relative smaller compared to the effect of strain error.

Correction for Rubber Membrane

It should be noted that the two membranes used in the sample preparation and testing process could have an effect on the measured RM values. The membrane effect depends on the thickness and the modulus of the rubber membrane, the sample size, and the axial strain of the specimen. The AASHTO T 294-94 method for RM testing does not specify how to consider this effect, however, the AASHTO T 297-94 method (AASHTO 1994f), which is a testing procedure for the consolidated undrained triaxial compression test on cohesive soils, specifies a method for the correction of rubber membrane. Based on this method, the following equation is used to correct the deviator stress for the effect of the rubber membrane if the error in deviator stress due to the strength of the membrane exceeds 5%:

$$\Delta\sigma_d = (4E_m * t_m * \varepsilon_1) / D \qquad (4\text{-}1)$$

where:

$\Delta\sigma_d$ = the correction to be subtracted from the measured deviator stress, psi (kPa),

E_m = Young's modulus of the membrane material, psi (kPa),

t_m = thickness of the membrane, in. (mm),

ε_1 = axial strain (decimal form), and

D = diameter of the specimen.

In the present test, the rubber membrane has a thickness of 0.5 mm and a Young's modulus of 200 psi (1378 kPa). The diameter of the specimen is 6 in (152 mm). In view of Tables A-1 through A-17 in Appendix A, the minimum and the maximum RM values obtained in this study are 41MPa and 397 MPa at the corresponding minimum and maximum deviator stresses of 21 kPa and 276 kPa, which result in the elastic strain in the range of $5.122*10^{-4}$ to $6.952*10^{-4}$. By taking all the above values into Eq. (4-1), it can be found that the amount of $\Delta\sigma_d$ is in the range of 0.01 to 0.1% of the deviator stress, which is much smaller than 5% specified by the AASHTO T 297-94 method. Hence, the membrane effect in the current tests is considered insignificant and was not included in the measured RM values.

Specimen Size

Another detrimental effect on the RM results could be the sample size. The maximum particle size of the aggregate used in this study is 1 in (25.4 mm). The diameter of the sample is 6 in (152 mm) which is six times of the maximum particle size. Generally, to avoid this detrimental effect, the minimum length (diameter here) of the sample should be ten times of the maximum particle size. This could be one of the reasons that caused the relative high deviations for the RM values at the coarser limit gradation (Figures A-5 and A-8).

4.7.2 Variability of the Replicate RM Test Results

The extent to which the RM values obtained from replicate specimens differ from each other is an important factor in determining the reliability of the RM values (Pandey, 1996). The variations in the individual RM values are measured by standard deviation (SD). The higher the magnitude of the SD, the larger the variation of RM values. For a good set of tests, it is desirable that the individual RM values not differ from the mean by any significant amount. In other wards, it is desirable and important to have a SD of smaller magnitude with respect to the mean value. The extent to which the individual values fall within a certain range or interval (confidence interval) depends on the number of observations (number of replicate specimens tested), the confidence coefficient desired, and the SD of the observations (Mendenhall and Sincich 1992). In this study, since the number of observations and the SD are known, the confidence coefficient, is determined as:

$$z_{\alpha/2}=e\sqrt{n}/s \qquad (4\text{-}2)$$

where e is the error in estimation, s is the SD, n is the number of observations, and $z_{\alpha/2}$ is the upper $\alpha/2$ critical value for the standard normal distribution.

In order to evaluate the confidence level of the RM values and hence the test data obtained from the present study, the RM values of the RS aggregate at 2% below the OMC are selected for this purpose. This set of data has the maximum sample standard deviations.

Based on the general experience of geotechnical testing, a 15% relative error was selected in the analysis. In other words, the goal here is to determine the confidence level in the measured RM values such that all the test results are within 15% (i.e., 15% below or above) of the mean RM values. Based on Eq. (4-1), the confidence levels were calculated for all of the RM values and are presented in Table 4-13. The mean confidence level for this case is about 90%, which means 90% of the obtained RM values fall within the range of 15% below or above the mean RM values. As mentioned previously, this is the worst case, and all other cases would have higher confidence levels since the measured SD values for these cases are lower than those used in this analysis. For example, the confidence levels of the RM values from the Sawyer aggregate at the finer limit gradation and OMC were calculated in Table 4-14. Overall, this set of data has the minimum sample standard deviations and the mean confidence level for this case is 98%, which means 98% of the individual RM values fall within the range of 15% below or above the mean RM values.

For the measured RM values, the relative error can be represented by the SD/mean RM values at different bulk stresses. Tables A-1 through A-17 in Appendix A present the RM values of all replicate specimens tested for the RS and the Sawyer aggregates. The SD values as a percentage of the mean RM values are also presented in these tables. A close observation of these values reveals that, although the SD values generally increase with increasing bulk stresses and RM values, the SD as a percentage of the mean RM values decreases with increasing RM values and bulk stresses. For example, for the RS aggregate at the coarser limit gradation and the OMC (Table A-5), the mean RM values at 84 kPa and 690 kPa bulk stresses are 93.77 MPa and 336.57 MPa, respectively, and the corresponding SD values are 25.94 MPa and 35.89 MPa, respectively. However, the SD values as a percentage of the mean RM values are 27.66% at 84 kPa bulk stress and 10.66% at 690 kPa bulk stress. Figures 4-18 and 4-19 show the relative error of the measured RM values as a function of bulk stress for the RS and the Sawyer aggregates, respectively. It can be observed that as the bulk stress increases, the relative error has a tendency to decrease. This indicates that the variation in RM values among replicates is smaller at higher bulk stresses than that at lower bulk stresses. This leads to the conclusion that the RM values obtained from the present study have a higher degree of reliability at the higher bulk stresses than that at the lower bulk stresses.

In view of Figures A1 through A17 in Appendix A, it can be observed that some cases present relative higher deviations among the replicate RM values. The reasons could be attributed to: (i) the strain error involved in the measurement; (ii) the non-uniform compaction effort used in the preparation of specimens; (iii) the effect of noise during the testing (particularly at the low bulk stress level); (iv) the different waiting times for the replicate specimens before the RM tests. For one specimen, the time needed for the RM test and the unconfined or triaxial compression tests is about two hours. The waiting time for the sixth specimen is much longer than that of the first specimen, this may cause some deviation in the RM values between the replicate specimens because of moisture migration, as an example.

By comparing the different cases in Figures 4-18 and 4-19, it can be found that the RM values at 2% below the OMC have the maximum relative errors for the RS and the Sawyer aggregates. The average relative errors for these two cases are 22.7% for the RS aggregate, and 20% for the Sawyer aggregate. Generally, this level of errors produced in geotechnical testing is acceptable. Actual error in most cases, however, is much smaller than these maximum error values.

Table 4-1 Mean RM Values from the Different Testing Procedures

Bulk Stress (kPa)	T 292-91I Mean RM (MPa)	T 292-91I SD (MPa)	Bulk Stress (kPa)	Haversine Mean RM (MPa)	Haversine SD (MPa)	Triangular Mean RM (MPa)	Triangular SD (MPa)	Rectangular Mean RM (MPa)	Rectangular SD (MPa)
483	228.9	14.4	84	118.2	42.0	60.7	7.1	63.8	8.9
551	253.6	7.6	104	141.3	28.2	72.7	12.6	76.6	12.8
621	241.0	24.9	125	149.2	23.8	90.0	14.0	93.6	9.0
689	234.6	29.6	136	158.2	26.3	81.3	25.8	81.8	7.2
378	143.8	22.5	171	172.4	27.6	100.9	20.4	100.5	19.3
447	174.8	21.1	205	182.5	35.1	107.7	16.6	116.1	19.6
516	195.1	22.3	276	249.3	36.6	104.6	26.1	125.4	27.1
585	202.0	21.6	345	247.5	36.8	128.6	27.9	152.8	21.6
241	93.0	18.0	414	240.9	33.9	148.8	39.1	156.6	20.4
276	112.1	16.7	378	252.6	40.0	118.2	26.4	136.6	17.9
345	147.8	16.8	412	274.0	50.0	132.4	38.8	149.4	17.8
414	168.9	13.9	516	302.6	37.8	168.5	45.9	183.6	20.1
136	77.7	7.1	517	311.4	41.8	156.6	20.9	169.0	12.4
171	103.8	17.1	552	334.7	32.5	169.9	20.3	189.2	17.8
205	122.6	17.6	690	367.6	40.7	207.6	17.7	233.8	26.0
97	80.8	13.4							
111	92.6	14.8							
125	102.8	14.7							

Table 4-2 Measured Recoverable Deformations from the T 292-91I and T 294-94 Testing Methods

Testing Method	Recoverable Deformation (1×10^{-3} in)	Test 1	Test 2	Test 3	Test 4	Test 5	Test 6
	Δ1 (at the 20th cycle)	7.8	8.8	6.8	7.8	8.8	8.8
T 292-91I	Δ2 (at the 50th cycle)	7.8	8.8	6.8	7.8	8.8	8.8
	(Δ2-Δ1)/Δ2 (%)	0.0	0.0	0.0	0.0	0.0	0.0
	Δ1 (at the 70th cycle)	9.8	7.8	9.8	7.8	8.8	10.8
T 294-94	Δ2 (at the 100th cycle)	9.6	7.8	9.6	7.8	8.8	10.6
	(Δ2-Δ1)/Δ2 (%)	2.1	0.0	2.1	0.0	0.0	1.9

1 in = 25.4 mm

Table 4-3 Mean RM Values of the RS Aggregate at the Three Different Gradations

Confining Pressure (kPa)	Deviator Stress (kPa)	Bulk Stress (kPa)	Median Mean RM (MPa)	Median SD (MPa)	Coarser Limit Mean RM (MPa)	Coarser Limit SD (MPa)	Finer Limit Mean RM (MPa)	Finer Limit SD (MPa)
21	21	84	118.2	42.0	93.8	26.0	83.8	31.0
21	41	104	141.3	28.2	140.2	16.1	82.4	17.3
21	62	125	149.2	23.8	144.2	38.7	88.8	23.3
34	34	136	158.2	26.3	156.1	42.2	82.4	24.9
34	69	171	172.4	27.6	175.1	41.1	97.0	16.9
34	103	205	182.5	35.1	177.3	34.8	103.1	13.0
69	69	276	249.3	36.6	215.9	46.6	108.9	21.5
69	138	345	247.5	36.8	229.8	41.0	121.7	14.5
69	207	414	240.9	33.9	240.6	36.4	129.6	14.7
103	69	378	252.6	40.0	236.4	36.6	125.1	13.6
103	103	412	274.0	50.0	249.8	44.4	133.0	29.0
103	207	516	302.6	37.8	293.5	52.9	153.0	19.1
138	103	517	311.4	41.8	298.3	56.5	160.8	32.5
138	138	552	334.7	32.5	297.9	47.6	172.1	31.6
138	276	690	367.6	40.7	336.6	35.9	198.7	26.4

Table 4-4 Mean RM Values of the Sawyer Aggregate at the Three Different Gradations

Confining Pressure (kPa)	Deviator Stress (kPa)	Bulk Stress (kPa)	Median Mean RM (MPa)	Median SD (MPa)	Coarser Limit Mean RM (MPa)	Coarser Limit SD (MPa)	Finer Limit Mean RM (MPa)	Finer Limit SD (MPa)
21	21	84	70.5	19.3	78.0	17.2	51.7	17.7
21	41	104	79.7	13.2	96.3	21.9	75.3	9.3
21	62	125	82.1	15.0	102.7	18.4	79.4	9.6
34	34	136	90.6	11.3	104.6	16.9	104.9	20.8
34	69	171	96.1	14.0	128.1	18.2	99.2	9.8
34	103	205	104.8	14.2	140.3	20.6	106.1	8.7
69	69	276	123.4	14.4	167.7	26.5	141.7	19.7
69	138	345	147.4	11.9	178.7	21.6	145.6	14.1
69	207	414	150.1	13.8	194.1	29.7	151.2	10.1
103	69	378	147.8	14.0	171.2	30.2	163.2	9.1
103	103	412	158.4	14.2	195.9	31.5	160.0	9.3
103	207	516	180.3	15.6	215.8	29.6	181.1	13.5
138	103	517	173.3	18.6	206.0	29.8	188.2	19.5
138	138	552	186.4	12.4	219.0	23.9	191.8	19.5
138	276	690	210.6	12.0	253.5	22.3	213.0	12.4

Table 4-5 Mean RM Values of the RS Aggregate at the Three Different Moisture Contents

Confining Pressure (kPa)	Deviator Stress (kPa)	Bulk Stress (kPa)	Optimum MC Mean RM (MPa)	Optimum MC SD (MPa)	2% Below OMC Mean RM (MPa)	2% Below OMC SD (MPa)	2% Above OMC Mean RM (MPa)	2% Above OMC SD (MPa)
21	21	84	118.2	42.0	102.6	37.3	65.5	18.1
21	41	104	141.3	28.2	139.4	30.1	96.6	20.1
21	62	125	149.2	23.8	188.7	50.5	105.4	20.7
34	34	136	158.2	26.3	209.4	66.3	122.0	17.3
34	69	171	172.4	27.6	200.7	48.4	125.8	17.5
34	103	205	182.5	35.1	232.3	40.0	131.5	18.3
69	69	276	249.3	36.6	260.2	59.0	192.2	32.1
69	138	345	247.5	36.8	312.2	58.9	183.2	19.8
69	207	414	240.9	33.9	303.4	46.3	184.2	22.9
103	69	378	252.6	40.0	271.2	80.3	184.8	28.9
103	103	412	274.0	50.0	321.8	69.7	210.0	30.4
103	207	516	302.6	37.8	352.3	53.9	234.8	23.7
138	103	517	311.4	41.8	339.8	81.5	235.8	32.3
138	138	552	334.7	32.5	380.8	74.5	266.8	40.5
138	276	690	367.6	40.7	396.0	62.3	284.7	29.7

Table 4-6 Mean RM Values of the Sawyer Aggregate at the Three Different Moisture Contents

Confining Pressure (kPa)	Deviator Stress (kPa)	Bulk Stress (kPa)	Optimum MC		2% Below OMC		2% Above OMC	
			Mean RM (MPa)	SD (MPa)	Mean RM (MPa)	SD (MPa)	Mean RM (MPa)	SD (MPa)
21	21	84	70.5	19.3	78.4	20.4	41.3	6.0
21	41	104	79.7	13.2	103.3	18.0	52.9	3.4
21	62	125	82.1	15.0	104.7	18.6	61.9	5.2
34	34	136	90.6	11.3	123.8	39.2	72.0	15.6
34	69	171	96.1	14.0	127.7	29.1	75.7	9.3
34	103	205	104.8	14.2	141.1	22.4	77.6	6.5
69	69	276	123.4	14.4	154.4	44.1	96.6	12.8
69	138	345	147.4	11.9	184.4	41.4	110.0	12.5
69	207	414	150.1	13.8	193.2	17.1	110.1	11.9
103	69	378	147.8	14.0	174.2	43.3	115.1	23.4
103	103	412	158.4	14.2	194.5	30.5	121.4	22.7
103	207	516	180.3	15.6	221.8	31.7	138.5	18.1
138	103	517	173.3	18.6	199.0	44.8	145.7	20.5
138	138	552	186.4	12.4	226.4	46.3	158.0	21.5
138	276	690	210.6	12.0	256.7	31.6	177.2	17.6

Table 4-7 Mean RM Values of the RS Aggregate at the Different Drainage Conditions

Confining Pressure (kPa)	Deviator Stress (kPa)	Bulk Stress (kPa)	Drained Mean RM (MPa)	Drained SD (MPa)	Undrained I Mean RM (MPa)	Undrained I SD (MPa)	Undrained II Mean RM (MPa)	Undrained II SD (MPa)
21	21	84	118.2	42.0	77.9	34.4	52.7	10.4
21	41	104	141.3	28.2	93.3	37.1	88.8	26.6
21	62	125	149.2	23.8	101.3	30.8	97.3	15.1
34	34	136	158.2	26.3	118.4	32.6	86.7	21.5
34	69	171	172.4	27.6	112.1	27.0	95.3	9.9
34	103	205	182.5	35.1	128.2	31.1	105.1	10.4
69	69	276	249.3	36.6	142.1	50.6	132.2	10.1
69	138	345	247.5	36.8	151.0	28.7	132.7	13.6
69	207	414	240.9	33.9	149.2	25.9	141.0	12.1
103	69	378	252.6	40.0	164.3	37.0	150.7	27.6
103	103	412	274.0	50.0	157.6	26.1	154.9	18.5
103	207	516	302.6	37.8	180.5	40.6	175.6	21.5
138	103	517	311.4	41.8	180.4	43.4	158.2	17.8
138	138	552	334.7	32.5	177.6	24.3	194.5	16.3
138	276	690	367.6	40.7	202.5	40.4	218.6	18.4

Table 4-8 Mean RM Values of the Sawyer Aggregate at the Different Drainage Conditions

Confining Pressure (kPa)	Deviator Stress (kPa)	Bulk Stress (kPa)	Drained		Undrained I		Undrained II	
			Mean RM (MPa)	SD (MPa)	Mean RM (MPa)	SD (MPa)	Mean RM (MPa)	SD (MPa)
21	21	84	70.5	19.3	52.6	3.4	52.4	9.9
21	41	104	79.7	13.2	58.8	5.7	59.9	9.4
21	62	125	82.1	15.0	64.4	2.5	63.9	9.3
34	34	136	90.6	11.3	59.2	4.7	57.4	8.7
34	69	171	96.1	14.0	66.4	2.9	65.4	5.1
34	103	205	104.8	14.2	75.7	2.5	71.3	7.6
69	69	276	123.4	14.4	89.0	3.9	91.7	12.4
69	138	345	147.4	11.9	96.2	4.8	96.2	12.2
69	207	414	150.1	13.8	107.2	3.7	102.8	8.9
103	69	378	147.8	14.0	107.3	8.8	98.6	20.7
103	103	412	158.4	14.2	109.7	12.9	103.6	26.3
103	207	516	180.3	15.6	130.1	13.6	118.7	16.9
138	103	517	173.3	18.6	138.4	20.8	131.6	19.5
138	138	552	186.4	12.4	134.9	15.8	135.1	23.0
138	276	690	210.6	12.0	162.2	21.2	150.6	14.3

Table 4-9 Pore Pressure (PP) Measured in the Undrained RM Tests (RS Aggregate)

Confining Pressure (kPa)	Deviator Stress (kPa)	Bulk Stress (kPa)	Undrained I Mean PP (kPa)	Undrained I SD (kPa)	Undrained II Mean PP (kPa)	Undrained II SD (kPa)
21	21	84	1.61	1.43	1.46	1.49
21	41	104	1.38	1.38	2.55	2.69
21	62	125	1.61	1.43	3.45	3.68
34	34	136	1.84	1.59	4.53	5.11
34	69	171	2.30	1.99	5.60	6.39
34	103	205	2.07	1.82	6.53	7.34
69	69	276	5.51	3.00	9.99	7.50
69	138	345	5.74	2.21	12.40	8.51
69	207	414	5.28	1.99	14.64	9.59
103	69	378	5.51	1.38	16.54	8.51
103	103	412	6.66	2.61	17.91	8.02
103	207	516	5.97	1.05	19.64	7.50
138	103	517	7.81	2.10	21.01	7.04
138	138	552	7.35	1.73	22.22	5.75
138	276	690	9.42	3.79	23.94	4.58

Table 4-10 Pore Pressure (PP) Measured in the Undrained RM Tests (Sawyer Aggregate)

Confining	Deviator	Bulk	Undrained I		Undrained II	
Pressure	Stress	Stress	Mean PP	SD	Mean PP	SD
(kPa)	(kPa)	(kPa)	(kPa)	(kPa)	(kPa)	(kPa)
21	21	84	2.58	3.10	3.72	3.10
21	41	104	2.81	3.32	4.55	3.98
21	62	125	2.43	3.56	5.51	4.16
34	34	136	3.86	4.65	8.68	6.44
34	69	171	3.55	3.98	10.75	5.86
34	103	205	3.74	3.81	13.50	7.98
69	69	276	4.96	5.89	15.19	7.87
69	138	345	5.00	5.58	16.89	8.50
69	207	414	5.70	6.18	19.86	7.30
103	69	378	9.25	8.68	22.97	9.53
103	103	412	9.94	9.07	26.15	11.19
103	207	516	10.47	8.93	29.71	12.64
138	103	517	13.40	11.39	32.42	13.63
138	138	552	14.95	12.96	34.22	12.75
138	276	690	14.97	12.08	37.29	11.92

Table 4-11 Expermental Error Analyzed and Standard Deviation Measured from the Last Five Cycle RM Test (RS Aggregate at the 2% below OMC and Median Gradation)

Case No.	σ_c (kPa)	σ_d (kPa)	θ (kPa)	RM_{96} (MPa)	RM_{97} (MPa)	RM_{98} (MPa)	RM_{99} (MPa)	RM_{100} (MPa)	Mean RM (MPa)	SD (MPa)	SD/Mean (%)
1	21	21	84	104.44	97.15	97.15	97.15	104.44	100.06	3.991	3.988
				±78/32%	±78/32%	±78/32%	±78/32%	±78/32%	±78/32%		
2	21	41	104	106.86	106.86	160.30	160.30	160.30	138.92	29.27	21.07
				±19/14%	±19/14%	±32/20%	±32/20%	±32/20%	±27/17%		
3	21	62	125	188.36	141.27	113.02	141.75	141.27	145.13	27.12	18.68
				±19/14%	±14/11%	±11/8.9%	±14/11%	±14/11%	±14/11%		
4	34	34	136	95.26	150.18	300.35	150.18	146.53	168.50	77.30	45.88
				±19/14%	±32/20%	±95/33%	±32/20%	±32/20%	±42/21%		
5	34	69	171	167.78	134.23	135.68	165.96	165.96	153.92	17.34	11.26
				±14/11%	±11/8.9%	±11/8.9%	±14/11%	±14/11%	±13/10%		
6	34	103	205	210.98	180.62	209.52	155.13	209.52	193.15	24.78	12.829
				±11/8.9%	±9.2/7.8%	±11/8.9%	±7.7/6.7%	±11/8.9%	±9.9/8.2%		
7	69	69	276	178.11	237.48	178.11	237.48	237.49	213.73	32.52	15.21
				±14/11%	±19/14%	±14/11%	±19/14%	±19/14%	±17/13%		
8	69	138	345	256.69	218.94	218.94	218.94	256.69	234.04	20.68	8.834
				±9.2/7.8%	±7.7/6.7%	±7.7/6.7%	±7.7/6.7%	±9.2/7.8%	±8.3/7.1%		

Table 4-11 Continued...

Case No.	σ_c (kPa)	σ_d (kPa)	θ (kPa)	RM_{96} (MPa)	RM_{97} (MPa)	RM_{98} (MPa)	RM_{99} (MPa)	RM_{100} (MPa)	Mean RM (MPa)	SD (MPa)	SD/Mean (%)
9	69	207	414	255.75	288.54	255.75	256.58	255.75	262.48	14.58	5.55
				±5.9/5.3%	±6.7/5.9%	±5.9/5.3%	±5.9/5.3%	±5.9/5.3%	±6.0/5.4%		
10	103	69	378	244.76	244.76	183.57	244.76	183.57	220.29	33.52	15.21
				±19/14%	±19/14%	±14/11%	±19/14%	±14/11%	±17/13%		
11	103	103	412	294.22	232.92	294.22	294.22	232.92	269.70	33.57	12.45
				±15/11%	±11/9.2%	±15/11%	±15/11%	±11/9.2%	±13/11%		
12	103	207	516	334.07	334.07	291.24	292.17	335.14	317.34	23.41	7.375
				±7.7/6.7%	±7.7/6.7%	±6.7/5.9%	±6.7/5.9%	±7.7/6.7%	±7.3/6.4%		
13	138	103	517	298.05	298.05	235.96	299.76	237.31	273.82	33.96	12.40
				±15/11%	±15/11%	±11/9.2%	±15/11%	±11/9.2%	±13/11%		
14	138	138	552	315.73	317.25	317.25	317.25	317.25	316.95	0.68	0.21
				±11/9.2%	±11/9.2%	±11/9.2%	±11/9.2%	±11/9.2%	±11/9.2%		
15	138	276	690	350.23	313.75	313.75	313.75	314.49	321.20	16.24	5.055
				±5.9/5.3%	±5.2/4.7%	±5.2/4.7%	±5.2/4.7%	±5.2/4.7%	±5.4/4.8%		

* RM_{96}, RM_{97}, RM_{98}, RM_{99}, and RM_{100} represent the RM values measured from the last five cycles.
* Mean RM represents the average RM value from the last five cycles, and SD is the standard deviation of the last five RM values.
* ± m/n % represents the corresponding relative RM error which means the real RM value is in the range of (1± m/n %) RM.

Table 4-12 Expermental Error Analyzed and Standard Deviation Measured from the Last Five Cycle RM Test (Sawyer Aggregate at the Finer Limit Gradation and OMC)

Case No.	σ_c (kPa)	σ_d (kPa)	θ (kPa)	RM_{96} (MPa)	RM_{97} (MPa)	RM_{98} (MPa)	RM_{99} (MPa)	RM_{100} (MPa)	Mean RM (MPa)	SD (MPa)	SD/Mean (%)
1	21	21	84	119.01	59.50	39.67	62.74	125.49	81.28	38.49	47.36
				±95/33%	±32/20%	±19/14%	±32/20%	±95/33%	±55/24%		
2	21	41	104	76.91	76.91	75.09	75.09	100.12	80.82	10.82	13.39
				±14/11%	±14/11%	±14/11%	±14/11%	±19/14%	±15/12%		
3	21	62	125	97.96	99.25	96.50	81.63	97.96	94.66	7.35	7.76
				±11/8.9%	±11/8.9%	±11/8.9%	±8.8/7.5%	±11/8.9%	±10/8.6%		
4	34	34	136	128.72	132.37	136.01	132.37	66.18	119.13	29.71	24.94
				±32/20%	±32/20%	±32/20%	±32/20%	±14/11%	±29/18%		
5	34	69	171	123.80	102.45	156.38	101.20	101.20	117.00	24.02	20.53
				±11/9.2%	±9.2/7.8%	±15/11%	±9.2/7.8%	±9.2/7.8%	±11/8.8%		
6	34	103	205	119.16	118.22	119.16	106.44	137.74	120.14	11.22	9.337
				±6.7/5.9%	±6.7/5.9%	±6.7/5.9%	±5.9/5.3%	±7.7/6.7%	±6.7/5.9%		
7	69	69	276	169.16	172.99	169.16	133.92	169.16	162.88	16.27	9.99
				±15/11%	±15/11%	±15/11%	±11/9.2%	±15/11%	±14/11%		
8	69	138	345	176.55	156.49	174.68	154.83	175.61	167.63	10.97	6.542
				±6.7/5.9%	±5.9/5.3%	±6.7/5.9%	±5.9/5.3%	±6.7/5.9%	±6.4/5.6%		

Table 4-12 Continued...

Case No.	σ_c (kPa)	σ_d (kPa)	θ (kPa)	RM_{96} (MPa)	RM_{97} (MPa)	RM_{98} (MPa)	RM_{99} (MPa)	RM_{100} (MPa)	Mean RM (MPa)	SD (MPa)	SD/Mean (%)
9	69	207	414	152.00	180.03	163.88	167.10	164.38	165.48	10.00	6.04
				±3.7/3.4%	±4.3/4.0%	±4.0/3.7%	±4.0/3.7%	±4.0/3.7%	±4.0/3.7%		
10	103	69	378	160.70	219.12	130.02	164.34	166.17	168.07	32.12	19.11
				±14/11%	±19/14%	±11/8.9%	±14/11%	±14/11%	±14/11%		
11	103	103	412	179.78	151.20	152.27	218.75	177.27	175.86	27.49	15.63
				±9.2/7.8%	±7.7/6.7%	±7.7/6.7%	±11/9.2%	±9.2/7.8%	±9.0/7.6%		
12	103	207	516	181.26	219.00	198.72	196.72	196.70	198.88	13.42	6.746
				±4.3/4.0%	±5.2/4.7%	±4.7/4.3%	±4.7/4.3%	±4.7/4.3%	±4.8/4.3%		
13	138	103	517	179.36	179.36	180.62	216.73	349.20	221.05	73.40	33.20
				±9.2/7.8%	±9.2/7.8%	±9.2/7.8%	±11/9.2%	±19/14%	±12/9.3%		
14	138	138	552	208.58	208.58	181.84	208.58	182.78	198.07	14.39	7.27
				±7.7/6.7%	±7.7/6.7%	±6.7/5.9%	±7.7/6.7%	±6.7/5.9%	±7.3/6.4%		
15	138	276	690	215.37	271.21	215.37	231.30	231.88	233.04	22.84	9.799
				±3.7/3.5%	±4.7/4.3%	±3.7/3.5%	±4.0/3.7%	±4.0/3.7%	±4.0/3.7%		

Table 4-13 Confidence Level Calculated from the Measured RM Values (RS Aggregate at the Median Gradation and 2% below OMC)

Bulk Stress (kPa)	RM (MPa)	SD (MPa)	EE (MPa)	Sample Number	$Z_{\alpha/2}$	Confidence Level (%)
84	102.6	37.3	15.39	6	1.011	68.8
104	139.4	30.1	20.91	6	1.702	91.0
125	188.7	50.5	28.31	6	1.373	83.0
136	209.4	66.3	31.41	6	1.662	90.4
171	200.7	48.4	30.11	6	1.524	87.2
205	232.3	40.0	34.85	6	2.134	96.6
276	260.2	59.0	39.03	6	1.620	89.4
345	312.2	58.9	46.83	6	1.948	94.8
414	303.4	46.3	45.51	6	2.408	98.4
378	271.2	80.3	40.68	6	1.241	78.6
412	321.8	69.7	48.27	6	1.696	91.0
516	352.3	53.9	52.85	6	2.402	98.4
517	339.8	81.5	50.97	6	1.532	87.4
552	380.8	74.5	57.12	6	1.878	94.0
690	396	62.3	59.40	6	2.335	98.0

Average Confidence Level (%) = 90%

Table 4-14 Confidence Level Calculated from the Measured RM Values (Sawyer Aggregate at the Finer Limit Gradation and OMC)

Bulk Stress (kPa)	RM (MPa)	SD (MPa)	EE (MPa)	Sample Number	$Z_{\alpha/2}$	Confidence Level (%)
84	51.7	17.7	7.76	6	0.142	71.6
104	75.3	9.3	11.30	6	0.001	99.8
125	79.4	9.6	11.91	6	0.000	100.0
136	104.9	20.8	15.74	6	0.032	93.6
171	99.2	9.8	14.88	6	0.000	100.0
205	106.1	8.7	15.92	6	0.000	100.0
276	141.7	19.7	21.26	6	0.004	99.2
345	145.6	14.1	21.84	6	0.000	100.0
414	151.2	10.1	22.68	6	0.000	100.0
378	163.2	9.1	24.48	6	0.000	100.0
412	160.0	9.3	24.00	6	0.000	100.0
516	181.1	13.5	27.17	6	0.000	100.0
517	188.2	19.5	28.23	6	0.000	100.0
552	191.8	19.5	28.77	6	0.000	100.0
690	213.0	12.4	31.95	6	0.000	100.0

Average Confidence Level (%) = 98%

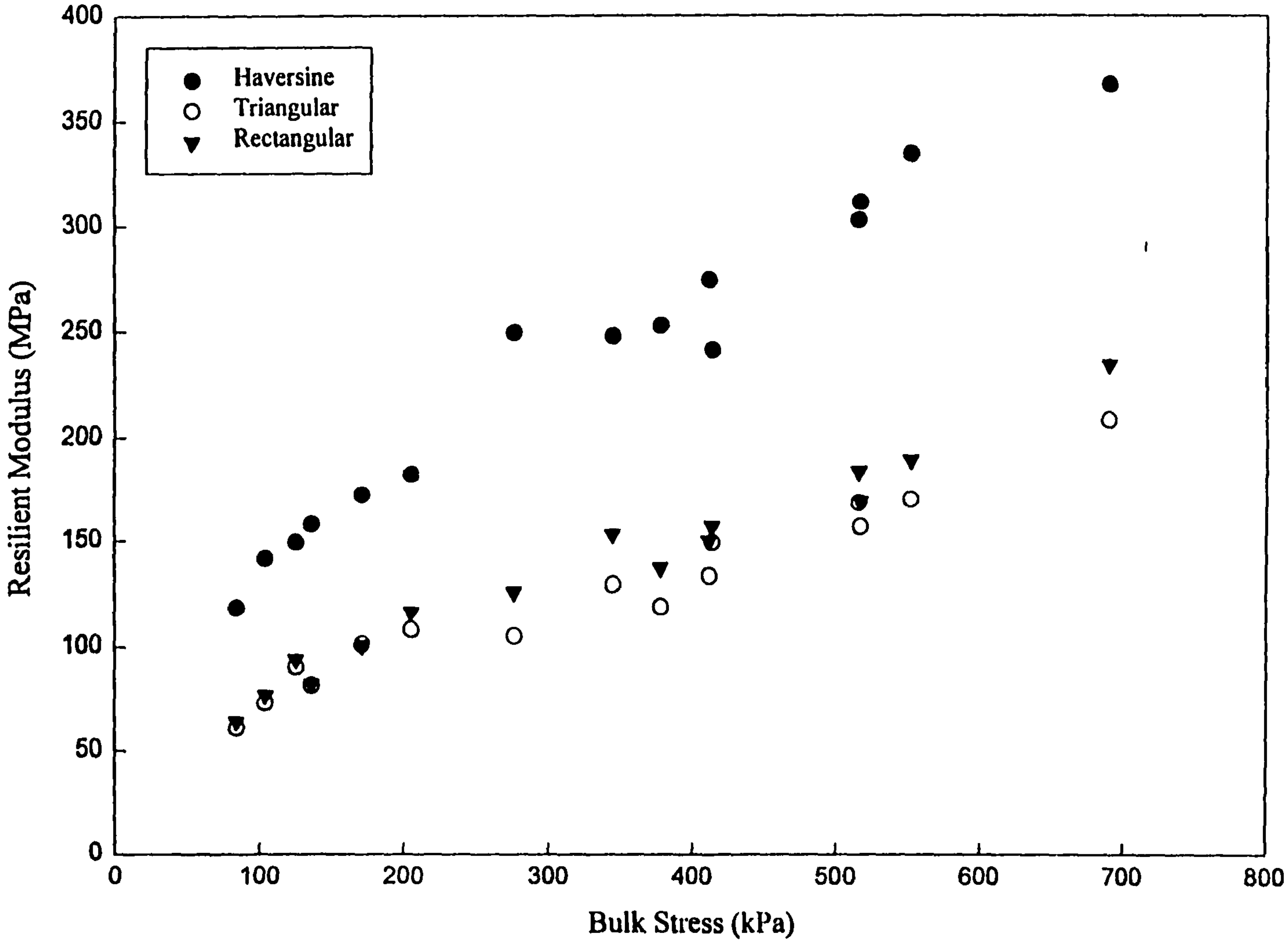

Figure 4-1 Mean RM Values from the Different Loading Waveforms (RS Aggregate)

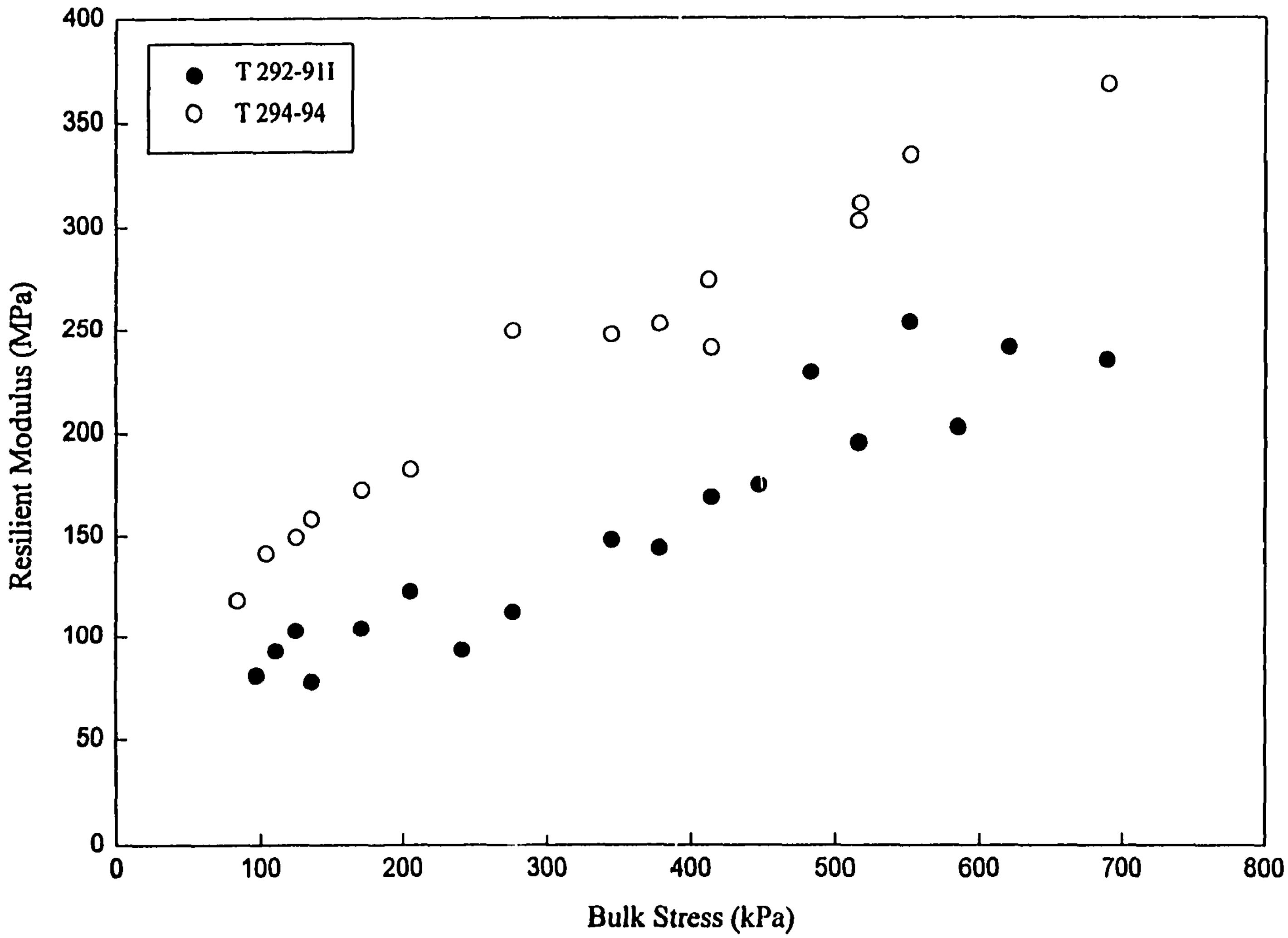

Figure 4-2 Mean RM Values from the AASHTO T 292-91I and T 294-94 Methods (RS Aggregate)

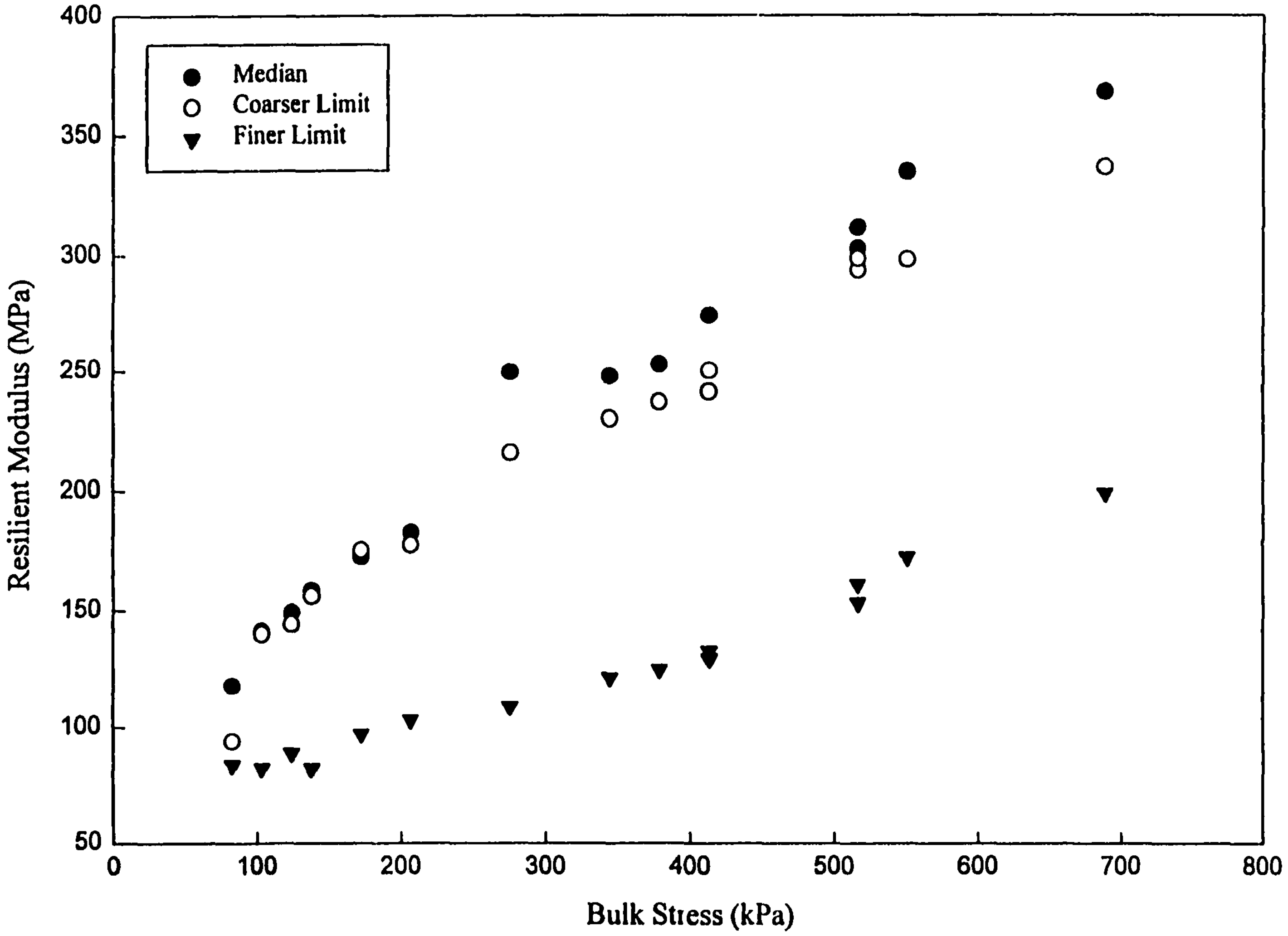

Figure 4-3 Mean RM Values of the RS Aggregate at the Different Gradations

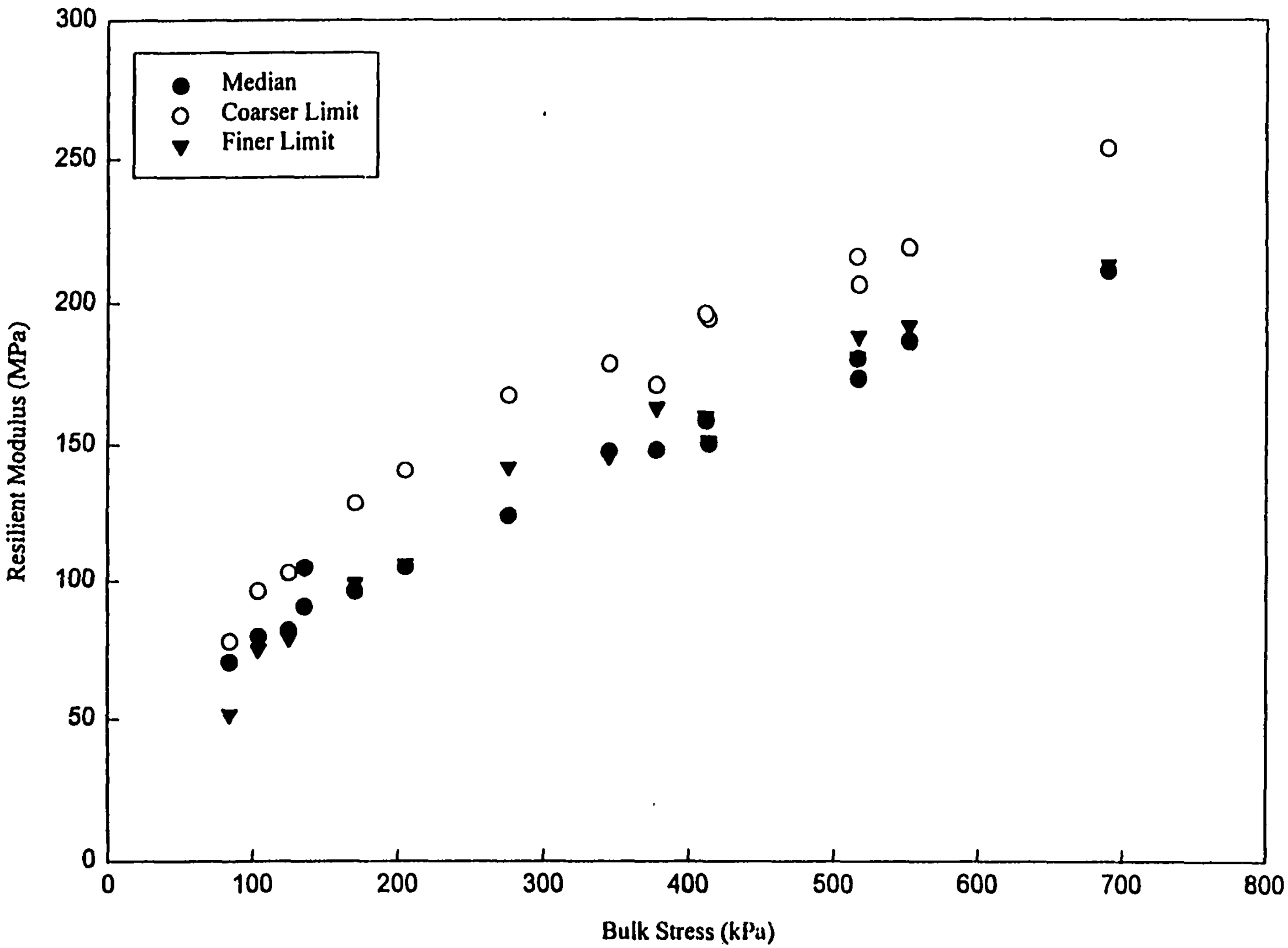

Figure 4-4 Mean RM Values of the Sawyer Aggregate at the Different Gradations

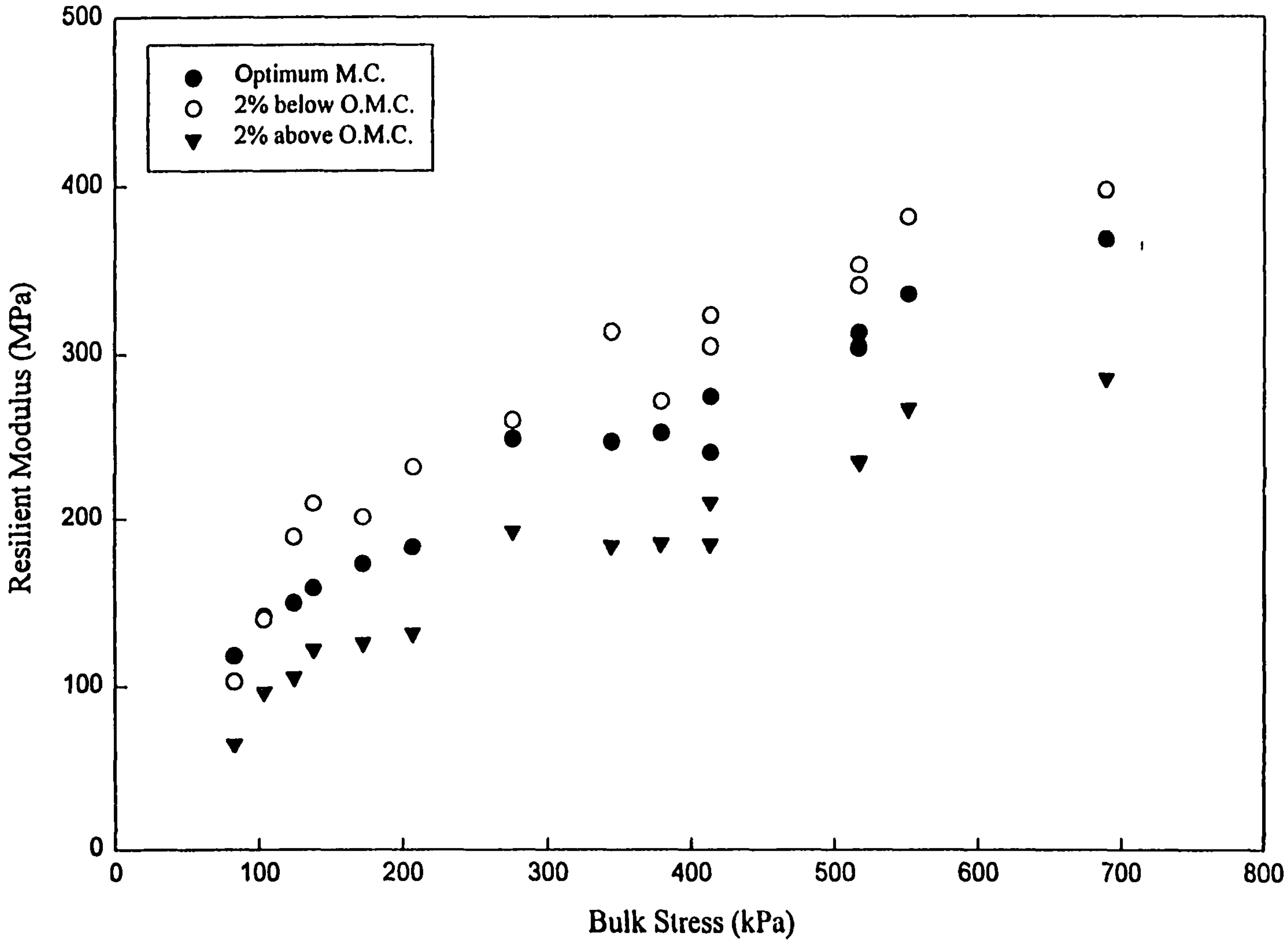

Figure 4-5 Mean RM Values of the RS Aggregate at the Different Moisture Contents

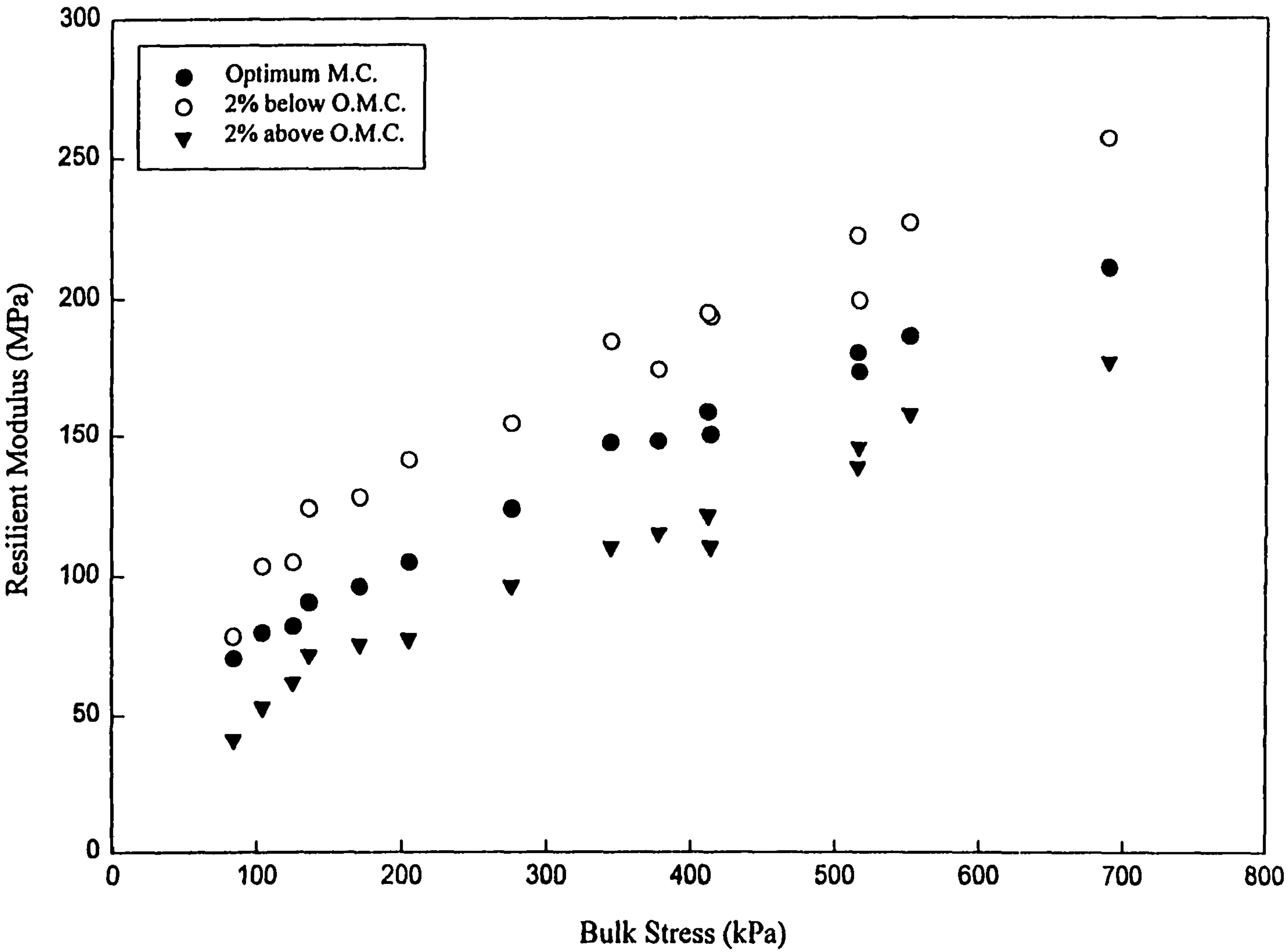

Figure 4-6 Mean RM Values of the Sawyer Aggregate at the Different Moisture Contents

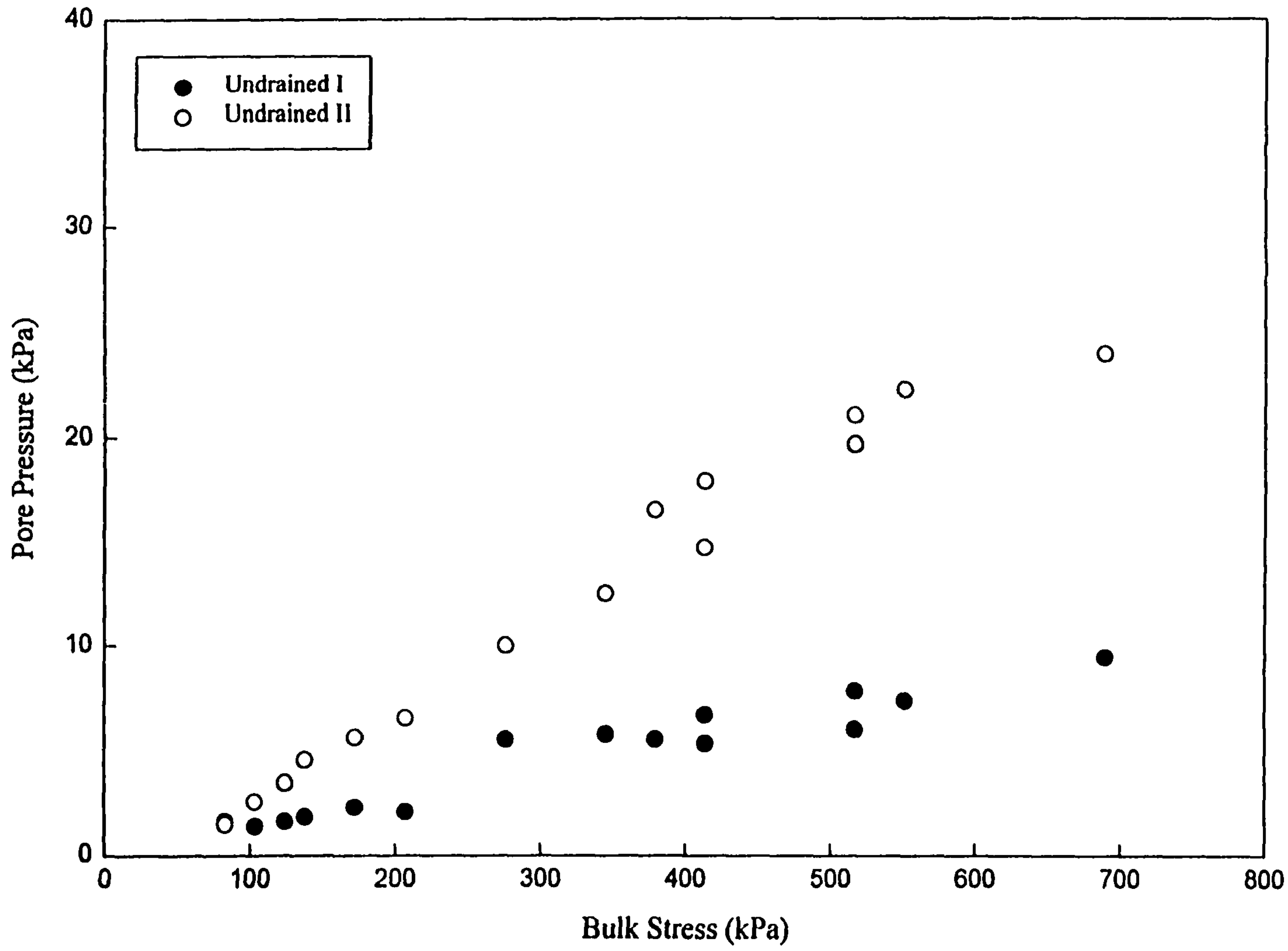

Figure 4-7 Pore Pressure Measured in the Undrained I and Undrained II RM Tests (RS Aggregate)

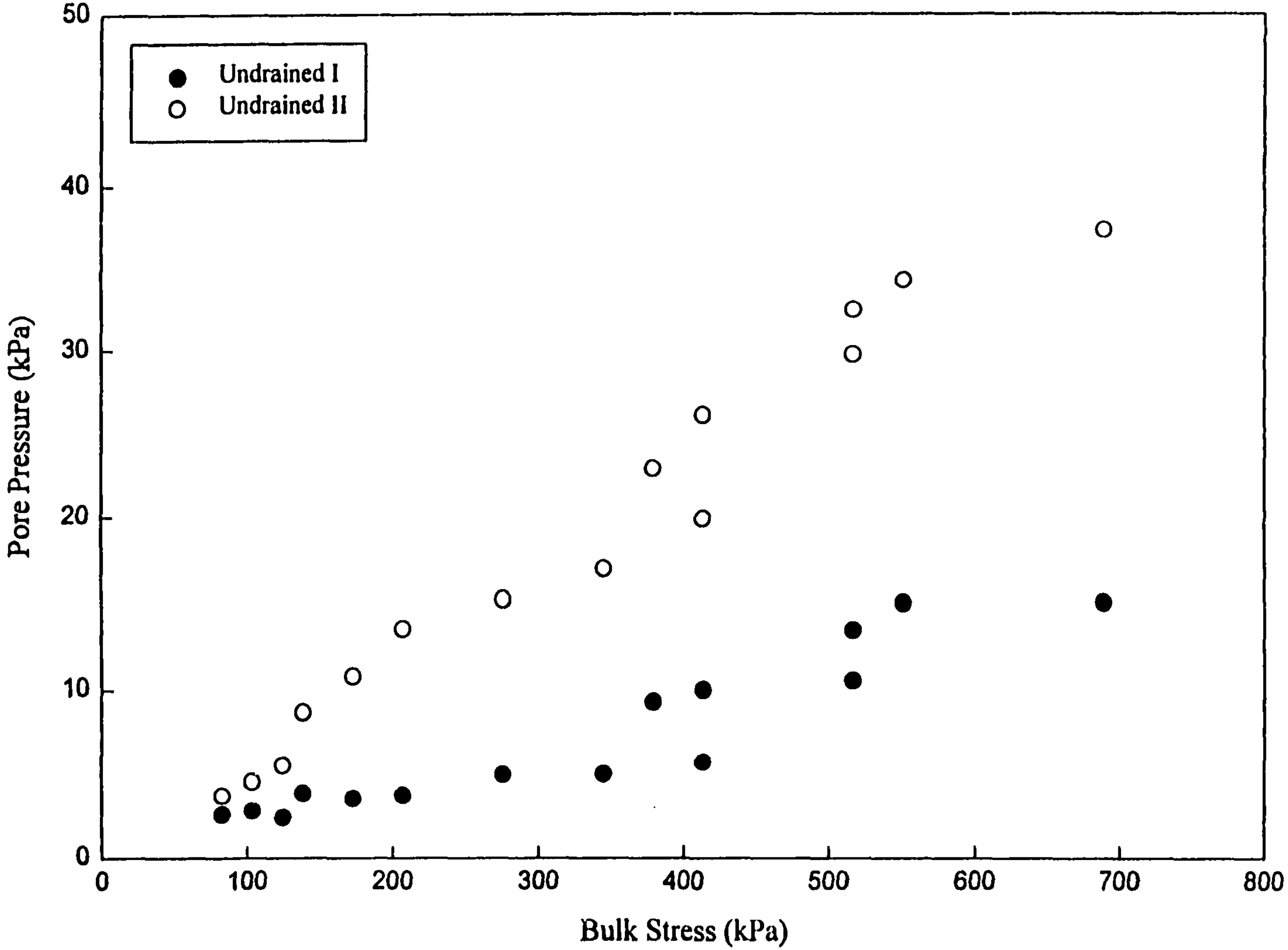

Figure 4-8 Pore Pressure Measured in the Undrained I and Undrained II RM Tests (Sawyer Aggregate)

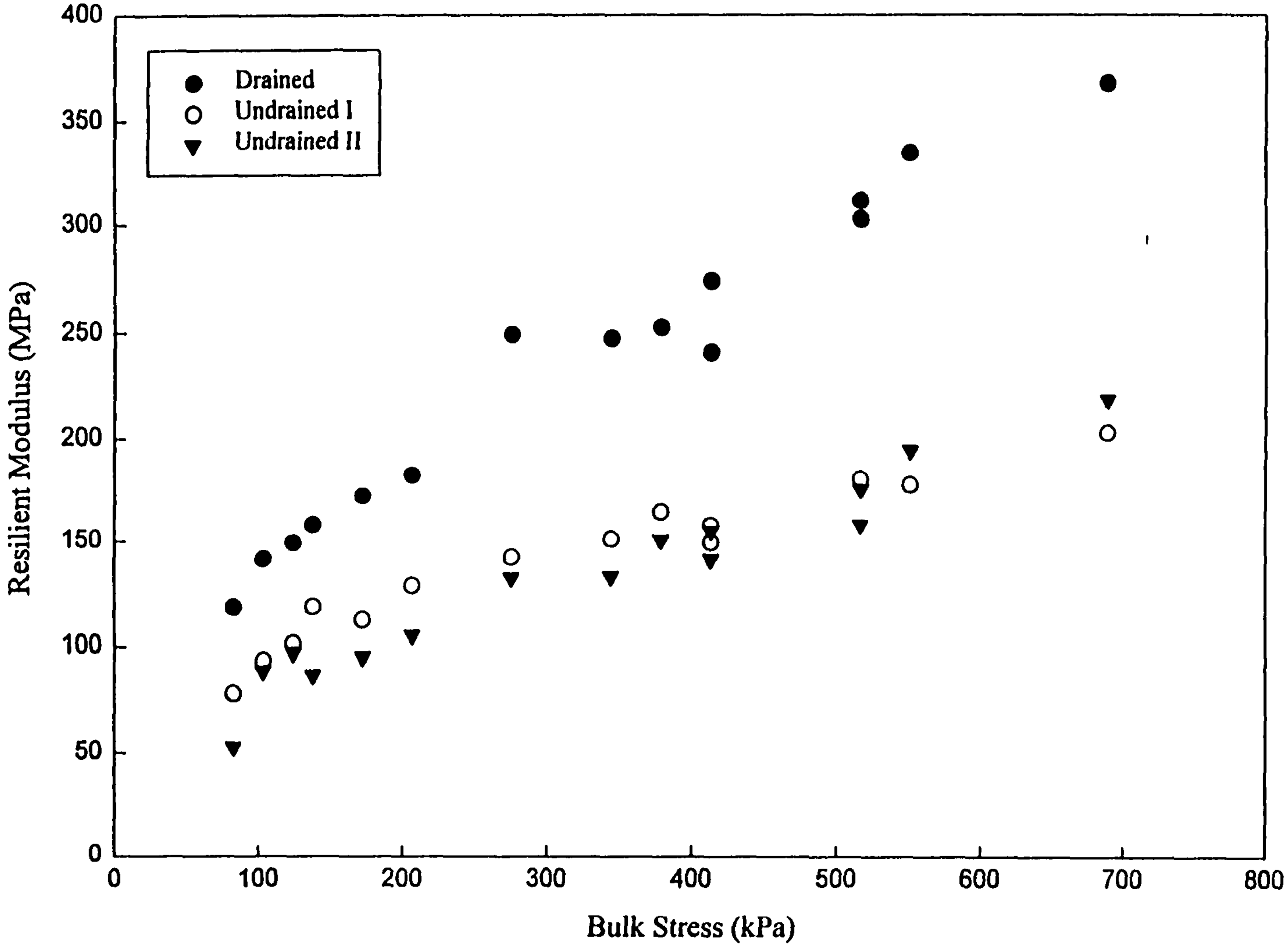

Figure 4-9 Mean RM Values of the RS Aggregate from the Drained and the Undrained Tests

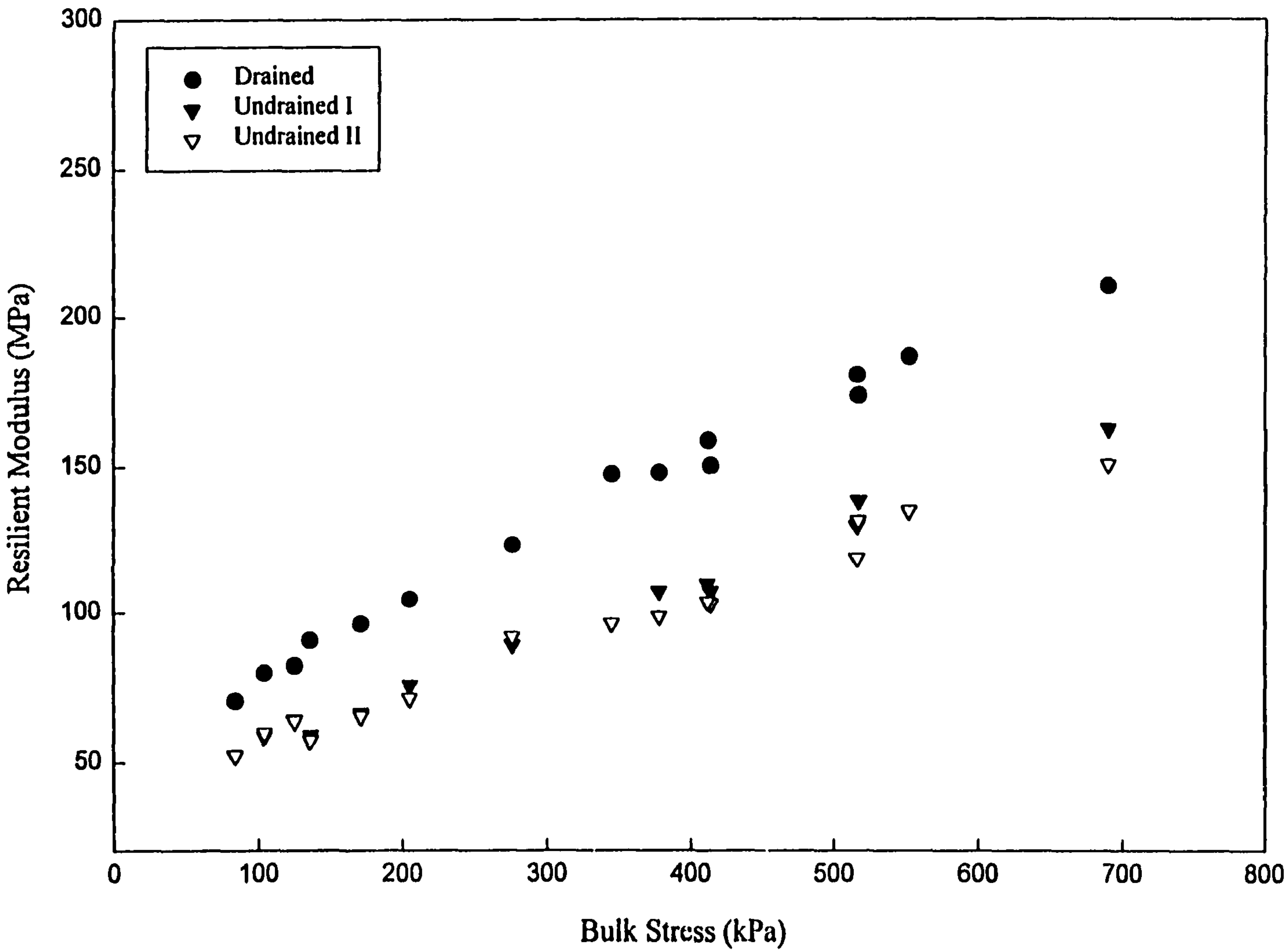

Figure 4-10 Mean RM Values of the Sawyer Aggregate from the Drained and the Undrained Tests

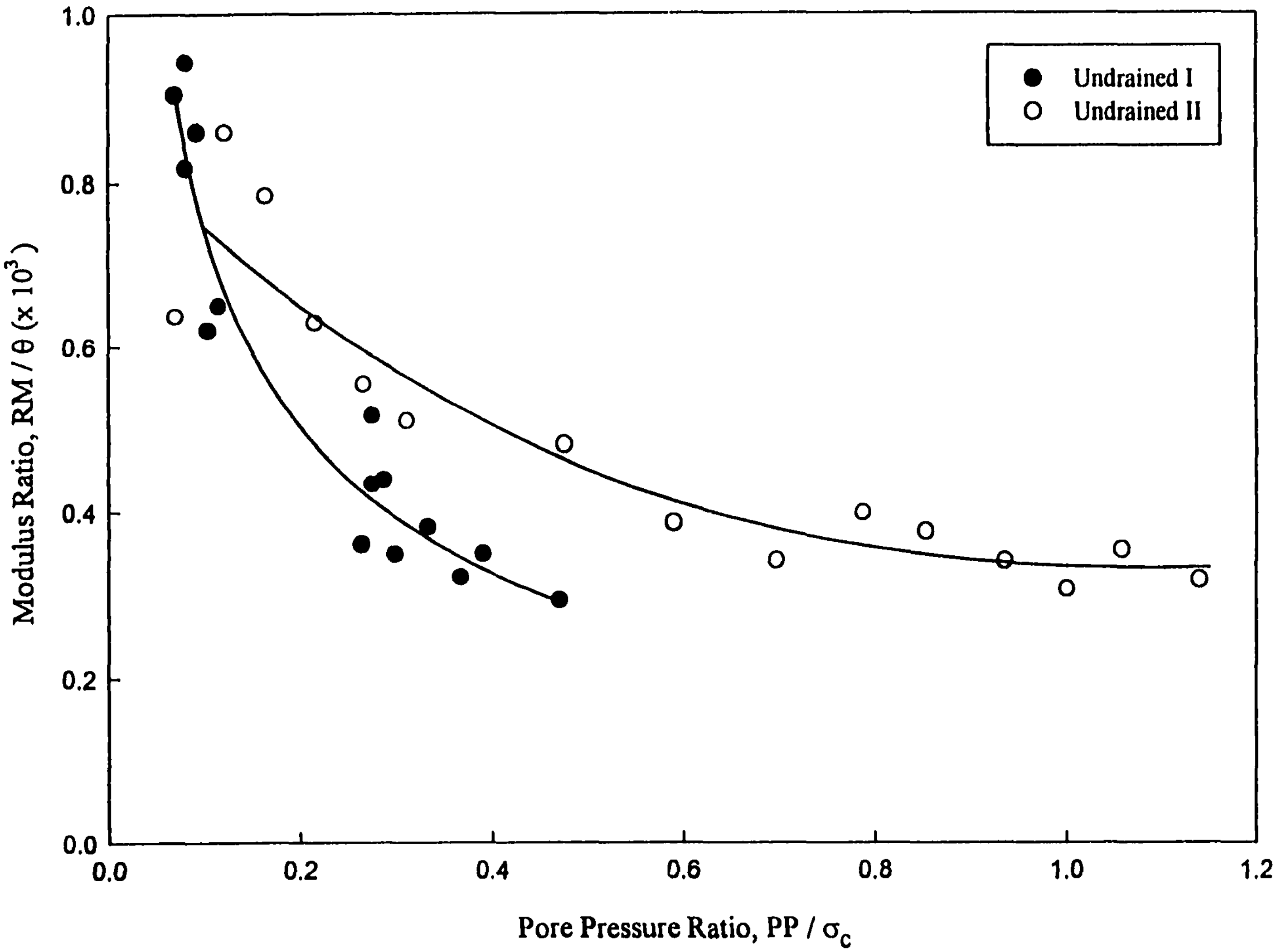

Figure 4-11 Variation of the Modulus Ratio with the Pore Pressure Ratio for the RS Aggregate

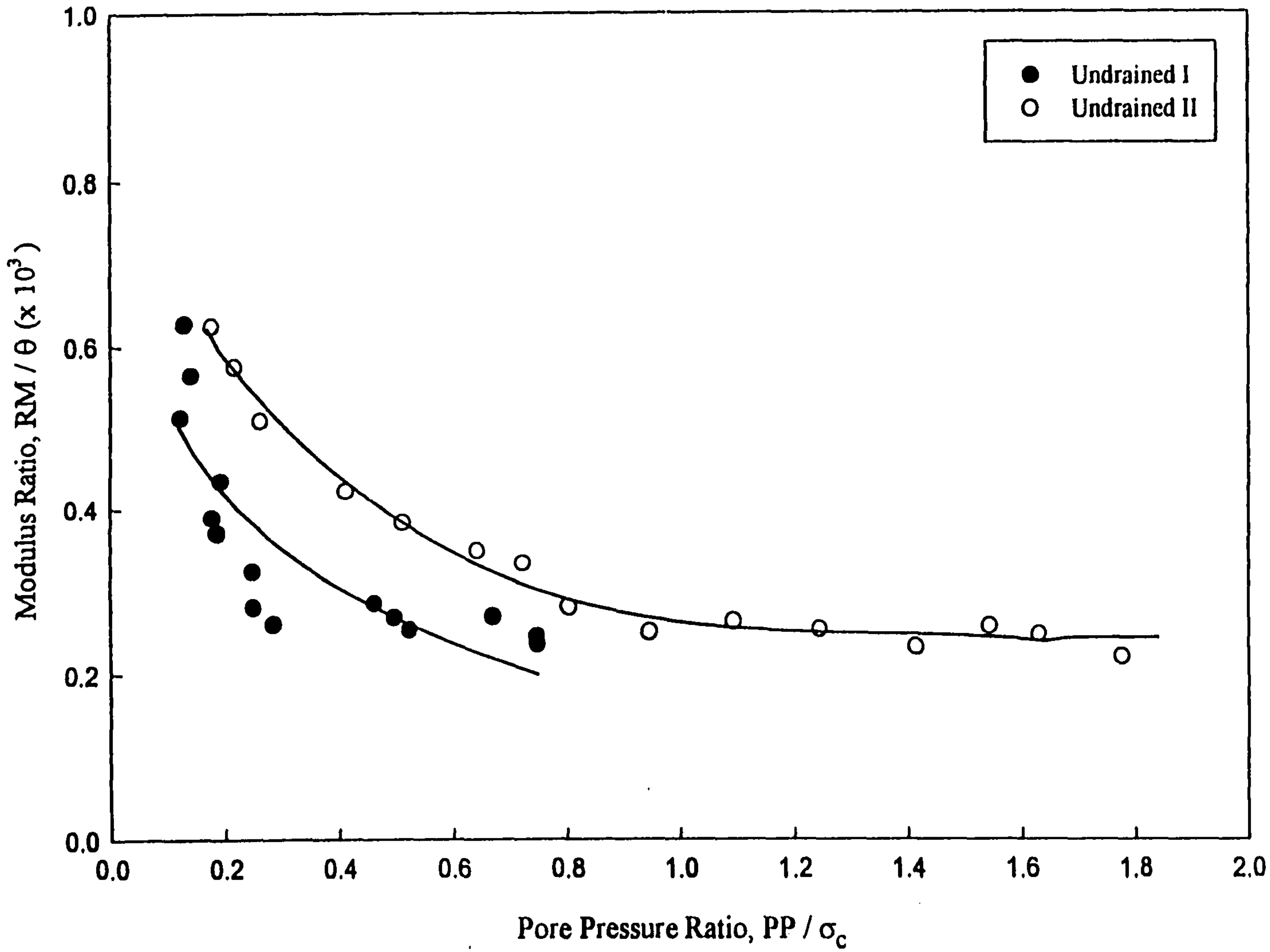

Figure 4-12 Variation of the Modulus Ratio with the Pore Pressure Ratio for the Sawyer Aggregate

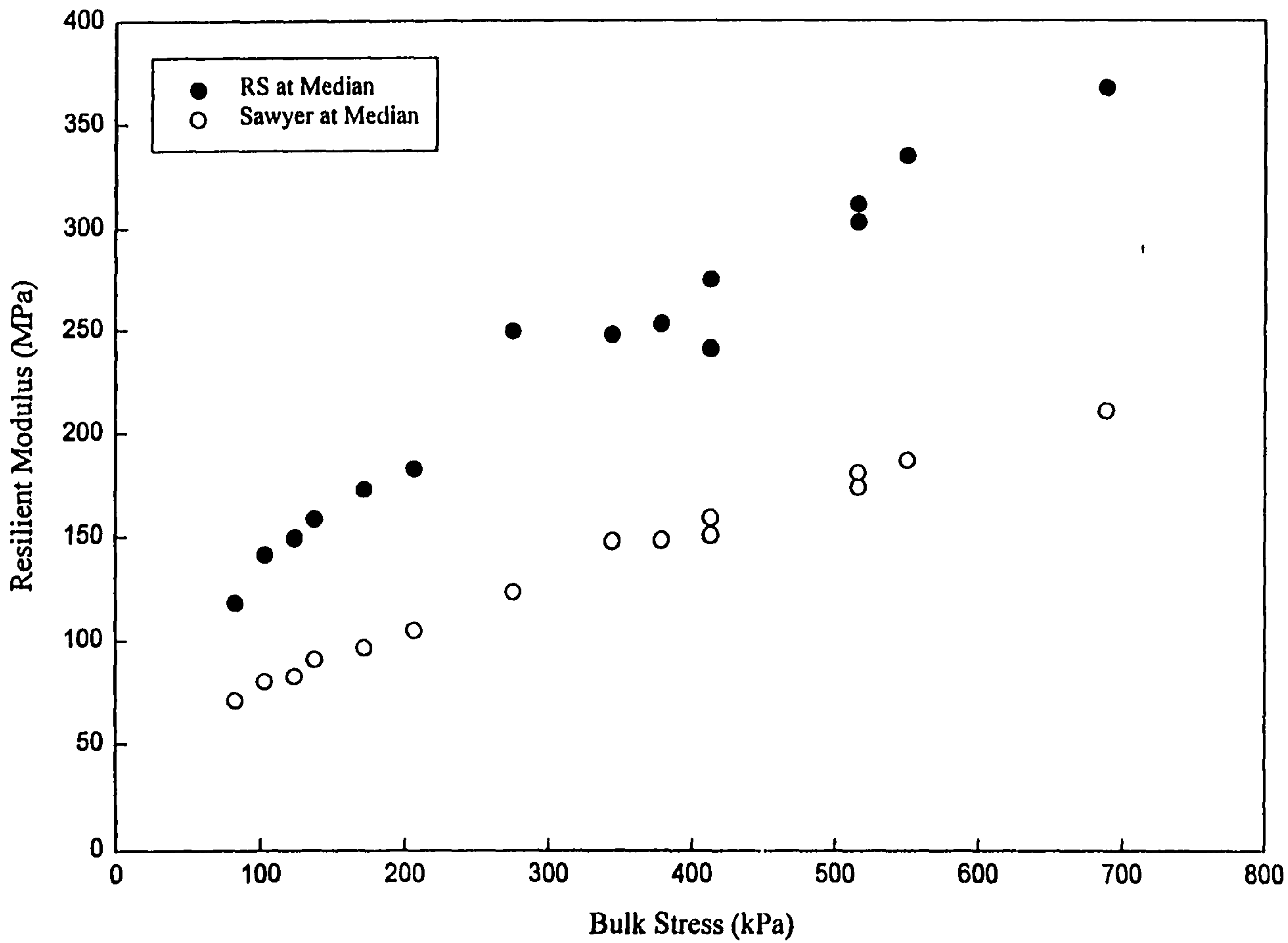

Figure 4-13 Mean RM Values of the RS and the Sawyer Aggregates at the Median Gradation

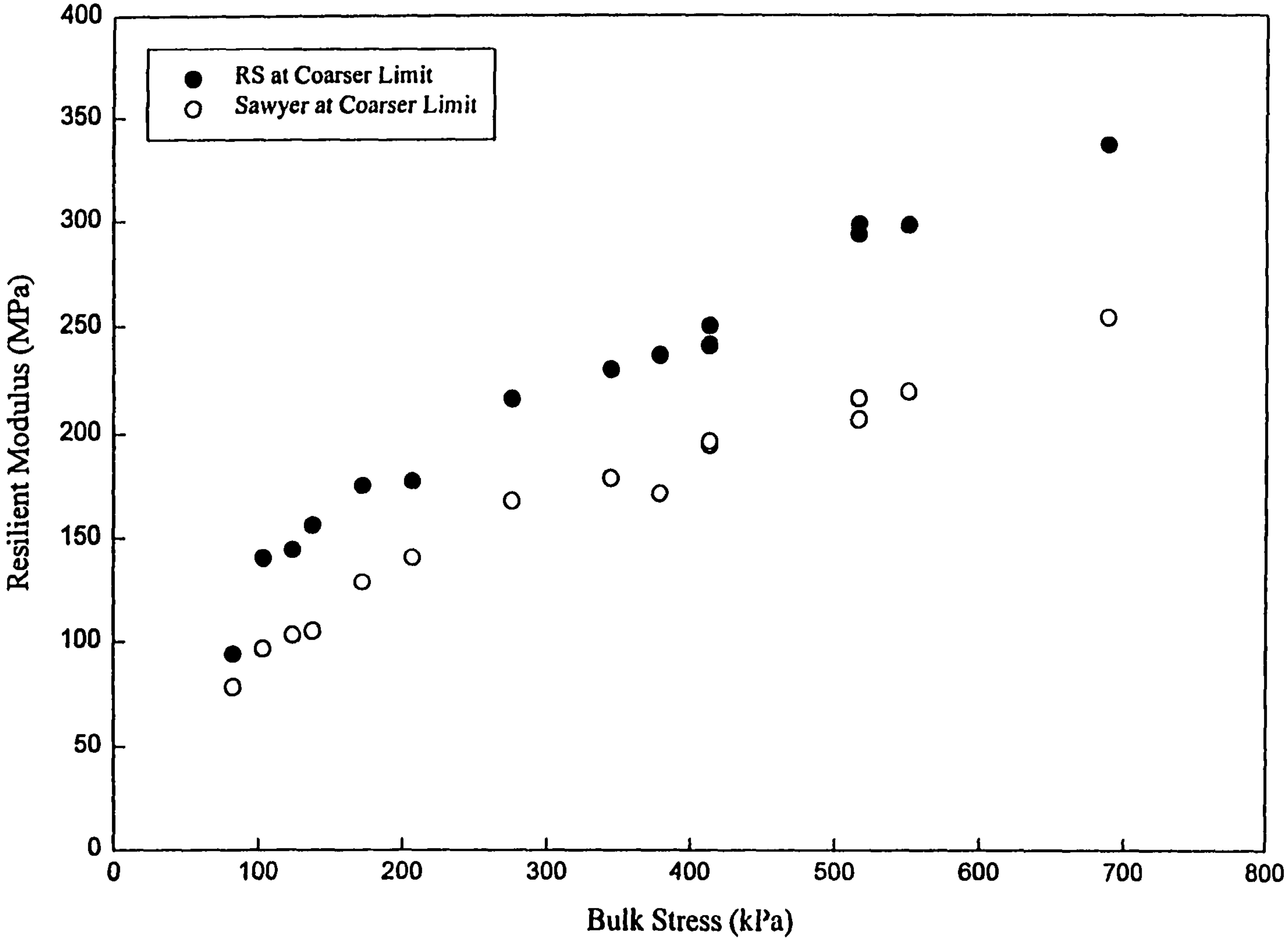

Figure 4-14 Mean RM Values of the RS and the Sawyer Aggregates at the Coarser Limit Gradation

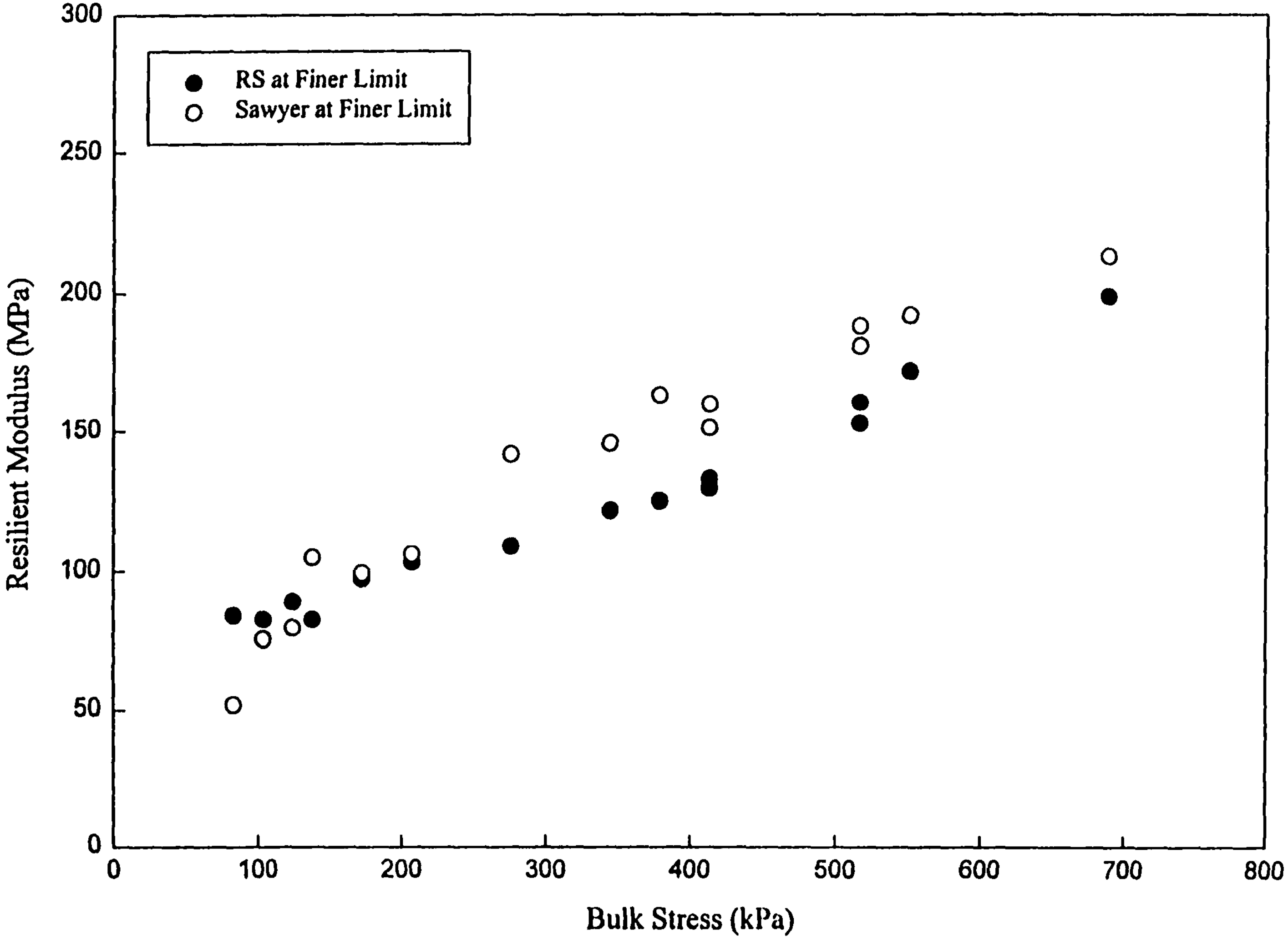

Figure 4-15 Mean RM Values of the RS and the Sawyer Aggregates at the Finer Limit Gradation

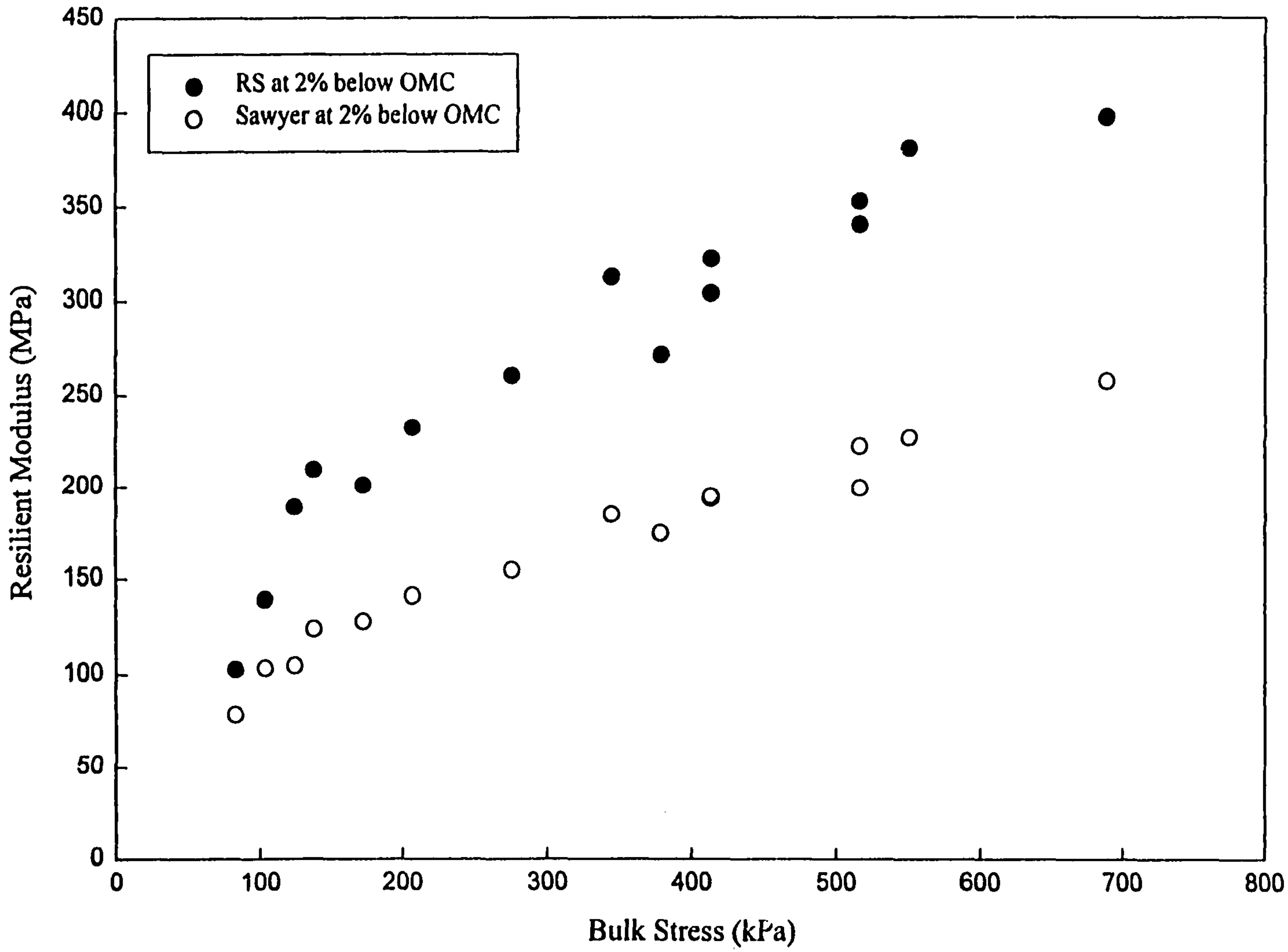

Figure 4-16 Mean RM Values of the RS and the Sawyer Aggregates at 2% below the OMC

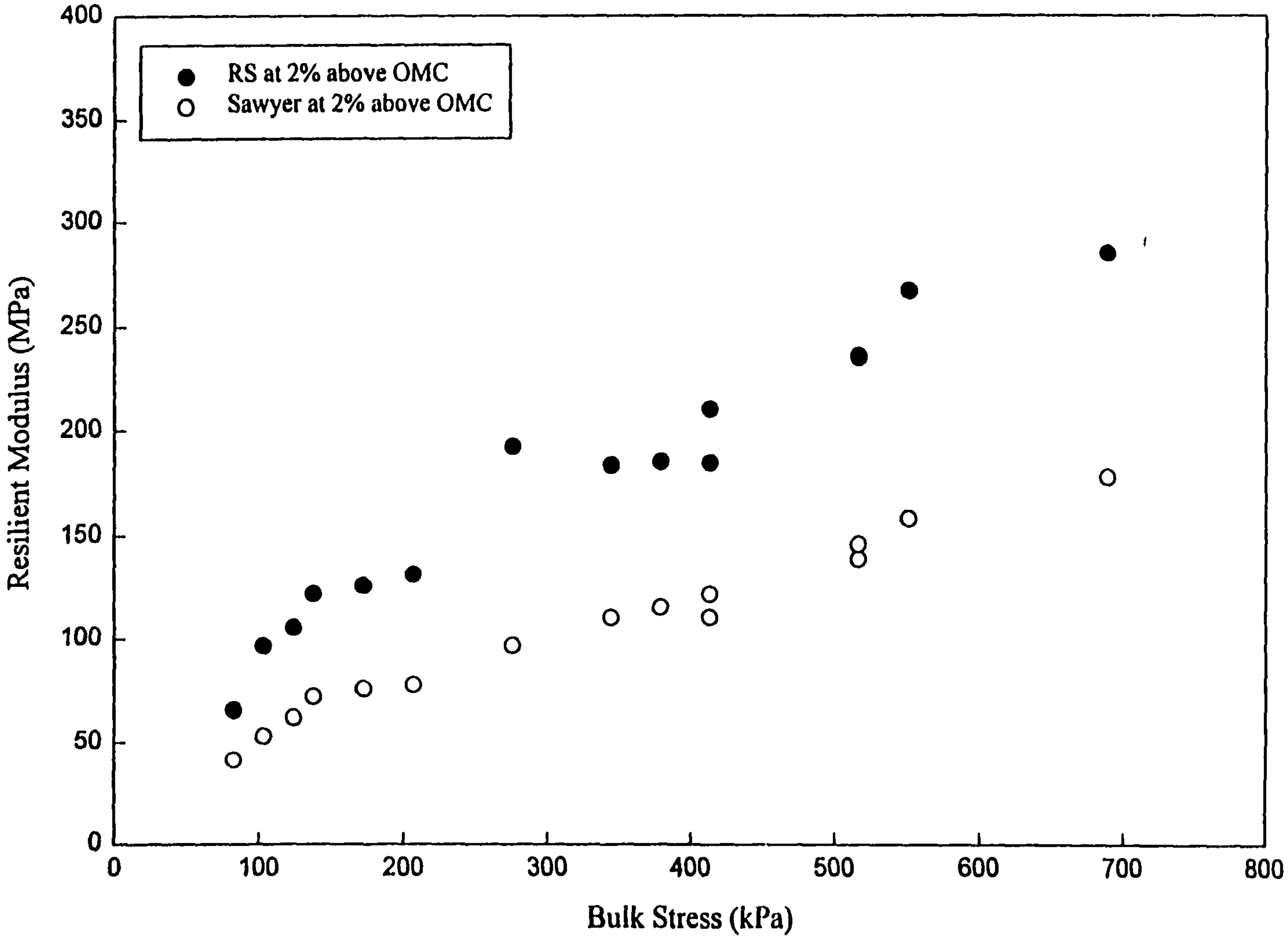

Figure 4-17 Mean RM Values of the RS and the Sawyer Aggregates at 2% above the OMC

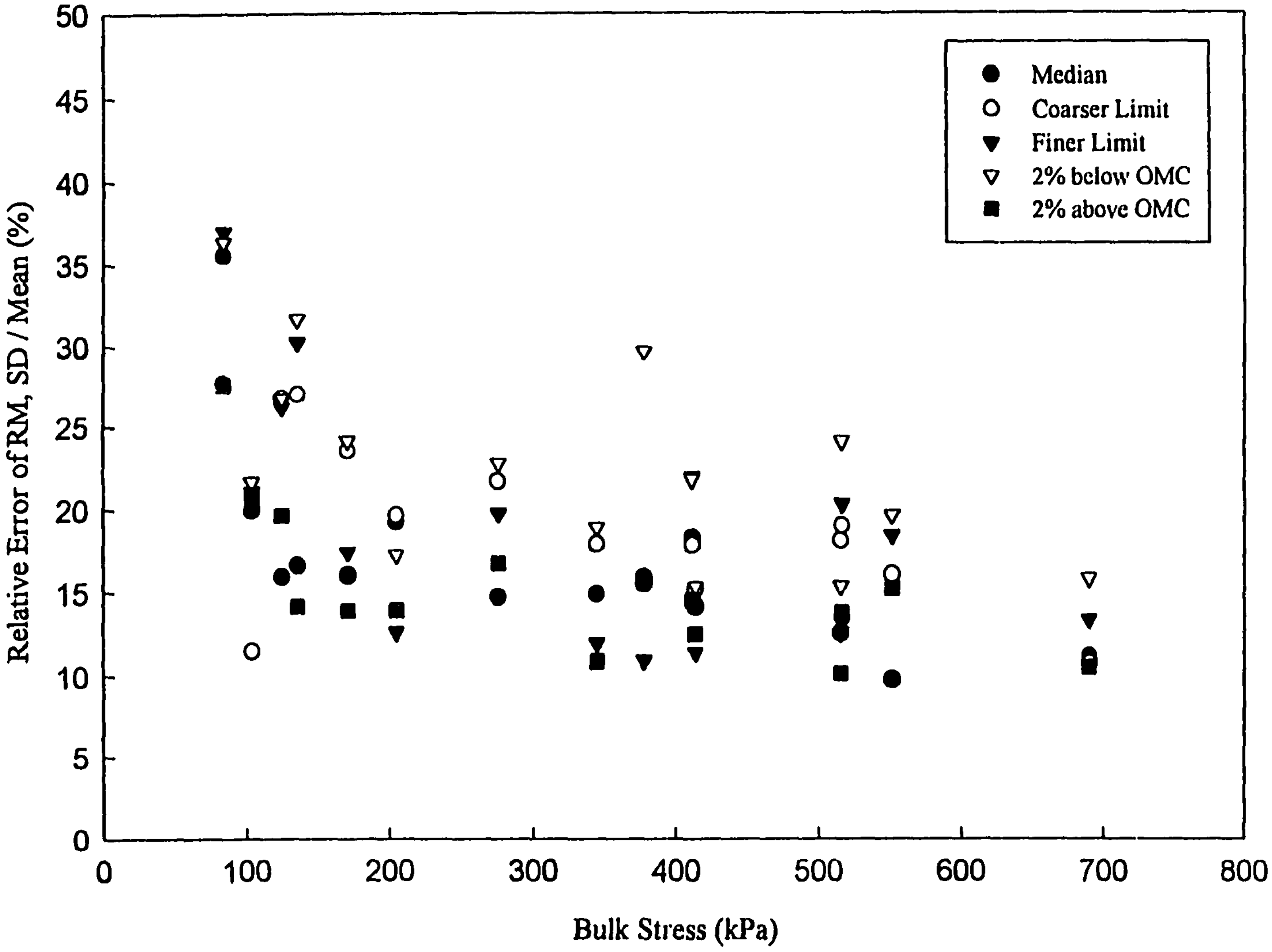

Figure 4-18 Relative Error of the RM Measurement with the Bulk Stress for the RS Aggregate

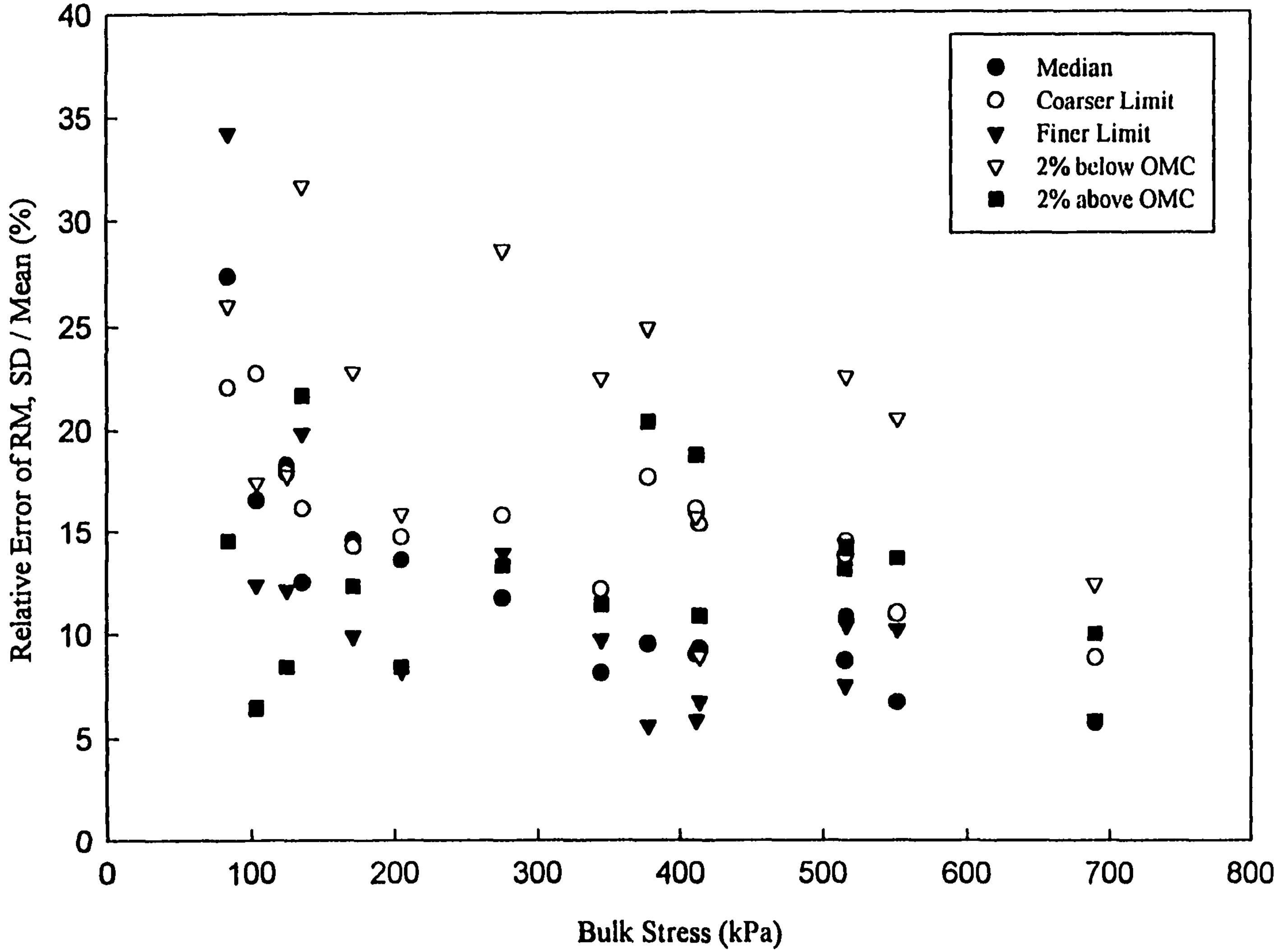

Figure 4-19 Relative Error of the RM Measurement with the Bulk Stress for the Sawyer Aggregate

CHAPTER 5

STATISTICAL CORRELATIONS

5.1 Introduction

Statistical correlations between RM and engineering index properties are useful in practice because the engineering index properties are less difficult and inexpensive to evaluate. This chapter presents the discussion on the statistical analysis conducted on the obtained RM values. The material model parameters, k_1 and k_2 , of the k-θ model are determined and discussed in light of different influencing factors. Finally, multiple linear regression models between the RM and various contributing factors are developed for the two aggregates used in this study.

5.2 Determination of Material Model Parameters

According to the AASHTO T 294-94 method, the RM values for aggregate materials can be conveniently represented by using the k-θ model given in Eq. (2-2). The k-θ model, which requires the determination of the regression constants k_1 and k_2, describes the resilient characteristics of the aggregate materials under varying bulk stress. Although this model has been widely used in pavement analyses, and recommended by AASHTO design procedure, it does not consider other important effects, for example, the shear effect which is believed to have an influence on RM values (Uzan 1985).

In the present study, regression analyses were performed to evaluate the k_1 and k_2 values for the different RM testing cases. Since six duplicate RM tests were conducted for each case, the RM values from five tests which resulted in 75 RM values were used to evaluate the k_1 and k_2 values, and the rest 15 RM values from one RM test were used to validate the obtained k-θ model. The parameters k_1 and k_2 thus obtained for all the cases are presented in Table 5-1 for the RS and the Sawyer aggregates, respectively. The standard deviations (SD) for the obtained k_1 and k_2 values along with the coefficient of determination (R^2) are also presented in the above table. In view of Table 5-1, as RM values changed due to different influencing factors, the k_1 values also vary significantly; however, the variation in k_2 is relatively insignificant. The k_1 and k_2 values in Table 5-1 conform the observations made by Rada and Witczak (1981) where six different granular materials were investigated (Table 2-3). By comparing the k_1 and k_2 values in the case of median gradation with the values obtained by Chen (1994) (Table 2-5), it can be observed that they are in the same range.

Typical values of k_1 and k_2 for unbound base and subbase aggregate materials are recommended by AASHTO Design Guide (AASHTO 1993) in case of no laboratory RM values provided in practical pavement design (Table 2-6). It can be observed that the moisture effect is considered in these values, and it has significant influence on the recommended k_1 values. Generally, the trend of increasing moisture content resulting in decrease of k_1 values can be observed among the AASHTO recommended values (Table 2-6). By comparing the k_1 and k_2 values with those obtained in this study, for example, the dry, damp, and wet conditions specified by AASHTO are compared with the cases of 2% below the OMC, the OMC, and 2% above the OMC used in this study, it can be observed that the AASHTO recommended k_1 values are much higher (about 1.5 time) than those obtained in this study. The k_2 values obtained in this study fall in the AASHTO suggested range (0.5 to 0.7). Since the RM values predicted from the k-θ model are much sensitive in terms of the k_1 parameter, therefore, it is possible that AASHTO recommended k_1 values are over-estimated for aggregate base materials. If so, it may result in an unconservative design in practice.

It should be noted that the k-θ model in Eq. (2-2) did not yield high R^2 values in the regression analyses for some cases. For example, in the cases having the finer limit gradation and 2% below the OMC for the RS aggregate, the R^2 values are found to be 0.6585 and 0.6628, respectively. For the Sawyer aggregate, the R^2 values are 0.6698 and 0.6673, respectively, for the cases having 2% below the OMC and the undrained I. Figures 5-1 through 5-14 show the graphical representations of the experimentally observed RM values and the k-θ model predicted RM values. In these figures, the experimentally measured RM data were not used in developing the corresponding k-θ models, therefore, these data can effectively examine the developed models. Generally, it can be observed that the k-θ models developed in this study can reasonably predict the RM values for the two aggregates in the corresponding cases.

Figures 5-15 and 5-16 show the variation of k_1 and k_2 as a function of gradation factor defined as percent passing the No. 200 sieve (0.075 mm). It can be observed that the RS aggregate produced higher k_1 value than that of the Sawyer aggregate. As the percentage of fines increases, the k_1 values decrease. However, there is not a clear trend present for the k_2 values. All k_2 values are located near the $k_2 = 0.5$ line as the percentage of fines increases. For both of the aggregates investigated in this study, the coarser limit gradation yielded the highest k_1 values, and the finer limit gradation yielded the lowest k_1 values.

Figures 5-17 and 5-18 show the variation of k_1 and k_2 as a function of the moisture content. It can be observed that as the moisture content increases, the k_1 decreases, and the k_2 increases but insignificantly. It is interesting to note that both of the aggregates exhibit a similar trend line for k_1 and k_2. Hence, it may be postulated that this relationship (form) is independent of the aggregate type. If so, it has significance in terms of practical application, because the k_1 and k_2 values for other moisture contents can be obtained using an interpolation.

Figures 5-19 and 5-20 show the variation of k_1 and k_2 as a function of the drainage condition. As the RM values decrease due to the change in drainage condition, for the RS aggregate, the k_1 value decreases from 10633 to 6538 kPa and the k_2 value decreases from 0.5403 to 0.4718. For the Sawyer aggregate, the corresponding decrease in k_1 is 7098 to 4818 kPa, while the k_2 values remain nearly unchanged at 0.5. Obviously, drainage condition has a significant effect on the k_1 values.

It is believed that the k_1 and k_2 values obtained in the present study can be used in the AASHTO pavement design equation when the pavement bases are constructed with the aggregates used in this study.

5.3 Statistical Correlations between RM and Other Material Properties

5.3.1 Overview of RM Correlation Model

The AASHTO Guide for Design of Pavement Structure (AASHTO 1993) suggests the use of resilient modulus to characterize the base material or subgrade soil. However, due to the complexity involved and the need for specialized equipment for RM testing, it is desirable to explore approximate methods for the estimation of RM values. Statistical correlations between RM and engineering index properties are often found to be useful in practical applications since the basic engineering index properties are relatively easy and inexpensive to evaluate. Previous research indicated that the RM values are neither intimately related to the PI of the granular materials nor to the conventional soil classification system used (Rada and Witczak 1981; Zaman et al. 1994). California Bearing Ratio (CBR) is widely used as an indicator of the strength characteristics of subgrade soils and aggregates in pavement design. However, due to the differences in the laboratory testing conditions, it was found that CBR values usually do not correlate well with the RM values (Rada and Witczak 1981; Chen 1994). Pandey (1996) attempted to correlate RM with unconfined compressive strength (U_C) and elastic modulus (EM) of a raw and stabilized marginal aggregate, called Meridian aggregate. It was found that the RM values cannot be correlated with the U_C and the EM values, for both raw and stabilized aggregates, with a reasonable degree of accuracy. Chen (1994) developed a correlation between the RM and the cohesion and friction angle; it was found that this correlation provided a better prediction of RM values for aggregate materials than that with CBR. A possible explanation is that deformation characteristics for the conventional triaxial compression test and RM test are more similar than those between the RM and the CBR tests (Chen 1994).

From the experimental results presented in Chapter 4, it is evident that the stress state has the most significant influence on the RM values. Gradation and moisture content also significantly influence the RM values of aggregate materials (Figures 4-3 and 4-5). It has been observed that the cohesion, friction angle, and unconfined compressive strength of both the aggregates used here are mainly dominated by the gradation and the moisture contents (Table 3-4). Therefore, an attempt is made here to develop a regression model in which RM is correlated with the stress state, static material properties, gradation, and moisture content.

5.3.2 Evaluation of Model Variables

Based on the discussion in section 5.3.1, all the possible influencing factors on the RM values could be listed as: bulk stress (θ), deviator stress (σ_d), moisture content (MC), gradation (percent passing No.200 sieve), cohesion (C), friction angle (ϕ), and unconfined compressive strength (U_C). The percent of fines passing No.200 (0.075mm) sieve is used to represent the gradation variable. It should be noted that some of these factors may not be independent and some factors may not have a significant influence on the RM values. In order to obtain the most significant factors to correlate RM values, the Least Square (LS) method was used to evaluate these factors in the light of their importance on the RM values.

The elastic modulus (EM) was not incorporated in the regression analysis partly because of the sensitivity in determining the EM values based on the initial slope of the stress-strain curves. A better approach to determine EM would be conducting tests with unloading-reloading cycles, but it was not pursed in this study.

Table 5-2 shows all the possible models with associated R^2 values. Here no parameters are estimated. It is observed that bulk stress (θ)gives the best one variable model with R^2 values of 0.4617 and 0.6672 for the RS and the Sawyer aggregates. The cohesion (C), friction angle (ϕ), and the unconfined compressive strength (U_C) have very little direct influence on the RM values. So the two variable models are evaluated based on the combination of variables of θ, σ_d, MC, and No.200. It was found that the best two variable model is the θ and MC model, R^2 values of 0.6162 and 0.8542 were obtained for the RS and the Sawyer aggregates, respectively. Furthermore, the three variable models were evaluated based on adding one variable (σ_d or No.200) in the θ, MC model. It was found that adding the No.200

variable in the θ, MC model is more critical than adding the σ_d variable for the RS aggregate in terms of increasing the R^2 value. The R^2 value increased from 0.6162 to 0.7534 due to adding the No.200 variable was observed for the RS aggregate. However, for the Sawyer aggregate, the R^2 value only slightly increases from 0.8542 to 0.8544 due to adding the No.200 variable. Additionally adding the variables of σ_d, C, ϕ, and U_C can not increase the R^2 value from the θ, MC, and No.200 model for both aggregates. Therefore, the three variables of θ, MC, and No.200 are the most significant influencing factors as such they are further used in establishing the multiple linear regression model.

5.3.3 Determination of Model Parameters

Based on the above obtained contributing factors, a multiple regression model between RM and these factors can be established. Multiple regression analysis can be either linear or nonlinear depending on the form of the unknown parameters. Usually, the functional form of the model known from physical phenomena leads to nonlinear regression analysis. In the present study, the analysis is restricted to linear regression because a prior knowledge of nonlinearity in parameters is not available. Also, in the cases of nonlinear regression, the evaluation of the parameters is difficult and a solution may not converge if the proper form of the nonlinearity in parameters is not included (Mendenhall and Sincich 1992).

In the present study, a multiple linear regression model between the RM and the bulk stress (θ), moisture content (MC), and aggregate gradation (No.200) is formulated as

$$RM / Pa = A_0 + A_1 * \theta / Pa + A_2 * MC + A_3 * No.200 \qquad (5\text{-}1)$$

where A_0, A_1, A_2, and A_3 are regression constants, and Pa is the atmospheric pressure

(101.3 kPa). The purpose of introducing the constant pressure of Pa is to obtain the non-dimensional coefficients A_i.

A databases having the RM values for different cases was established first in order to evaluate the regression coefficients A_i for the two selected aggregates. Six duplicate RM tests and five different factors considered in the experimental program (the median, finer limit, and coarser limit gradations, 2% below OMC, 2% above OMC) resulted in a total of 450 RM values. These RM values were separated into two groups. Test 1 through Test 5 having a total of 375 RM values were used to develop the model, and all of Test 6 having a total of 75 RM values were used to validate the obtained models. The following numerical values of the regression constants were obtained for the RS and the Sawyer aggregates, respectively:

$A_0 = 3433$; $A_1 = 354$; $A_2 = -291$; and $A_3 = -138$ (RS aggregate).

$A_0 = 1637$; $A_1 = 250$; $A_2 = -177$; and $A_3 = -0.81$ (Sawyer aggregate).

The coefficients of determination (R^2) of the regression analyses are 0.7534 and 0.8544 for the RS and the Sawyer aggregates, respectively. A comparison between the experimental observations and the model predictions is presented in Figures 5-19 and 5-20 for the RS and the Sawyer aggregates, respectively. It can be observed that both models reasonably fit the experimental data. By comparing the multiple regression model with the k-θ model in terms of R^2 values, it can be observed that both models present the same level of R^2 values. However, the multiple regression model has a wide range of applications since the RM values of the two selected aggregates at different gradations and moisture contents can be predicted by using the multiple regression model, and hence it has a significance in the practical pavement design.

Table 5-1 Material Parameters k_1 and k_2 of the RS and the Sawyer Aggregates

Material Type	Case	k_1 (kPa)	SD (kPa)	k_2	SD	R^2
RS	Median	10633	2191	0.5403	0.0344	0.8139
	Coarser Limit	11037	2746	0.5213	0.0415	0.7351
	Finer Limit	8710	2171	0.4603	0.0418	0.6585
	2% below OMC	14306	4181	0.5091	0.0489	0.6628
	2% above OMC	5909	1278	0.5893	0.0359	0.8317
	Undrained I	9198	3422	0.4718	0.0624	0.6271
	Undrained II	6539	1738	0.5247	0.0444	0.8034
Sawyer	Median	7098	930	0.5162	0.0219	0.9061
	Coarser Limit	8110	1550	0.5235	0.0319	0.8272
	Finer Limit	5554	852	0.5610	0.0255	0.8996
	2% below OMC	11063	2860	0.4728	0.0434	0.6698
	2% above OMC	2815	606	0.6281	0.0357	0.8518
	Undrained I	4846	1516	0.5092	0.0532	0.6673
	Undrained II	4819	1181	0.5166	0.0409	0.7712

Table 5-2 Measure of Fit for Models with Different Variables

Number in Model	Variables	R^2 (RS)	R^2 (Sawyer)
1	No.200	0.1233	0.0185
1	MC	0.1545	0.1870
1	σ_d	0.3065	0.4551
1	θ	0.4617	0.6672
2	MC, No.200	0.2917	0.1870
2	σ_d, No.200	0.4298	0.4736
2	σ_d, MC	0.4610	0.6421
2	θ, σ_d	0.4623	0.6674
2	θ, No.200	0.5850	0.6857
2	θ, MC	0.6162	0.8542
3	θ, σ_d, No.200	0.5856	0.6860
3	σ_d, MC, No.200	0.5981	0.6421
3	θ, MC, σ_d	0.6168	0.8542
3	θ, MC, No.200	0.7534	0.8544
4	θ, MC, No.200, σ_d	0.7539	0.8544
5	θ, MC, No.200, σ_d, C	0.7555	0.8568

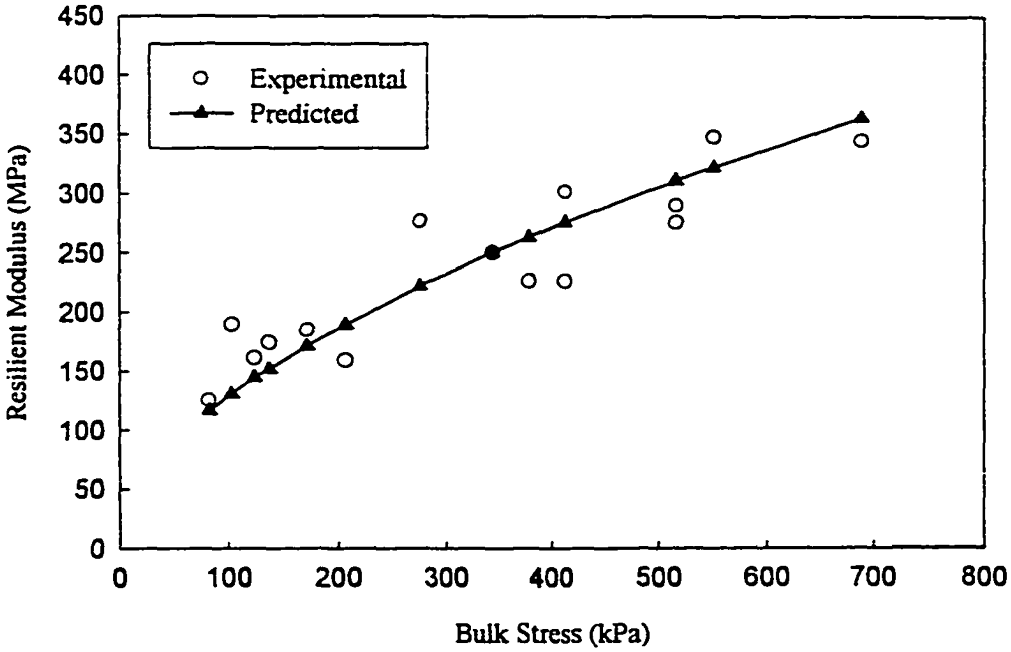

Figure 5-1 Experimental and the k-θ Model Predicted RM Values of the RS Aggregate at the Median Gradation

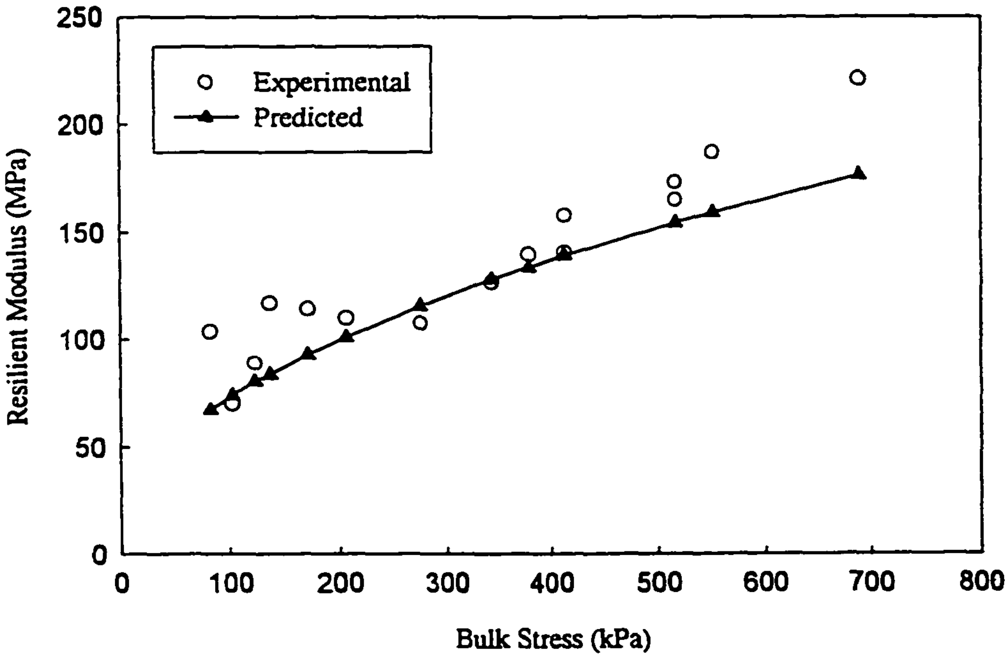

Figure 5-2 Experimental and the k-θ Model Predicted RM Values of the RS Aggregate at the Finer Limit Gradation

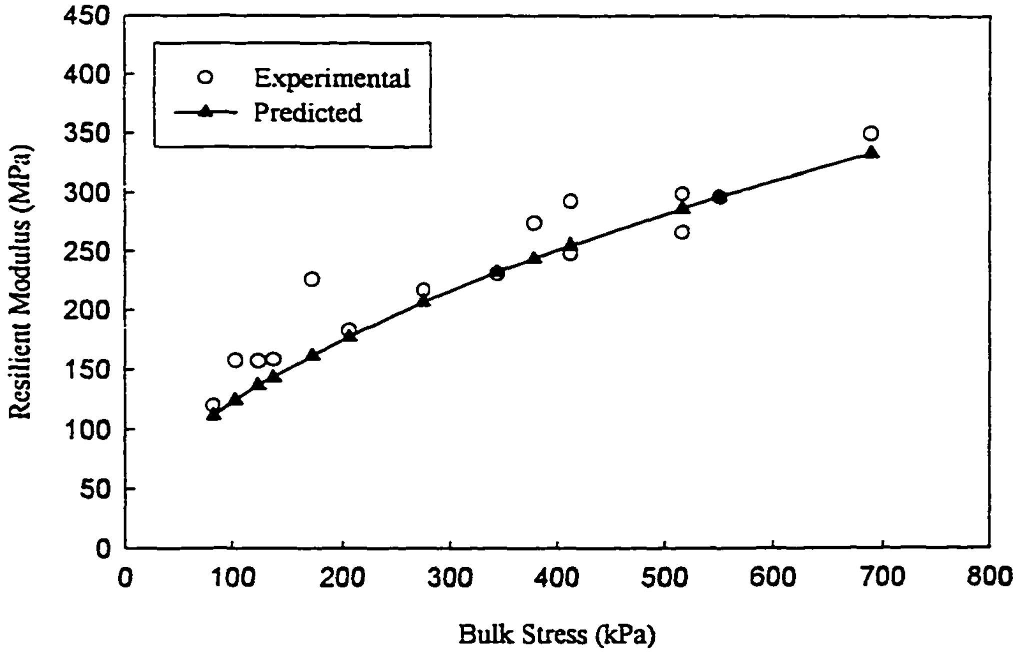

Figure 5-3 Experimental and the k-θ Model Predicted RM Values of the RS Aggregate at the Coarser Limit Gradation

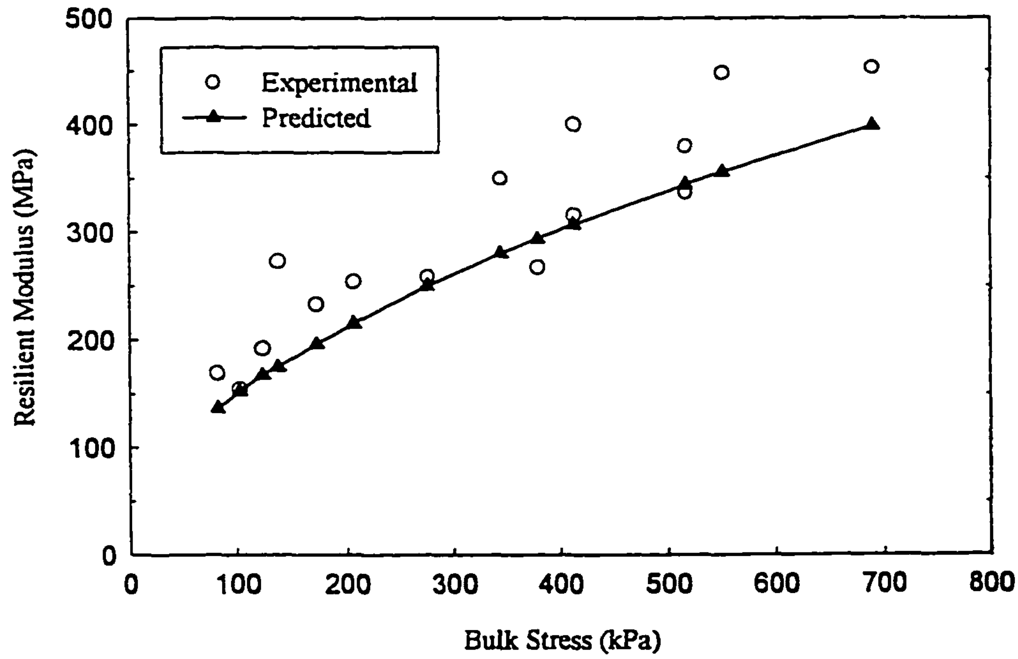

Figure 5-4 Experimental and the k-θ Model Predicted RM Values of the RS Aggregate at 2% below the OMC

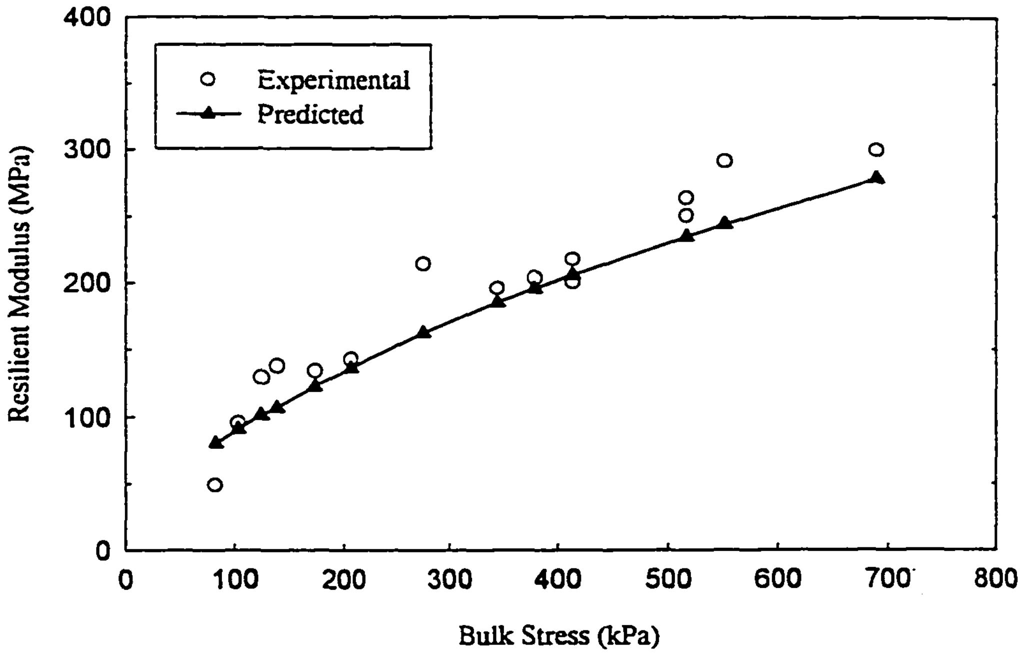

Figure 5-5 Experimental and the k-θ Model Predicted RM Values of the RS Aggregate at 2% above the OMC

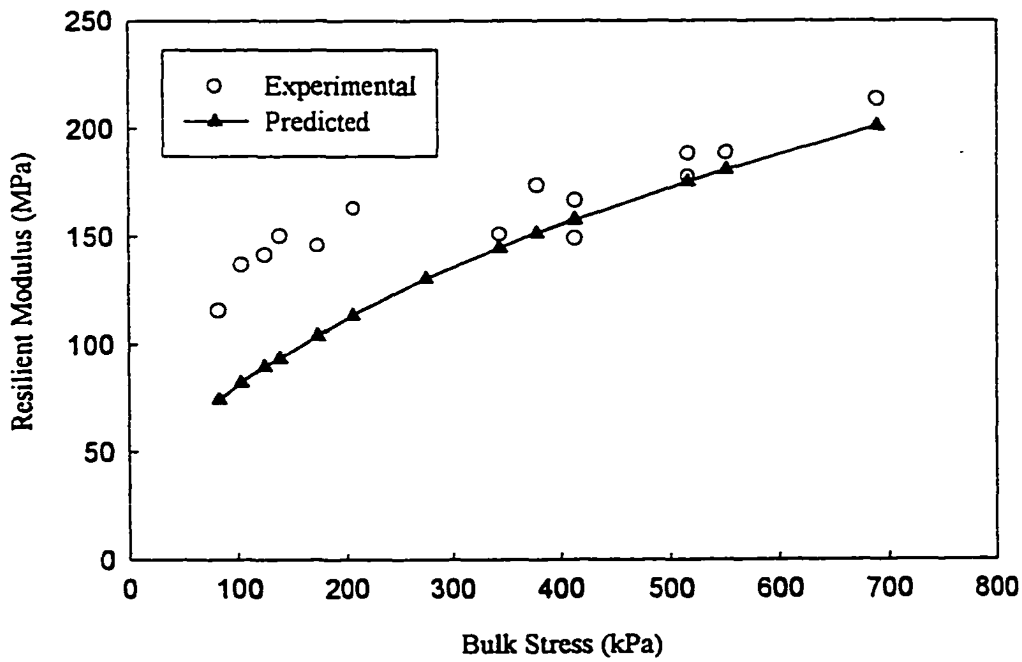

Figure 5-6 Experimental and the k-θ Model Predicted RM Values of the RS Aggregate from the Undrained I Test

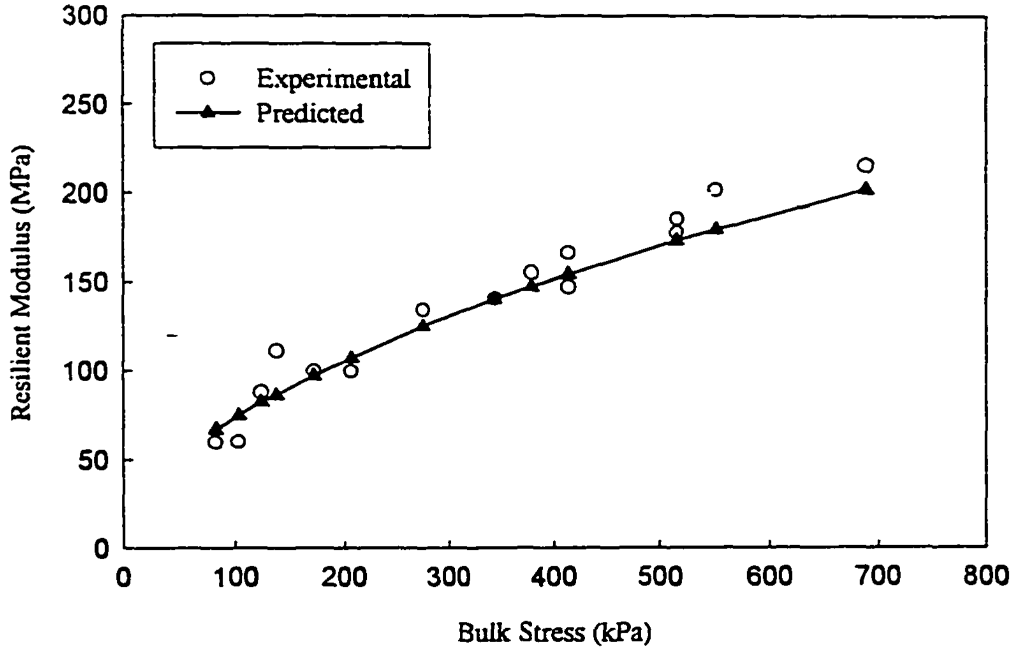

Figure 5-7 Experimental and the k-θ Model Predicted RM Values of the RS Aggregate from the Undrained II Test

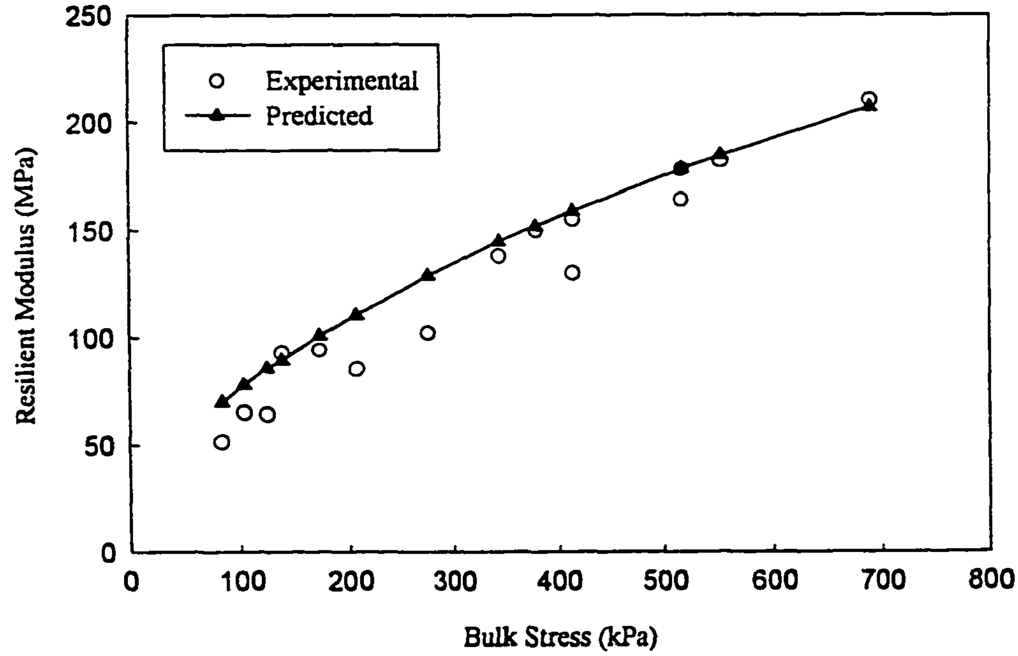

Figure 5-8 Experimental and the k-θ Model Predicted RM Values of the Sawyer Aggregate at the Median Gradation

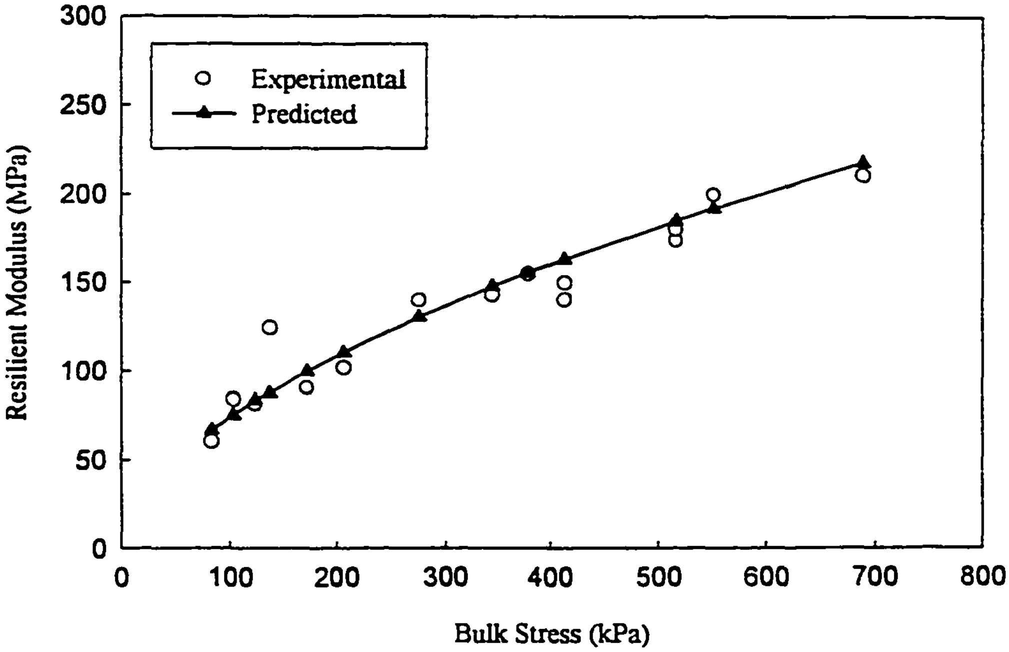

Figure 5-9 Experimental and the k-θ Model Predicted RM Values of the Sawyer Aggregate at the Finer Limit Gradation

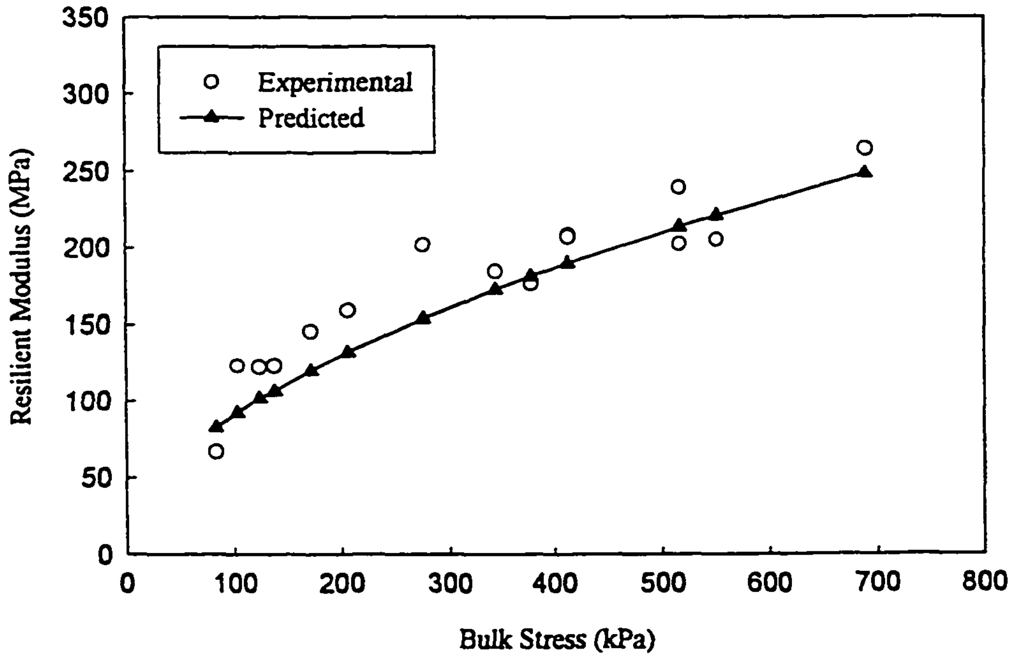

Figure 5-10 Experimental and the k-θ Model Predicted RM Values of the Sawyer Aggregate at the Coarser Limit Gradation

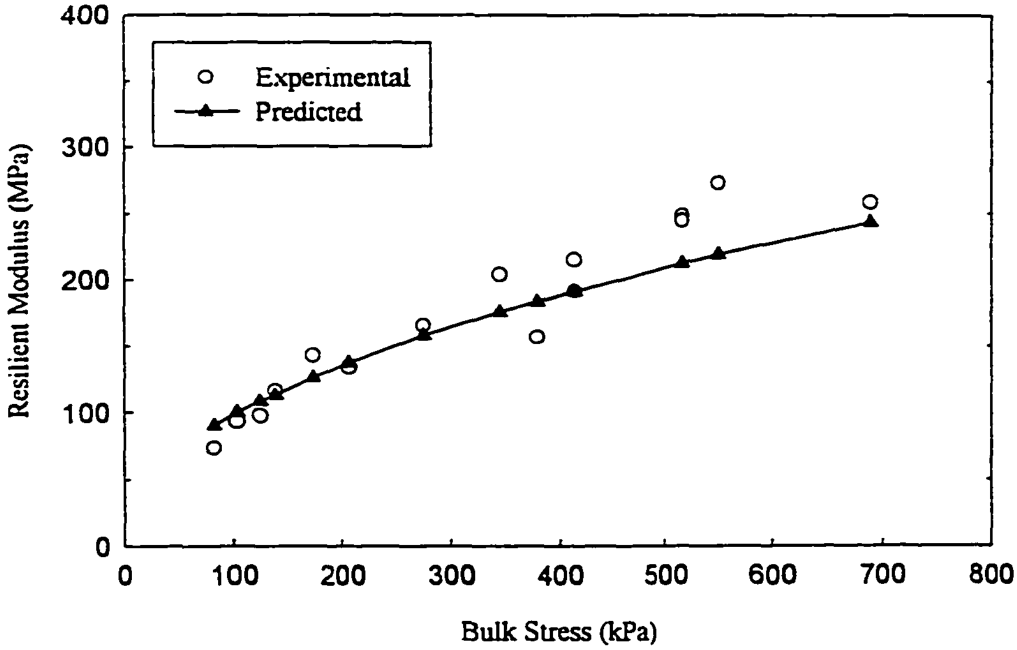

Figure 5-11 Experimental and the k-θ Model Predicted RM Values of the Sawyer Aggregate at 2% below the OMC

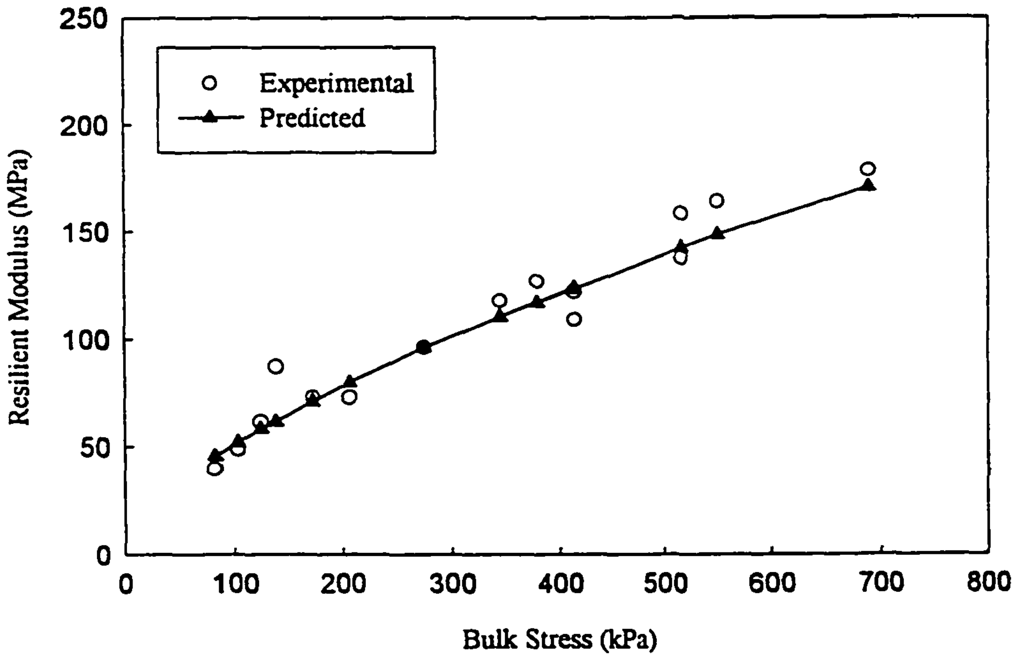

Figure 5-12 Experimental and the k-θ Model Predicted RM Values of the Sawyer Aggregate at 2% above the OMC

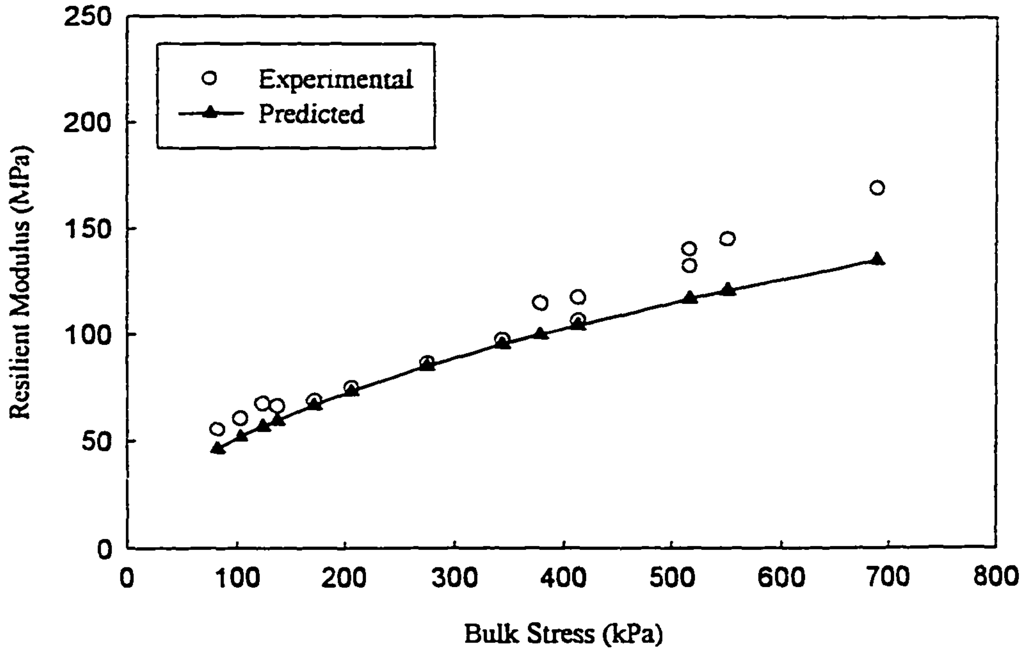

Figure 5-13 Experimental and the k-θ Model Predicted RM Values of the Sawyer Aggregate from the Undrained I Test

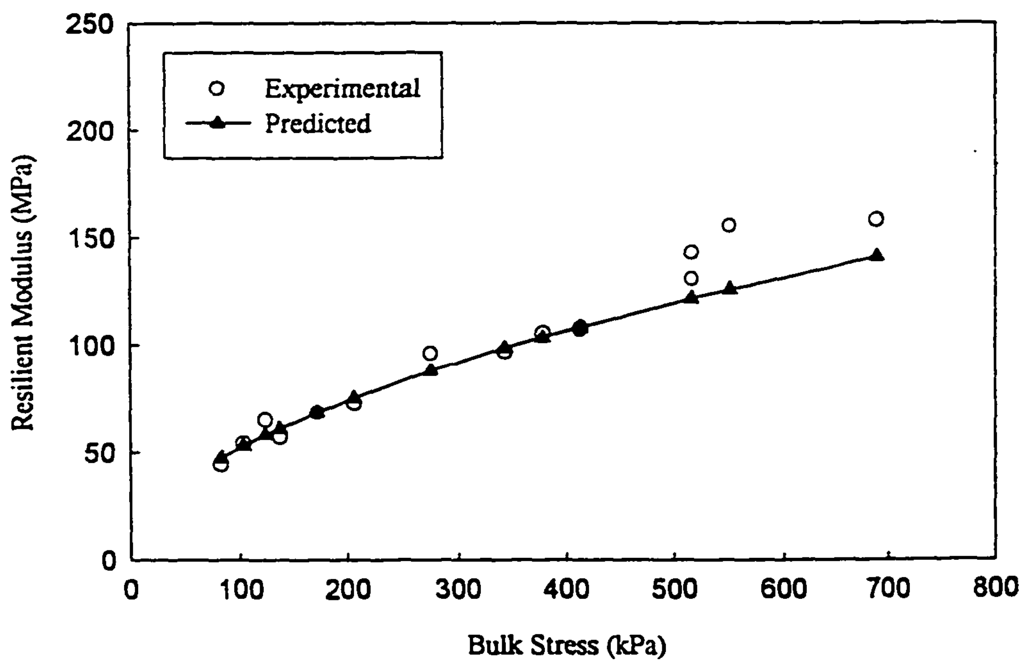

Figure 5-14 Experimental and the k-θ Model Predicted RM Values of the Sawyer Aggregate from the Undrained II Test

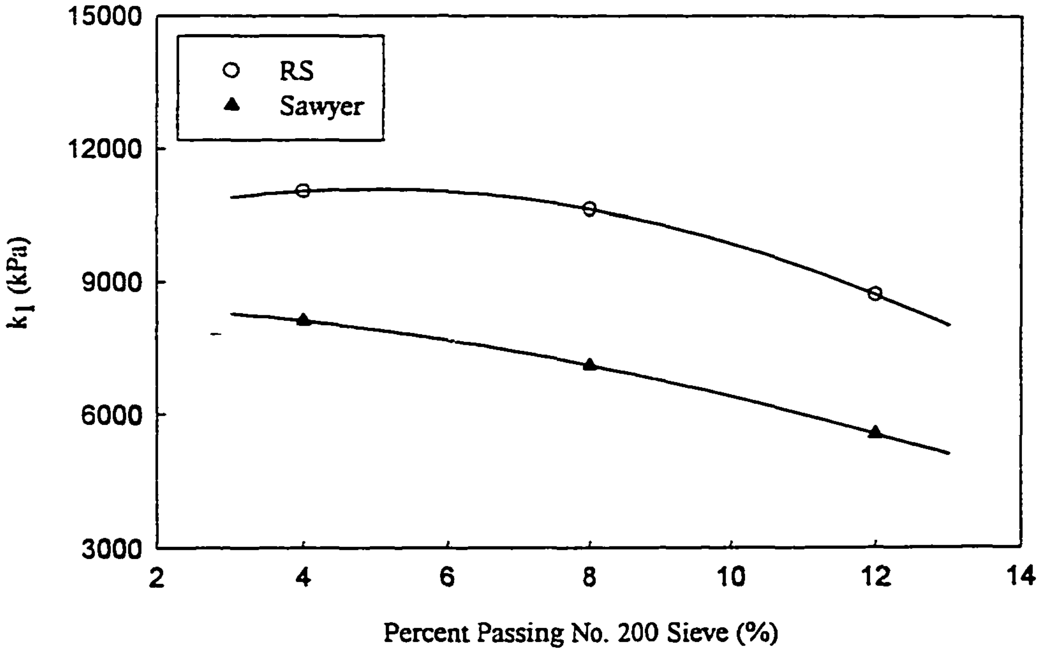

Figure 5-15 Variation of k_1 Values with the No. 200 (0.075 mm) Percent Passing

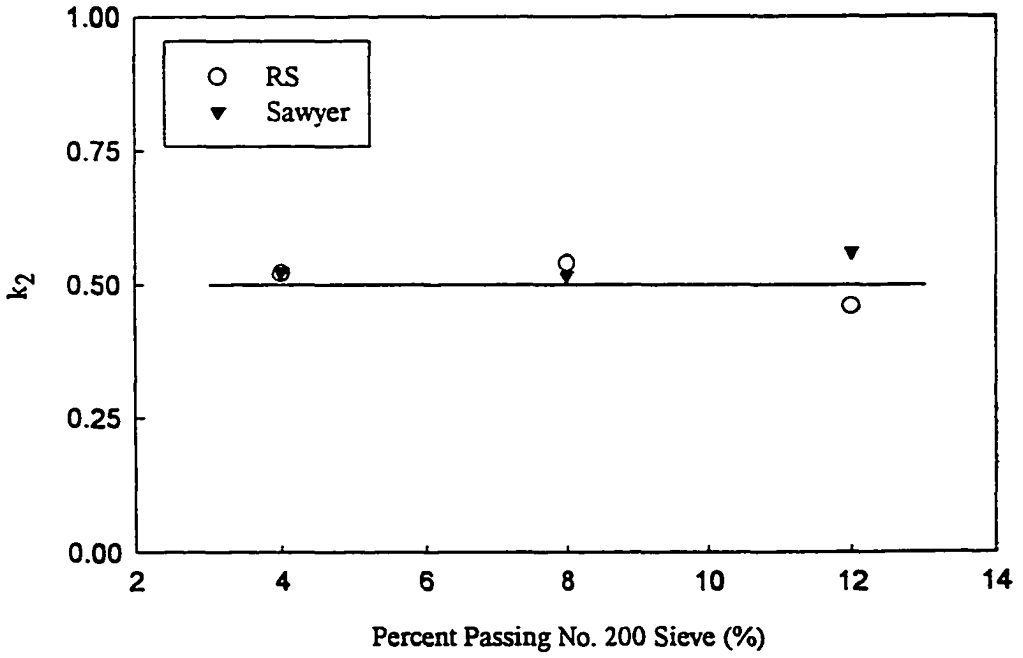

Figure 5-16 Variation of k_2 Values with the No. 200 (0.075 mm) Percent Passing

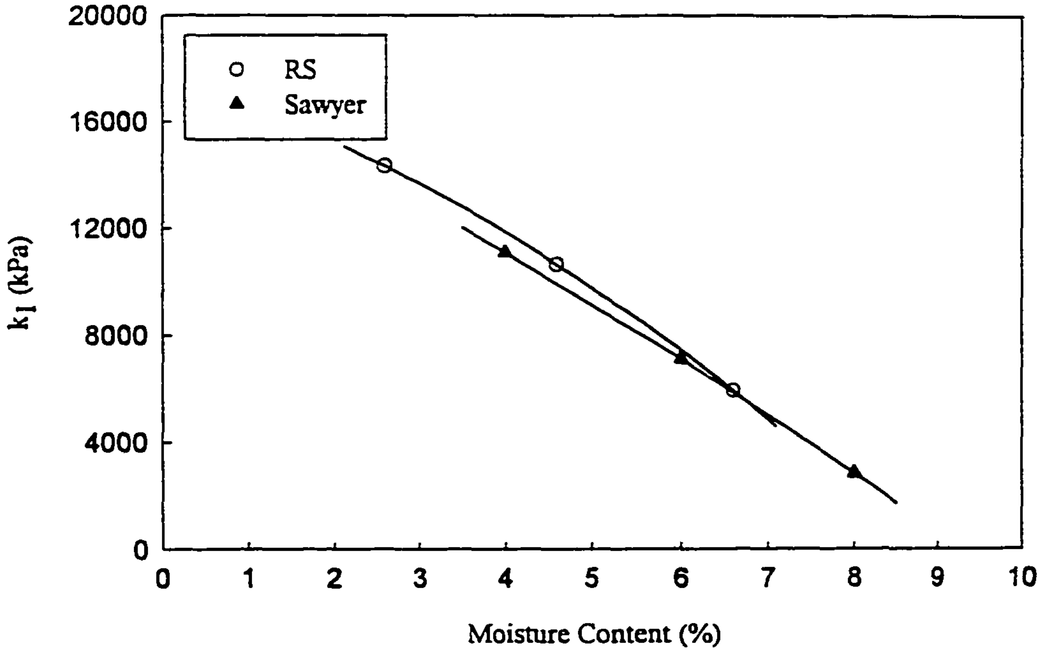

Figure 5-17 Variation of k_1 Values with Moisture Content

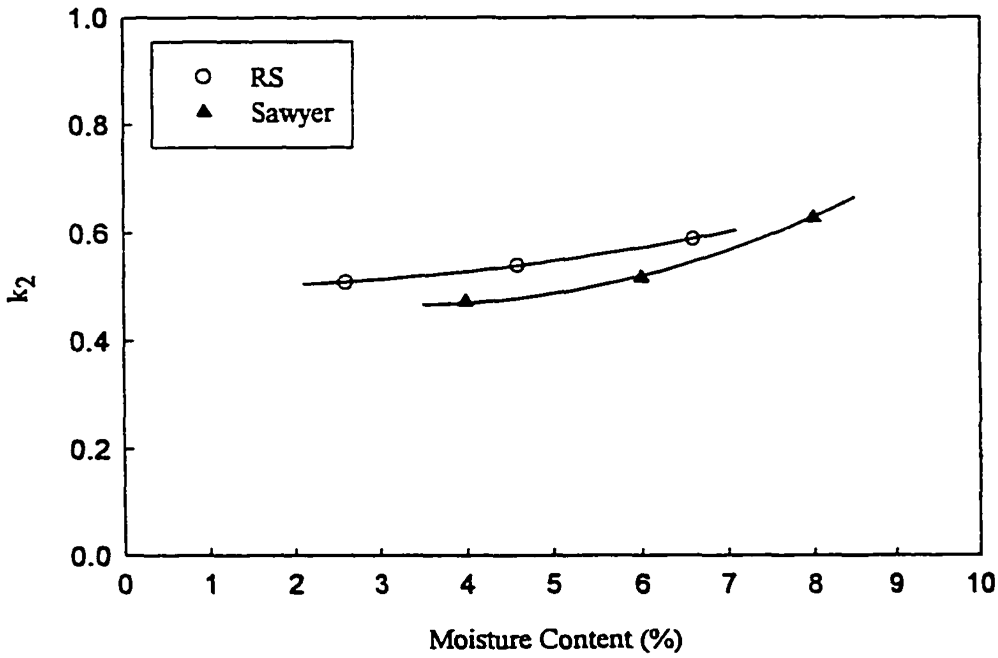

Figure 5-18 Variation of k_2 Values with Moisture Content

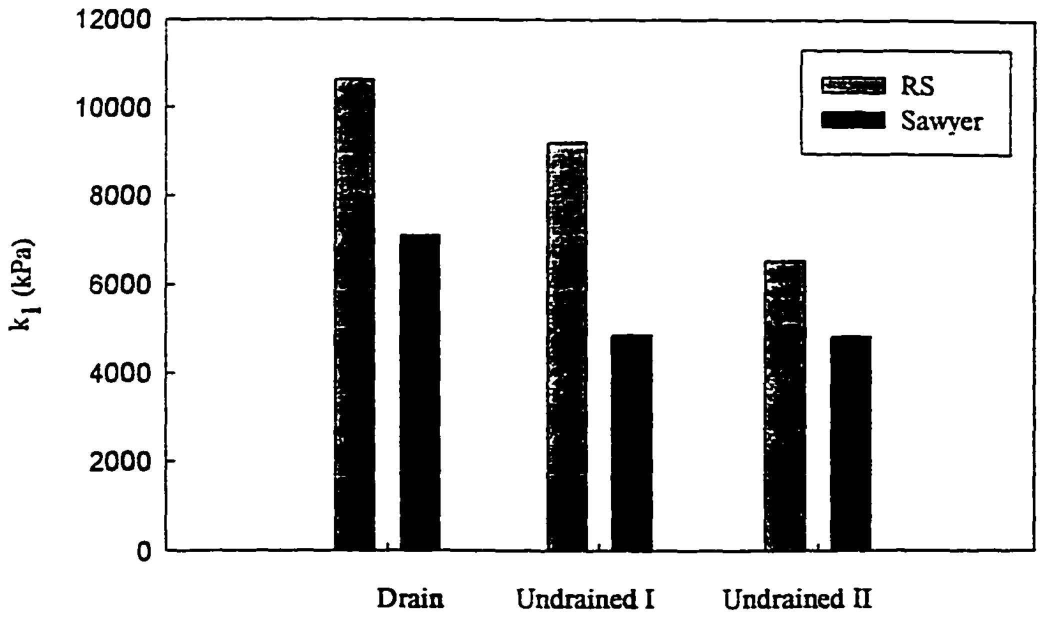

Figure 5-19 Variation of k_1 Values with Drainage Condition

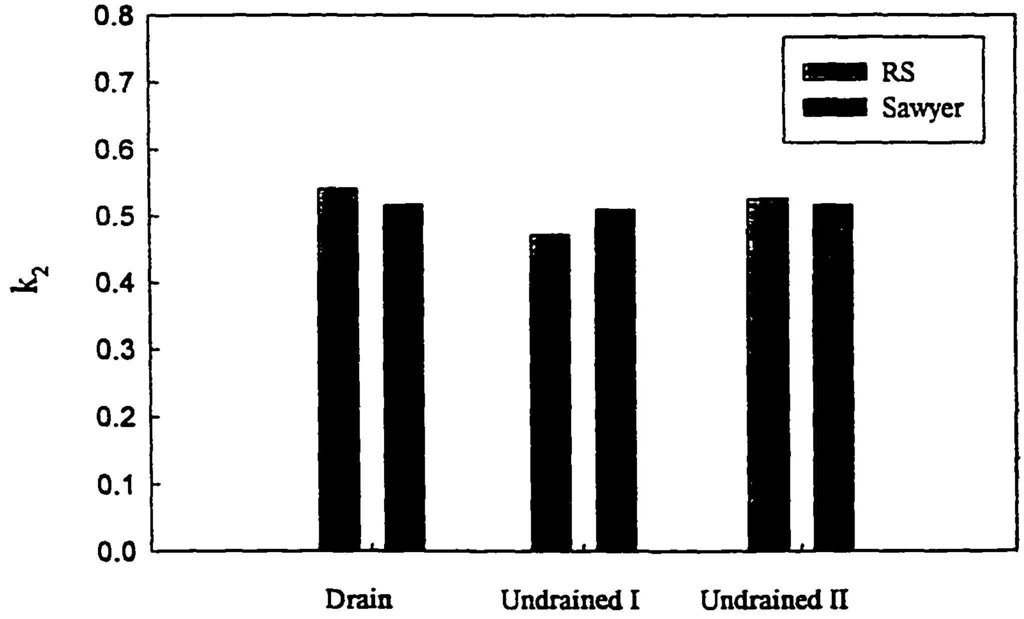

Figure 5-20 Variation of k_2 Values with Drainage Condition

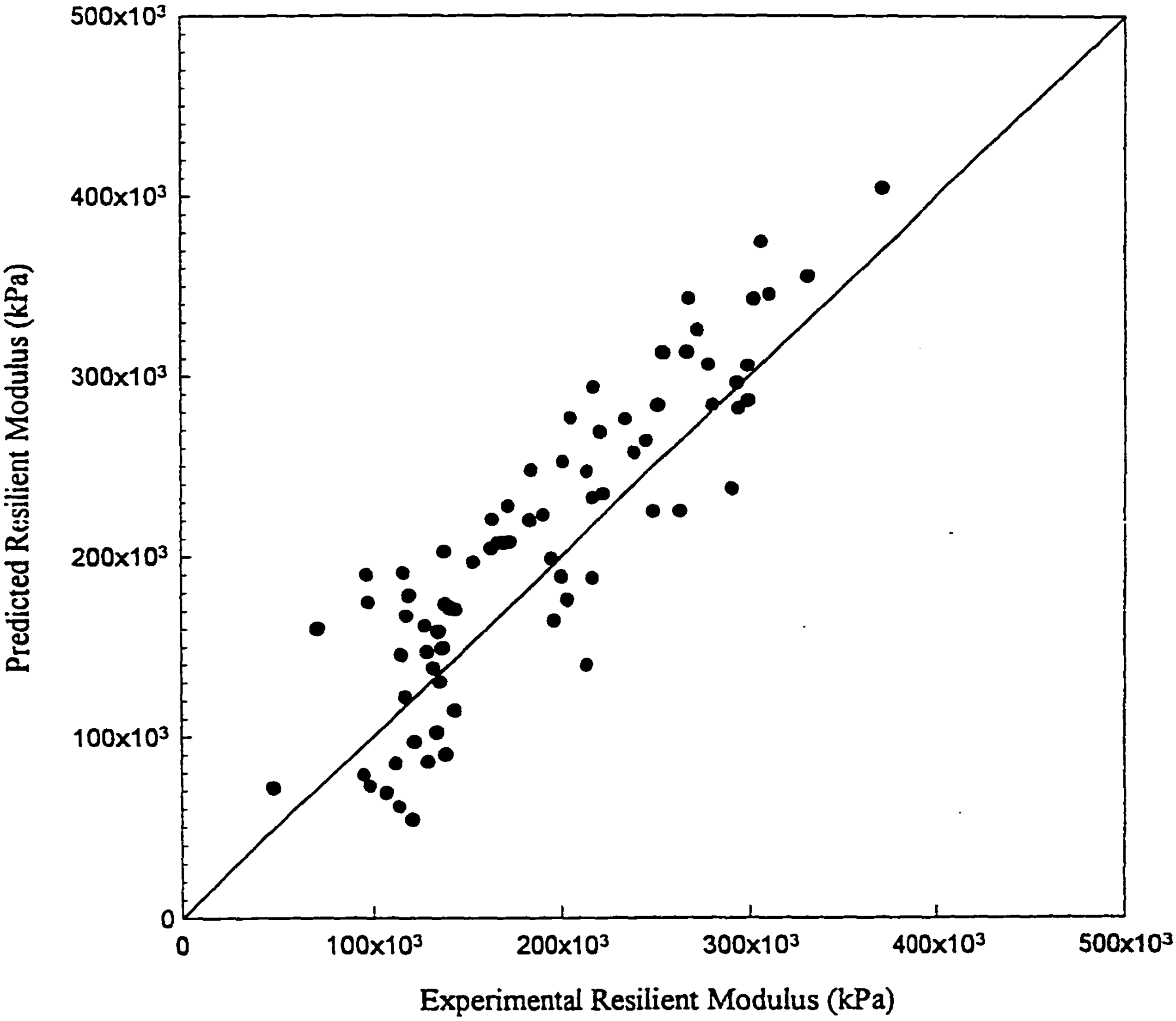

Figure 5-21 Experimental and the Multiple Model Predicted RM Values of the RS Aggregate

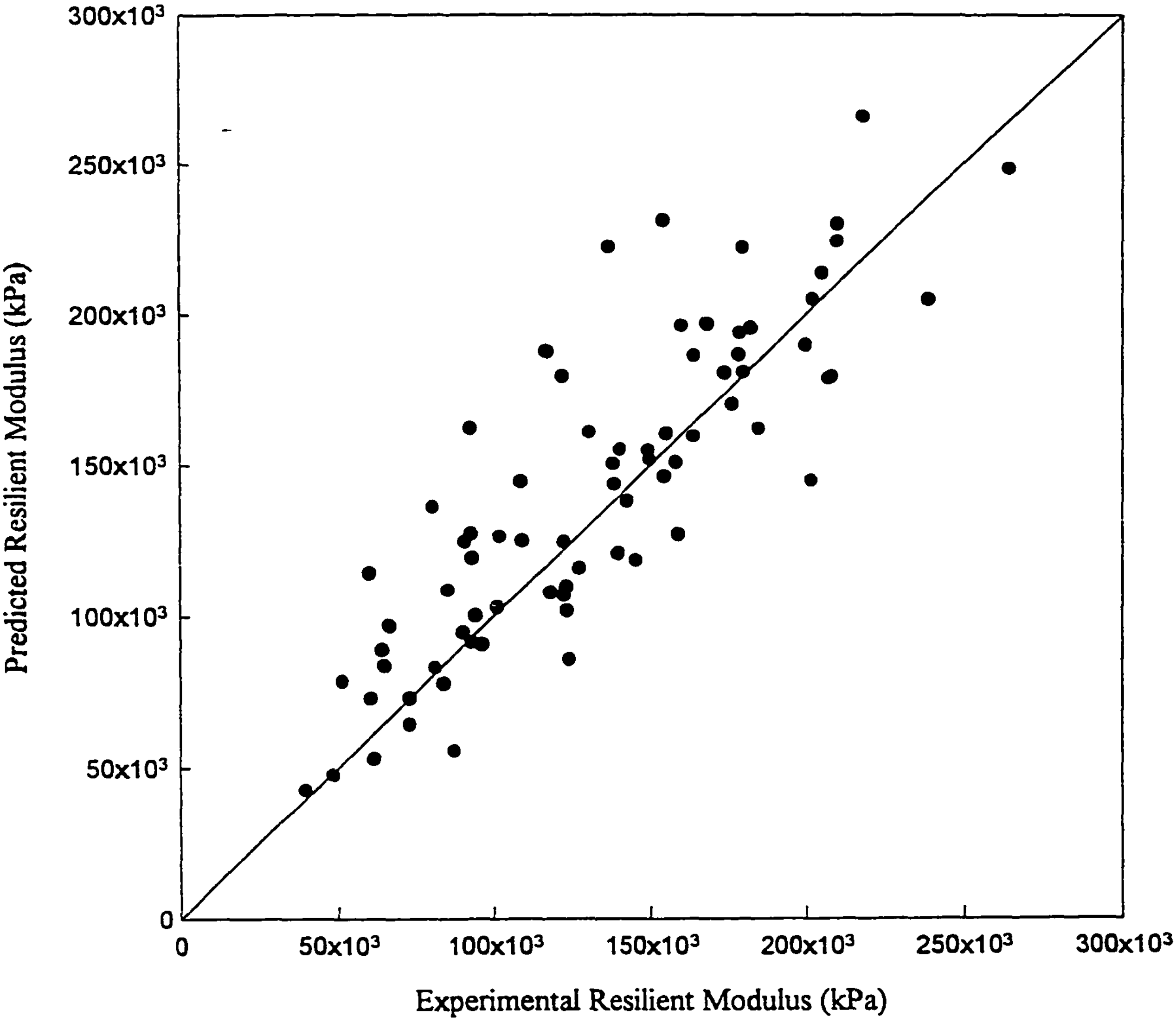

Figure 5-22 Experimental and the Multiple Model Predicted RM Values of the Sawyer Aggregate

CHAPTER 6

LAYER COEFFICIENTS AND FLEXIBLE PAVEMENT DESIGN

6.1 Introduction

The layer coefficients which are used in the AASHTO flexible pavement design are calculated in this chapter. The effects of gradation, moisture content, and drainage condition on layer coefficients are investigated for the two selected aggregates. The methodology adopted for computing the layer coefficients is also discussed in this chapter. Finally, the application of layer coefficients in the design of flexible pavements using the AASHTO design methodology and the influence of layer coefficients on the design results are explained with the help of several design examples.

6.2 Layer Coefficients

The pavement design procedure recommended by AASHTO is based on the results of the extensive AASHTO Road Test conducted in Ottawa, Illinois in the late 1950s (HRB 1962). The current design guide (AASHTO 1993) still uses the empirical performance equations obtained from the AASHTO Road Test, but they were modified and extended to make them applicable to other regions. Also, some new design concepts such as the reliability and RM for soil support are added.

In the AASHTO flexible pavement design procedure, structural number (SN), which provides a link between the structural design of a pavement and its performance, is defined as a function of layer thickness, layer coefficient, and drainage coefficient as follows:

$$SN = a_1 D_1 m_1 + a_2 D_2 m_2 + a_3 D_3 m_3 + \ldots\ldots + a_n D_n m_n \qquad (6\text{-}1)$$

where, a_1, a_2, ..., a_n are the layer coefficients of layer 1, layer 2, ...layer n, respectively; D_1, D_2, ..., D_n are the thicknesses of the layer 1, layer 2, ... layer n, respectively; and m_1, m_2, ...m_n are the drainage coefficients of layer 1, layer 2, ..., layer n, respectively.

For a three layer flexible pavement system shown in Figure 6-1, layer 1 corresponds to the asphalt concrete (AC) layer, layer 2 is the aggregate base layer, and layer 3 is the subgrade layer. The layer coefficients (a_i) in Eq. (6-1) express an empirical relationship between SN and thickness and represent a measure of the relative ability of a unit thickness of a given material to function as a structural component of the pavement (AASHTO 1993). Layer coefficients can be determined from test roads, as was done in the AASHTO Road Test, or from correlations with material properties (Van Til et al. 1972). It is recommended that the layer coefficient be based on RM, which is a more fundamental material property and can be measured in laboratory using the AASHTO T 294-94 method (Huang 1993).

The RM of aggregate base varies with the state of stress (bulk stress θ) within the base layer and the values of the material parameters k_1 and k_2 as described by the k-θ model (Eq. (2-2)). The bulk stresses within the base layer vary with the roadbed soil resilient modulus and the thickness of the surface layer (Huang 1993). Typical values of θ within the pavement base layer given by AASHTO (AASHTO 1993) are shown in Table 6-1. Hence, given k_1, k_2, and θ, RM at a point within the base layer can be computed using Eq. (2-2). According to the AASHTO design guide (AASHTO 1993), the relationship between the layer coefficient (a_2) of the aggregate base material and its RM is given by the following empirical equation:

$$a_2 = 0.249 (\log RM) - 0.977 \qquad (6\text{-}2)$$

Computation of layer coefficient, a_2, therefore, involves computing the bulk stress within the base layer for various thicknesses of the AC layer, base layer, and the RM of subgrade soil. Since the bulk stress within the base layer is not a constant, it also varies through the depth of the layer, hence, it is desirable to compute one representative bulk stress value, termed the equivalent layer bulk stress (ELBK), for one particular thickness of the base layer (Pandey 1996). For each set of AC thickness, base layer thickness and roadbed soil RM, one ELBK is computed. The RM value for each ELBK is then computed using Eq. (2-2). Finally, the RM value thus computed is converted to a layer coefficient using Eq. (6-2). Therefore, for each set of AC thickness, AC RM value, and base layer thickness, one unique layer coefficient value for that particular base layer is computed.

6.3 Overview of MICH-PAVE

A nonlinear finite element computer program, MICH-PAVE, was used in this study to compute ELBK. MICH-PAVE has been used widely for stress, strain, fatigue, and rut depth analyses in multi-layered flexible pavement systems (Huang 1993). Comparison of the results from MICH-PAVE, CHEV5L and ILLI-PAVE showed that MICH-PAVE and CHEV5L give similar strains and displacements for linear analysis. For nonlinear analysis, MICH-PAVE and ILLI-PAVE give very similar stresses (Harichandran et al. 1990). Chen (1994) compared the results of analyses using several available computer programs and concluded that MICH-PAVE is one of the most appropriate codes available for the routine structural analysis of flexible pavements. MICH-PAVE can effectively analyze the flexible pavement response including the influence of such factors as dual-wheel or single-wheel loading and of stress-dependency of the associated materials (Chen 1994).

It is well known that aggregate materials and subgrade soils are nonlinear with an resilient modulus varying with the level of stresses (Huang 1993). By using a method of successive approximations, MICH-PAVE characterizes the nonlinear behavior of aggregate materials by using the k-θ model described in Eq. (2-2). For the subgrade soil, Eqs. (6-3) and (6-4) in following are used to describe the nonlinear material behavior of subgrade soil (Harichandran et al. 1990).

$$RM = k_2 + k_3*[k_1 - \sigma_d] \qquad \text{when } k_1>\sigma_d \qquad (6\text{-}3)$$

$$RM = k_2 + k_4*[\sigma_d - k_1] \qquad \text{when } k_1<\sigma_d \qquad (6\text{-}4)$$

in which k_1, k_2, k_3, and k_4 are material constants and can be determined from laboratory tests, and σ_d is the deviator stress.

The accuracy of a finite element analysis is directly related to the mesh fineness. To achieve an acceptable level of accuracy, especially in the vicinity of the load, the mesh must be sufficiently fine. Figure 6-2 shows the finite element mesh generated in MICH-PAVE. Each layer is divided into a number of finite elements with the mesh being finer closer to the wheel load and coarser farther away from the wheel load both in the horizontal and vertical directions. The optimal numbers of elements in vertical and horizontal directions are generated based on the thickness (D_i) of each layer and the radius of the loaded area (a). In the present analysis, the number of elements located within 0 - a, a - 3a, 3a - 6a, and 6a - 10a in the horizontal direction are 4, 4, 3, and 2, respectively. In the vertical direction, however, the optimal element number is determined by the thickness and location of each layer. It was found that increasing the number of elements in the mesh described above did not significantly change the calculated ELBK results. Hence, the optimal mesh generated by MICH-PAVE was used in present finite element analyses.

The subgrade layer of a pavement section is actually semi-infinite, MICH-PAVE uses a flexible boundary at a limited depth beneath the surface of the subgrade instead of a rigid boundary at a large depth. The subgrade below the flexible boundary is considered as a homogeneous half space. This is an improvement over the other computer programs in that it greatly reduces the number of finite elements required. Consequently, the memory and computational requirements of the nonlinear finite element method are significantly reduced without sacrificing accuracy (Harichandran et al. 1990).

6.4 Determination of Equivalent Layer Bulk Stress

Figure 6-1 shows the three layered flexible pavement system used in this study for ELBK computation. The materials which comprise the AC, base, and subgrade layers are assumed as hot mix asphalt (HMA), aggregate, and soft clay. The material properties of the AC, base, and subgrade layers are given in Table 6-2. It is believed that Poisson's ratio does not significantly influence the calculated results in pavement analysis (Huang 1993). A number between 0 to 0.5 can be reasonably assumed for each layer. In this study, the Poisson's ratios were assumed as 0.35, 0.38, and 0.45 for the AC, base, and subgrade layers. Also, the unit weights of 150 pcf (24 kN/m^3), 140 pcf (22 kN/m^3), and 115 pcf (18 kN/m^3) were assumed for the HMA, aggregate base, and soft clay subgrade layers, respectively.

For the aggregate base layer, the k_1 and k_2 values of the k-θ model can be assumed as 5000 psi (34.5 MPa) and 0.5. These values come from the AASHTO Design Guide (AASHTO 1993) at the condition of damp state. Generally, for aggregate material, the cohesion (C) and friction angle (ϕ) can be reasonably assumed as 0 and 45°.

Thompson and Elliott (1985) reported typical k_1, k_2, k_3, and k_4 values for very soft, soft, medium, and stiff fine-grained soils, respectively. For the soft clay material, the k_1, k_2, k_3, and k_4 values of 6 psi (41.1 kPa), 3020 psi (20.84 MPa), 110, and 178 were reported. These values are used in this study for calculating the RM values of the subgrade layer. Generally, for soft clay material, the cohesion (C) can be reasonably assumed as 6 psi (41.4 kPa) and the friction angle (ϕ) can be assumed as 0. The material properties selected for each layer are also presented in Figure 6-1.

The 18-kip (80-kN) single-axle load with a tire pressure of 100 psi (690 kPa) is used in the ELBK calculation. This single-axle load is applied over two tires, so each tire applies a load of 9000 lb (40-kN) which results a radius of 5.35 in (13.6 cm) loaded area.

It is known that the bulk stress within the base layer varies with the modulus of AC and base layers and the thickness of AC layer. In order to capture the ELBK in a reasonable range, following different thicknesses and modulus of AC and base layers are selected in this study.

Thickness of AC layer: 76, 152, and 228 mm;

Modulus of AC layer: 1725, 3450, and 5175 MPa;

Thickness of base layer: 76, 152, 228, and 304 mm.

The above selected AC layer thickness and RM value as well as the base layer thickness are the magnitudes usually encountered in practical pavement design. The various sets of AC thicknesses and RM values and base layer thicknesses selected result in 36 different cases, as shown in Table 6-3 along with the corresponding ELBK values. The ELBK values obtained are also graphically presented in Figure 6-3.

In view of Figure 6-3, as the RM value and the thickness of the AC layer increase, the

ELBK shows a decreasing trend. It is consistent with the general concept that as the AC layer becomes more stiff, more load is carried or more energy is absorbed by the AC layer. Thus the stresses induced in the sub-layers are reduced. Also, it can be observed that the thickness of the base layer has a very small influence on the values of ELBK when the modulus and thickness of AC layer are unchanged. So the conclusion can be made that a representative bulk stress such as the ELBK can be used for the whole base layer at one combination of the modulus and thickness of AC layer.

By comparing the ELBK values obtained in Table 6-3 with the typical bulk stress values of base course suggested by AASHTO (Table 6-1), it can be observed that the ELBK values obtained in the present study are in the range suggested by AASHTO design guide (AASHTO 1993).

A regression equation for computation of ELBK, further for computation of RM, was established based on the data presented in the Table 6-3. The dependent variables such as thickness of AC layer (D_{ac}), thickness of base layer (D_{bs}), modulus of AC layer (E_{ac}), and the modulus of subgrade soil (E_s) were evaluated first based on their relative relationships with the ELBK values. The following approach was used in the evaluation. For any one of the variables, as keeping the other variables unchanged, the relative relationship of the single variable with the ELBK can be obtained, and this form of relationship is further used in the multiple nonlinear regression analysis. It was found that the ELBK has polynomial relationships with the variables of D_{ac}, D_{bs}, and E_{ac} individually. As the D_{ac} and E_{ac} increase, the ELBK shows a decreasing trend. Generally, increasing the RM of subgrade will result in decreasing the ELBK values. Based on these relationships, a nonlinear multiple regression analysis was performed, and the regression equation that can be used to calculate the ELBK is obtained as follows:

$$ELBK = 1510*D_{ac}^{0.3} - 90*D_{bs}^{-0.05} - 72*(\log E_{ac})^{0.5}$$

$$- 254*(\log E_s)^{-1} + 52 \qquad (R^2 = 0.8621) \qquad (6\text{-}5)$$

in which the D_{ac} and D_{bs} are the thicknesses of AC and base layers, E_{ac} and E_s are the resilient modulus of AC and subgrade layers. In the above equation, the unit of thickness is mm and the unit of modulus is kPa.

6.5 Determination of Layer Coefficients

Based on the ELBK values obtained, the equivalent layer resilient modulus (ELRM), for a particular set of AC layer thickness, RM value, and base layer thickness, can be determined by Eq. (6-6)

$$ELRM = k_1 (ELBK)^{k_2} \qquad (6\text{-}6)$$

The k_1 and k_2 values are material-dependent parameters and could be determined by laboratory RM tests. The ELRM value obtained from Eq. (6-6) is the representative RM for the entire base layer, since MICH-PAVE evaluates the ELBK in the section of the layer that lies within an assumed 2:1 load distribution zone, it is possible to adequately reflect the stress-dependent variation of the RM within the layer (Chen 1994). Subsequently, by using the k_1 and k_2 values of the RS and the Sawyer aggregates which were obtained in Chapter 5 (Table 5-1), the ELRM can be calculated from Eq. (6-6). Further, the layer coefficients (a_2) based on the ELRM of the base layer were calculated by using Eq. (6-2). The layer coefficients obtained for the RS aggregate at the three different gradations, three different moisture contents, and two drainage conditions are presented in Tables 6-4, 6-5, and 6-6, respectively.

Similarly, the layer coefficients of the Sawyer aggregate at the corresponding conditions are presented in Tables 6-7, 6-8, and 6-9, respectively.

As indicated in Eq. (6-2), the larger the RM values, the larger the layer coefficients. So the median gradation (Table 6-4) of the RS aggregate gives the highest layer coefficient among the different gradations studied. For the Sawyer aggregate, the coarser limit gradation (Table 6-7) yields the highest layer coefficients among the three different gradations selected. For example, for Case 1, layer coefficient of 0.1256 for the median gradation is higher than the layer coefficient of 0.0619 for the finer limit gradation and slightly higher than the layer coefficient of 0.1185 for the coarser limit gradation in the RS aggregate.

Similarly, the 2% below the OMC (Tables 6-5 and 6-8) yields the highest layer coefficients among the three different moisture contents studied. For example, for Case 4, layer coefficient of 0.1409 for 2% below the OMC is higher than the layer coefficients of 0.1281 and 0.0915 for the OMC and 2% above the OMC in the RS aggregate. It can also be observed in Tables 6-6 and 6-9 that the layer coefficients for the drained conditions are significantly higher than those under the undrained conditions for both aggregates. Layer coefficients were reduced about 50% when the drainage condition changed from drain to undrain. For example, for Case 1, the drained condition yielded a layer coefficient of 0.1256 for the RS aggregate; however, the undrained condition only yielded a layer coefficient of 0.0654 for the same aggregate base.

In view of Tables 6-4 though 6-9, some cases yield small negative layer coefficient values. Pandey (1996) reported that the layer coefficients that have a negative value do not have any practical significance and therefore, should be considered as values approaching zero. The layer coefficient is a measure of the relative ability of the material to function as a structural component of the pavement (AASHTO 1993). Hence, layer coefficients having values approaching zero essentially mean that the material has insignificant structural support in the pavement system. In contrast, the layer coefficients of the RS aggregate are higher than those of the Sawyer aggregate at different cases, hence, the RS aggregate is more suitable for use as base course than the Sawyer aggregate in pavement design. Several design examples involving the variations of layer coefficients at different conditions are compared in terms of the design loading and the design thickness of the base layer in the section of 6.6.

It can be observed that the thickness of the base layer has an insignificant effect on the layer coefficients when the modulus and thickness of AC layer is unchanged. For example, the layer coefficient of the RS aggregate at the median gradation is 0.1256 for Case 1 and it is 0.1228 for Case 10, where the corresponding base thicknesses are 76 mm and 304 mm, respectively. The reason is that the thickness of the base layer has an insignificant effect on the ELBK values when the modulus and thickness of AC layer is unchanged. Thus, it can be concluded that one representative layer coefficient value can be chosen for a base layer at one combination of the modulus and thickness of AC layer.

It should be noted that in the ELBK calculation (section 6.4) the RM of the base layer was determined from the k-θ model in Eq. (2-2) with k_1 equaling 5000 psi (34.5 MPa) and k_2 equaling 0.5. These k_1 and k_2 values correspond to the damp condition specified by the AASHTO design guide (AASHTO 1993). In view of Table 2-6, the variation of k_2 is relatively small and it is independent of the moisture conditions. Therefore, in order to demonstrate the effect of base layer RM on the ELBK, the k_1 values corresponding to the wet and dry conditions such as 2000 psi (13.8 MPa) and 8000 psi (55.1 MPa) were used to calculate the ELBK for Case 3, Case 6 , Case 9, and Case 12. The calculated ELBK values for these cases are presented in Figure 6-4 which shows that the influence of base layer RM on the ELBK is insignificant. The mean ELBK for these cases is around 55 kPa (7.97 psi). As the k_1 varies in the range of 2000 to 8000 psi ($k_2 = 0.5$), by taking the ELBK as 7.97 psi in Eq. (6-6), the ELRM values are in the range of 38.9 to 155 MPa. This range of ELRM is able to cover the ELRM values used in the layer coefficient calculation. For example, the maximum k_1 and k_2 values for both aggregates are obtained from the case of 2% below the OMC. The minimum k_1 and k_2 values, on the other hand, are obtained from the undrained II case (Table 5-1). These two sets of k_1 and k_2 values result in the ELRM in the range of 53.5 to 110 MPa and 38 to 74 MPa for the RS and the Sawyer aggregates, respectively. Evidently, the combined ELRM range for both aggregates is from 38 to 110 MPa, which is covered by the ELBK values used in the layer coefficient calculation.

It also should be noted that all the layer coefficients obtained above correspond to certain gradation and moisture content. In a practical design, if the material gradation and moisture content used are different from those studied in this research, the layer coefficients for these cases can be obtained using an interpolation. In this study, a multiple linear regression analysis was attempted in order to facilitate the application of the layer coefficients for other moisture contents and gradations for the RS and the Sawyer aggregates.

From the previous analysis, the possible variables that may have influences on layer coefficient (a_2) values could be the thickness of AC layer (D_{ac}), thickness of base layer (D_{bs}), modulus of AC layer (E_{ac}), moisture content (MC), and the gradation effect (No.200). Here, the amount of fines passing the No.200 (0.075mm) sieve is used to represent the gradation effect. In order to select the most critical factors to correlate a_2 values, the Least Square (LS) method which was described in Chapter 5 was used here again to evaluate these factors.

Table 6-10 shows all the possible models for the RS and the Sawyer aggregates with associated R^2 values. It was observed that the D_{ac} gives the best one variable model with R^2 values of 0.5044 and 0.5339 for both aggregates. The D_{bs} has very little direct influence on the a_2 values. So the two variable models were evaluated based on the combination of variables of D_{ac}, E_{ac}, MC, and No.200. It was found that the best two variable model is the D_{ac} and MC model, R^2 values of 0.7211 and 0.8904 were obtained for both aggregates, respectively. Furthermore, the three variable models were evaluated based on adding one variable (E_{ac} or No.200) in the D_{ac}, MC model. It was found that adding the No.200 variable in the D_{ac}, MC model is more significant than adding the E_{ac} variable in terms of increasing the R^2 value for the RS aggregate. The R^2 value increased from 0.7211 to 0.8676 due to adding the No.200 variable was observed. However, for the Sawyer aggregate, adding the E_{ac} variable is more critical than adding the No.200 variable in terms of increasing the R^2 value. The R^2 value increased from 0.8904 to 0.9485 due to adding the E_{ac} variable was observed. The next consideration is the four variable model, it was found that either adding the E_{ac} variable or the No.200 variable in the corresponding best three variable models increases the R^2 values from 0.8676 to 0.9226 and 0.9485 to 0.9510 for the RS and the Sawyer aggregates, respectively. Additionally adding the variable of D_{bs} cannot increase the R^2 value from the best four variable models for both aggregates. Therefore, the four variables of D_{ac}, MC, No.200, and E_{ac} were used next to develop the regression model for estimating the layer coefficient (a_2).

Multiple linear regression analyses were performed to correlate a_2 values with the D_{ac}, MC, No.200, and E_{ac} for the RS and the Sawyer aggregate, respectively. For each aggregate, three different gradations and two different moisture contents at the 36 different cases result in 180 layer coefficients values that were used in the regression analyses. The following regression equations were obtained for the RS and the Sawyer aggregates:

i. Layer coefficient a_2 for the RS aggregate:

$$a_2 = 0.5546 - 0.4579*10^{-3}*D_{ac} - 0.0146*MC$$
$$- 0.6062*10^{-2}*No.200 - 0.0476*\log E_{ac}$$
$$R^2 = 0.9226 \tag{6-7}$$

ii. Layer coefficient a_2 for the Sawyer aggregate:

$$a_2 = 0.5274 - 0.4872*10^{-3}*D_{ac} - 0.0179*MC$$
$$- 0.8613*10^{-3}*No.200 - 0.0506*\log E_{ac}$$
$$R^2 = 0.9510 \tag{6-8}$$

in which: D_{ac} (mm) = thickness of AC layer, E_{ac} (kPa) = RM of AC layer, MC (%) = moisture content, and No.200 (%) = percent of fines passing the No.200 (0.075mm) sieve.

6.6 Design of AASHTO Flexible Pavements

The layer coefficients determined above can be used in the flexible pavement design according to the AASHTO design guide (AASHTO 1993). The RS and the Sawyer aggregates at different conditions were used as the base layer and the relative performance of the whole pavement can be evaluated by comparison of SN (Structure Number) and the corresponding ESAL (Equivalent Single Axle Load). In the present design, the SN and ESAL were computed for an overall standard deviation (S_0) of 0.35, initial serviceability index (P_i) of 4.2, and the terminal serviceability index (P_t) of 2.5. These values of S_0, P_i, and P_t correspond to the values observed at the AASHTO Road Test (AASHTO 1993). Based on the AASHTO recommendation, a reliability level of 90% was selected as an input parameter in this study.

The initial and terminal serviceability indexes are used to compute the change in serviceability, ΔPSI, to be used in the design equations. The initial serviceability index (P_i) is a function of pavement type and construction quality. Typical value from the AASHTO Road Test was 4.2 for flexible pavement. The terminal serviceability index (P_t) is the lowest index that will be tolerated before rehabilitation, resurfacing, and reconstruction become necessary. An index of 2.5 or higher is suggested for design of major highways and 2.0 for highways with lower traffic. S_0 is the standard deviation between the predicted number of ESAL and the allowable number of ESAL for a given reliability level. The allowable number of ESAL is the load applications to cause the reduction of present serviceability index from P_i to P_t.

For the RS aggregate, Case 3, Case 6, Case 9, and Case 12 were selected for the comparison of SN and ESAL. The thickness and the RM value of the AC layer are 228 mm (9 in) and 1725 MPa (250 ksi), and the road bed soil RM is 51.75 MPa (7.5 ksi). Only the thickness of base layer changes among these cases. The SN and ESAL were computed using the AASHTO Flexible Pavement Design Computer Software (AASHTO 1986), and the results obtained are presented in Table 6-11.

Design ESAL of 1,000,000 is recommended by the Asphalt Institute for urban minor arterial and light industrial streets (AI 1991b). In view of Table 6-11, as the thickness of the base layer increased to 228 mm (9 in) and 304 mm (12 in), if the median and the coarser limit gradations for the RS aggregate are used as the base layer, the ESALs (1,220,600 and 1,642,400 for the median gradation, 1,076,300 and 1,405,700 for the coarser limit gradation) can satisfy the requirement recommended by the Asphalt Institute. However, the finer limit gradation cannot yield the required design ESAL for all of the thicknesses of base layers considered. On the other hand, as moisture varies within ±2% of the OMC, the material presents a very good performance when its moisture reaches the 2% below the OMC. For example, the 1,381,300 and 1,913,300 ESALs are obtained for 228 mm (9 in) and 304 mm (12 in) base layer, respectively. However, as the moisture increased to 2% above the OMC, only 519,800 and 530,500 ESALs are obtained for the corresponding thicknesses of base layers. From this example, one conclusion can be made that the service life of a pavement will reduce significantly if the pavement base layer is designed based on the optimum moisture, however, the actual moisture is often above the optimum during the rainfall or some other reasons.

Similar observations can be made when the undrained condition is pursued in the field. For example, the ESALs of 1,220,600 and 1,642,400 are obtained for 228 mm (9 in) and 304 mm (12 in) base layers under the drained condition. However, only 519,800 of ESALs was obtained if the drainage condition was changed to undrain. Hence, half of the service life or two third of the service life will be lost for pavements including the 228 mm or 304 mm base layers, if the undrained condition is pursued in the field.

In practical application, if the moisture content of aggregate base is different from the study cases given at here, for example, the moisture content is 1% below or 1% above the OMC, the layer coefficients predicted by Eqs. (6-7) and (6-8) can be used in design practice. The following design examples based on the Sawyer aggregate show this application. Assume that the coarser limit gradation for the Sawyer aggregate at the OMC, 1% below, and 1% above the OMC is used as a base layer, respectively. The thicknesses of the base layer are 76 mm, 152 mm, 228 mm, and 304 mm, respectively. The thickness of the AC layer is assumed to be 178 mm, and its RM value is 3450 MPa. Based on these parameters, the layer coefficients for each base layer were predicted by using Eq. (6-8). Furthermore, the SN and ESAL of the pavements at the different bases were computed and the results obtained are presented in Table 6-12.

In view of Table 6-12, the Sawyer aggregate at 1% below the OMC gave the highest design ESAL. As the base thickness increases from 76 mm to 304 mm, the ESAL increasing from 1,024,700 to 1,767,300 was observed. At the OMC, the 76 mm base which gave 815,400 design ESAL cannot satisfy the AI requirement. However, as the thickness of base layer increases to 152 mm, a design ESAL of 1,017,200 was obtained. For the Sawyer aggregate at 1% above the OMC, none of these bases can produce a desired design ESAL.

Since the RS aggregate generally gave higher layer coefficients than those of the Sawyer aggregate (Tables 6-4 to 6-9), it is interested to compare the design results between the RS and the Sawyer aggregates. It is expected that for the same design ESAL, the RS aggregate would require less base thickness than the Sawyer aggregate. For example, the RS aggregate in Case 6, which has 152 mm (6 in) base and 228 mm AC layers, gave a design ESAL of 1,057,000 when the moisture is 2% below the OMC. It was found that for the same thickness of AC layer and base moisture content, it requires a 457 mm (18 in) thick base for the Sawyer aggregate to produce the same design ESAL. Therefore, it can be concluded that using the RS aggregate as a base layer is more efficient than using the Sawyer aggregate in pavement design.

Table 6-1 Typical Values of Bulk Stress (θ) for Base Course (After AASHTO 1993)

Asphalt Concrete Thickness (in)	Roadbed Soil Resilient Modulus (psi)		
	3000	7500	15000
Less than 2	20	25	30
2 to 4	10	15	20
4 to 6	5	10	15
Greater than 6	5	5	5

1 in = 25.4 mm; 1 psi = 6.9 kPa

Table 6-2 Material Constant Inputs for ELBK Computation Using MICH-PAVE

Layer Type	Poisson's Ratio	Unit Weight (pcf)	k_0	k_1 (psi)	k_2	k_3	k_4	c (psi)	ϕ (deg.)
AC	0.35	150	0.7						
Base	0.38	140	0.6	5000.0	0.50			0.0	45.0
Soil	0.45	115	0.8	6.2	3021	1110	178	6.0	0.0

1psi = 6.9 kPa; 1pcf = 0.1572 kN/m^3

Table 6-3 The Various Combinations of AC layer Thickness (D_{ac}), AC Layer RM (E_{ac}), Base Layer Thickness (D_2), Corresponding Case Number, and ELBK

E_{ac}	Base Thickness	D_{ac}, mm (in)								
		76 (3)			152 (6)			228 (9)		
kPa	D_2	Case	ELBK		Case	ELBK		Case	ELBK	
(psi)	mm (in)	No.	psi	kPa	No.	psi	kPa	No.	psi	kPa
1725000	76 (3)	Case 1	27.62	190.59	Case 2	12.60	86.92	Case 3	7.83	54.00
(250000)	152 (6)	Case 4	28.92	199.52	Case 5	12.60	86.92	Case 6	7.59	52.37
	228 (9)	Case 7	30.08	207.53	Case 8	13.00	89.71	Case 9	7.00	48.29
	304 (12)	Case 10	26.27	181.26	Case 11	11.98	82.66	Case 12	7.20	49.69
3450000	76 (3)	Case 13	21.70	149.73	Case 14	9.17	63.26	Case 15	5.88	40.56
(500000)	152 (6)	Case 16	21.73	149.95	Case 17	9.26	63.88	Case 18	5.93	40.95
	228 (9)	Case 19	22.53	155.45	Case 20	8.86	61.11	Case 21	6.19	42.69
	304 (12)	Case 22	20.42	140.87	Case 23	8.22	56.69	Case 24	6.44	44.40
5175000	76 (3)	Case 25	17.35	119.68	Case 26	7.52	51.88	Case 27	5.37	37.02
(750000)	152 (6)	Case 28	18.33	126.49	Case 29	7.33	50.55	Case 30	5.64	38.91
	228 (9)	Case 31	19.31	133.22	Case 32	7.27	50.17	Case 33	5.89	40.62
	304 (12)	Case 34	17.93	123.68	Case 35	7.43	51.24	Case 36	6.11	42.18

Table 6-4 Layer Coefficients (a_2) of the RS Aggregate at the Three Different Gradations

E_{ac}	Base Thickness	Median Gradation			Finer Limit Gradation			Coarser Limit Gradation		
	D_2	D_{ac} (mm)			D_{ac} (mm)			D_{ac} (mm)		
		76	152	228	76	152	228	76	152	228
(kPa)	(mm)	a_2	a_2	a_2	a_2	a_2	a_2	a_2	a_2	a_2
1725000	76	0.1256	0.0824	0.0562	0.0619	0.0278	0.0071	0.1185	0.0750	0.0486
	152	0.1281	0.0824	0.0545	0.0639	0.0278	0.0058	0.1211	0.0750	0.0469
	228	0.1303	0.0841	0.0500	0.0656	0.0292	0.0022	0.1233	0.0767	0.0424
	304	0.1228	0.0796	0.0516	0.0597	0.0256	0.0035	0.1158	0.0722	0.0440
3450000	76	0.1123	0.0649	0.0404	0.0514	0.0140	-0.0053	0.1052	0.0574	0.0327
	152	0.1124	0.0654	0.0410	0.0515	0.0144	-0.0049	0.1052	0.0579	0.0332
	228	0.1144	0.0630	0.0433	0.0530	0.0125	-0.0031	0.1072	0.0554	0.0355
	304	0.1089	0.0589	0.0454	0.0488	0.0092	-0.0014	0.1018	0.0513	0.0377
5175000	76	0.1000	0.0540	0.0354	0.0417	0.0054	-0.0093	0.0927	0.0464	0.0276
	152	0.1030	0.0526	0.0382	0.0441	0.0042	-0.0071	0.0958	0.0449	0.0304
	228	0.1059	0.0521	0.0405	0.0463	0.0039	-0.0053	0.0987	0.0445	0.0328
	304	0.1018	0.0533	0.0426	0.0431	0.0048	-0.0036	0.0946	0.0457	0.0349

Table 6-5 Layer Coefficients (a_2) of the RS Aggregate at the Three Different Moisture Contents

E_{ac}	Base Thickness	Optimum Moisture			2% below Optimum			2% above Optimum		
	D_2	D_{ac} (mm)			D_{ac} (mm)			D_{ac} (mm)		
		76	152	228	76	152	228	76	152	228
(kPa)	(mm)	a_2	a_2	a_2	a_2	a_2	a_2	a_2	a_2	a_2
1725000	76	0.1256	0.0824	0.0562	0.1382	0.0919	0.0639	0.0885	0.0373	0.0063
	152	0.1281	0.0824	0.0545	0.1409	0.0919	0.0621	0.0915	0.0373	0.0043
	228	0.1303	0.0841	0.0500	0.1432	0.0938	0.0573	0.0941	0.0394	-0.0010
	304	0.1228	0.0796	0.0516	0.1352	0.0890	0.0590	0.0853	0.0340	0.0008
3450000	76	0.1123	0.0649	0.0404	0.1240	0.0732	0.0470	0.0728	0.0166	-0.0124
	152	0.1124	0.0654	0.0410	0.1241	0.0738	0.0476	0.0729	0.0172	-0.0118
	228	0.1144	0.0630	0.0433	0.1262	0.0712	0.0501	0.0752	0.0143	-0.0091
	304	0.1089	0.0589	0.0454	0.1204	0.0668	0.0524	0.0688	0.0094	-0.0065
5175000	76	0.1000	0.0540	0.0354	0.1108	0.0615	0.0417	0.0582	0.0036	-0.0184
	152	0.1030	0.0526	0.0382	0.1140	0.0600	0.0446	0.0618	0.0019	-0.0151
	228	0.1059	0.0521	0.0405	0.1171	0.0596	0.0471	0.0652	0.0015	-0.0123
	304	0.1018	0.0533	0.0426	0.1127	0.0608	0.0494	0.0603	0.0028	-0.0099

Table 6-6 Layer Coefficients (a_2) of the RS Aggregate at the Different Drainage Conditions

E_{ac}	Base Thickness	Drained			Undrained I			Undrained II		
	D_2	D_{ac} (mm)			D_{ac} (mm)			D_{ac} (mm)		
		76	152	228	76	152	228	76	152	228
(kPa)	(mm)	a_2	a_2	a_2	a_2	a_2	a_2	a_2	a_2	a_2
1725000	76	0.1256	0.0824	0.0562	0.0680	0.0264	0.0013	0.0628	0.0179	-0.0093
	152	0.1281	0.0824	0.0545	0.0704	0.0264	-0.0004	0.0654	0.0179	-0.0111
	228	0.1303	0.0841	0.0500	0.0725	0.0281	-0.0046	0.0676	0.0197	-0.0157
	304	0.1228	0.0796	0.0516	0.0653	0.0238	-0.0031	0.0599	0.0150	-0.0141
3450000	76	0.1123	0.0649	0.0404	0.0552	0.0096	-0.0139	0.0490	-0.0003	-0.0257
	152	0.1124	0.0654	0.0410	0.0553	0.0102	-0.0134	0.0491	0.0003	-0.0251
	228	0.1144	0.0630	0.0433	0.0572	0.0078	-0.0112	0.0511	-0.0022	-0.0228
	304	0.1089	0.0589	0.0454	0.0520	0.0038	-0.0091	0.0455	-0.0065	-0.0205
5175000	76	0.1000	0.0540	0.0354	0.0434	-0.0009	-0.0187	0.0362	-0.0116	-0.0309
	152	0.1030	0.0526	0.0382	0.0463	-0.0022	-0.0161	0.0393	-0.0131	-0.0281
	228	0.1059	0.0521	0.0405	0.0490	-0.0026	-0.0138	0.0423	-0.0135	-0.0256
	304	0.1018	0.0533	0.0426	0.0451	-0.0015	-0.0118	0.0381	-0.0123	-0.0234

Table 6-7 Layer Coefficients (a_2) of the Sawyer Aggregate at the Three Different Gradations

E_{ac}	Base Thickness	Median Gradation			Finer Limit Gradation			Coarser Limit Gradation		
	D_2	D_{ac} (mm)			D_{ac} (mm)			D_{ac} (mm)		
		76	152	228	76	152	228	76	152	228
(kPa)	(mm)	a_2	a_2	a_2	a_2	a_2	a_2	a_2	a_2	a_2
1725000	76	0.0647	0.0208	-0.0058	0.0631	0.0131	-0.0171	0.0865	0.0423	0.0156
	152	0.0672	0.0208	-0.0075	0.0660	0.0131	-0.0191	0.0891	0.0423	0.0138
	228	0.0694	0.0226	-0.0120	0.0685	0.0152	-0.0242	0.0913	0.0441	0.0093
	304	0.0619	0.0180	-0.0104	0.0599	0.0099	-0.0224	0.0837	0.0395	0.0109
3450000	76	0.0512	0.0031	-0.0218	0.0477	-0.0071	-0.0353	0.0729	0.0245	-0.0005
	152	0.0513	0.0036	-0.0212	0.0478	-0.0064	-0.0347	0.0730	0.0250	0.0000
	228	0.0533	0.0011	-0.0189	0.0501	-0.0093	-0.0321	0.0750	0.0225	0.0023
	304	0.0478	-0.0031	-0.0167	0.0439	-0.0140	-0.0296	0.0695	0.0183	0.0046
5175000	76	0.0387	-0.0080	-0.0269	0.0335	-0.0197	-0.0411	0.0603	0.0133	-0.0057
	152	0.0418	-0.0095	-0.0241	0.0370	-0.0213	-0.0380	0.0635	0.0119	-0.0029
	228	0.0447	-0.0099	-0.0217	0.0403	-0.0218	-0.0352	0.0664	0.0114	-0.0004
	304	0.0405	-0.0087	-0.0196	0.0356	-0.0205	-0.0328	0.0622	0.0126	0.0017

Table 6-8 Layer Coefficients (a_2) of the Sawyer Aggregate at the Three Different Moisture Contents

E_{ac}	Base Thickness	Optimum Moisture			2% below Optimum			2% above Optimum		
	D_2	D_{ac} (mm)			D_{ac} (mm)			D_{ac} (mm)		
		76	152	228	76	152	228	76	152	228
(kPa)	(mm)	a_2	a_2	a_2	a_2	a_2	a_2	a_2	a_2	a_2
1725000	76	0.0647	0.0208	-0.0058	0.0894	0.0474	0.0220	0.0311	-0.0213	-0.0530
	152	0.0672	0.0208	-0.0075	0.0919	0.0474	0.0203	0.0341	-0.0213	-0.0551
	228	0.0694	0.0226	-0.0120	0.0940	0.0491	0.0160	0.0368	-0.0192	-0.0605
	304	0.0619	0.0180	-0.0104	0.0867	0.0447	0.0175	0.0277	-0.0246	-0.0586
3450000	76	0.0512	0.0031	-0.0218	0.0765	0.0304	0.0067	0.0150	-0.0425	-0.0721
	152	0.0513	0.0036	-0.0212	0.0766	0.0310	0.0072	0.0151	-0.0418	-0.0715
	228	0.0533	0.0011	-0.0189	0.0785	0.0286	0.0094	0.0175	-0.0448	-0.0687
	304	0.0478	-0.0031	-0.0167	0.0732	0.0246	0.0115	0.0109	-0.0498	-0.0661
5175000	76	0.0387	-0.0080	-0.0269	0.0645	0.0198	0.0018	0.0000	-0.0557	-0.0782
	152	0.0418	-0.0095	-0.0241	0.0675	0.0184	0.0044	0.0037	-0.0574	-0.0749
	228	0.0447	-0.0099	-0.0217	0.0703	0.0180	0.0067	0.0072	-0.0579	-0.0720
	304	0.0405	-0.0087	-0.0196	0.0663	0.0192	0.0088	0.0022	-0.0565	-0.0695

Table 6-9 Layer Coefficients (a_2) of the Sawyer Aggregate at the Different Drainage Conditions

E_{ac}	Base Thickness	Drained			Undrained I			Undrained II		
	D_2	D_{ac} (mm)			D_{ac} (mm)			D_{ac} (mm)		
		76	152	228	76	152	228	76	152	228
(kPa)	(mm)	a_2	a_2	a_2	a_2	a_2	a_2	a_2	a_2	a_2
1725000	76	0.0647	0.0208	-0.0058	0.0293	-0.0152	-0.0421	0.0270	-0.0149	-0.0403
	152	0.0672	0.0208	-0.0075	0.0319	-0.0152	-0.0438	0.0295	-0.0149	-0.0420
	228	0.0694	0.0226	-0.0120	0.0341	-0.0134	-0.0484	0.0316	-0.0132	-0.0463
	304	0.0619	0.0180	-0.0104	0.0264	-0.0180	-0.0468	0.0244	-0.0176	-0.0448
3450000	76	0.0512	0.0031	-0.0218	0.0156	-0.0331	-0.0583	0.0141	-0.0319	-0.0556
	152	0.0513	0.0036	-0.0212	0.0157	-0.0326	-0.0578	0.0142	-0.0314	-0.0551
	228	0.0533	0.0011	-0.0189	0.0177	-0.0351	-0.0554	0.0162	-0.0337	-0.0529
	304	0.0478	-0.0031	-0.0167	0.0122	-0.0393	-0.0532	0.0109	-0.0377	-0.0508
5175000	76	0.0387	-0.0080	-0.0269	0.0029	-0.0444	-0.0635	0.0022	-0.0425	-0.0605
	152	0.0418	-0.0095	-0.0241	0.0061	-0.0458	-0.0606	0.0051	-0.0439	-0.0578
	228	0.0447	-0.0099	-0.0217	0.0090	-0.0463	-0.0582	0.0079	-0.0443	-0.0555
	304	0.0405	-0.0087	-0.0196	0.0048	-0.0451	-0.0561	0.0039	-0.0431	-0.0535

Table 6-10 Measure of Fit for Models with Different Variables

Number in Model	Variables	R^2 (RS)	R^2 (Sawyer)
1	log E_{ac}	0.0549	0.0581
1	No.200	0.1297	0.0532
1	MC	0.2167	0.3564
1	D_{ac}	0.5044	0.5339
2	No.200, log E_{ac}	0.1847	0.1114
2	MC, log E_{ac}	0.2717	0.4146
2	MC, No.200	0.3633	0.3589
2	D_{ac}, log E_{ac}	0.4342	0.5921
2	D_{ac}, No.200	0.6341	0.5872
2	D_{ac}, MC	0.7211	0.8904
3	MC, No.200, log E_{ac}	0.4182	0.4171
3	D_{ac}, No.200, log E_{ac}	0.6890	0.6453
3	D_{ac}, MC, log E_{ac}	0.7760	0.9485
3	D_{ac}, MC, No.200	0.8676	0.8929
4	D_{ac}, MC, No.200, log E_{ac}	0.9226	0.9510
5	D_{ac}, MC, No.200, log E_{ac}, D_{bs}	0.9226	0.9510

Table 6-11 Comparison of SN and ESAL for the RS Aggregate at the Different Cases

	Case 3		Case 6		Case 9		Case 12	
	SN	ESAL	SN	ESAL	SN	ESAL	SN	ESAL
Median	3.14	727,300	3.30	982,400	3.42	1,220,600	3.59	1,642,400
Finer	2.99	541,300	3.00	552,300	2.99	541,300	3.01	563,500
Coarser	3.12	699,700	3.25	895,600	3.35	1,076,300	3.50	1,405,700
2% below	3.16	755,700	3.34	1,057,000	3.49	1,381,300	3.68	1,913,300
2% above	2.99	541,300	3.00	552,300	2.97	519,800	2.98	530,500
Undrained I	2.97	519,800	2.97	519,800	2.97	519,800	2.97	519,800
Undrained II	2.97	519,800	2.97	519,800	2.97	519,800	2.97	519,800

Table 6-12 Comparison of SN and ESAL for the Sawyer Aggregate at the Different Cases

	D_{base} = 76 mm D_{ac} = 178 mm E_{ac} = 3450 MPa		D_{base} = 152 mm D_{ac} = 178 mm E_{ac} = 3450 MPa		D_{base} = 228 mm D_{ac} = 178 mm E_{ac} = 3450 MPa		D_{base} = 304 mm D_{ac} = 178 mm E_{ac} = 3450 MPa	
	SN	ESAL	SN	ESAL	SN	ESAL	SN	ESAL
Coarser at OMC	3.12	699,700	3.25	895,600	3.35	1,076,300	3.50	1,405,700
1% below OMC	3.16	755,700	3.34	1,057,000	3.49	1,381,300	3.68	1,913,300
1% above OMC	2.99	541,300	3.00	552,300	2.97	519,800	2.98	530,500

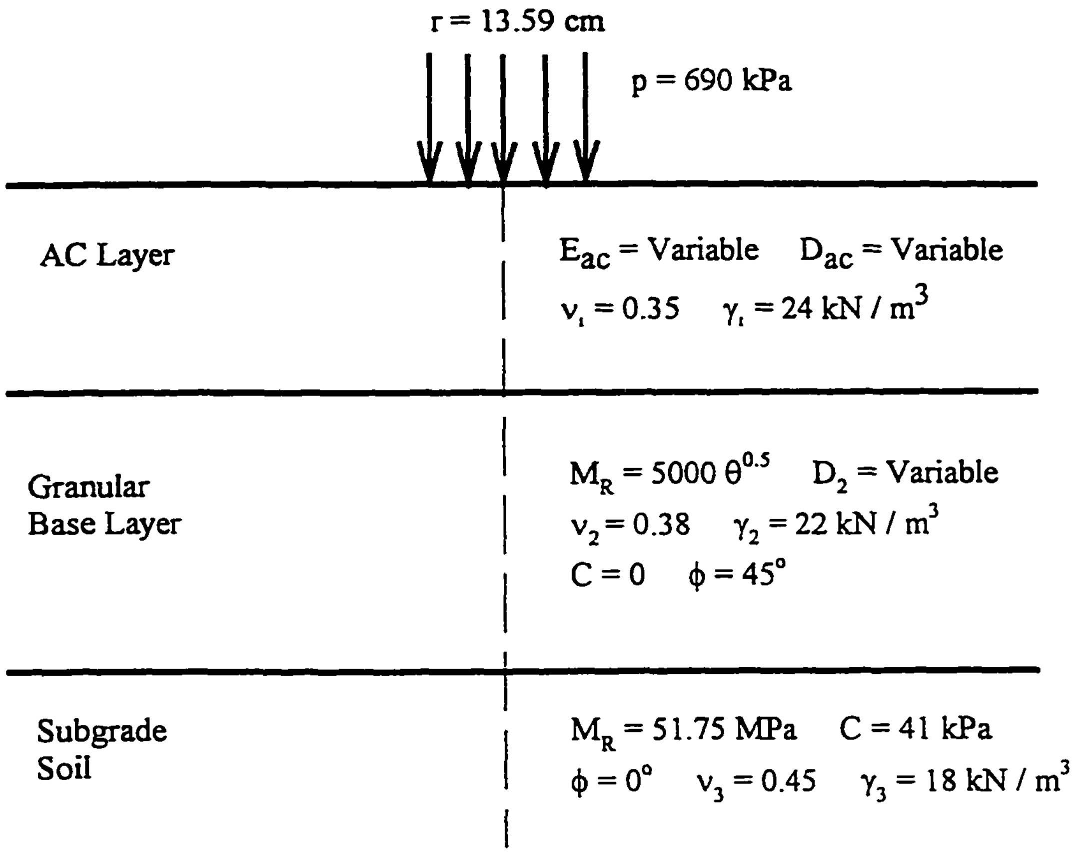

Figure 6-1 Pavement Configuration Used for the ELBK Calculation

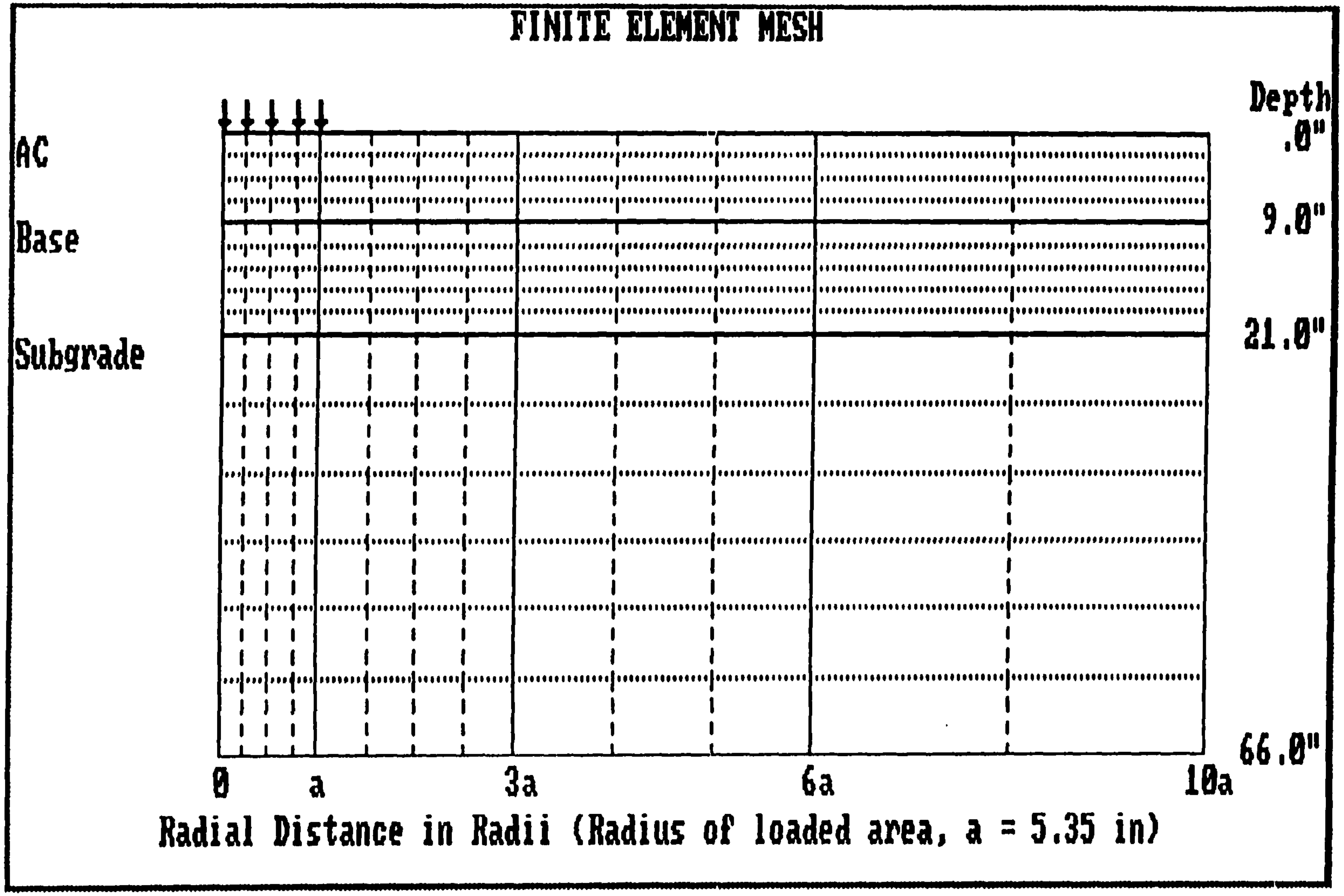

Figure 6-2 Finite Element Mesh Used in This Study for ELBK Calculation

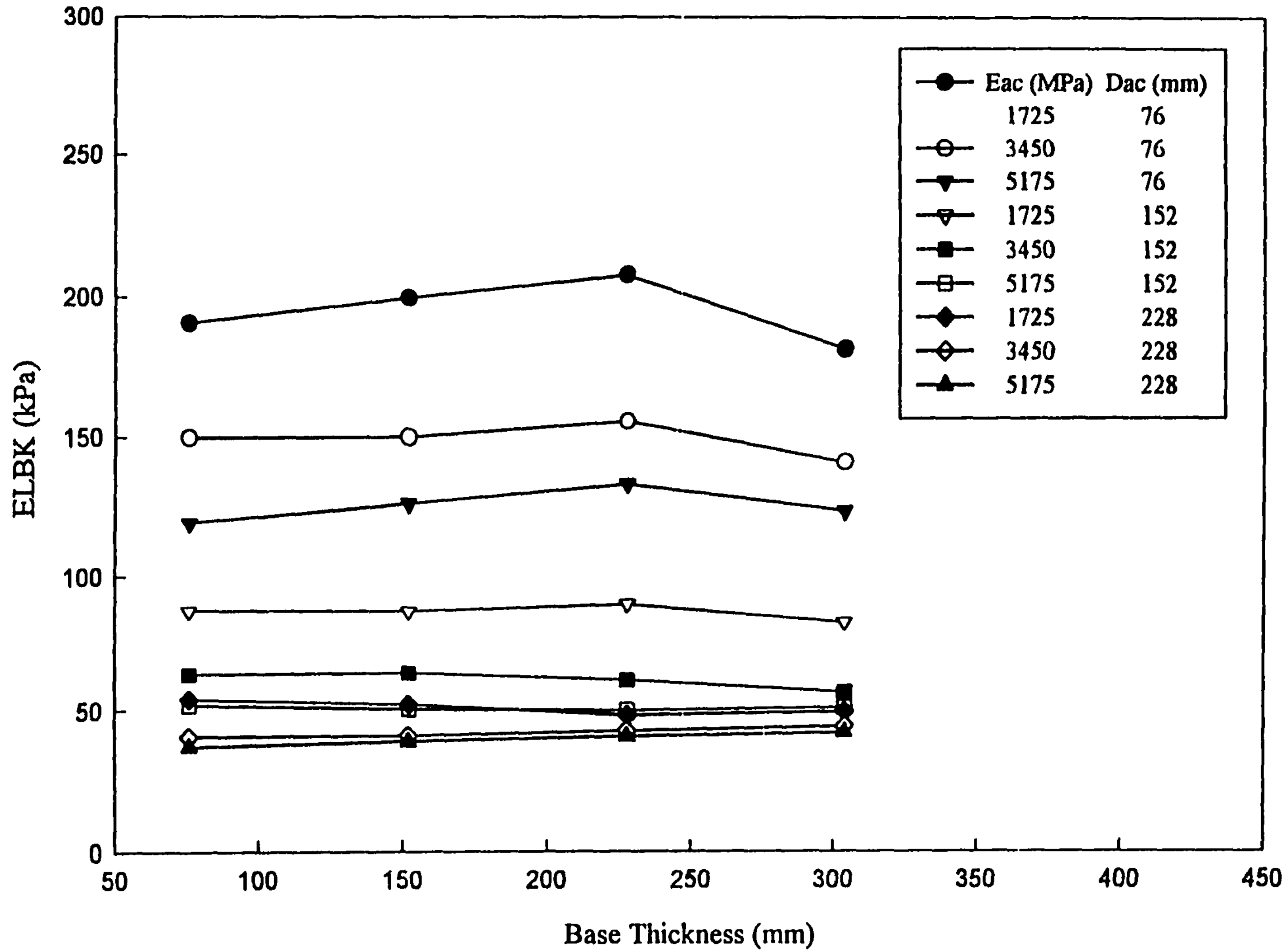

Figure 6-3 Effect of Base Layer Thickness on the ELBK Values

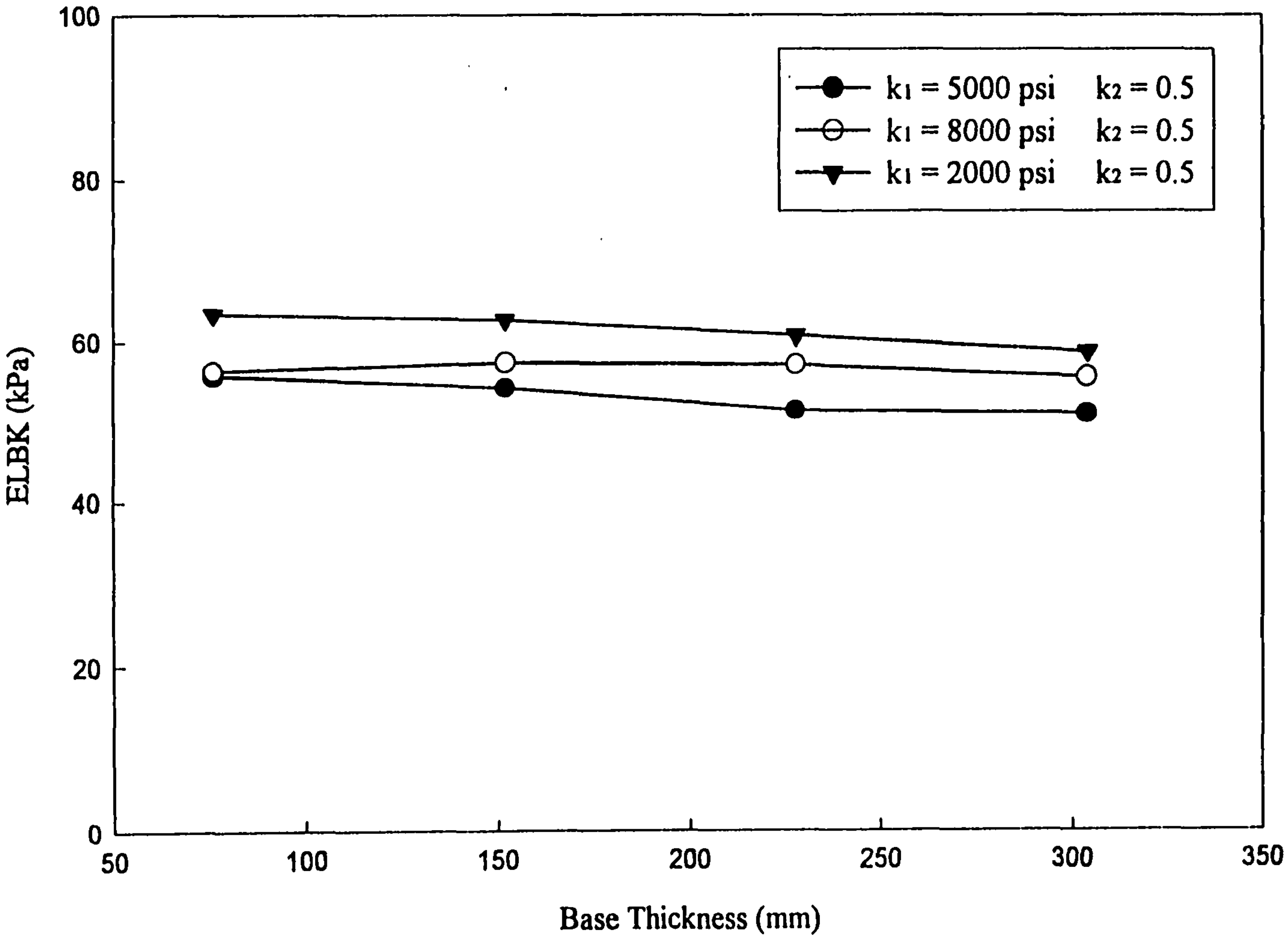

Figure 6-4 Effect of Base Layer RM on the ELBK Values

CHAPTER 7

SUMMARY, CONCLUSIONS, AND RECOMMENDATIONS

7.1 Introduction

This chapter presents a summary of this study and conclusions drawn from the data obtained and the analyses performed in the preceding chapters. Finally, recommendations for further research are suggested.

7.2 Summary

An evaluation of resilient modulus (RM) for aggregate materials and its application in AASHTO flexible pavement design were conducted in this study. Two most commonly encountered aggregates, Richard Spur (RS) limestone and Sawyer sandstone, that are used as good quality subbase/base of roadways in Oklahoma, were selected and tested under cyclic loading to evaluate the RM by using the AASHTO T 294-94 method. The effects of testing procedure, gradation, moisture content, drainage condition, and aggregate type on the RM values were investigated based on the obtained test results. The material model parameters and the layer coefficients which are used in the AASHTO flexible pavement design were determined and the effects of gradation, moisture content, and drainage condition on these values were evaluated.

Material property tests, such as grain size distribution, moisture-density relationship, Los Angeles abrasion, specific gravity, and Atterberg limits tests, were conducted first for the two selected aggregates. Following the RM tests, unconfined compressive strength and triaxial compression tests were also conducted on the specimens to evaluate the material properties including cohesion, friction angle, and unconfined compressive strength.

To ensure the same gradation among the various aggregate types, the median gradation was selected to investigate the effects of testing procedure, moisture content, and drainage condition on the RM values. However, in order to investigate the effect of gradation on the RM values, three gradations, namely, the coarser limit, the median, and the finer limit specified by the ODOT were selected. RM test specimens of 152 mm diameter and 304 mm height were prepared according to the AASHTO designation T 294-94. The test specimens were compacted at the OMC and above 95% of the MDD value obtained from the moisture-density tests.

The AASHTO T 294-94 testing procedure was used in most of the majority RM tests in this study. The major differences between the standard and the interim testing procedures (AASHTO T 294-94 and T292-91I) were compared and their effects on the RM values were investigated in terms of sample conditioning, applied stress sequence, number of loading cycles, loading duration, and loading waveform.

Three moisture contents, namely, OMC, 2% below and 2% above the OMC, were selected to investigate the effect of moisture content on the RM values.

Two types of undrained RM tests, undrained I and undrained II, were conducted in order to simulate the different traffic situations in the field. For the RS aggregate, the specimen were tested at the OMC. However, for the Sawyer aggregate, the specimens were prepared at the OMC and then soaked in a water tank for one week period in order to increase the degree of saturation. The effects of drainage condition, pore pressure, and degree of saturation on the RM values were investigated.

The k-θ model was implemented on both of the aggregates in order to obtain the material parameters k_1 and k_2. The model is found to describe the resilient characteristics of the two selected aggregates reasonably well. In addition, multiple linear regression models between the RM values and the bulk stress (θ), moisture content, and gradation were established for the two aggregates investigated.

The AASHTO flexible pavement design methodology uses layer coefficients to relate the structural design of the pavement with its performance (AASHTO 1993). Layer coefficient (a_2) values corresponding to the base layer were determined for each combination of the three different AC layer RM values, three different AC layer thicknesses, and four different base layer thicknesses. MICH-PAVE, a finite element software, was used to calculate the equivalent layer bulk stress (ELBK) for each of the cases. Furthermore, the layer coefficients were determined from the ELBK for each of the cases. The effects of gradation, moisture content, and drainage condition on layer coefficients were investigated, and regression equations between the layer coefficients and the various contributing factors, such as the AC layer RM and thickness, the material gradation, and the moisture content, were established. Finally, the application of layer coefficients in the design of flexible pavement using the AASHTO design methodology and the influence of layer coefficients on the design results were explained with the help of several design examples.

7.3 Conclusions

From the data obtained and the analyses presented in the preceding chapters, the following conclusions are made.

1. The RM values obtained from the AASHTO T 294-94 method are nearly 32 to 122%

higher than those from the AASHTO T 292-91I method due to the different stress sequences and loading waveforms used in the two testing procedures. The haversine waveform used in the AASHTO T 294-94 method produces higher RM values than those from the triangular and rectangular waveforms due to the different loading durations, rest periods, and loading frequency used in these waveforms.

2. The variabilities of the RM values due to the three different gradations which are specified by Oklahoma DOT are found different for the two investigated aggregates. For the RS aggregate, the median gradation produces substantially higher RM values (41 to 129% higher) than the finer limit gradation but only slightly higher values (0 to 26% higher) than the coarser limit gradation. However, for the Sawyer aggregate, the coarser limit gradation produces the highest RM values (nearly 10 to 36% higher than the finer limit and the median gradations), and the RM values of the median and the finer limit gradations are nearly the same.

3. An increase in moisture content leads to a decrease in RM values. The variations of the RM values between 2% below the OMC and the OMC are nearly -13 to 27% (RS aggregate) and 11 to 37% (Sawyer aggregate), while the variations between the OMC and 2% above the OMC are more than 25 to 80% (RS aggregate) and 18 to 71% (Sawyer aggregate), respectively. Although 2% above the OMC cannot cause the specimen saturation, the decreasing of RM values is obvious. So, the RM values will decrease significantly when the specimens reach the state of saturation.

4. As the fines increase in a gradation, the cohesion (C) increases and the friction angle (ϕ) decreases. On the other hand, as the moisture changed, regardless which side of the OMC, the cohesion (C) decreases compared to the case of OMC. However, the

friction angle (ϕ) increases as the moisture increased.

5. Cyclic loading of unsaturated aggregate materials under undrained conditions induces pore pressure, thereby reducing the effective stress and material stiffness. The pore pressure generation increases with increasing the degree of saturation. Also, as the pore pressure ratio increases, the modulus ratio decreases.

6. The RM values obtained from the drained tests are 34 to 97% and 25 to 58% higher than those from the undrained tests for the RS and the Sawyer aggregates, respectively. This may be due to (i) the increased density and decreased moisture content in the specimens used in the drained tests; (ii) the pore pressure generated in the specimens used in the undrained tests.

7. The strain error caused by the data acquisition system is the major reason for the measured RM errors. The RM errors depend on the level of resilient strain, and therefore depend on the confining pressure (σ_c) and deviator stress (σ_d). For the stress ratio $\sigma_d/\sigma_c \leq 1$, if the bulk stress (θ) $\leq$ 84 kPa, RM errors as great as 78% and 55% of the measured RM values are evident for the RS and the Sawyer aggregates, respectively. However, if the θ > 136 kPa, relatively lower RM errors are produced (6.4 to 17% of the measured RM values). For the stress ratio $\sigma_d/\sigma_c > 1$, at any level of bulk stress, the yielded RM errors are relatively small (3 to 27% of the measured RM values). Generally, the RM values measured in this study are more reliable at the higher bulk stress (θ > 136 kPa) than those at the lower bulk stress. Caution should be exercised in practical application when the bulk stress $\theta \leq$ 84 kPa.

8. As RM values changed due to the different effects, the k_1 value has been significantly

influenced. However, the variation of k_2 value among the different cases is not significant. Generally, assuming the k_2 value as 0.5 is a safe assumption for design purposes. The k_1 value, however, should be carefully selected in the design practice, since the variation of k_1 value is significant for different conditions, and also it is associated with the aggregate type.

9. As the fines increased in a gradation, the k_1 value decreases. However, the k_2 value keeps unchanged (near 0.5). On the other hand, as the moisture increased, generally, the k_1 value decreases and the k_2 value slightly increases.

10. As RM values decrease from the drained to the undrained conditions, the k_1 value decreases and the k_2 value keeps nearly same for both aggregates. Drainage conditions have a significant effect on the k_1 value.

11. The multiple linear regression model developed in this study includes the most important factors that have influences on RM values, hence, it can be used to predict the RM values of the investigated aggregate bases if the different moisture content and gradation are used in the pavement design and construction.

12. The ELBK values obtained in this study are in the range suggested by AASHTO design guide (AASHTO 1993). As the RM and the thickness of AC layer increase, the ELBK shows the decreasing trend. Also, it can be observed that the thickness and RM of the base layer have a very small influence on the ELBK values.

13. The service life of a pavement will be reduced significantly for the pavement designed based on the OMC, however, the actual moisture is often above the optimum during rainfall. Similarly, half of the service life or two third of the service life will be lost for the pavement designed based on the drained conditions, if the undrained conditions

are pursued in the field.

14. The layer coefficients of the RS aggregate are higher than those of the Sawyer aggregate in the different cases, hence, using the RS aggregate as the base layer is more effective than using the Sawyer aggregate in the pavement design. The regression equations for predicting the layer coefficients developed in this study include the most important factors and, hence, it is believed that these equations can be used in the practice if different conditions such as the different moisture content, gradation, and thickness and RM of AC layer are met in the field.

7.4 Recommendations

The following recommendations are made for further studies.

1. Gradation has a significant effect on RM values. From the practical point, if the material gradation located outside the ODOT gradation band is selected as paving material, its RM values could be significantly different with the values from the gradation within the ODOT band. The influence of gradation on RM values should be studied at the gradations that are located outside the ODOT gradation band, such as above the finer limit or below the coarser limit gradations. This will lead to a complete understanding of the gradation effect on RM values.
2. Moisture content has a significant effect on the stiffness of aggregate materials. In further study, the moisture content effect on RM values should be conducted by compacting specimens at the OMC, and then drying and soaking the specimens to obtain a different degree of saturation. This will lead to the same dry density among the different specimens, and hence, the moisture effect on RM can be isolated. The

worst scenario regarding the moisture effect is when a specimen is at or near saturation. Since most of the pavement bases are constructed under the drain conditions, hence conducting the RM test at the drain conditions by using the specimen at or near saturation is highly recommended in the further study.

3. Test results from this study indicate that aggregate material is very sensitive to moisture content. Further studies should be conducted to investigate the moisture sensitivity of aggregate materials at different gradations, particularly for the gradations with different percentages of fine particles.

4. The drainage condition has a significant effect on RM values. In the present study, the undrained RM test was conducted with aggregate having the ODOT median gradation and optimum moisture content. The influence of undrained conditions on RM values could be different if the different aggregate gradations and moisture contents are used. Hence, the drainage effect should be studied at gradations corresponding to the ODOT coarser limit and the finer limit gradations, also at varied moisture contents.

5. The RM values measured from the laboratory cyclic triaxial tests in the current study are very sensitive in terms of the accuracy of the elastic strain measurement. Therefore, it is recommended that a more accurate data acquisition system be used in a future study. Also, a more accurate measurement of pore pressure can be achieved by using a miniature probe within the specimen. Although it was not within the scope of this research, it should be considered in a future study.

6. Gradation analyses should be conducted after the sample preparation and RM testing processes to investigate (i) if the segregation of particles is produced due to the

vibration and compaction used in the sample preparation; and (ii) if the particles are broken down due to the sample compaction and cyclic triaxial testing. These analyses are important in terms of the cyclic behavior of aggregate materials.

7. A comparison between the field and the laboratory RM values of the aggregates should be made to determine whether variations occur between these values as a result of the various field conditions. In a further study, it is recommended to conduct the in-situ FWD tests on the aggregate bases investigated in this study to obtain the backcalculated field moduli. Therefore, the correlation between the field and the laboratory determined RM values can be established for these aggregates.

REFERENCES

American Association of State Highway and Transportation Officials (AASHTO) (1972). *AASHTO interim guide for design of pavement structures.* AASHTO, Washington, D.C.

American Association of State Highway and Transportation Officials (AASHTO) (1982). "Suggested method of test for resilient modulus of subgrade soils, AASHTO DESIGNATION: T 274-82," Washington, D.C.

American Association of State Highway and Transportation Officials (AASHTO) (1991). "Interim method of test for resilient modulus of subgrade soils and untreated base/subbase materials, AASHTO DESIGNATION: T 292-91I," Washington, D.C.

American Association of State Highway and Transportation Officials (AASHTO) (1992a). "Interim method of test for resilient modulus of unbound base/subbase materials and subgrade soils - SHRP Protocol P46, AASHTO DESIGNATION: T 294-92I," Washington, D.C.

American Association of State Highway and Transportation Officials (AASHTO) (1992b). "Unconfined compressive strength of cohesive soil, AASHTO DESIGNATION: T 208-92," Washington, D.C.

American Association of State Highway and Transportation Officials (AASHTO) (1993). *AASHTO guide for design of pavement structures.* AASHTO, Washington, D.C.

American Association of State Highway and Transportation Officials (AASHTO) (1993a). "Moisture-Density relations of soils using a (4.55-kg) 10-lb rammer and an (457-mm) 18-in. Drop, AASHTO DESIGNATION: T 180-93," Washington, D.C.

American Association of State Highway and Transportation Officials (AASHTO) (1993b). "Sieve analysis of fine and coarse aggregates, AASHTO DESIGNATION: T 27-93," Washington, D.C.

American Association of State Highway and Transportation Officials (AASHTO) (1994a). "Standard method of test for resilient modulus of unbound granular base/subbase materials and subgrade soils - SHRP Protocol P46, AASHTO DESIGNATION: T 294-94," Washington, D.C.

American Association of State Highway and Transportation Officials (AASHTO) (1994b). "Determining the liquid limits of soils, AASHTO DESIGNATION: T 89-94," Washington, D.C.

American Association of State Highway and Transportation Officials (AASHTO) (1994c). "Determining the plastic limit and plasticity index of soils, AASHTO DESIGNATION: T 90-

94," Washington, D.C.

American Association of State Highway and Transportation Officials (AASHTO) (1994d). "Resistance to degradation of small-size coarse aggregate by abrasion and impact in the Los Angeles machine, AASHTO DESIGNATION: T 96-94," Washington, D.C.

American Association of State Highway and Transportation Officials (AASHTO) (1994e). "Specific gravity and absorption of fine aggregate, AASHTO DESIGNATION: T 84-94," Washington, D.C.

American Association of State Highway and Transportation Officials (AASHTO) (1994f). "Consolidated, undrained triaxial compression test on cohesive soils, AASHTO DESIGNATION: T 297-94," Washington, D.C.

Asphalt Institute (AI). (1982a). *Thickness Design.* Manual (MS-1), Research and Development of the Asphalt Institute, Ninth Edition, Research Report 82-2.

Asphalt Institute (AI), (1982b). "Method of test of for resilient modulus of soil," Laboratory Manual Series No. 11 (MS-11), Appendix C, College Park, M.D.

Asphalt Institute (AI) (1991a). "Computer program DAMA (CP-1/1991 Revision)-Pavement Structural Analysis Using Mult-Layered Elastic Theory," Lexington, KY.

Asphalt Institute (AI) (1991b). *Thickness design- asphalt pavements for highways and streets.* Manual Series No. 1 (MS-1), College Park, M.D.

Barksdale, R.D. (1971). "Compressive stress pulse times in flexible pavements for use in dynamic testing," *Highway Research Record, No. 345*, Highway Research Board, Washington, D.C., 32-44.

Barksdale, R.D. (1972). "Laboratory evaluation of rutting in base course materials," *Proceedings, Third International Conference on the Structural Design of Asphalt Pavements*, London, England, Vol. 1, 161-174.

Barksdale, R.D., et al. (1975). "Test procedures for characterizing dynamic stress-strain properties of pavement materials," Special Report 162. Transportation Research Board, National Research Council, Washington, D.C.

Barksdale, R.D. and Itani, S.Y. (1989). "Influence of aggregate shape on base behavior," *Transportation Research Record, No. 1227*, Transportation Research Board, Washington, D.C., 173-182.

Barksdale, R.D., Rix, G.J., Itani, S., Khosla, P. N., Kim. R., Lambe, P. C., and Rahman, M. S. (1990). "Laboratory determination of resilient modulus for flexible pavement design," Interim Report No. I, Georgia Tech Project E20-634, National Cooperative Highway

Research Program, Transportation Research Board, Washington, D.C.

Bowles, J.E. (1988). *Foundation analysis and design*. The fourth edition, McGraw Hill Publishing Company, New York, N.Y.

Brown and Pappin, J.W. (1981). "Analysis of pavements with granular bases," *Transportation Research Record No. 810*, Transportation Research Board, Washington, D.C., 17-23.

Burczyk, J.M., Ksaibati, K., Sprecher, R.A. and Farrar, M.J. (1994). "Factors influencing determination of a subgrade resilient modulus value," *Transportation Research Record No. 1462*, Transportation Research Board, Washington, DC, 72-78.

Chen, D.H. (1994). "Resilient modulus of aggregate bases and a mechanistic-empirical methodology for flexible pavements," PhD dissertation, School of Civil Engineering and Environmental Science, University of Oklahoma, Norman, Oklahoma.

Chen, D.H., Zaman, M.M., and Laguros, J.G. (1994a). "Resilient modulus of aggregate materials: variability due to testing procedure and aggregate type," *Transportation Research Record, No. 1462*, Transportation Research Board, Washington, D.C., 57-64.

Chen, D.H., Zaman, M.M., and Laguros, J.G. (1994b). "Characterization of base/subbase materials under repetitive loading," *Journal of Testing and Evaluation, Vol. 23, No. 3*, ASTM, Philadelphia, Pennsylvania, 180-188.

Chen, D.H., Zaman, M.M., and Laguros, J.G. (1994c). "Selection of a distress model for prediction of pavement service life," *Proceedings, The Third material Engineering Conference: New Materials and Method for Repair*, Nov. 14-16, San Diego, California, American Society of Civil Engineers, New York, N.Y., 1073-1080.

Chen, D.H., Zaman, M., Laguros, J., Soltani, A. (1995). "Assessment of computer programs for analysis of flexible pavement structure," *Transportation Research Record, No. 1482*, Transportation Research Board, Washington, D.C., 123-133.

Cosentino, P.J. and Chen, Y. (1991). " Correlating resilient moduli from pressuremeter tests to laboratory California Bearing Ratio," *Transportation Research Record, No. 1309*, Transportation Research Board, Washington, D.C., 56-65.

Das, B.M. (1990). *Principles of Geotechnical Engineering*. Second Edition. PWS Publishers.

Darter, M.I., Smith, K.D., and Hall, K.T. (1993). Concrete pavement backcalculation results from field studies," *Transportation Research Record, No. 1377*, Transportation Research Board, Washington, D.C., 7-16.

Elliott, R.P. (1992). "Selection of subgrade modulus for AASHTO flexible pavement design," *Transportation Research Record, No. 1354*, Transportation Research Board, Washington, D.C., 39-44.

Elliott, R.P. and Thornton, S.I. (1988). "Resilient modulus and AASHTO pavement design," *Transportation Research Record, No. 1196*, Transportation Research Board, Washington, D.C., 116-124.

Harichandran, R.S., Yeh, M.S., and Baladi G.Y. (1989). "MICH-PAVE User's Manual," *Final Report, FHWA-MI-RD-89-032*, Department of Civil and Environmental Engineering, Michigan State University, East Lansing, Michigan.

Harichandran, R.S., Yeh, M.S., and Baladi G.Y. (1990). "MICH-PAVE: A nonlinear finite element program for analysis of flexible pavements," *Transportation Research Record, No. 1286*, Transportation Research Board, Washington, D.C., 123-131.

Haynes, J.H. and Yoder, E.J. (1963). "Effects of repeated loading on gravel and crushed stone base course materials used in the AASHTO road test," *Highway Research Record No. 39*, Highway Research Board, Washington, D.C., 82-96.

Hicks, R.G. (1970). "Factors influencing the resilient properties of granular materials," Ph.D. dissertation, University of California at Berkeley, California.

Hicks, R.G. and Monismith, C.L. (1971). "Factors influencing the resilient properties of granular materials," *Transportation Research Record, No. 345*, Transportation Research Board, Washington, D.C., 15-31.

Ho, R.K.H. (1989). "Repeated load tests on untreated soils, a Florida experience," workshop on Resilient Modulus Testing, Oregon State University, Corvallis, Oregon, March 28-30, 1989.

HRB, (1962). The AASHTO Road Test, Report 5; Pavement research; Report 6; Special Studies; and Report 7: Summary Report, Special Reports 61E, 61F, and 61G, Highway Research Board.

Huang, Y.H. (1993). *Pavement analysis and design*. Prentice-Hall, Inc., Englewood Cliffs, N.J.

Huffman, G.G., Alfonsi, P.P., Dalton, R.C., Duarte-Vivas, A., and Jeffries, E.L. (1975). *Geology and Mineral Resources of Choctaw County, Oklahoma.* Bulletin 120, Oklahoma Geological Survey.

Irwin, L.H. (1993). "Report of the discussion group on practical limitations and what can be done to overcome them," *Transportation Research Record, No. 1377*, Transportation Research Board, Washington, D.C., 1-12.

Johnson, E.G. and Hicks, R.G. (1987). "Evaluation of effect of uncrushed base layers on pavement performance," *Transportation Research Record, No. 1117*, Transportation Research Board, Washington, D.C., 11-20.

Kalcheff, I.V. and Hicks, R.G. (1973). "A test procedure for determining the resilient properties of granular materials," *Journal of Testing and Evaluation, Vol. 1, No. 6*, ASTM, Philadelphia, Pennsylvania, 472-479.

Kamal, M.A., Dawson, A.R., Farouki, O.T., Hughes, A.B., and Sha'at, A.A. (1993). "Field and laboratory evaluation of the mechanical behavior of unbound granular materials in pavements," *Paper presented at 72nd Annual Meeting of the Transportation Research Board*, Washington, D.C., January 12, 1993.

Khedr, S. (1985). "Deformation characteristics of granular base course in flexible pavements," *Transportation Research Record, No. 1043*, Transportation Research Board, Washington, D.C., 131-138.

Laguros, J.G., Zaman, M.M., and Chen, D.H. (1993). "Resilient modulus of select aggregate bases and their correlations with other engineering properties,"*Report No 2189, ORA 125-6073*, School of Civil Engineering and Environmental Science, University of Oklahoma, Norman, Oklahoma.

Lambe, T.W. and Whitman, R.V. (1969). *Soil Mechanics*. John Wiley & Sons, Inc., New York, N.Y.

Lary, J.A. and Mahoney, J.P. (1984). "Seasonal Effects on the Strength of Pavement Structures," *Transportation Research Record, No. 954*, Transportation Research Board, Washington, D.C., 41-49.

Lee, S.W., Mahoney, J.P., and Jackson, N.C. (1988). "Verification of backcalculation of pavement moduli," *Transportation Research Record, No. 1196*, Transportation Research Board, Washington, D.C., 85-95.

Lotfi, H.A., Schwartz, C.W., and Witczak, M.W. (1988). "Compaction specification for the control of pavement subgrade rutting," *Transportation Research Record, No. 1196*, Transportation Research Board, Washington, D.C., 108-115.

Lotfi, H.A. and Witczak, M.W. (1985). "Dynamic characterization of cement-treated base and subbase materials," *Transportation Research Record, No. 1031*, Transportation Research Board, Washington, D.C., 41-48.

Maree, J.H., Vanzyl, N.J.W., and Freeme C.R. (1982). "Effective moduli and stress dependance of pavement materials as measured in some Heavy-Vehicle Simulater tests," *Transportation Research Record, No. 852*, Transportation Research Board, Washington, D.C., 52-60.

May, R.W. and Witczak, W.M. (1981). "Effective granular modulus to model pavement responses," *Transportation Research Record, No. 810*, Transportation Research Board, Washington, D.C., 1-17.

Mendenhall, W. and Sincich, T. (1992). *Statistics for engineering and the sciences*. Third Edition, Dellen Publishing Company, San Francisco, California.

Mohammad, L.N., Puppala, A.J., and Prasad, A. (1994). "Influence of testing procedure and LVDT location on resilient modulus of soils," *Transportation Research Record, No. 1462*, Transportation Research Board, Washington, D.C., 91-101.

Monismith, C.L. (1992). "Analytically based asphalt pavement design and rehabilitation: theory and practice, 1962-1992," *Transportation Research Record, No. 1354*, Transportation Research Board, Washington, D.C., 5-26.

Morris, J. and Haas, R.C.G. (1974). "Dynamic testing of bituminous mixtures for pavement deformation response," *Special Technical Publication No. 561*, ASTM, Philadelphia, Pennsylvania, 115-131.

Nataatmadja, A. (1994). " Stress-strain relations for base course materials under repeated loading," Transactions of the Institution of Engineers, Australia. Vol. CE36, No. 4, 299-308.

Oklahoma Department of Transportation (ODOT) (1996). *Standard Specifications for Highway Construction*. 1996 Edition, Oklahoma City, Oklahoma.

Pandey, K.K. (1996). "Evaluation of resilient modulus and layer coefficients of a coal ash stabilized marginal aggregate base for AASHTO flexible pavement design," Ph.D. dissertation, School of Civil Engineering and Environmental Science, University of Oklahoma, Norman, Oklahoma.

Pezo, R.F., Claros, G., Hudson, W.R., and Stoke, K. H. (1992). "Development of a reliable resilient modulus test for subgrade and non-granular subbase materials for use in routine pavement design," *Research Report 1177-4f*, Center for Transportation Research, Bureau of Engineering Research. The University of Texas at Austin.

Powell, W.D. et al. (1984). "The structural design of bituminous pavements," *TRRL Laboratory Report 1132*, Transport and Road Research Laboratory, U.K.

Raad, L., Minassian, G. H. and Gartin, S. (1990). "Characterization of saturated granular bases under repeated loads," *Transportation Research Record No. 1369*, Transportation Research Board, Washington, D.C., 73-82.

Rada, G. and Witczak, M. (1981). "Comprehensive evaluation of laboratory moduli results for granular material," *Transportation Research Record, No. 810*, Transportation Research Board, Washington, D.C., 23-33.

Rahman, M., Thomas, C., and Zaman, M.M. (1996). "Field evaluation of drainable bases in Oklahoma," *ORA Report 125-4299*, School of Civil Engineering and Environmental Science, the University of Oklahoma, Norman, Oklahoma.

Rahman, M., Sudharsanan, S., Muraleetharan, K.K., and Zaman, M.M. (1997). "Modeling Time-Dependent Behavior of Pavement Drainage Using Linear System Identification and Neural Network Techniques," *Transportation Research Record No. 1582*, Transportation Research Board, Washington, D.C., 34-41.

Rowland, T.L. (1972). *General Survey of Carbonate Mineral Deposits in Oklahoma.* Oklahoma Geology Notes, Vol. 32, No. 3, Oklahoma Geological Survey.

Seed, H.B. and McNeill, R.L. (1958). "Soil deformation under repeated stress applications," *Special Technical Publication No. 32*, ASTM, Philadelphia, Pennsylvania, 177-197.

Seed, H.B., Chan, C.K., and Lee, C.E. (1962). "Resilience characteristics of subgrade soils and their relation to fatigue failure in asphalt pavements," *Proceeding, International Conference on Structural Design of Asphalt Pavement*, University of Michigan, 611-636.

Seed, H.B. (1967). "Factors influencing the resilient deformations of untreated aggregate base in two layer pavements subject to repeated loading." *Highway Research Record No. 190*, Highway Research Board, Washington, D.C., 19-57.

Shell (1978), International Petroleum, Co. Ltd., *Shell Pavement Design Manual.*

Spangler M.G. and Handy R.L. (1973). *Soil Engineering.* Intext Educational Publishers, New York, NY.

Terrel, R.L., Awad, I.S., and Foss, L.R. (1974). "Techniques for characterizing bituminous materials using a versatile triaxial testing system," *Special Technical Publication No. 561*, ASTM, Philadelphia, Pennsylvania, 47-66.

Thom, N.H. (1988). "Design of road foundations," Ph.D. Dissertation, University of Nottingham, U.K.

Thom, N.H. and Brown, S.F. (1987). "The effect of moisture on the structural performance of a crushed limestone road base, " *Paper presented at the 1987 Annual Transportation Research Board Meeting*, Washington, D.C.

Thompson, M.R. and Elliot, R.P. (1985) "ILLI-PAVE-Based Response Algorithms for Design of Conventional Flexible Pavements," *Transportation Research Record No. 1043*, Transportation Research Board, Washington, D.C., 50-57.

Thompson, M.R. (1987). "ILLI-PAVE based full-depth asphalt concrete pavement design procedure," *Proceedings, Sixth International Conference on Structural Design of Asphalt*

Pavements, Ann Arbor, MI.

Thompson, M.R. (1989). "Factors affecting the resilient moduli of soil and granular materials," Workshop on Resilient Modulus Testing, Oregon State University, Corvallis, Oregon, March 28-30, 1989.

Thompson, M.R. and Barenberg, E.J. (1989). *Calibrated mechanistic structural analysis procedures for pavements: Vol. 1, Final Report*, NCHRP Project 1-26, Transportation Research Board, National Research Council, Washington, D.C.

Thompson, M.R. and Barenberg, E.J. (1990). "ILLI-PAVE PC Version-USER'S MANUAL," NCHRP I-26 Deliverable, Transportation Faculties Group, University of Illinois at Urbana-Champaign, April, 1990.

Thompson, M.R. and Smith, K.L. (1990). "Repeated triaxial characterization of granular bases," *Transportation Research Record, No. 1278*, Transportation Research Board, Washington, D.C., 7-17.

Tian, P., Zaman, M.M., and Laguros, J.G. (1997). "Influence of testing procedure on resilient modulus of aggregate materials," *Proceedings, Ninth International Conference of the Association for Computer Methods and Advances in Geomechanics*, Wuhan, P.R. China, November 2-7, 1997. Volume 2, 795-800.

Tian, P., Zaman, M.M., and Laguros, J.G. (1997a). "Drained and undrained resilient moduli of aggregate materials," Submitted to the *Journal of Experimental Mechanics* for Possible Publication, Aug., 1997. (In Review).

Tian, P., Zaman, M.M., and Laguros, J.G. (1997b). "Resilient moduli of aggregate materials: variability due to gradation and moisture content," Submitted to ASTM for Possible Publication in the *Journal of Testing and Evaluation*, Nov, 1997. (In Review).

Tian, P., Zaman, M.M., and Laguros, J.G. (1998). "Gradation and moisture effects on resilient moduli of aggregate bases," Accepted for Publication in *Transportation Research Record*, Transportation Research Board, Washington, D.C. (In Press).

Ullidtz, P. (1977). "Overlay and stage by stage design," *Proceedings, Fourth International Conference on Structural Design of Asphalt Pavements*, Ann Arbor, MI.

Uzan, J. (1985). "Characterization of granular material," *Transportation Research Record, No. 1022*, Transportation Research Board, Washington, D.C., 52-59.

Van Til, C.J., McCullough, Vallerga, B.A., and Hicks, R.G. (1972). "Evaluation of AASHO interim guides for design of pavement structures," *NCHRP Report No. 128*, Highway Research Board, Washington, D.C.

Verstraeten, J., Veverka, V., and Francken, L. (1982). "Rational and practical designs of asphalt pavements to avoid cracking and rutting," *Proceeding, Fifth International Conference on the Structural Design of Asphalt Pavements.*

Vinson, T.S. (1989). "Fundamentals of resilient modulus testing," *Workshop on Resilient Modulus Testing*, Oregon State University, Corvallis, Oregon, March 28-30, 1989.

Witczak, M.W. and Uzan, J. (1988). "Granular material characterization," *The Universal Airport Pavement Design System, Report I of IV*, University of Maryland.

WU, F. (1993). "Laboratory versus nondestructive testing for pavement design," *Journal of Transportation Engineering*, Vol 119, No. 6, American Society of Civil Engineers, New York, N.Y. 934-938

Zaman, M.M., Laguros, J.G., and Danayak, R. (1991). "Assessment of resilient modulus testing methods and their application to design of pavements," *Report No. FHWA/OK 91(08), ORA 158-342,* University of Oklahoma, Norman, Oklahoma.

Zaman, M.M., Chen, D.H., and Laguros, J. (1994). "Resilient modulus of granular materials," *Journal of Transportation Engineering*, Vol. 120, No. 6, American Society of Civil Engineers, New York, N.Y., 967-988.

APPENDIX A

Table A-1 RM Values of the RS Aggregate at the Median Gradation and the OMC (T 292-91I)

Confining Pressure (kPa)	Deviator Stress (kPa)	Bulk Stress (kPa)	RM Test 1 (MPa)	RM Test 2 (MPa)	RM Test 3 (MPa)	RM Test 4 (MPa)	RM Test 5 (MPa)	RM Test 6 (MPa)	Mean RM Value (MPa)	Standard Deviation (MPa)	St. Dev./ Mean (%)
138	69	483	222.06	249.76	226.34	242.80	212.28	220.27	228.92	14.37	6.28
138	138	551	265.20	248.18	248.04	259.27	255.07	245.90	253.61	7.59	2.99
138	207	621	258.58	191.68	254.93	252.59	247.42	240.94	241.02	24.94	10.35
138	276	689	264.09	179.90	256.86	237.15	232.19	237.22	234.57	29.59	12.61
103	69	378	168.39	109.55	166.74	144.07	129.12	144.69	143.76	22.45	15.62
103	138	447	188.17	139.59	201.95	174.45	166.81	177.90	174.81	21.11	12.08
103	207	516	210.15	154.13	218.28	195.33	201.39	191.61	195.15	22.33	11.44
103	276	585	218.83	165.64	226.34	196.99	209.59	194.57	201.99	21.61	10.70
69	34	241	112.93	76.62	118.44	79.37	84.06	86.47	92.98	18.01	19.36
69	69	276	132.77	99.08	134.42	103.14	102.59	100.53	112.09	16.73	14.93
69	138	345	156.61	122.50	173.56	144.90	144.35	144.62	147.76	16.80	11.37
69	207	414	179.35	148.20	186.79	168.46	171.70	159.09	168.93	13.87	8.21
34	34	136	75.24	72.41	90.67	80.20	71.38	76.55	77.74	7.07	9.09
34	69	171	95.15	88.54	135.80	108.93	100.25	94.19	103.81	17.11	16.48
34	103	205	118.16	107.14	157.02	122.30	113.82	117.27	122.62	17.60	14.36
21	34	97	80.34	72.90	107.07	76.48	70.21	77.51	80.75	13.38	16.56
21	48	111	84.40	86.33	121.26	92.26	79.86	91.29	92.57	14.78	15.97
21	62	125	97.70	93.57	132.49	99.35	97.63	95.91	102.78	14.69	14.29

Table A-2 RM Values of the RS Aggregate at the Median Gradation and the OMC (Haversine Waveform, T 294-94)

Confining Pressure (kPa)	Deviator Stress (kPa)	Bulk Stress (kPa)	RM Test 1 (MPa)	RM Test 2 (MPa)	RM Test 3 (MPa)	RM Test 4 (MPa)	RM Test 5 (MPa)	RM Test 6 (MPa)	Mean RM Value (MPa)	Standard Deviation (MPa)	St. Dev./ Mean (%)
21	21	84	125.12	168.60	62.56	145.31	72.41	135.18	118.20	41.96	35.50
21	41	104	189.20	153.72	105.07	137.87	129.95	132.01	141.30	28.24	19.99
21	62	125	160.95	172.66	172.18	128.71	145.59	114.86	149.16	23.79	15.95
34	34	136	173.90	195.88	133.67	135.94	173.01	136.56	158.16	26.27	16.61
34	69	171	184.58	171.56	203.88	155.51	191.34	127.47	172.39	27.58	16.00
34	103	205	158.47	239.22	173.56	199.53	186.31	138.08	182.53	35.08	19.22
69	69	276	276.63	250.18	237.77	300.40	236.60	194.23	249.30	36.57	14.67
69	138	345	249.76	303.16	245.28	261.75	235.22	190.03	247.53	36.78	14.86
69	207	414	225.65	279.18	238.53	253.41	264.99	183.48	240.87	33.88	14.06
103	69	378	226.06	276.29	205.46	308.33	276.36	223.24	252.62	40.05	15.85
103	103	412	301.44	251.00	226.82	335.82	314.25	214.49	273.97	49.98	18.24
103	207	516	275.19	358.90	294.13	307.36	327.62	252.59	302.63	37.80	12.49
138	103	517	289.45	390.39	298.20	284.76	324.93	280.84	311.43	41.77	13.41
138	138	552	347.81	356.49	305.30	325.62	379.43	293.72	334.73	32.48	9.70
138	276	690	344.50	413.12	345.40	383.02	408.85	310.81	367.62	40.65	11.06

Table A-3 RM Values of the RS Aggregate at the Median Gradation and OMC (Rectangular Waveform, T 294-94)

Confining Pressure (kPa)	Deviator Stress (kPa)	Bulk Stress (kPa)	RM Test 1 (MPa)	RM Test 2 (MPa)	RM Test 3 (MPa)	RM Test 4 (MPa)	Mean RM Value (MPa)	Standard Deviation (MPa)	St. Dev./ Mean (%)
21	21	84	72.69	69.31	60.22	52.98	63.80	8.93	14.00
21	41	104	86.81	88.61	66.76	64.35	76.63	12.85	16.77
21	62	125	99.22	103.01	83.85	88.47	93.64	8.97	9.58
34	34	136	88.12	87.92	76.55	74.69	81.82	7.20	8.80
34	69	171	114.17	119.47	79.79	88.40	100.46	19.34	19.25
34	103	205	135.11	130.50	95.36	103.63	116.15	19.62	16.89
69	69	276	136.08	158.75	105.55	101.21	125.40	27.11	21.62
69	138	345	162.40	178.66	132.63	137.59	152.82	21.59	14.13
69	207	414	172.80	175.63	137.66	140.42	156.63	20.37	13.01
103	69	378	153.65	150.41	120.02	122.37	136.61	17.88	13.09
103	103	412	160.12	166.32	126.57	144.55	149.39	17.76	11.89
103	207	516	192.30	206.29	159.99	175.90	183.62	20.06	10.93
138	103	517	182.65	175.35	155.03	162.95	168.99	12.37	7.32
138	138	552	200.64	201.95	163.64	190.51	189.18	17.78	9.40
138	276	690	248.66	244.87	194.92	246.73	233.79	25.96	11.11

Table A-4 RM Values of the RS Aggregate at the Median Gradation and OMC (Triangular Waveform, T 294-94)

Confining Pressure (kPa)	Deviator Stress (kPa)	Bulk Stress (kPa)	RM Test 1 (MPa)	RM Test 2 (MPa)	RM Test 3 (MPa)	RM Test 4 (MPa)	Mean RM Value (MPa)	Standard Deviation (MPa)	St. Dev./ Mean (%)
21	21	84	51.81	65.32	67.32	58.36	60.70	7.06	11.63
21	41	104	73.03	87.50	56.70	73.65	72.72	12.60	17.32
21	62	125	84.88	104.59	72.97	97.70	90.04	14.01	15.56
34	34	136	64.21	107.97	54.71	98.32	81.30	25.82	31.76
34	69	171	94.19	116.51	74.89	117.82	100.85	20.42	20.25
34	103	205	101.28	118.16	87.43	123.88	107.69	16.57	15.38
69	69	276	92.74	127.33	73.45	125.05	104.64	26.12	24.96
69	138	345	112.79	160.95	98.94	141.52	128.55	27.95	21.74
69	207	414	126.98	188.30	105.28	174.45	148.76	39.11	26.29
103	69	378	102.04	142.00	89.57	139.25	118.22	26.40	22.33
103	103	412	111.62	167.01	88.19	162.81	132.41	38.77	29.28
103	207	516	143.24	210.70	116.65	203.32	168.48	45.90	27.24
138	103	517	125.26	168.25	166.46	166.26	156.56	20.88	13.34
138	138	552	139.87	175.70	184.03	180.17	169.94	20.34	11.97
138	276	690	183.34	224.82	214.76	207.60	207.63	17.67	8.51

Table A-5 RM Values of the RS Aggregate at the Coarser Limit Gradation and the OMC

Confining Pressure (kPa)	Deviator Stress (kPa)	Bulk Stress (kPa)	RM Test 1 (MPa)	Test 2 (MPa)	Test 3 (MPa)	Test 4 (MPa)	Test 5 (MPa)	Test 6 (MPa)	Mean RM Value (MPa)	Standard Deviation (MPa)	St. Dev./ Mean (%)
21	21	84	109.76	66.83	72.55	121.82	119.68	72.00	93.77	25.94	27.66
21	41	104	124.23	140.28	146.41	155.09	157.02	117.89	140.15	16.10	11.49
21	62	125	106.66	147.10	205.12	151.79	156.33	97.91	144.15	38.67	26.83
34	34	136	120.23	140.35	232.88	165.98	157.85	119.27	156.09	42.16	27.01
34	69	171	144.90	168.67	213.11	182.10	225.72	116.37	175.14	41.13	23.48
34	103	205	144.69	202.91	228.75	167.70	182.17	137.46	177.28	34.84	19.65
69	69	276	175.83	214.83	301.02	215.86	216.41	171.35	215.89	46.56	21.56
69	138	345	185.27	229.51	304.61	227.78	230.54	200.84	229.76	41.04	17.86
69	207	414	199.05	254.79	298.82	237.98	247.76	205.39	240.63	36.37	15.12
103	69	378	166.39	249.35	247.97	234.47	273.74	246.59	236.42	36.62	15.49
103	103	412	190.51	254.86	307.36	218.48	292.48	235.22	249.82	44.43	17.78
103	207	516	233.09	297.10	387.36	288.90	298.89	255.41	293.46	52.86	18.01
138	103	517	224.48	314.87	380.33	337.13	265.89	267.19	298.31	56.53	18.95
138	138	552	234.81	305.02	379.43	299.30	295.86	272.84	297.88	47.57	15.97
138	276	690	289.04	339.19	391.77	343.40	349.60	306.40	336.57	35.89	10.66

Table A-6 RM Values of the RS Aggregate at the Finer Limit Gradation and the OMC

Confining Pressure (kPa)	Deviator Stress (kPa)	Bulk Stress (kPa)	RM Test 1 (MPa)	RM Test 2 (MPa)	RM Test 3 (MPa)	RM Test 4 (MPa)	RM Test 5 (MPa)	RM Test 6 (MPa)	Mean RM Value (MPa)	Standard Deviation (MPa)	St. Dev./ Mean (%)
21	21	84	51.12	109.41	50.64	103.56	67.73	120.51	83.83	31.05	37.04
21	41	104	70.42	79.24	70.76	69.86	90.12	113.89	82.38	17.31	21.01
21	62	125	63.87	72.21	75.86	88.88	125.26	106.73	88.80	23.30	26.24
34	34	136	59.46	73.10	52.30	116.79	94.26	98.39	82.38	24.89	30.21
34	69	171	80.06	92.88	74.96	114.10	108.38	111.89	97.05	16.93	17.45
34	103	205	84.75	103.69	93.02	110.03	105.21	121.95	103.11	13.01	12.62
69	69	276	81.65	118.92	88.26	107.55	140.14	117.06	108.93	21.51	19.75
69	138	345	108.59	123.54	101.35	126.78	141.59	128.50	121.72	14.54	11.94
69	207	414	115.75	126.16	109.55	140.56	144.90	140.62	129.59	14.70	11.35
103	69	378	111.20	130.57	105.42	139.66	129.39	134.49	125.12	13.63	10.89
103	103	412	114.37	132.49	86.26	157.99	163.57	143.17	132.98	28.96	21.78
103	207	516	152.27	139.80	122.23	165.22	172.94	165.64	153.02	19.12	12.50
138	103	517	157.23	150.89	107.48	173.28	206.56	169.15	160.77	32.48	20.20
138	138	552	165.29	176.04	114.17	186.99	207.25	182.65	172.07	31.58	18.35
138	276	690	197.81	191.20	150.96	220.89	209.66	221.58	198.68	26.35	13.26

Table A-7 RM Values of the Sawyer Aggregate at the Median Gradation and the OMC

Confining Pressure (kPa)	Deviator Stress (kPa)	Bulk Stress (kPa)	RM Test 1 (MPa)	Test 2 (MPa)	Test 3 (MPa)	Test 4 (MPa)	Test 5 (MPa)	Test 6 (MPa)	Mean RM Value (MPa)	Standard Deviation (MPa)	St. Dev./ Mean (%)
21	21	84	58.36	55.26	102.04	75.65	80.20	51.40	70.48	19.29	27.36
21	41	104	66.01	74.96	96.80	84.33	91.22	64.97	79.72	13.22	16.58
21	62	125	74.00	68.07	95.70	94.74	96.05	64.21	82.13	14.98	18.24
34	34	136	69.93	89.43	96.60	103.69	90.81	93.02	90.58	11.33	12.51
34	69	171	93.91	70.07	107.69	105.49	105.00	94.39	96.09	14.05	14.62
34	103	205	104.11	90.53	115.48	111.96	121.13	85.37	104.76	14.24	13.59
69	69	276	123.47	110.72	137.59	136.84	129.88	102.18	123.45	14.39	11.65
69	138	345	148.34	131.60	150.27	166.46	149.72	138.14	147.42	11.94	8.10
69	207	414	160.40	140.90	153.78	168.53	146.69	130.22	150.09	13.79	9.19
103	69	378	132.22	147.93	136.49	172.39	147.93	149.86	147.80	14.00	9.47
103	103	412	184.24	141.80	151.24	158.75	159.43	155.16	158.44	14.19	8.95
103	207	516	197.26	165.36	175.07	200.64	179.28	164.26	180.31	15.56	8.63
138	103	517	188.17	142.62	159.85	191.61	179.14	178.31	173.28	18.64	10.76
138	138	552	201.81	172.66	172.59	193.40	195.47	182.24	186.36	12.37	6.64
138	276	690	223.93	193.06	204.15	224.34	207.80	210.28	210.59	12.03	5.71

Table A-8 RM Values of the Sawyer Aggregate at the Coarser Limit Gradation and the OMC

Confining Pressure (kPa)	Deviator Stress (kPa)	Bulk Stress (kPa)	RM Test 1 (MPa)	RM Test 2 (MPa)	RM Test 3 (MPa)	RM Test 4 (MPa)	RM Test 5 (MPa)	RM Test 6 (MPa)	Mean RM Value (MPa)	Standard Deviation (MPa)	St. Dev./ Mean (%)
21	21	84	77.58	84.82	108.38	60.36	70.14	66.49	77.96	17.18	22.03
21	41	104	93.50	99.77	115.48	63.11	82.61	123.12	96.26	21.89	22.74
21	62	125	99.84	108.66	120.92	74.83	89.78	122.16	102.70	18.43	17.95
34	34	136	103.42	96.74	126.64	94.81	83.30	122.92	104.64	16.94	16.19
34	69	171	134.42	130.01	137.80	93.15	127.47	145.45	128.05	18.22	14.23
34	103	205	140.14	141.93	154.68	101.01	144.83	158.95	140.26	20.60	14.69
69	69	276	159.85	179.48	160.19	123.88	181.07	201.60	167.68	26.48	15.79
69	138	345	179.62	176.11	215.45	150.89	165.43	184.51	178.67	21.64	12.11
69	207	414	196.78	194.85	237.98	149.10	177.90	208.28	194.15	29.74	15.32
103	69	378	189.61	213.87	167.22	125.33	155.16	176.18	171.23	30.20	17.64
103	103	412	217.79	203.26	231.37	149.10	166.74	207.11	195.89	31.49	16.07
103	207	516	227.78	230.06	236.74	163.57	197.54	239.15	215.81	29.64	13.73
138	103	517	242.73	199.74	239.01	167.43	184.65	202.29	205.98	29.79	14.46
138	138	552	234.67	231.44	243.35	178.18	220.82	205.25	218.95	23.88	10.91
138	276	690	259.27	262.85	274.98	211.80	247.42	264.44	253.46	22.26	8.78

Table A-9 RM Values of the Sawyer Aggregate at the Finer Limit Gradation and the OMC

Confining Pressure (kPa)	Deviator Stress (kPa)	Bulk Stress (kPa)	RM Test 1 (MPa)	Test 2 (MPa)	Test 3 (MPa)	Test 4 (MPa)	Test 5 (MPa)	Test 6 (MPa)	Mean RM Value (MPa)	Standard Deviation (MPa)	St. Dev./ Mean (%)
21	21	84	81.30	50.23	34.59	49.61	33.97	60.43	51.69	17.70	34.24
21	41	104	80.82	66.49	82.68	76.62	61.25	83.85	75.28	9.33	12.39
21	62	125	94.67	79.17	65.04	80.54	75.86	81.30	79.43	9.56	12.03
34	34	136	119.13	126.64	91.02	91.15	77.44	123.88	104.88	20.84	19.87
34	69	171	116.99	99.28	101.77	90.74	95.98	90.26	99.17	9.85	9.93
34	103	205	120.16	111.20	96.80	99.70	107.42	101.35	106.11	8.67	8.17
69	69	276	162.88	161.09	148.69	123.54	114.72	139.45	141.73	19.68	13.88
69	138	345	167.63	150.75	126.29	136.70	149.65	142.42	145.57	14.08	9.67
69	207	414	165.50	161.64	149.10	143.93	146.69	140.07	151.16	10.15	6.71
103	69	378	168.05	173.77	161.64	150.89	170.53	154.61	163.25	9.13	5.59
103	103	412	175.83	158.81	153.03	159.02	163.98	149.44	160.02	9.26	5.79
103	207	516	198.85	191.82	163.02	172.53	186.37	173.77	181.06	13.50	7.46
138	103	517	221.03	198.02	163.57	185.62	181.14	179.76	188.19	19.54	10.38
138	138	552	198.09	189.06	160.19	184.93	218.96	199.81	191.84	19.47	10.15
138	276	690	233.02	218.21	196.78	204.70	215.04	210.21	212.99	12.42	5.83

Table A-10 RM Values of the RS Aggregate at the Median Gradation and 2% below the OMC

Confining Pressure (kPa)	Deviator Stress (kPa)	Bulk Stress (kPa)	RM Test 1 (MPa)	RM Test 2 (MPa)	RM Test 3 (MPa)	RM Test 4 (MPa)	RM Test 5 (MPa)	RM Test 6 (MPa)	Mean RM Value (MPa)	Standard Deviation (MPa)	St. Dev./ Mean (%)
21	21	84	100.04	113.41	69.93	66.42	169.01	97.08	102.65	37.26	36.30
21	41	104	138.90	179.97	97.63	112.38	154.54	153.03	139.41	30.12	21.61
21	62	125	145.03	213.04	275.60	144.00	192.23	162.19	188.68	50.53	26.78
34	34	136	168.53	305.09	204.77	133.39	272.57	172.25	209.43	66.33	31.67
34	69	171	153.92	257.55	242.53	154.89	232.61	162.81	200.72	48.42	24.12
34	103	205	193.13	269.33	277.05	183.21	253.55	217.66	232.32	39.96	17.20
69	69	276	213.73	297.51	356.21	195.26	258.44	240.12	260.21	58.98	22.67
69	138	345	234.05	364.21	373.71	257.13	349.81	294.55	312.24	58.91	18.87
69	207	414	262.51	359.45	352.97	251.49	315.49	278.70	303.44	46.31	15.26
103	69	378	220.27	397.48	335.27	188.92	267.06	218.14	271.19	80.31	29.61
103	103	412	269.67	331.13	400.58	229.30	400.45	299.37	321.75	69.65	21.65
103	207	516	317.35	418.02	401.14	294.89	380.05	302.20	352.27	53.85	15.29
138	103	517	273.81	413.61	462.53	283.52	336.99	268.09	339.76	81.46	23.98
138	138	552	316.94	431.11	462.87	294.82	448.13	330.93	380.80	74.51	19.57
138	276	690	321.21	414.23	478.37	343.26	453.02	370.06	396.69	62.31	15.71

Table A-11 RM Values of the RS Aggregate at the Median Gradation and 2% above the OMC

Confining Pressure (kPa)	Deviator Stress (kPa)	Bulk Stress (kPa)	RM Test 1 (MPa)	RM Test 2 (MPa)	RM Test 3 (MPa)	RM Test 4 (MPa)	RM Test 5 (MPa)	RM Test 6 (MPa)	Mean RM Value (MPa)	Standard Deviation (MPa)	St. Dev./Mean (%)
21	21	84	55.60	51.88	81.85	60.98	93.77	49.13	65.54	18.10	27.62
21	41	104	79.92	89.64	131.60	106.17	77.10	95.36	96.63	20.12	20.83
21	62	125	82.54	115.61	123.47	101.42	80.54	128.98	105.43	20.70	19.64
34	34	136	103.97	132.91	119.40	138.83	99.28	137.73	122.02	17.31	14.18
34	69	171	101.56	146.69	140.69	120.23	112.17	133.60	125.82	17.46	13.87
34	103	205	114.51	132.70	159.78	128.91	110.24	142.62	131.46	18.29	13.91
69	69	276	147.45	222.75	223.30	168.94	176.73	214.14	192.22	32.14	16.72
69	138	345	149.17	198.91	195.47	190.65	169.29	195.68	183.19	19.80	10.81
69	207	414	153.51	197.95	209.73	183.89	159.92	200.02	184.17	22.90	12.44
103	69	378	129.05	185.27	206.42	201.05	183.83	203.26	184.81	28.92	15.65
103	103	412	161.29	222.55	242.18	230.47	186.10	217.52	210.02	30.37	14.46
103	207	516	187.34	238.74	247.01	247.28	238.12	250.11	234.77	23.74	10.11
138	103	517	177.69	244.39	266.44	232.40	230.47	263.61	235.83	32.26	13.68
138	138	552	200.57	287.24	316.11	255.14	251.00	290.83	266.82	40.50	15.18
138	276	690	236.33	315.70	309.43	269.88	277.39	299.37	284.68	29.67	10.42

Table A-12 RM Values of the Sawyer Aggregate at the Median Gradation and 2% below the OMC

Confining Pressure (kPa)	Deviator Stress (kPa)	Bulk Stress (kPa)	RM Test 1 (MPa)	RM Test 2 (MPa)	RM Test 3 (MPa)	RM Test 4 (MPa)	RM Test 5 (MPa)	RM Test 6 (MPa)	Mean RM Value (MPa)	Standard Deviation (MPa)	St. Dev./Mean (%)
21	21	84	96.05	101.70	73.38	88.19	50.71	60.08	78.35	20.38	26.02
21	41	104	121.06	126.36	93.15	106.38	79.51	93.29	103.29	18.03	17.46
21	62	125	108.52	125.54	97.56	125.40	80.13	90.81	104.66	18.57	17.75
34	34	136	170.32	120.78	116.03	168.81	74.07	92.95	123.82	39.20	31.66
34	69	171	168.74	132.08	142.69	120.85	121.20	80.61	127.69	29.10	22.79
34	103	205	167.91	163.36	134.01	144.83	127.47	108.79	141.06	22.40	15.88
69	69	276	222.20	133.11	165.22	175.76	137.52	92.67	154.42	44.09	28.55
69	138	345	199.81	172.66	203.74	243.77	164.95	121.75	184.45	41.42	22.46
69	207	414	211.25	196.37	191.27	211.80	180.24	168.39	193.22	17.14	8.87
103	69	378	225.17	172.46	156.33	225.03	149.31	116.99	174.21	43.35	24.88
103	103	412	209.59	169.22	214.83	237.36	175.83	160.12	194.49	30.49	15.68
103	207	516	250.31	213.25	247.76	248.80	190.72	179.69	221.75	31.71	14.30
138	103	517	251.49	175.83	244.53	211.94	173.63	136.70	199.02	44.85	22.53
138	138	552	243.91	183.76	272.57	252.24	251.49	154.40	226.39	46.34	20.47
138	276	690	278.98	241.08	257.89	305.98	238.05	218.41	256.73	31.57	12.30

Table A-13 RM Values of the Sawyer Aggregate at the Median Gradation and 2% above the OMC

Confining Pressure kPa	Deviator Stress kPa	Bulk Stress kPa	RM Test 1 MPa	RM Test 2 MPa	RM Test 3 MPa	RM Test 4 MPa	RM Test 5 MPa	RM Test 6 MPa	Mean RM Value MPa	Standard Deviation MPa	St. Dev./ Mean %
21	21	84	51.74	35.83	44.51	36.24	39.82	39.76	41.32	5.99	14.50
21	41	104	54.57	56.57	50.64	56.43	50.92	48.51	52.94	3.38	6.38
21	62	125	66.56	56.91	54.71	67.52	64.35	61.46	61.92	5.22	8.43
34	34	136	85.71	66.01	56.36	84.13	52.64	87.23	72.01	15.64	21.71
34	69	171	88.40	73.31	70.83	85.02	63.59	73.03	75.70	9.29	12.27
34	103	205	87.02	77.24	69.38	83.30	75.93	72.97	77.64	6.53	8.41
69	69	276	114.86	93.36	87.02	107.35	80.41	96.32	96.55	12.75	13.21
69	138	345	121.54	111.27	94.81	120.30	94.32	117.96	110.03	12.50	11.36
69	207	414	124.85	117.47	91.29	114.99	102.87	109.14	110.10	11.86	10.77
103	69	378	133.60	129.26	77.10	129.12	94.60	127.05	115.12	23.44	20.36
103	103	412	140.35	145.45	88.47	131.46	100.32	122.23	121.38	22.66	18.67
103	207	516	156.82	151.44	113.06	151.51	120.51	137.87	138.53	18.13	13.09
138	103	517	167.08	153.58	117.13	154.82	122.99	158.33	145.65	20.47	14.05
138	138	552	167.08	172.59	124.71	180.52	138.83	163.98	157.95	21.51	13.62
138	276	690	194.23	192.02	151.58	186.86	160.12	178.59	177.23	17.62	9.94

Table A-14 RM Values of the RS Aggregate at the Median Gradation and the OMC (Undrained Test I)

Confining Pressure (kPa)	Deviator Stress (kPa)	Bulk Stress (kPa)	RM Test 1 (MPa)	RM Test 2 (MPa)	RM Test 3 (MPa)	RM Test 4 (MPa)	Mean RM Value (MPa)	Standard Deviation (MPa)	St. Dev./ Mean (%)
21	21	84	97.91	45.13	52.71	115.75	77.87	34.36	44.12
21	41	104	59.05	65.94	111.27	136.84	93.27	37.15	39.83
21	62	125	76.48	78.06	109.07	141.59	101.30	30.77	30.37
34	34	136	126.16	72.83	124.23	150.27	118.37	32.59	27.53
34	69	171	99.63	83.16	119.75	145.79	112.08	27.00	24.09
34	103	205	112.86	93.29	143.66	163.09	128.22	31.14	24.29
69	69	276	96.67	100.59	177.28	193.68	142.05	50.61	35.63
69	138	345	156.33	113.48	183.21	151.03	151.01	28.71	19.01
69	207	414	155.51	114.72	177.28	149.10	149.15	25.93	17.39
103	69	378	187.34	109.55	186.72	173.63	164.31	37.05	22.55
103	103	412	169.43	118.92	175.70	166.53	157.64	26.10	16.55
103	207	516	184.65	125.60	223.51	188.30	180.52	40.59	22.48
138	103	517	188.23	125.26	230.75	177.56	180.45	43.38	24.04
138	138	552	189.96	141.25	190.44	188.79	177.61	24.25	13.65
138	276	690	219.10	143.45	234.26	213.25	202.51	40.36	19.93

Table A-15 RM Values of the RS Aggregate at the Median Gradation and the OMC (Undrained Test II)

Confining Pressure (kPa)	Deviator Stress (kPa)	Bulk Stress (kPa)	RM Test 1 (MPa)	RM Test 2 (MPa)	RM Test 3 (MPa)	RM Test 4 (MPa)	Mean RM Value (MPa)	Standard Deviation (MPa)	St. Dev./ Mean (%)
21	21	84	38.17	60.70	52.30	59.74	52.73	10.40	19.73
21	41	104	104.04	117.68	73.10	60.22	88.76	26.64	30.02
21	62	125	82.27	115.13	104.25	87.57	97.30	15.13	15.55
34	34	136	58.50	89.36	88.26	110.86	86.75	21.52	24.80
34	69	171	82.54	105.83	93.57	99.15	95.27	9.86	10.35
34	103	205	105.83	119.40	95.70	99.49	105.11	10.41	9.90
69	69	276	141.59	135.25	117.89	134.01	132.18	10.09	7.64
69	138	345	113.00	143.04	134.29	140.49	132.70	13.64	10.28
69	207	414	123.88	151.65	141.59	146.89	141.00	12.13	8.60
103	69	378	125.12	135.04	187.61	154.89	150.67	27.57	18.30
103	103	412	134.29	174.04	144.83	166.39	154.89	18.48	11.93
103	207	516	145.03	194.44	177.49	185.55	175.63	21.54	12.26
138	103	517	137.66	150.06	167.15	177.76	158.16	17.80	11.26
138	138	552	170.32	205.46	200.84	201.39	194.50	16.25	8.36
138	276	690	193.88	233.85	231.30	215.24	218.57	18.40	8.42

Table A-16 RM Values of the Sawyer Aggregate at the Median Gradation and the Soaked Specimen (Undrained Test I)

Confining Pressure (kPa)	Deviator Stress (kPa)	Bulk Stress (kPa)	RM Test 1 (MPa)	RM Test 2 (MPa)	RM Test 3 (MPa)	RM Test 4 (MPa)	RM Test 5 (MPa)	Mean RM Value (MPa)	Standard Deviation (MPa)	St. Dev./ Mean (%)
21	21	84	49.95	55.67	55.88	49.40	55.26	53.23	3.26	6.12
21	41	104	51.47	54.84	58.50	65.18	60.22	58.04	5.23	9.01
21	62	125	61.32	59.05	63.73	65.18	67.25	63.31	3.21	5.08
34	34	136	58.36	43.68	55.33	57.05	66.08	56.10	8.07	14.38
34	69	171	64.70	60.77	69.18	63.32	68.49	65.29	3.54	5.41
34	103	205	72.97	68.83	76.82	78.48	74.41	74.30	3.73	5.01
69	69	276	91.84	62.08	92.81	85.23	86.19	83.63	12.50	14.95
69	138	345	102.32	76.55	94.26	91.09	96.94	92.23	9.69	10.50
69	207	414	112.44	92.53	105.97	103.83	106.38	104.23	7.28	6.99
103	69	378	113.89	55.95	95.70	105.21	114.44	97.04	24.21	24.95
103	103	412	122.44	64.97	93.57	105.55	117.34	100.77	22.91	22.74
103	207	516	144.28	91.71	111.55	132.22	132.22	122.39	20.80	17.00
138	103	517	161.23	59.25	110.72	141.31	140.14	122.53	39.70	32.40
138	138	552	148.55	72.55	113.41	132.77	144.90	122.44	31.08	25.38
138	276	690	184.17	101.28	133.67	161.78	169.01	149.98	32.82	21.88

Table A-17 RM Values of the Sawyer Aggregate at the Median Gradation and the Soaked Specimen (Undrained Test II)

Confining Pressure (kPa)	Deviator Stress (kPa)	Bulk Stress (kPa)	RM Test 1 (MPa)	RM Test 2 (MPa)	RM Test 3 (MPa)	RM Test 4 (MPa)	RM Test 5 (MPa)	Mean RM Value (MPa)	Standard Deviation (MPa)	St. Dev./ Mean (%)
21	21	84	40.72	52.30	61.46	62.91	44.44	52.36	9.90	18.91
21	41	104	47.27	60.63	70.76	66.56	54.29	59.90	9.41	15.70
21	62	125	52.71	56.22	73.86	71.59	64.97	63.87	9.27	14.51
34	34	136	45.20	54.29	68.83	61.39	57.12	57.37	8.73	15.23
34	69	171	58.77	60.98	69.52	69.11	68.49	65.37	5.09	7.79
34	103	205	60.36	69.18	72.48	81.30	72.97	71.26	7.56	10.61
69	69	276	76.75	87.37	110.31	88.26	96.05	91.75	12.44	13.56
69	138	345	83.30	93.77	116.03	90.81	96.87	96.16	12.20	12.68
69	207	414	88.67	101.35	112.44	104.31	107.21	102.80	8.89	8.65
103	69	378	81.23	110.79	122.30	73.10	105.42	98.57	20.67	20.97
103	103	412	89.16	100.59	145.03	75.17	107.90	103.57	26.27	25.37
103	207	516	103.14	121.33	138.70	99.91	130.63	118.74	16.91	14.25
138	103	517	97.22	139.25	135.53	143.31	142.83	131.63	19.49	14.81
138	138	552	99.84	143.86	151.65	124.43	155.51	135.06	23.05	17.06
138	276	690	126.02	157.30	161.02	150.41	158.06	150.56	14.26	9.47

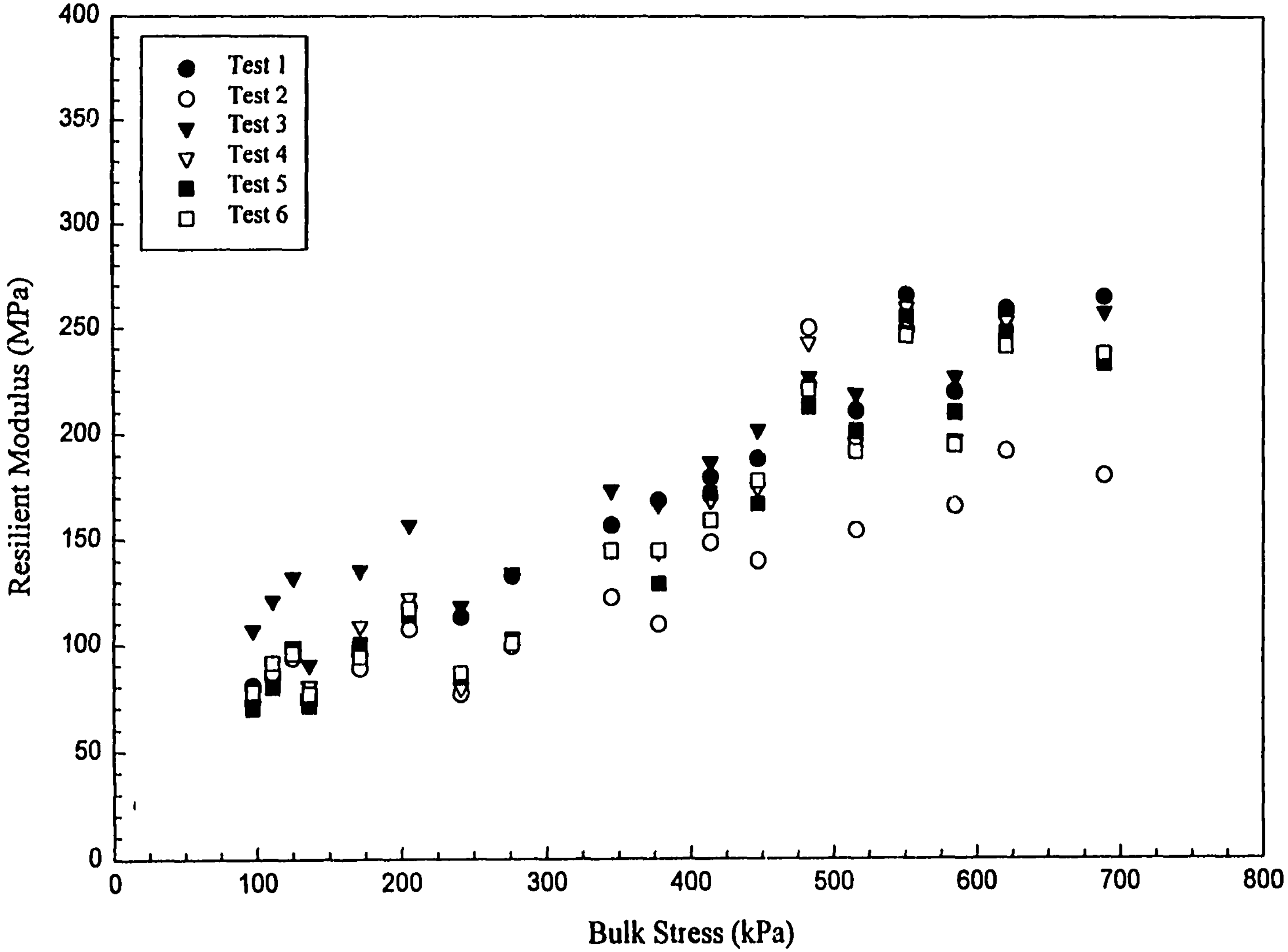

Figure A-1 RM Values of the RS Aggregate at the Median Gradation and the OMC (AASHTO T 292-91I)

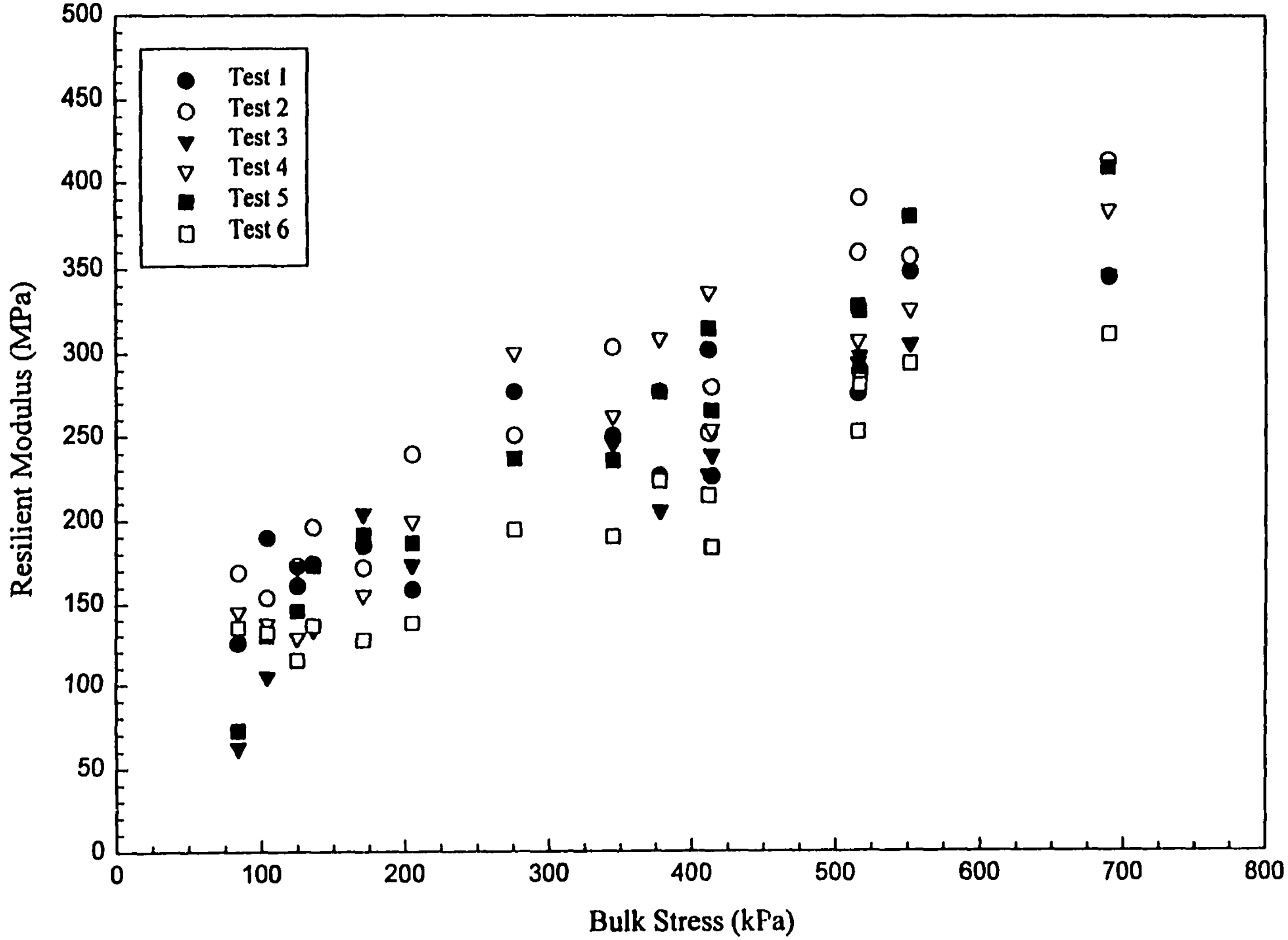

Figure A-2 RM Values of the RS Aggregate at the Median Gradation and the OMC (AASHTO T 294-94)

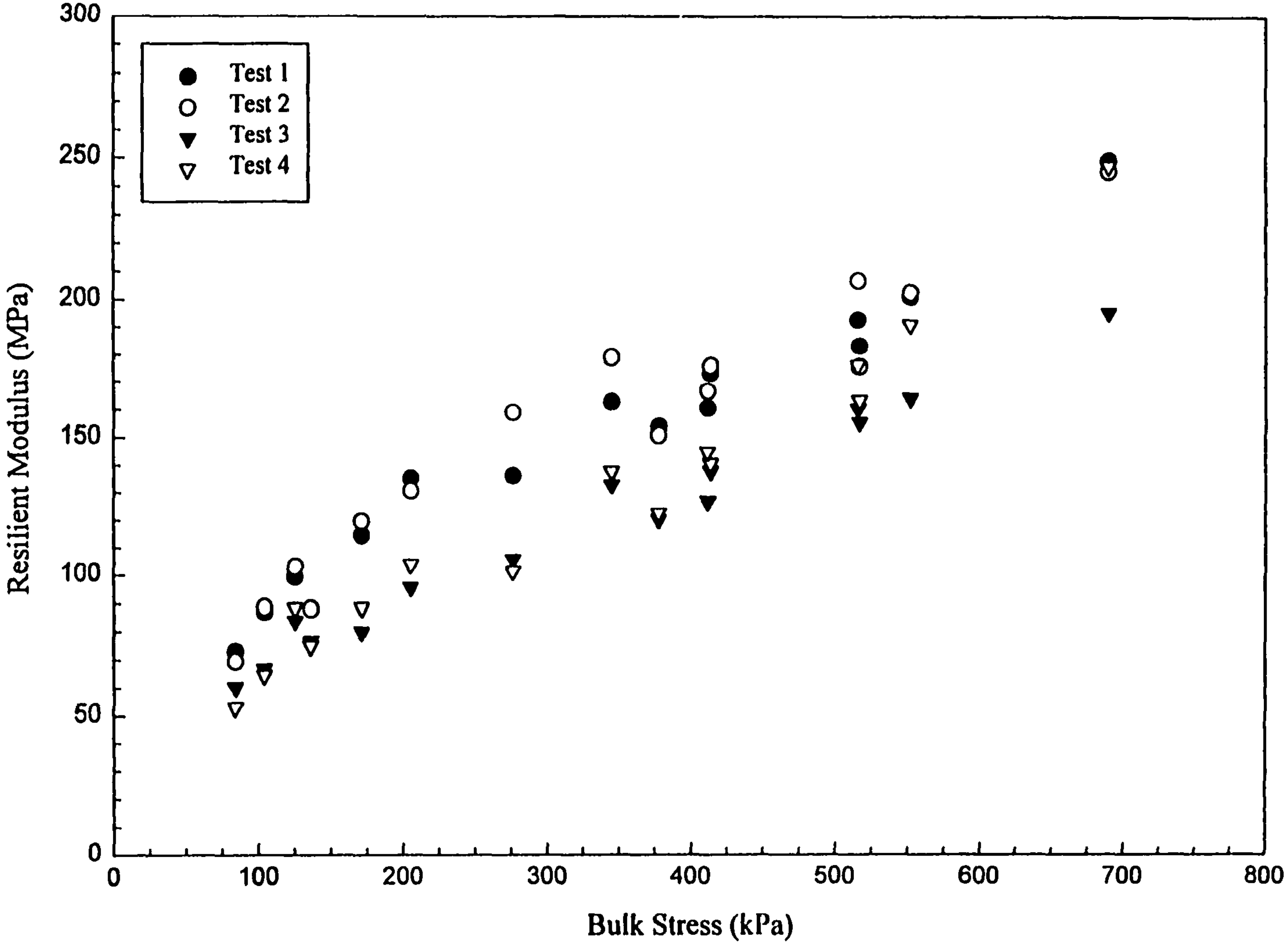

Figure A-3 RM Values of the RS Aggregate at the Median Gradation and the OMC (Rectangular Waveform, T 294-94)

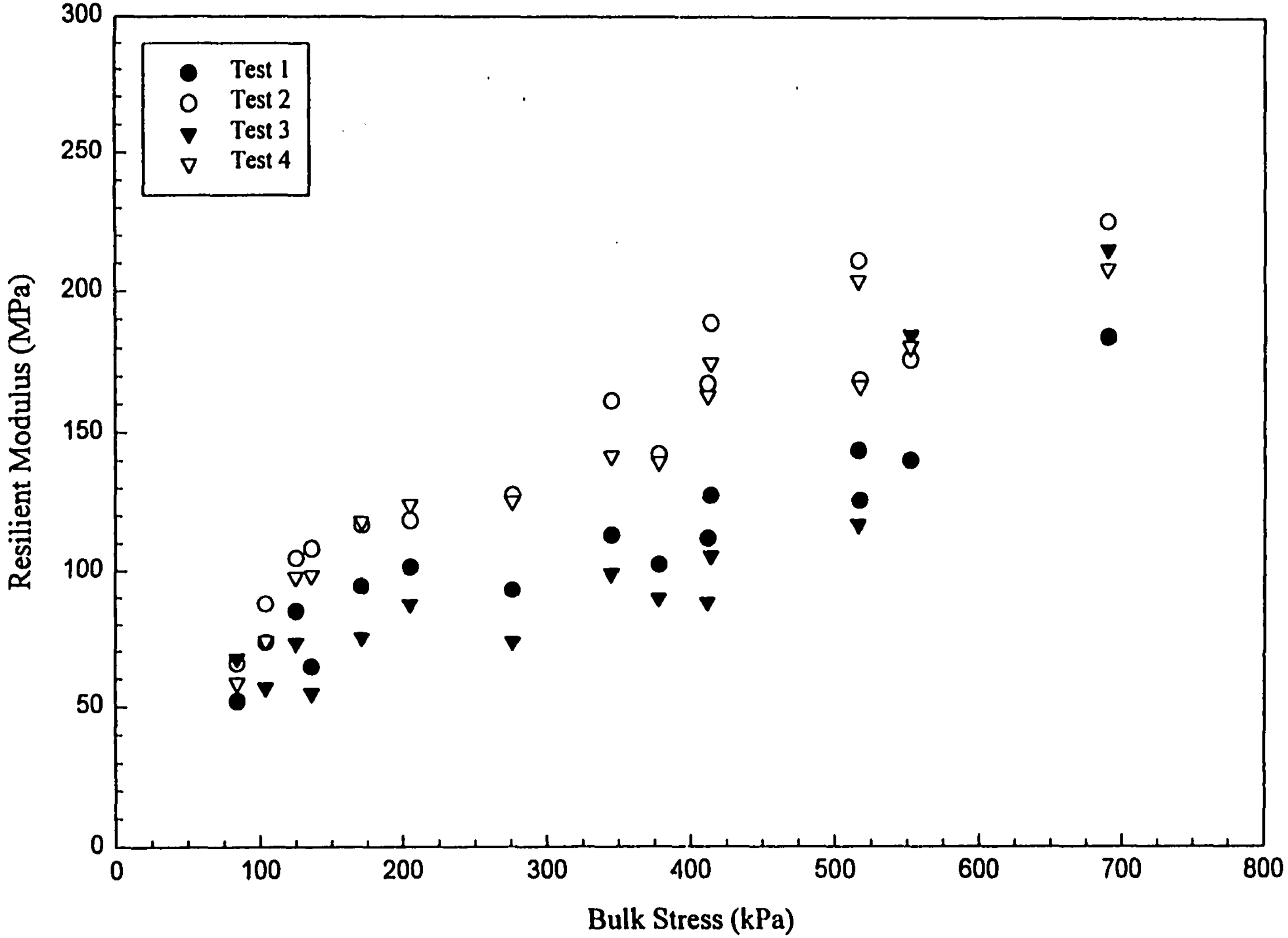

Figure A-4 RM Values of the RS Aggregate at the Median Gradation and the OMC (Triangular Waveform, T 294-94)

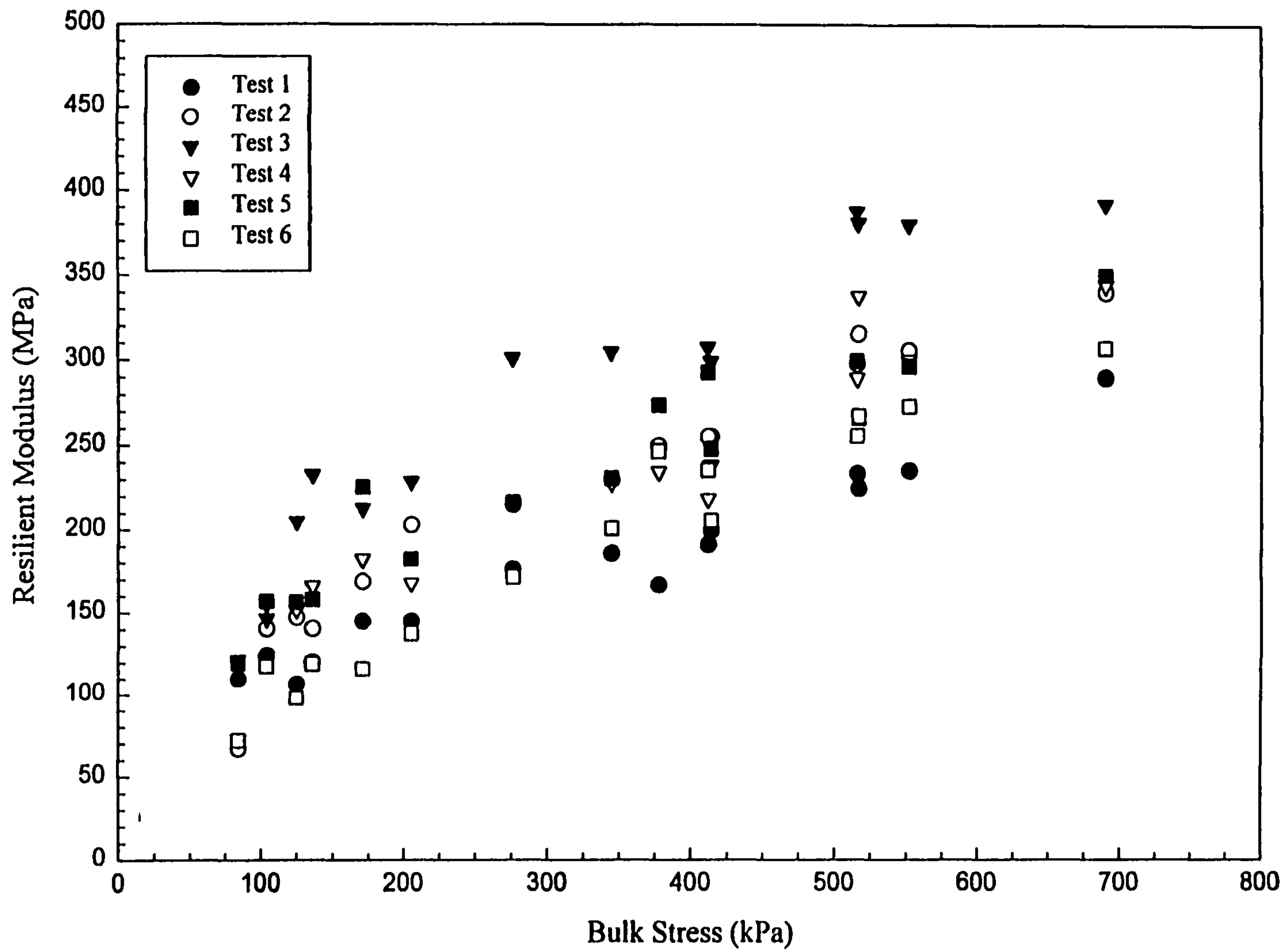

Figure A-5 RM Values of the RS Aggregate at the Coarser Limit Gradation and the OMC

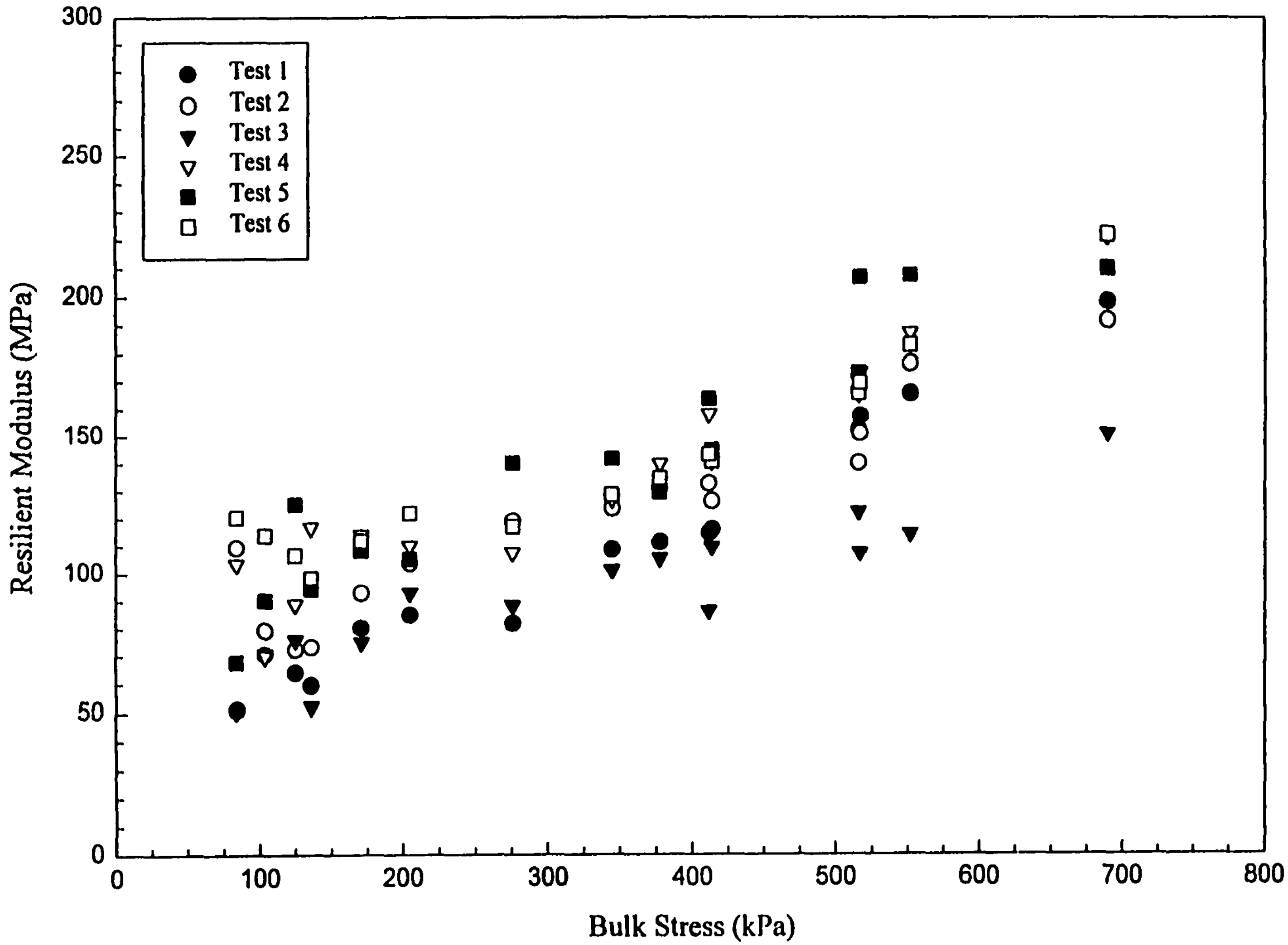

Figure A-6 RM Values of the RS Aggregate at the Finer Limit Gradation and the OMC

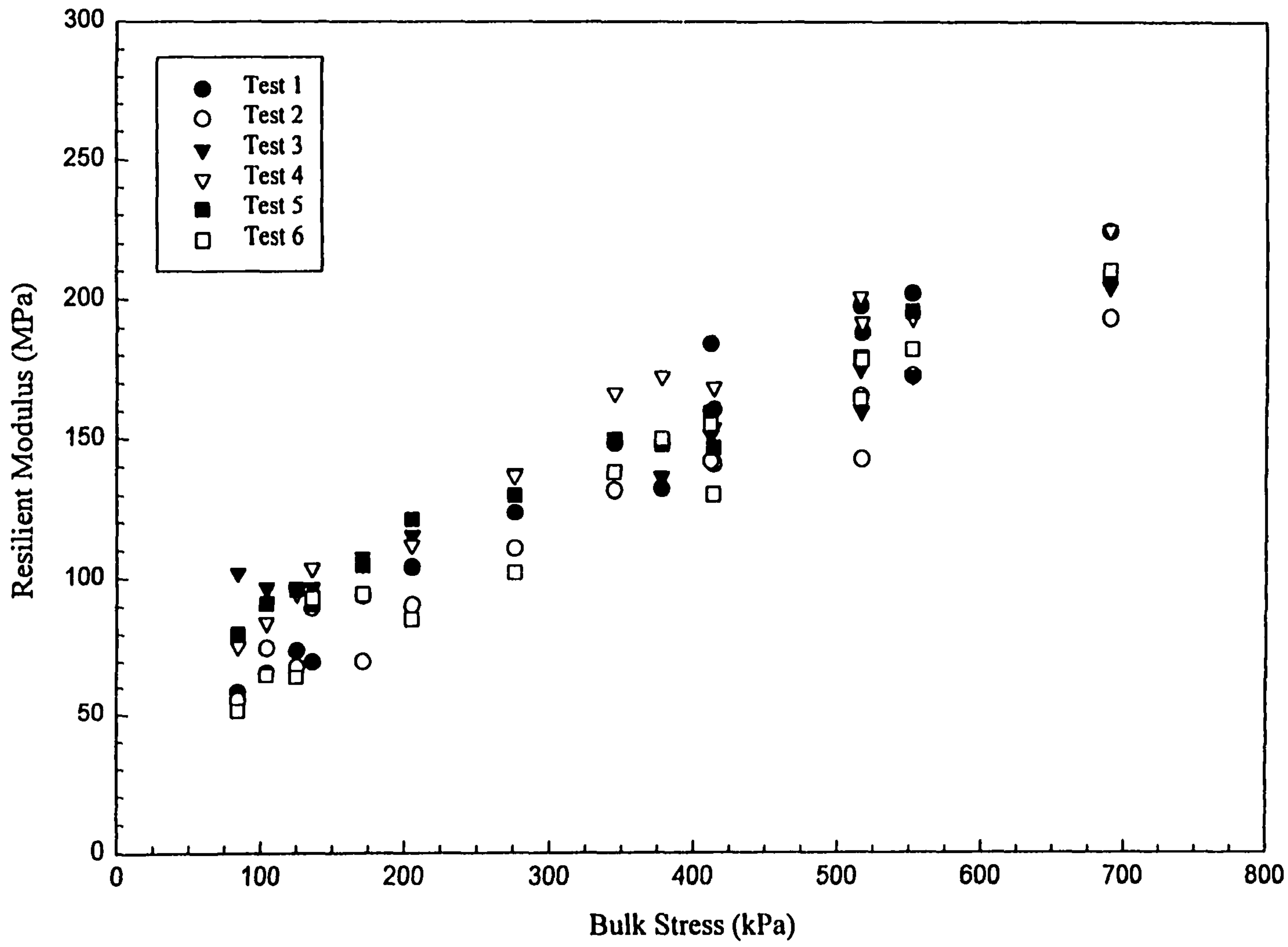

Figure A-7 RM Values of the Sawyer Aggregate at the Median Gradation and the OMC

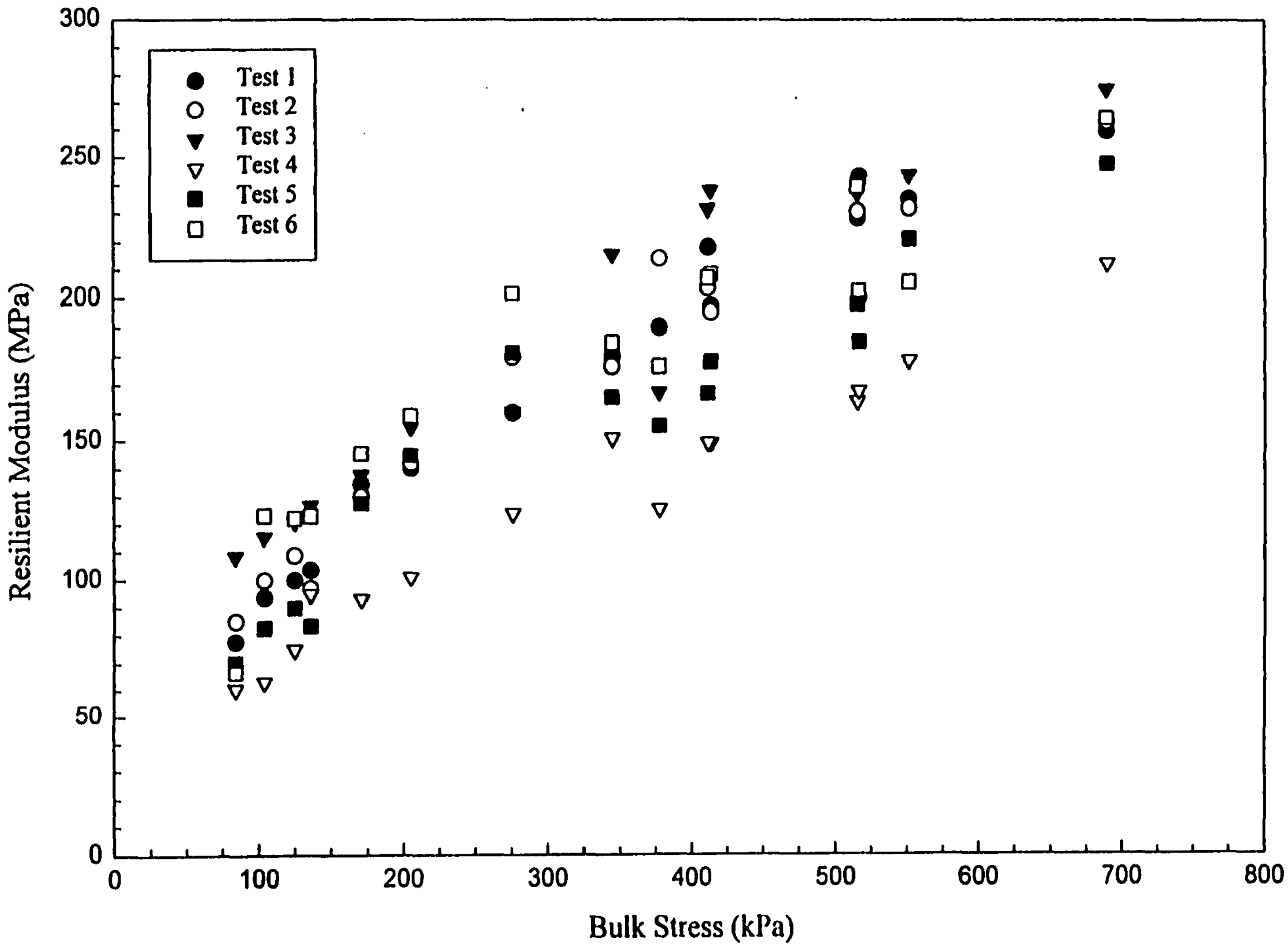

Figure A-8 RM Values of the Sawyer Aggregate at the Coarser Limit Gradation and the OMC

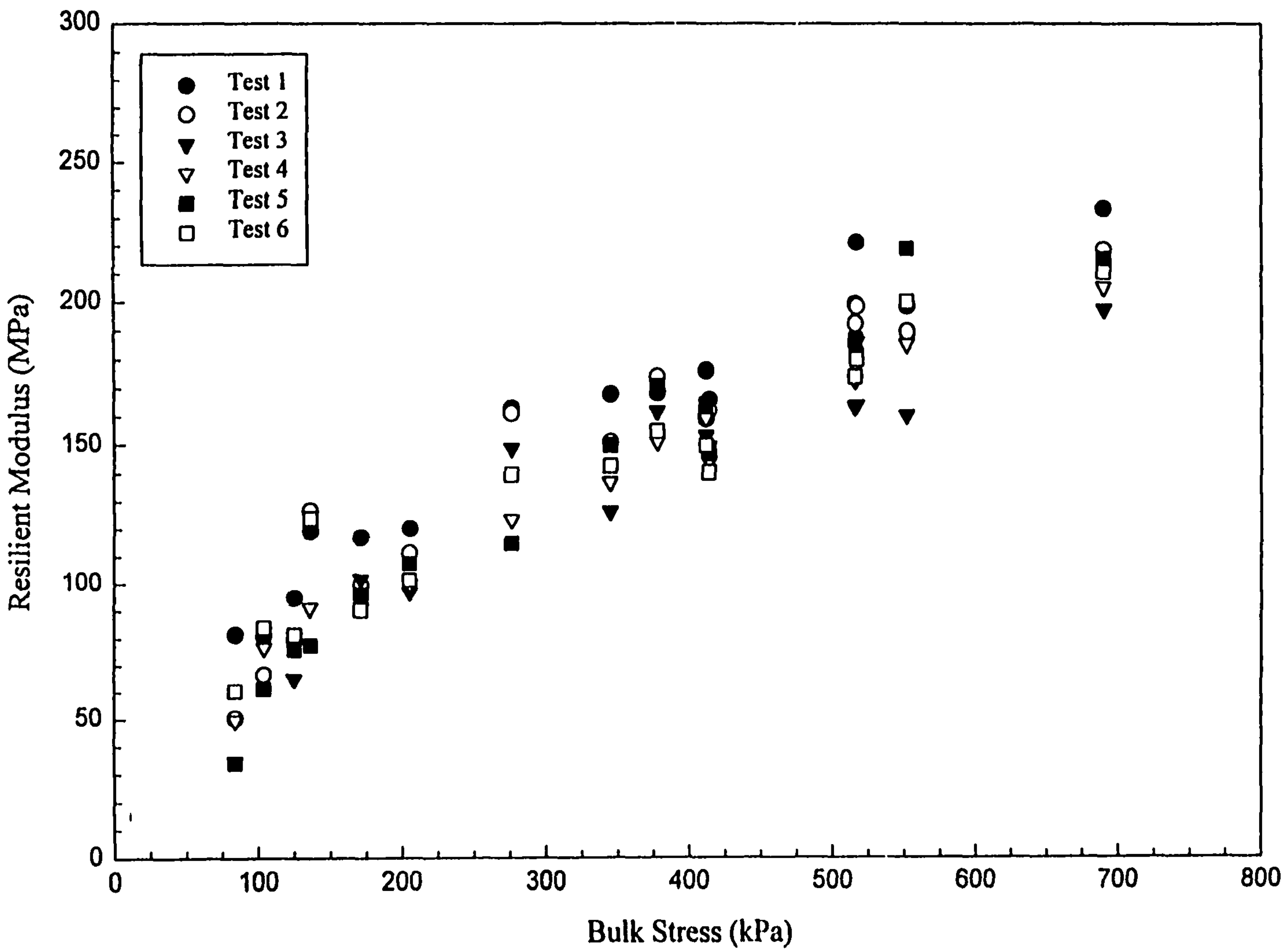

Figure A-9 RM Values of the Sawyer Aggregate at the Finer Limit Gradation and the OMC

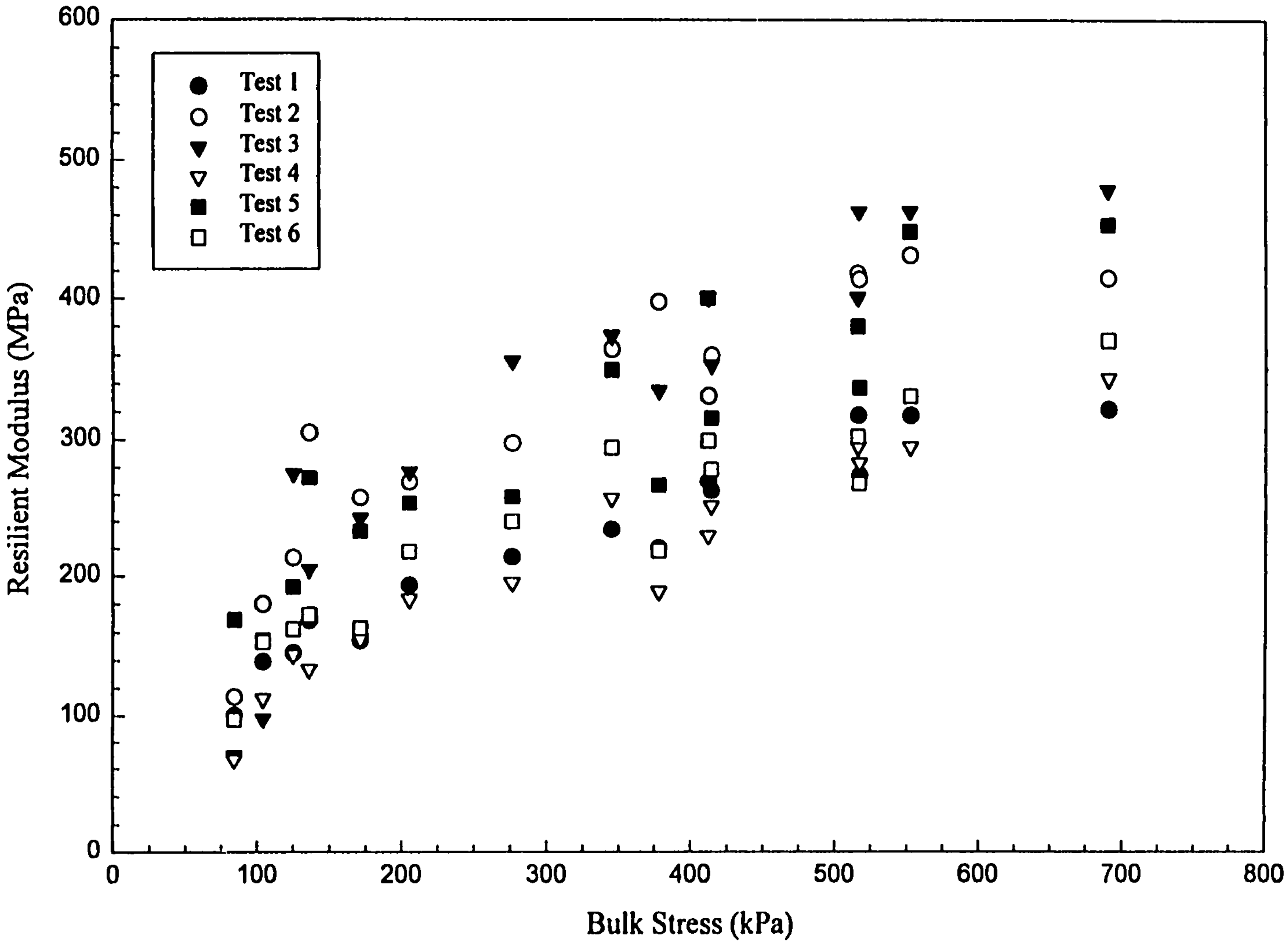

Figure A-10 RM Values of the RS Aggregate at the Median Gradation and 2% below the OMC

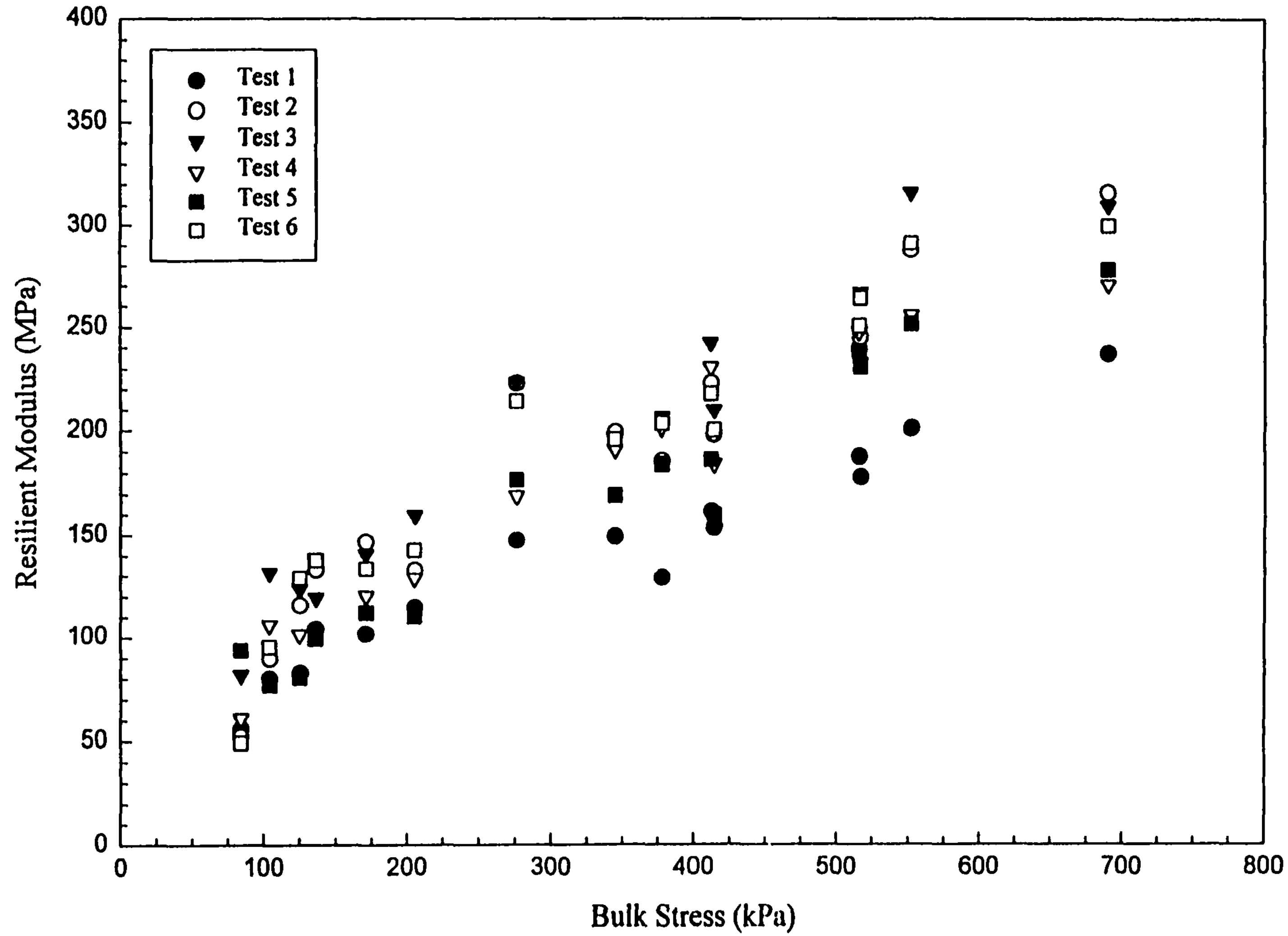

Figure A-11 RM Values of the RS Aggregate at the Medain Gradation and 2% above the OMC

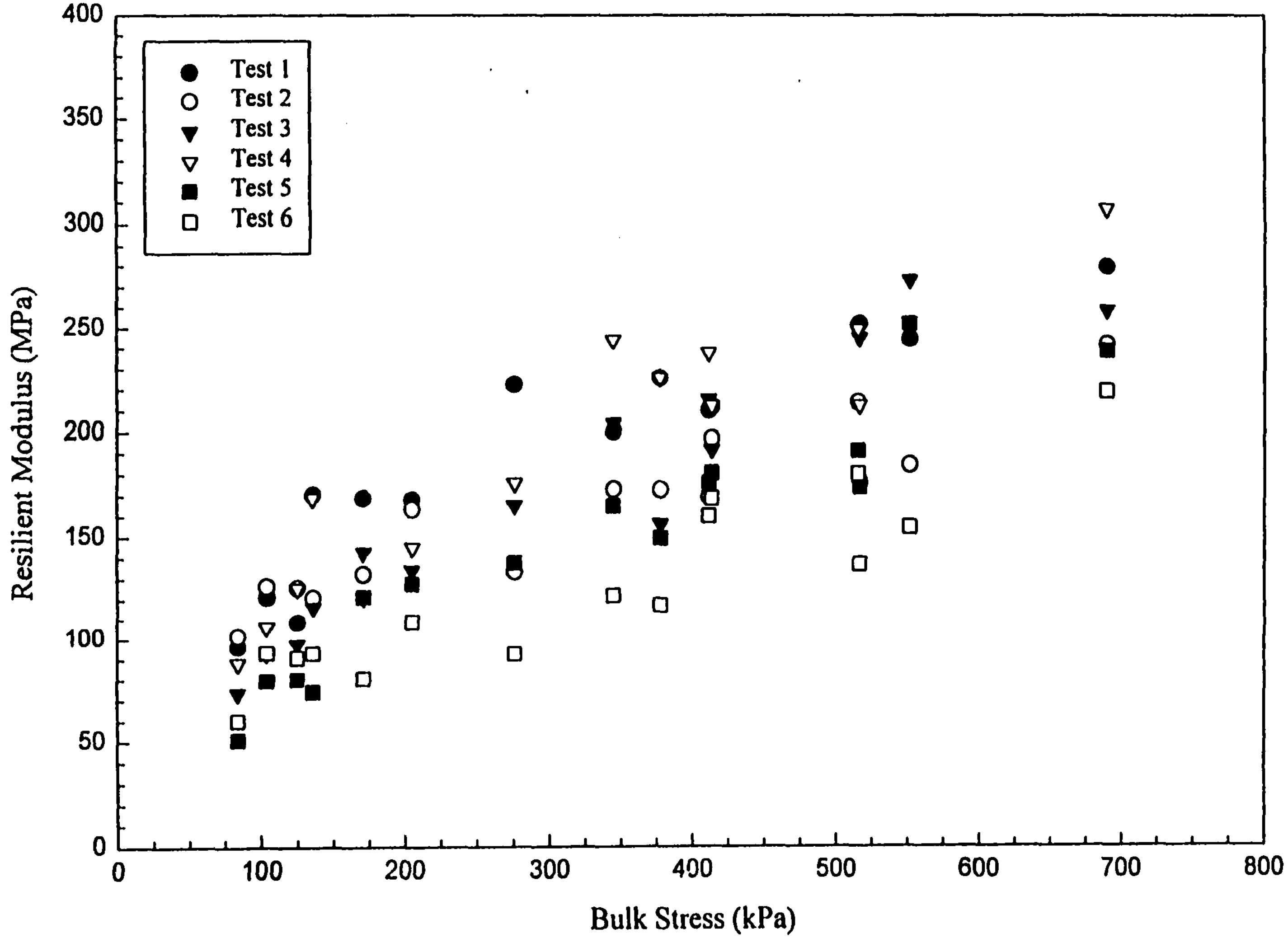

Figure A-12 RM Values of the Sawyer Aggregate at the Median Gradation and 2% below the OMC

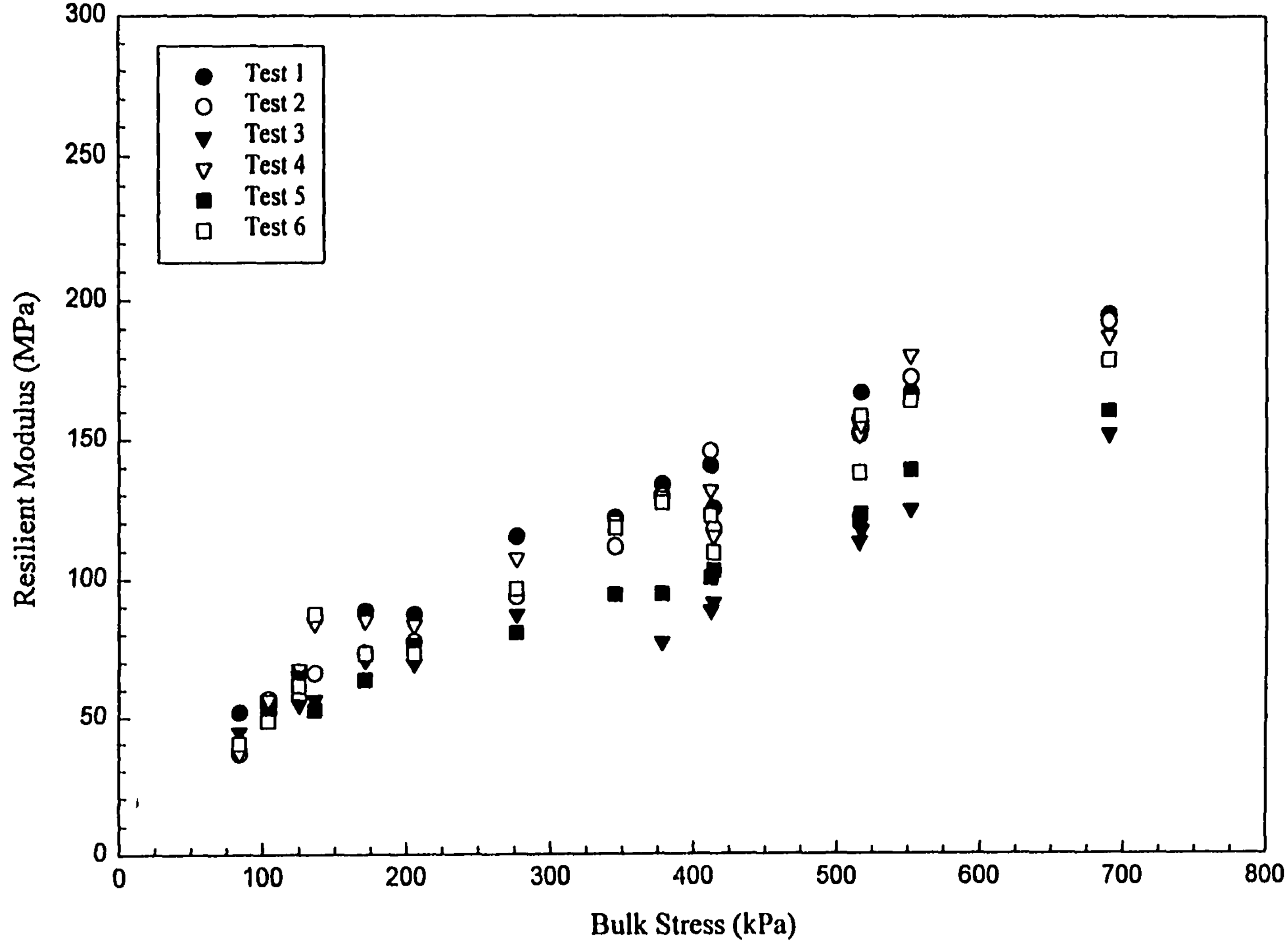

Figure A-13 RM Values of the Sawyer Aggregate at the Median Gradation and 2% above the OMC

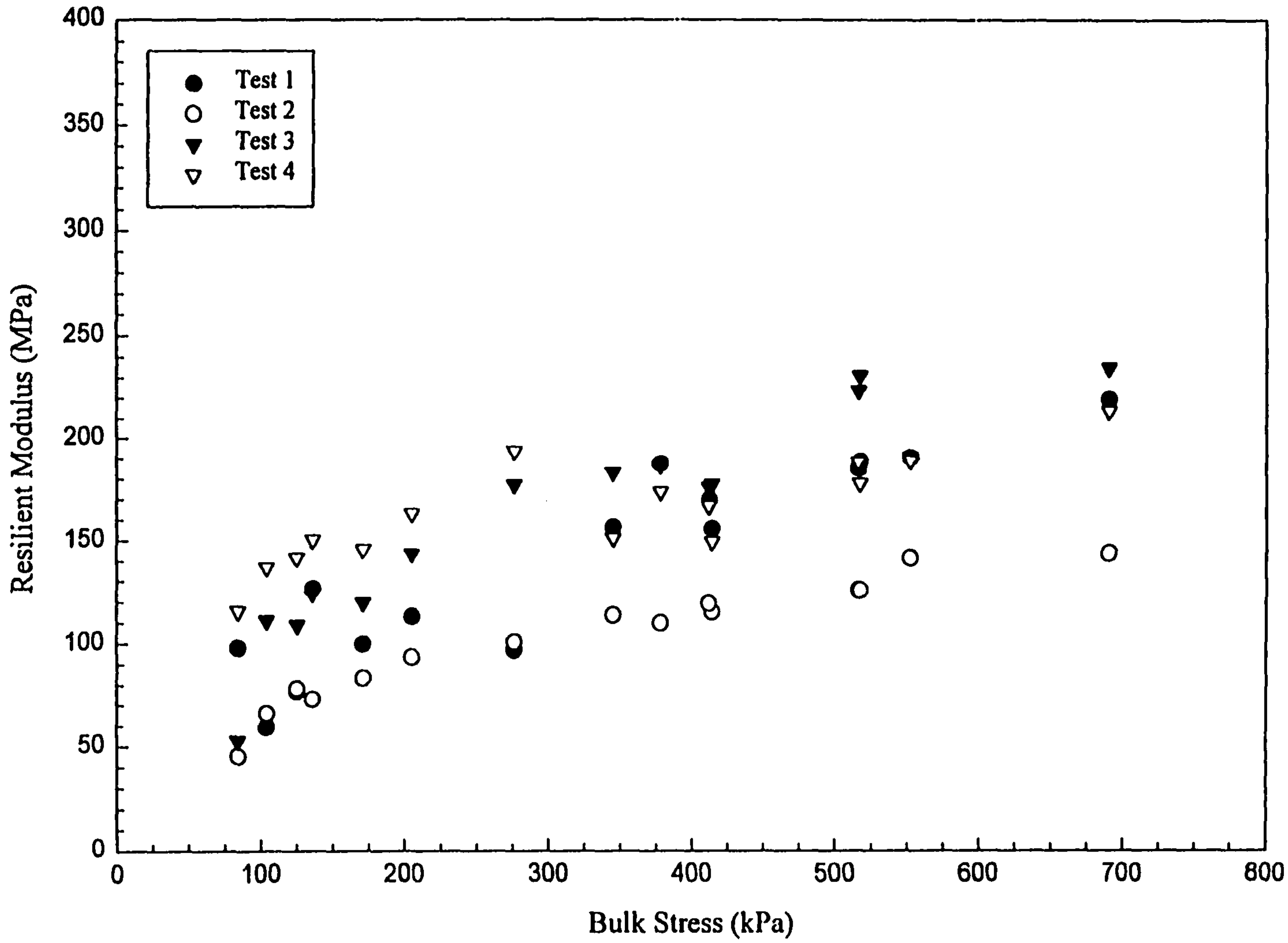

Figure A-14 RM Values of the RS Aggregate at the Median Gradation and the OMC (Undrained I)

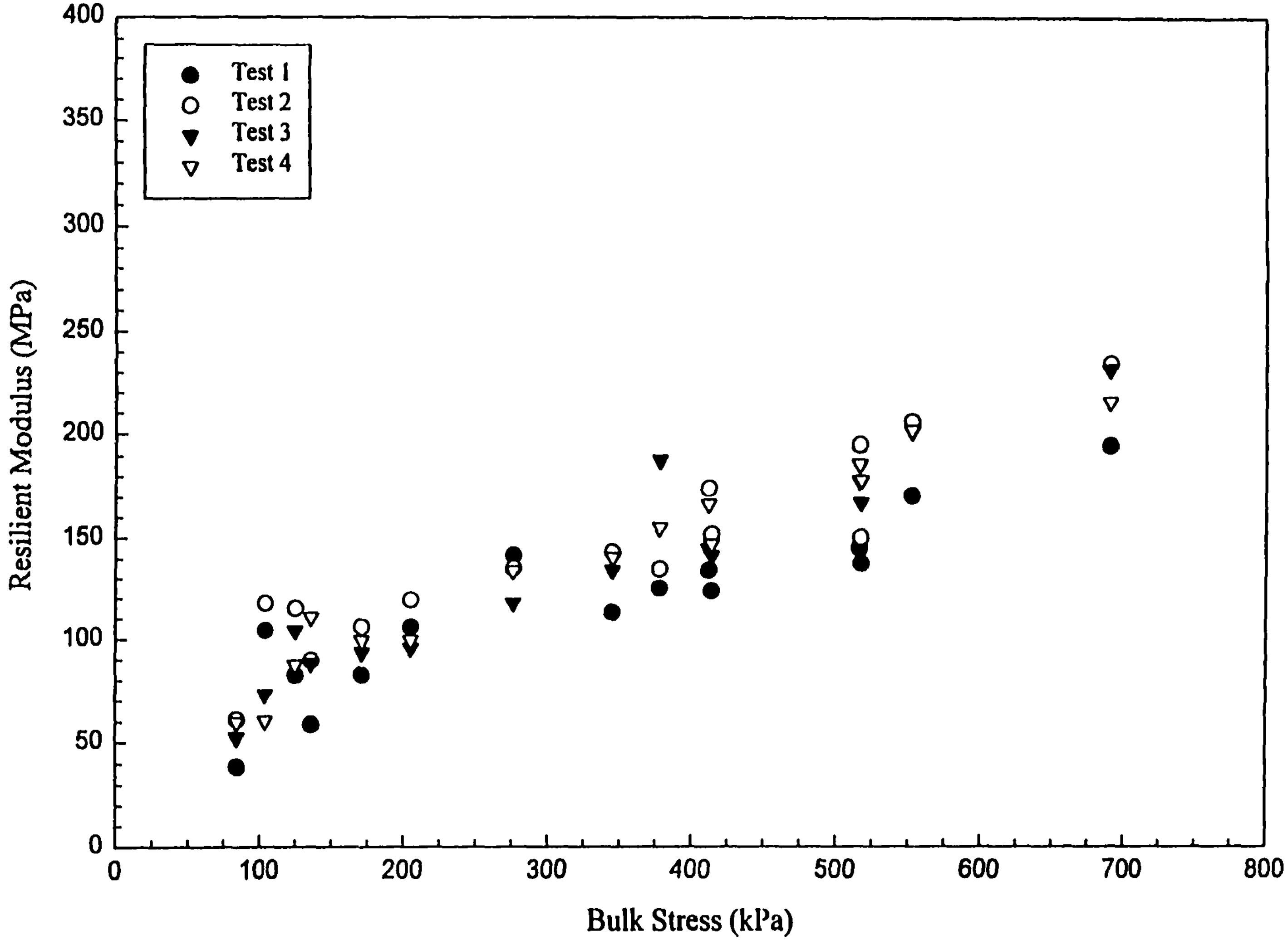

Figure A-15 RM Values of the RS Aggregate at the Median Gradation and the OMC (Undrained II)

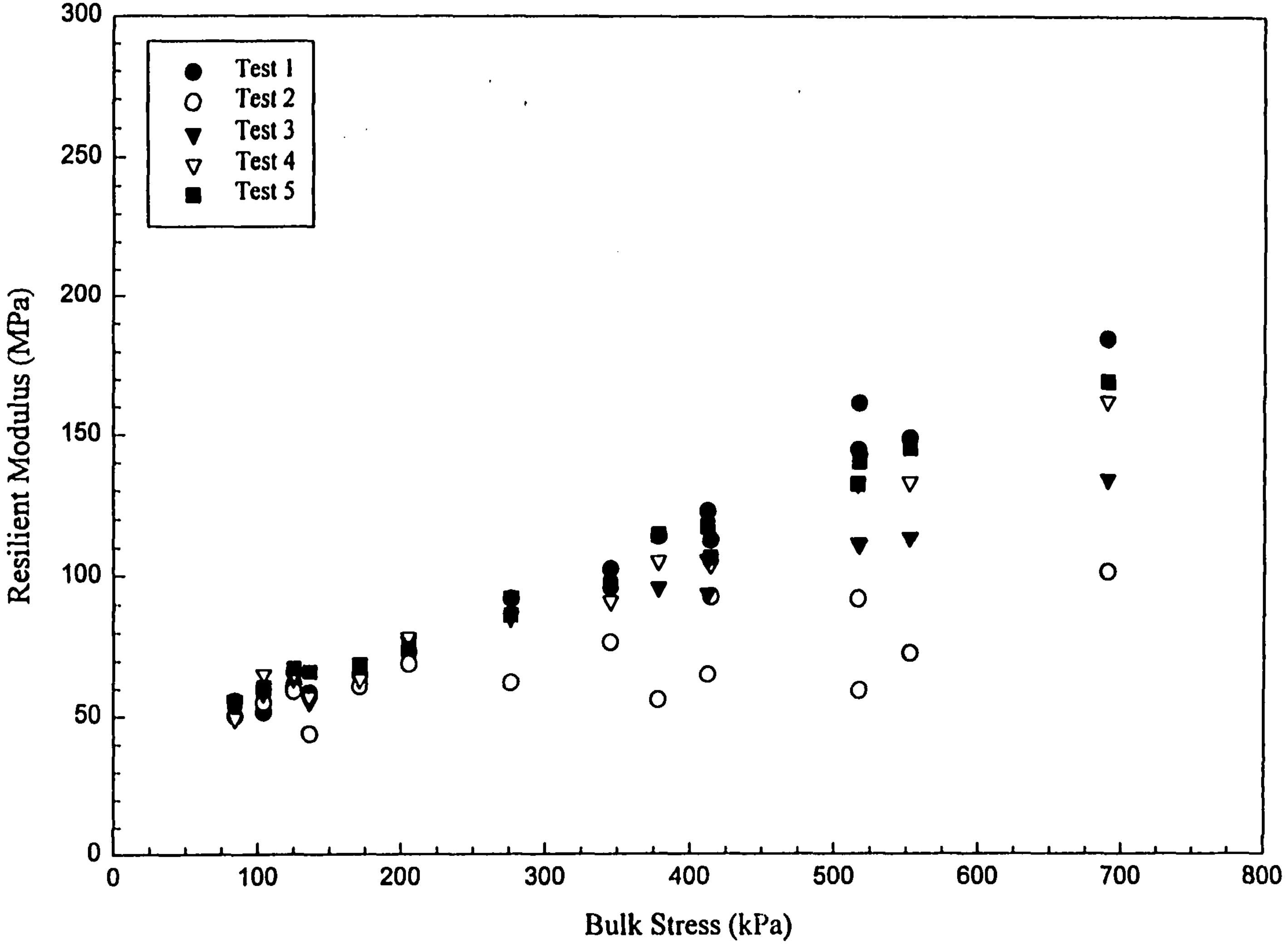

Figure A-16 RM Values of the Sawyer Aggregate at the Median Gradation with the Soaked Specimen (Undrained I)

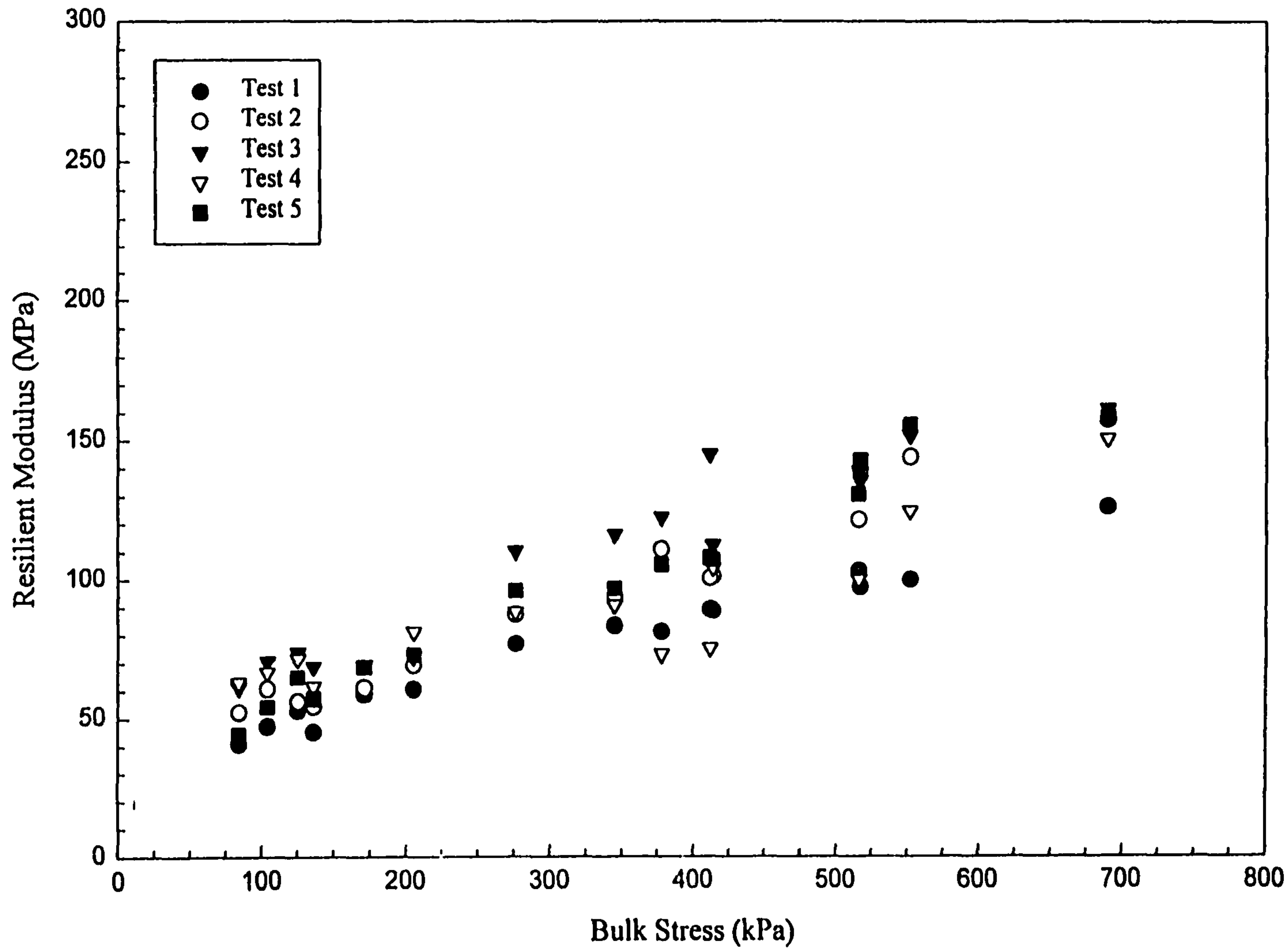

Figure A-17 RM Values of the Sawyer Aggregate at the Median Gradation with the Soaked Specimen (Undrained II)

APPENDIX B

Table B-1 Conversion Factors from SI to English Units

Length	1 m 1 cm 1 mm 1 m 1 cm 1 mm	3.281 ft 3.281×10^{-2} ft 3.281×10^{-3} ft 39.37 in. 0.3937 in. 0.03937 in.
Area	1 m^2 1 cm^2 1 mm^2 1 m^2 1 cm^2 1 mm^2	10.764 ft^2 10.764×10^{-4} ft^2 10.764×10^{-6} ft^2 1550 $in.^2$ 0.155 $in.^2$ 0.155×10^{-2} $in.^2$
Volume	1 m^3 1 cm^3 1 m^3 1 cm^3	35.32 ft^3 35.32×10^{-4} ft^3 61,023.4 $in.^3$ 0.061023 $in.^3$
Force	1 N 1 kN 1 kgf 1 KN 1 KN 1 metric ton 1 N/m	0.2248 lb 224.8 lb 2.2046 lb 0.2248 kip 0.1124 U.S. ton 2204.6 lb 0.0685 lb/ft
Stress	1 N/m^2 1 kN/m^2 1 kN/m^2 1 kN/m^2 1 kN/m^2	20.885×10^{-3} lb/ft^2 20.885 lb/ft^2 0.01044 U.S. ton/ft^2 20.885×10^{-3} kip/ft^2 0.145 lb/$in.^2$
Unit Weight	1 kN/m^3 1 kN/m^3	6.361 lb/ft^3 0.003682 lb/$in.^3$

IMAGE EVALUATION TEST TARGET (QA-3)

150mm

6"

APPLIED IMAGE . Inc
1653 East Main Street
Rochester, NY 14609 USA
Phone: 716/482-0300
Fax: 716/288-5989